



UNIVERSITAT DE
BARCELONA

Advanced multimodal neuromonitoring

Applicability for the pathophysiological study of intracranial pressure plateau waves

Nicolás Gonzalo de Riva Solla

ADVERTIMENT. La consulta d'aquesta tesi queda condicionada a l'acceptació de les següents condicions d'ús: La difusió d'aquesta tesi per mitjà del servei TDX (www.tdx.cat) i a través del Dipòsit Digital de la UB (diposit.ub.edu) ha estat autoritzada pels titulars dels drets de propietat intel·lectual únicament per a usos privats emmarcats en activitats d'investigació i docència. No s'autoritza la seva reproducció amb finalitats de lucre ni la seva difusió i posada a disposició des d'un lloc aliè al servei TDX ni al Dipòsit Digital de la UB. No s'autoritza la presentació del seu contingut en una finestra o marc aliè a TDX o al Dipòsit Digital de la UB (framing). Aquesta reserva de drets afecta tant al resum de presentació de la tesi com als seus continguts. En la utilització o cita de parts de la tesi és obligat indicar el nom de la persona autora.

ADVERTENCIA. La consulta de esta tesis queda condicionada a la aceptación de las siguientes condiciones de uso: La difusión de esta tesis por medio del servicio TDR (www.tdx.cat) y a través del Repositorio Digital de la UB (diposit.ub.edu) ha sido autorizada por los titulares de los derechos de propiedad intelectual únicamente para usos privados enmarcados en actividades de investigación y docencia. No se autoriza su reproducción con finalidades de lucro ni su difusión y puesta a disposición desde un sitio ajeno al servicio TDR o al Repositorio Digital de la UB. No se autoriza la presentación de su contenido en una ventana o marco ajeno a TDR o al Repositorio Digital de la UB (framing). Esta reserva de derechos afecta tanto al resumen de presentación de la tesis como a sus contenidos. En la utilización o cita de partes de la tesis es obligado indicar el nombre de la persona autora.

WARNING. On having consulted this thesis you're accepting the following use conditions: Spreading this thesis by the TDX (www.tdx.cat) service and by the UB Digital Repository (diposit.ub.edu) has been authorized by the titular of the intellectual property rights only for private uses placed in investigation and teaching activities. Reproduction with lucrative aims is not authorized nor its spreading and availability from a site foreign to the TDX service or to the UB Digital Repository. Introducing its content in a window or frame foreign to the TDX service or to the UB Digital Repository is not authorized (framing). Those rights affect to the presentation summary of the thesis as well as to its contents. In the using or citation of parts of the thesis it's obliged to indicate the name of the author.

DOCTORAL THESIS

**ADVANCED MULTIMODAL NEUROMONITORING:
applicability for the pathophysiological study
of intracranial pressure plateau waves**

PhD Student:
Nicolás Gonzalo de Riva Solla

Directors:
Neus Fàbregas Julià Ph.D.
Ricard Valero Castell Ph.D.

Departament de Cirurgia i Especialitats Quirúrgiques
Facultat de Medicina. Universitat de Barcelona



UNIVERSITAT DE
BARCELONA

Facultat de Medicina
i Ciències de la Salut

Los Dres **Neus Fàbregas Julià** y **Ricard Valero Castell**, como Directores del trabajo de Tesis Doctoral: “**ADVANCED MULTIMODAL NEUROMONITORING: APPLICABILITY FOR THE PATHOPHYSIOLOGICAL STUDY OF INTRACRANIAL PRESSURE PLATEAU WAVES**”

Certificamos:

Que esta Tesis ha sido realizada, bajo nuestra dirección, por **Nicolás Gonzalo de Riva Solla** para optar al Grado de Doctor.

Los artículos que se incluyen en esta Tesis cumplen las condiciones vigentes en la Facultad de Medicina de la Universitat de Barcelona para la presentación de tesis doctorales por publicaciones.

En Barcelona a 11 de octubre de 2017.

Dra Neus Fàbregas Julià

Dr Ricard Valero Castell

“One size does not fit all...”

Acknowledgements

Agradecimientos

Agraiments

A la Dra Fàbregas i al Dr Valero, a la Neus i en Ricard. Pel seu grandíssim suport i paciència infinita. I no haver deixat mai de creure (“never stopped believing”).

To the “family” of the “Brain Physics Group” in Cambridge with a special mention for Zofia (Czosnyka), Karol (Budohoski), Georgios (Varsos) and Luzius Steiner. But specially, I want to thank Marek (Czosnyka) and Peter (Smielewski). Thank you for teaching me the real value of “doing science” while being so humble, curious and anxious about knowledge no matter how brilliant you are. A lesson for life.

To all the colleagues and coworkers at the Neurosciences Critical Care Unit (NCCU) at my time at Addenbrooke’s. Y a mis compañeros en la UCI-Quirúrgica que tanto me enseñan y con los que tantas vivencias he compartido a lo largo de estos años.

A Fran, Isa, Kike y Paola. Porque somos un equipo y nada se puede conseguir sin apoyarnos entre todos. Esta Tesis es un ejemplo más.

A mis compañeros neurocirujanos del hospital Clínic. Por su apoyo en un proyecto que comenzó aquí, y que busca aumentar nuestro conocimiento para dar lo mejor de nosotros mismos y, sobre todo, ayudar a nuestros pacientes.

A mis padres y hermanos, que con sus enseñanzas y su apoyo incondicional me permitieron estar hoy aquí. Dar solo las gracias se queda en muy poco...

Un recuerdo muy especial a mi tío Pepe (José García Prendes-Pando) y mi tía Pili (Pilar González Posada) que tanto creyeron en mí en el minuto cero de este viaje.

A mi familia de México, a la que tanto quiero. Los Cotenein, los Angelitos Negros, Mati, el “Negro y Jan”. Un muégano que siempre parece cerca, aunque esté lejos.

Pero sobre todo quiero darle las gracias a Lola y a Emma... por el tiempo “robado”, por vuestra Luz, y porque haceis que la Vida (y mi Vida), sea “fantástica” y llena de alegría. OS AMO.

Abbreviations and Acronyms

a_1	pulse amplitude (first harmonic) of ABP
ABP	arterial blood pressure
AVDO ₂	arterio-venous (jugular) difference of oxygen
AMP	ICP pulse amplitude
AUC	area under the curve
BBB	blood-brain barrier
C_a	cerebrovascular compliance
CBF	cerebral blood flow
CCP	critical closing pressure
CCP ₁	fundamental harmonic model of critical closing pressure
CCPm	multi-parameter mathematical model of CCP based on the concept of impedance.
CM	closing margin
CMRO ₂	cerebral metabolic rate of oxygen
CO	cardiac output
CPPm	mean cerebral perfusion pressure
CSF	cerebrospinal fluid
CVR	cerebrovascular resistance
dCA	dynamic cerebral autoregulation
DAI	diffuse axonal injury
DC	decompressive craniectomy
EVD	external ventricular drainage
f	frequency
f_1	pulse amplitude (first harmonic) of blood FV
FV	cerebral blood flow velocity

FVm	mean blood flow velocity in the middle cerebral artery
FVd	diastolic blood flow velocity in the middle cerebral artery
FVs	systolic blood flow velocity in the middle cerebral artery
HR	heart rate
ICP	intracranial pressure
LLA	lower limit of cerebral autoregulation
LDF	laser Doppler flowmetry
MAP	mean arterial blood pressure
MMM	multimodality monitoring
MRI	magnetic resonance imaging
Mx	mean velocity index of cerebrovascular autoregulation
NCCU	Neurosciences Critical Care Unit
nICP	non-invasive intracranial pressure
NIRS	near-infrared emission spectroscopy
PaCO ₂	arterial partial pressure of carbon dioxide
PaO ₂	arterial partial pressure of oxygen
PbtO ₂	brain tissue oxygen pressure
PET	positron emission tomography
PI	Gosling pulsatility index
PRx	cerebrovascular pressure reactivity index
PVI	pressure-volume index
rCBF	regional cerebral blood flow
R _a	cerebrovascular resistance (CVR in the print publication)
RAP	volume-pressure compensatory reserve index
RBC	red blood cells
RI	Pourcelot resistance index
SAH	subarachnoid haemorrhage
sCA	static cerebral autoregulation

SjO_2	jugular saturation of oxygen
SRoR	static rate of autoregulation
TBI	traumatic brain injury
TCD	transcranial Doppler
THRT	transient hyperaemia response test
ULA	upper limit of cerebral autoregulation
WT	wall tension
WT_1	fundamental harmonics model wall tension
WT_m	multi-parameter mathematical model of wall tension based on the concept of impedance
$ z $	cerebrovascular impedance
$ z_1 $	cerebrovascular impedance with frequency equal to HR

Index

SUMMARY	1
INTRODUCTION	5
1. Brain Physics: cerebral physiology and brain monitoring	7
1.1 Cerebral blood flow and metabolism	7
1.1.1 Regulation of cerebral blood flow	8
1.1.1.1 Cerebral autoregulation	8
1.1.1.2 Cerebrovascular carbon dioxide and oxygen reactivity	15
1.1.1.3 Flow-metabolism neurovascular coupling and hypothermia	16
1.1.1.4 Cardiac output	17
1.1.1.5 Integrated regulation of cerebral blood flow	18
1.1.2 Monitoring cerebral blood flow	19
1.1.3 Transcranial Doppler	21
1.1.3.1 Pulsatility index definition	24
1.1.3.2 Clinical applications of pulsatility index	25
1.2 Intracranial Pressure	26
1.3 Critical Closing Pressure	32
2. Traumatic brain injury	35
2.1 Definition and epidemiology	35
2.2 Clinical assessment and classification: the GCS scale	35
2.3 Physiological changes after a traumatic brain injury	37
2.3.1 Intracranial hypertension	37
2.3.2 Plateau waves	40
3. ICM+ [®] software for multimodal brain monitoring	42
3.1 Multimodal neuromonitoring	42
3.2 The ICM+ [®] software	43
3.2.1 Principles of ICM+ [®] software	43
3.2.2 Integrated physiological study of plateau waves	48
HYPOTHESIS AND AIMS	51
SUBJECTS AND METHODS. RESULTS (PUBLICATIONS)	55

DISCUSSION	81
CONCLUSIONS	95
REFERENCES	99
OTHER SCIENTIFIC MERITS RELATED TO THIS INVESTIGATION	113

Summary

INTRODUCTION Multimodal neuromonitoring increases the knowledge of the physiopathology underlying the plateau waves of intracranial pressure (ICP). The transcranial Doppler (TCD) pulsatility index (PI) is considered a descriptor of the distal cerebrovascular resistance (CVR).

Critical closing pressure (CCP) denotes a threshold of arterial blood pressure (ABP) below which blood vessels collapse and cerebral blood flow (CBF) ceases increasing the ischemic risk. Although theoretically could be useful, its clinical applicability is limited for methodological reasons.

HYPOTHESIS 1) PI could be determined by the interaction of multiple haemodynamic variables and not only by CVR; 2) CCP, estimated with a cerebrovascular impedance model, increases during plateau waves.

AIMS 1) to define which factors influence TCD pulsatility index of cerebral blood flow velocity; 2) to measure CCP and verify a new method to its calculation during plateau waves.

SUBJECTS AND METHODS Recordings from patients with severe head-injury undergoing monitoring of arterial blood pressure, ICP, cerebral perfusion pressure (CPP), and TCD assessed cerebral blood flow velocities (FV) were analysed. The Gosling pulsatility index (PI) was compared between baseline and ICP plateau waves (n = 20 patients) or short-term (30–60 min) hypocapnia (n = 31). In addition, a modeling study was conducted with the “spectral” PI (calculated using fundamental harmonic of FV) resulting in a theoretical formula expressing the dependence of PI on balance of cerebrovascular impedances.

Analysis with a validated specific software (ICM+®). Both studies are based in a multiparametric method new model of cerebrovascular impedance; first a retrospective study of 2 opposing physiological conditions comparing basal PI to: a) plateau waves (n= 20 patients, 38 plateau waves); and b) moderate hyperventilation (n=31); next CCP was calculated in the plateau waves group (n= 20). According to Burton’s model, wall tension (WT) was estimated as: $WT = CCP - PIC$.

RESULTS 1) during plateau waves PI increases significantly while CVR diminishes. During hypocapnia both PI and CVR increase; 2) CCP increases significantly in the plateau of the wave while WT lowers a 34.3%.

CONCLUSIONS 1) Transcranial Doppler PI is usually misinterpreted as a descriptor of distal CVR. There is a complex relationship between PI and multiple haemodynamic variables; 2) Critical closing pressure (CCP) increases during plateau waves but wall tension (WT) diminishes. A new mathematical model to calculate CCP is presented which allows a more physiological interpretation.

Keywords Cerebral hemodynamics _ Critical closing pressure _ Intracranial pressure _ Mathematical modeling _ Plateau waves _ Transcranial Doppler _ Traumatic brain injury _ Wall tension

Introduction

1. BRAIN PHYSICS: CEREBRAL PHYSIOLOGY AND BRAIN MONITORING

Scientists have studied the brain for centuries. The brain is the part of the central nervous system that is housed in the cranial vault and has a very complex biomechanics.

Brain physics is the area of science that summarizes physical interactions between volumes, flows and pressures within the brain. Hence, a good understanding of these relationships is needed in order to clearly understand the basics of cerebral physiology, and particularly of cerebral haemodynamics.

The brain is a unique vital organ with a high metabolic rate that requires a continuous supply of energy, and its oxygen demand exceeds that of all organs except the heart. Although cerebral parenchyma comprises only 2% of the body weight it disproportionately consumes 20% of the total body resting oxygen consumption and 25% of the glucose used by the whole body, and is dependent on a constant supply of 12-15% of the cardiac output (700 mL min^{-1} in the young adult). As cerebral function is totally dependent on oxidative phosphorylation of glucose to provide ATP, the brain is dependent on a stable supply of cerebral blood flow¹⁻³.

1.1 Cerebral blood flow and metabolism

Mean resting cerebral blood flow (CBF) in young adults is about $55\text{-}60 \text{ mL (100 g brain tissue)}^{-1} \text{ min}^{-1}$. This mean value represents two very different categories of flow: 75 and $45 \text{ mL (100 g brain tissue)}^{-1} \text{ min}^{-1}$ for grey and white matter, respectively. Regional CBF (rCBF) and glucose consumption decline with age, along with marked reductions in brain neurotransmitter content, and less consistent decreases in neurotransmitter binding.

In health, oxygen delivery by CBF is efficiently matched to the cerebral metabolic rate for oxygen (CMRO₂), which usually is about $3.3 \text{ mL (100 g brain tissue)}^{-1} \text{ min}^{-1}$. There is a basal consumption of energy (around 40%) for the maintenance of the cellular integrity and the electrochemical gradients, synthesis of proteins, lipids and carbohydrates and neurotransmitters management; besides there is a “functional” consumption (60%) for the electrical activity of the neurons².

In physiological conditions, there is an excellent flow–metabolism coupling whereby CMRO₂ is directly related to CBF and the arterio-jugular differences in oxygen content (AVDO₂). The lack of storage of substrates and the high metabolic rate of the brain accounts for the organ’s sensitivity to hypoxia. CBF and oxygen consumption thresholds identified for ischemic and irreversible injuries are $18 \text{ mL (100 g brain tissue)}^{-1} \text{ min}^{-1}$ and $1.0 \text{ mL (100 g brain tissue)}^{-1} \text{ min}^{-1}$, respectively⁴.

Optimal cerebral perfusion is essential to avoiding tissue ischemia and overperfusion. There are two common theories to explain the relationship between cerebral perfusion and systemic hemodynamics. The first is based on an analogy to *Ohm’s law* regarding the relationship between resistance, pressure, and flow: ‘organ perfusion (flow) depends on arterial blood pressure (ABP) and cerebrovascular resistance (CVR)’. The other is based on the *distribution of the cardiac output (CO)*: ‘the blood flow of the brain is a portion of the CO that is determined by the value of CO and the percentage of share based on the brain’s metabolic need’¹.

Application of the Ohm's law to cerebrovascular haemodynamics translates to the following equation, where CPP stands for 'cerebral perfusion pressure':

$$\text{CBF} = \frac{\text{CPP}}{\text{CVR}}$$

The driving pressure in most organs is the difference between arterial and venous pressure. However, the pressure perfusing the brain (CPP) is the difference between mean arterial pressure (MAP) and either the intracranial pressure (ICP) or the pressure within the cerebral veins (whichever is greater)⁵. As the brain lies in a closed cavity, when ICP is elevated there is a collapse of the bridging pial veins and venous sinuses, which then act as Starling resistors. Therefore, coupling between the ICP and pressure in bridging and cortical veins provides the basis for this definition of CPP⁶.

CVR is influenced in physiologic states by constriction and dilatation of the arterioles in the brain. In pathologic states, focal changes in resistance can be seen immediately behind an area of significant stenosis.

The main goal of brain cerebrovascular haemodynamics is to keep CBF stable despite possible alterations in CPP and CVR. The interaction of different physiological mechanisms is responsible of this goal.

1.1.1 Regulation of cerebral blood flow

CBF is rigorously regulated by a set of powerful mechanisms to safeguard the matching of cerebral metabolic demand and supply. Classically these mechanisms have been considered to be cerebral autoregulation, neurovascular coupling and cerebrovascular carbon dioxide (and oxygen) reactivity. However, actual evidence shows that also an alteration in cardiac output, either acutely or chronically, may lead to a change in CBF that is independent of other CBF-regulating parameters including blood pressure and carbon dioxide⁷.

1.1.1.1 Cerebral autoregulation

Cerebral blood flow autoregulation is the intrinsic ability of the cerebral vasculature to maintain a stable blood flow for a given magnitude of cerebral metabolic rate despite fluctuations in mean arterial blood pressure. Under normal circumstances, CBF is regulated mainly through changes in arteriolar diameter, which, in turn, drive changes in CVR in accordance with Poiseuille's Law. Decreases in ABP (or CPP) result in cerebral arteriolar vasodilation, while elevations induce vasoconstriction.

This homeostatic mechanism was first demonstrated by Fog (1937) in cats^{8,9} but it was not accepted until 1959 when Lassen described this phenomenon using the classic triphasic autoregulation curve which was constructed from CBF measurements in several different

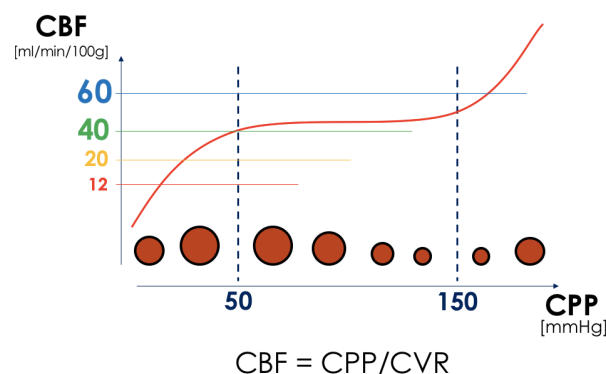
human studies using Kety and Schmidt's nitrous oxide method¹⁰.

Various neurogenic (through pial vessels innervation)¹¹, myogenic (changes in arteriolar transmural pressure)¹² and metabolic pathways (involving nitric oxide and adenosine)¹³ have been involved in mediation of cerebral vasomotor reactions, but the exact molecular mechanisms still remain elusive¹⁴.

As shown in **figure 1-1**, cerebral autoregulation is visualized as a correlation plot of CBF (axis of ordinate) against CPP or ABP (axis of abscissas).

Figure 1-1. Classical curve of cerebral autoregulation (also known as Lassen's curve)¹⁰. CBF is maintained through active changes in vascular diameter of the arterioles despite fluctuations in CPP. The three elements of the resulting curve are (1) the lower limit, LLA; (2) the upper limit, ULA; and (3) the plateau. The lower and upper limits are the two inflection points indicating the boundary of pressure-independent flow (the plateau) and the start of pressure-passive flow.

Reproduced with permission from the Brain Physics Lab, University Neurosurgery Unit, Addenbrooke's Hospital, Cambridge, UK.



As we see in **figure 1-1**, the most quoted are a LLA of 50 mm Hg, an ULA of 150 mmHg, and the plateau (CBF) around 45-50mL (100 g brain tissue)⁻¹ min⁻¹. Below the LLA, CBF would be completely dependent on MAP (or CPP) with the consequent risk of cerebral ischemia. On the other hand, above the ULA we would have the same condition (CBF directly dependent on MAP or CPP) but in this case the risks would be related to the damage of the blood-brain barrier and the consequent risk for oedema or even bleeding.

However, these classical reference numbers are the means of various groups of subjects in different studies, without any note of the standard deviations or range of distribution^{10,11}. That explains why these inflection points are usually represented as “sharp points” instead of a more physiological round “shoulder” limits as seen in **figure 1-1**. Also the flat plateau (zero tilt) of the autoregulation curve is an idealized drawing, as it may execute on a slightly tilted plateau different to pressure-passive flow¹⁵.

There is a wide range of interindividual and study-to-study variations regarding these LLA and

ULA in health and disease, and published figures in humans vary considerably¹⁶. Experts in the field remark the importance of individualizing these limits or, as a reference for clinical practice, consider a theoretical LLA with a 75% of the MAP value taken as a reference. Cerebral hypoperfusion symptoms could be expected when MAP of the patient would become about 40-50% of the initial reference value¹⁷.

The position of the LLA also depends on the mechanism of hypotension. If it is related to vasodilating drugs (i.e. low sympathetic tone), the LLA will shift more to the left compared to cases related to hypovolemia (due to the generalized increment of the sympathetic tone in this last group)¹⁸.

The cerebral autoregulation curve is shifted to the right in patients with chronic arterial hypertension. As both upper (ULA) and lower (LLA) limits are shifted, CBF becomes more pressure-dependent at low “normal” arterial pressures in return for cerebral protection at higher arterial pressures. Studies suggest that long-term (over 1 year) antihypertensive therapy can restore cerebral autoregulation limits towards normal¹⁹.

Considering all these facts, the autoregulation curve conceived by Lassen is not a ‘one-size-fits-all’ phenomenon; rather, its position and shape may change following changes in pertinent physiological and medical conditions.

Cerebrovascular autoregulation can be thought of as comprising both fast (*dynamic*) and slow (*static*) components in terms of the changes in CVR in response to changes in pulsatile and mean CPP, respectively²⁰. Measurement of cerebral autoregulation is a complicated process. Besides the technical limitations there are many physiological variables that can affect the CBF either directly or through metabolic coupling.

- *Static cerebrovascular autoregulation (sCA)*

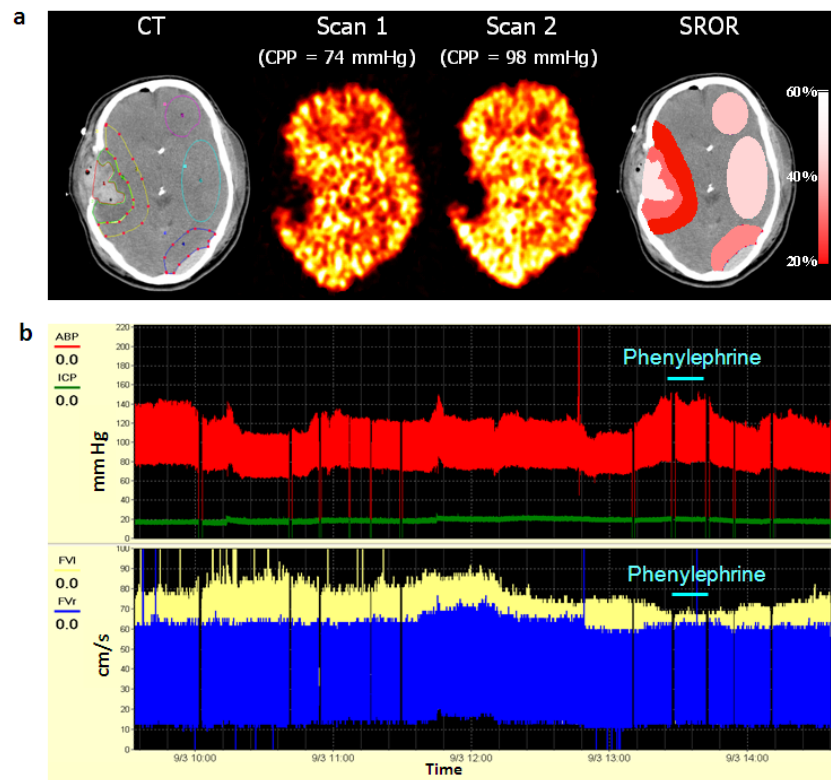
Static measurements evaluate the change in CVR in response to the pharmacological manipulation of MAP allowing sufficient time for the flow and pressure to plateau. In fact, the static rate of autoregulation (SRoR) is calculated by measuring CBF at two stable blood pressure levels, and determining the ratio of change in the two parameters; that is, the percentage change in CVR divided by the percentage change in MAP (or CPP if available, see **figure 1-2**).

$$SRoR = \frac{\% \text{ change in CVR}}{\% \text{ change in CPP}}$$

If CVR does not change with change in CPP (or MAP), autoregulation is said to be impaired.

Static measurements are considered the gold standard for testing cerebrovascular autoregulation. The best approach is to measure it with direct perfusion methods, such as ¹³³Xe clearance, magnetic resonance imaging (MRI) and positron emission tomography (PET) scan, which all enable calculation of absolute CBF values.

Figure 1-2. Static rate of cerebral autoregulation (SRoR). The figure shows assessment of SRoR during pharmacological-induced hypertension. It is calculated as percentage change of CVR divided by the percentage change in CPP. **a)** Direct CBF measurement and SRoR calculation using a PET scan. Noradrenaline was infused to increase CPP. **b)** SRoR calculated with a CBF surrogate (transcranial Doppler). ABP was increased with injection of a vasopressor (phenylephrine, light blue bar). Right side CBF velocity (dark blue) responded positively and left side (in yellow) negatively. Left side SRoR was 120% (preserved) and right side SRoR was 64% (altered). *Reproduced with permission from the Brain Physics Lab, University Neurosurgery Unit, Addenbrooke's Hospital, Cambridge, UK.*



However, despite being quantitative and providing results that are simple to interpret, these techniques have several drawbacks. First, assessment of CBF at two steady states can provide information about the long-term (outcome) performance of cerebral autoregulation but not the dynamic process itself¹⁶. Furthermore, as use of these techniques requires pharmacological induction of changes in ABP, they are not suitable for critically ill patients in whom blood-pressure stimuli may be undesirable, nor for sequential monitoring¹⁴.

- *Dynamic cerebrovascular autoregulation (dCA)*

Described as a concept in 1989 by Aaslid *et al*, it refers to the fast component of cerebrovascular autoregulation that tends to be affected earlier than sCA and in consequence is more vulnerable to a variety of insults²¹.

For practical reasons including availability and the capacity to measure blood flow continuously, surrogate markers of CBF have been frequently measured and adopted for monitoring dCA. Such methods include transcranial Doppler (TCD), laser Doppler flowmetry (LDF), partial pressure of brain tissue oxygen (pbtO₂) and thermal-diffusion regional CBF, as well as near-infrared spectroscopy (NIRS) technologies¹⁴. These surrogate measurements place emphasis on the dynamic process (fast component) of autoregulatory reactions- that is, changes that occur within seconds after a fall or rise in perfusion pressure.

Owing to the heterogeneity of these modalities, both in terms of the nature of the monitored parameter as well as their spatial characteristics (white matter versus grey matter, and unilateral versus bilateral), interpretation of results is often challenging.

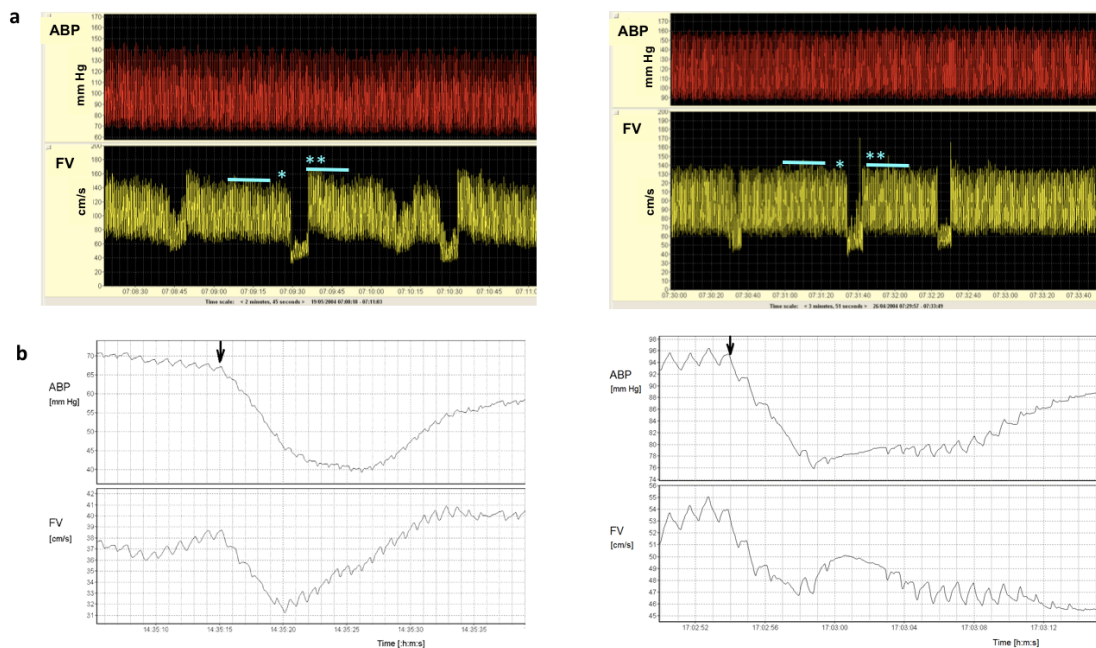
In contrast to calculation of the SRoR, no uniform and accepted method exists for calculation of dCA¹⁶; however, they can be broadly divided into those that require a short blood-pressure stimulus and those that rely on spontaneous fluctuations of blood pressure, which are less invasive.

Measurement with blood-pressure stimulus (figure 1-3):

- *Transient hyperemic response test (THRT)*: originally described by Giller et al, it uses TCD to determine the magnitude of the increase in CBF velocity that occurs after the common carotid artery is relieved from a brief period of compression (5 seconds)²². The observed hyperaemia is a consequence and manifestation of autoregulatory vasodilatation that occurs during compression; lack of a hyperaemic response, therefore, is suggestive of dysautoregulation. Similar reactions can also be evoked using NIRS-derived parameters.
- *Thigh-cuff deflation method*: described by Aaslid et al, it uses systemic hypotension induced by deflation of a previously inflated thigh cuff²¹. This hypotension is accompanied by a sudden drop in CBF velocity (measured with TCD) with subsequent recovery, which is again a manifestation of autoregulatory vasodilatation and decreasing CVR. The rate of recovery can be calculated and used as an index of autoregulation: fast recovery indicates functional autoregulation.

The fact that the observer controls the exact time and grade of the stimulation imparts precision to these techniques, as stimuli can be graded to create a favourable signal-to-noise ratio¹⁶.

Figure 1-3. Dynamic cerebral autoregulation (dCA) assessed with short-lived blood pressure stimulus. **a)** Transient hyperaemic response test with a 5 seconds compression (*) and then release (**) of the common carotid artery. Intact autoregulation (left) shows a positive hyperemic response of blood FV measured with TCD in the middle cerebral artery. When autoregulation is impaired (right), no hyperaemic response is seen. **b)** Thigh-cuff test: following rapid deflation of a thigh cuff (black arrow), intact autoregulation leads to rapid return of FV to baseline preceding normalization of ABP (left). Impaired autoregulation shows a slow return of FV to baseline (right). *Reproduced with permission from the Brain Physics Lab, University Neurosurgery Unit, Addenbrooke's Hospital, Cambridge, UK.*



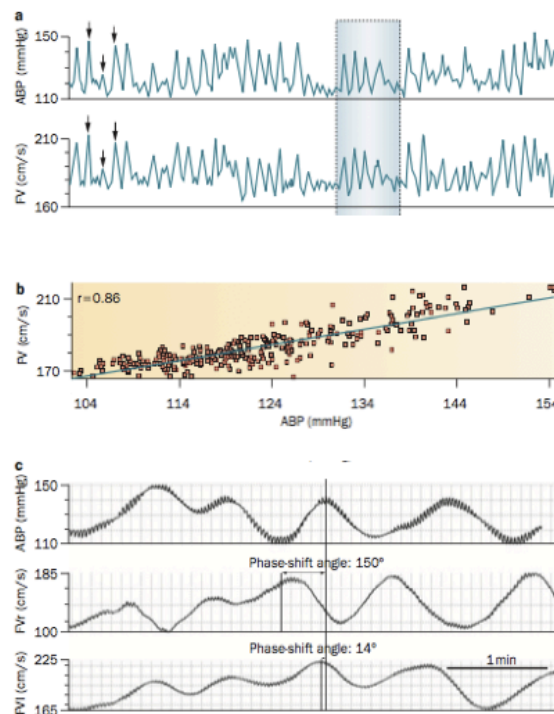
Noninvasive measurements (figure 1-4).

Methods are available that enable continuous autoregulation monitoring relying on the observation of spontaneous responses of CBF to spontaneous ABP fluctuations without the requirement of external stimuli. Hemodynamic oscillations with a period between 20 seconds and 3 minutes (the so called ‘slow waves’) are the best inputs for this assessment¹⁶.

These methods are based on waveform analysis as the signal-to-noise ratio and subsequent precision is less favourable than in the testing methods previously explained. This loss of precision is compensated by the ability to repeat the measurements frequently and autoregulation is calculated continuously by assessment of either the speed or the direction of changes in any of the surrogate markers of CBF in relation to the speed or direction of the ABP change. Again, large heterogeneities exist in methods to calculate autoregulatory parameters, and such variability has particular importance when assessment of autoregulation is based on spontaneous fluctuations (figure 1-4).

- *Time-based methods* assess the correlation between ABP and surrogate markers of CBF, and follow the concept that in a passive system (such as autoregulatory failure), the correlation between these two parameters will be high²³.
- *Frequency-based methods* involve application of a mathematical-transfer function analysis and assess the phase relationship (*'phase-shift'* = *which variable changes before which*) between fluctuations of ABP and surrogate markers of CBF within a defined frequency band. In this model, a near-zero phase shift indicates passivity and impaired autoregulation, while a negative phase shift (indicating surrogate CBF changes before ABP) indicates intact autoregulation^{24,25}.

Figure 1-4. Dynamic cerebral autoregulation assessed with spontaneous fluctuations of blood pressure. **a)** Spontaneous ABP and FV fluctuations (arrows); **b)** Time-based methods determine the moving correlation coefficient between ABP and FV; **c)** Frequency-based methods single out the slow waves with filters and measures the phase shift angle between both signals (high phase-shift = preserved autoregulation on the right side-FVr, low phase-shift = impaired autoregulation on the left side-FVl). *Modified from Budohoski KP et al. Nat. Rev. Neurol. 2013, (9): 152-63.*



Currently, TCD remains the most commonly used non-invasive method for monitoring surrogate markers of CBF. As TCD measures CBF velocity and only in a particular artery, commonly the middle cerebral artery (MCA), this may introduce a source of inaccuracy²⁶. Nevertheless, TCD has been extensively validated both for estimating CBF sufficiency and for monitoring autoregulation²⁷.

NIRS is gaining recognition as a non-invasive method to monitor cerebral autoregulation as it has been shown to accurately reflect the dynamic changes in CBF²⁸. Experimental work using a piglet model of induced hypotension demonstrated that NIRS-based assessment of autoregulation was reliable and correlated well with more-established invasive methods²⁹. However, a particular limitation for NIRS is that it is prone to extracranial contamination of the signal, particularly when extracranial tissue is extensively swollen (e.g. after neurosurgery)³⁰.

Although in general there is a good concordance between static and dynamic cerebrovascular autoregulation testing, sCA is more robust than dCA as the former is not affected by latency changes³¹.

1.1.1.2 Cerebrovascular carbon dioxide and oxygen reactivity

The execution of cerebral autoregulation relies on the robust cerebrovascular reactivity that engenders dilation to a decrease in CPP and constriction to an increase in CPP. However, carbon dioxide (CO₂) is a largely known powerful modulator of cerebral vasomotor tone and through changes in arterial blood CO₂ partial pressure (PaCO₂) has a major influence in the regulation of CBF^{32,33}.

At a normal ABP, a change in PaCO₂ exerts a profound effect on cerebral perfusion with a 2-4% linear change in CBF for every 1-mmHg change in PaCO₂³⁴. Carbon dioxide diffuses rapidly across the blood-brain barrier, increases the concentration of extracellular fluid H⁺ ions, and causes vasodilation³⁵. However, the arteriolar tone modifies the effects of PaCO₂ on CBF, and severe hypotension can abolish the ability of the cerebral circulation to respond to PaCO₂ changes³⁶.

Hypercapnia increases CBF by cerebral vasodilation. As a consequence, the plateau of the Lassen's autoregulation curve is progressively shifted upward and shortened, the lower limit (LLA) is shifted rightward, and the upper limit (ULA) is shifted leftward (**figure 1-5, left**). The extent of these changes depends on the balance between the severity of hypercapnia and the buffering capacity of the sympathetic nervous activity. At severe hypercapnia, when cerebral resistance vessels are maximally dilated, the plateau is lost and the pressure-flow relationship is linear³³.

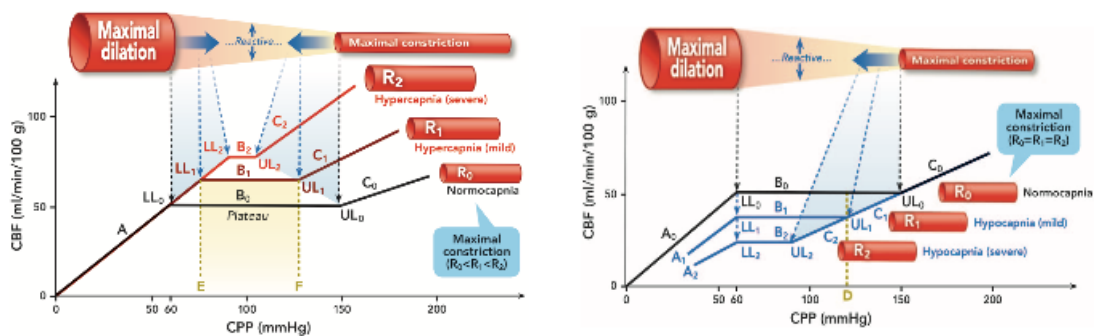
During hypercarbia, vasodilation occurs in the normal cerebral vasculature. As a consequence, *cerebral blood flow steal* may happen as there is a decreased blood flow in relatively ischemic areas of the brain as a result of hypercarbia-induced vasodilation in non-ischemic areas³⁷.

Conversely, hypocapnia decreases CBF due to cerebral vasoconstriction and results in the plateau descending to lower CBF with an unremarkable change of the LLA³⁸ (**figure 1-5, right**). However, how the upper limit moves is not clear and different speculations have been stated³³. In this case, vasoconstriction in the normal areas of the brain induced by hypocapnia can redistribute blood to ischemic areas, the so called *inverse steal* (or 'Robin Hood') phenomenon³⁹.

Within physiological limits, arterial blood oxygen partial pressure (PaO₂) does not affect CBF. Hypoxia-induced cerebral vasodilation begins to rise CBF when PaO₂ falls to 50 mmHg and roughly increases two-fold at a PaO₂ of 30 mmHg because of tissue hypoxia and concomitant

lactic acidosis. Hyperoxia may be associated with only minimal decreases (<10%) in CBF. Therefore oxygen regulates CBF both alone and via an integrated mechanism that involves interplay with CO₂, perfusion pressure, and maybe other physiological processes³⁵.

Figure 1-5. Effect of hypercapnia (*left*) and hypocapnia (*right*) on cerebral autoregulation. Autoregulation curves are in black at normocapnia, red at hypercapnia and blue at hypocapnia. Cerebral resistance vessels are drawn in red and R = calibers of the vessels. A = curve below the LL of autoregulation (LL), B = the plateau at normocapnia (B₀), mild hypercapnia or hypocapnia (B₁) and severe hypercapnia or hypocapnia (B₂); C = the curve above the upper limit (UL) at normocapnia (C₀), mild hypercapnia or hypocapnia (C₁) and severe hypercapnia or hypocapnia (C₂). Taken from Meng L et al. *Anesthesiology* 2015, 122 (1): 196-205.



1.1.1.3 Flow-metabolism neurovascular coupling and hypothermia

Increases in local neuronal activity are accompanied by increases in regional cerebral metabolic rate. Until recently, increases in regional cerebral blood flow (rCBF) and oxygen consumption produced during such functional activation were thought to be closely coupled to the CMRO₂ of utilization of both oxygen (CMRO₂) and glucose.

However, recent research has shown that the key mechanism responsible for the rCBF increase during functional activation is a tight coupling (a linear relationship), between rCBF and glucose metabolism. On the other side, oxygen metabolism only increases to a minor degree, causing an uncoupling of rCBF and oxidative metabolism⁴⁰.

The disproportionate increase in glucose utilization leads to regional anaerobic glucose utilization with a consequent decrease in oxygen extraction ratio. Functional recruitment of capillaries attempting to accommodate the cerebral tissue's increased demand for glucose supply during neural activation and recent evidence supporting a key function for astrocytes in rCBF regulation are the mechanisms involved⁴¹.

Hypothermia is known to reduce both the active and the basal components of metabolism, thereby increasing the period of ischemia tolerated. The cerebral metabolic rate (CMRO₂) decreases by 5-7% for each 1°C fall in body temperature⁴² while pyrexia has the reverse effect. Accordingly, there is a parallel reduction in CBF with the decrease in cerebral metabolic rate⁴³.

1.1.1.4 Cardiac Output

A recent review of the overall evidence shows that, even though the ABP remains stable or within the autoregulatory range, acute or chronic alterations in cardiac output (CO) lead to a change in CBF that is independent of other CBF-regulating parameters including ABP and CO₂⁷. This is a clinically relevant issue because both acute and chronic changes in CO are frequently encountered in clinical care. CO contributes to the regulation of CBF likely via the sympathetic nervous activity, with or without the renin–angiotensin system depending on the acuteness or chronicity of change (**figure 1-6**).

Although there are methodological heterogeneities between studies with some inconsistent results there seems to be a causal relationship between *acute changes in CO* and CBF, where each percentage of change in CO would correspond to a 0.35% change in CBF⁷. The speculative involved mechanism would be a change in CVR due to the sympathetic innervation of the cerebral resistance vessels incurred by central blood volume alterations, as ABP remained relatively stable. During acute central blood volume alteration, the extent of the CBF change is much smaller (about one third) than the change in peripheral regional blood flow probably due to the concomitant protective effects of the other previously explained CBF-regulating mechanisms⁴⁴ and to the redistribution of flow from the periphery to the brain due to a major role of the sympathetic nervous system in the peripheral tissues vascular beds.

On the other hand, there is also extensive evidence showing that CBF is reduced in patients diagnosed with *chronically reduced CO* due to chronic heart failure compared to healthy controls. The extent of the CBF reduction correlates with the severity of the chronic heart failure assessed using New York Heart Association functional classification⁴⁵ and the left ventricular ejection fraction⁴⁶.

In both acute and chronic CO reduction on CBF, the differential extent of vasoconstriction of different vascular beds shunts the flow from the periphery to the brain resulting in a lesser extent of CBF reduction than both the CO and the peripheral blood flow.

The mechanism underlying the CBF reduction in patients with chronic heart failure is unclear but likely related to the neurohormonal activation incurred by a failing heart (**figure 1-6**). The hyperactivity of both the sympathetic nervous system and the renin–angiotensin–aldosterone axis provokes vasoconstriction of not only the peripheral vascular beds but also the cerebral vascular bed. This relentless cerebral hypoperfusion and neurohormonal hyperactivity likely contribute to the dysfunction of the neurovascular unit increasing the risk of cognitive dysfunction, abnormal brain aging and Alzheimer's disease⁷.

The lesser extent to which CBF changes compared with that of CO or peripheral blood flow during acute or chronic CO alterations can be explained by the fact that the extent to which CBF is changed is determined by the integrated effect of all CBF-regulating mechanisms (**figure 1-6**). Other powerful CBF-regulating mechanisms unrelated to CO may buffer the effect of CO on CBF, causing a lesser flow change in the brain compared with the organs that are not influenced by these mechanisms.

Unfortunately, studies on the association between CO and CBF in patients with varying neurologic (vasospasm, ischemic stroke), medical (sepsis, hepatic failure) and surgical conditions (cardiac surgery, neurosurgery, head injuries) are confounded by methodologic limitations. The use of vasoactive drugs is a remarkable aspect, as vasoactive agents that primarily increase ABP such as phenylephrine or norepinephrine may have unpredictable effects on CO. In contrast, dobutamine and volume augmentation can increase the CO but not necessarily ABP. The effect of a vasopressor on CBF likely depends on the drug being used, the disease state, and the functional status of the regulatory mechanisms of brain perfusion. However, it seems that interventions that enhance cardiac performance may improve perfusion of the ischemic brain, especially in patients with impaired cardiac function.

1.1.1.5 Integrated Regulation of cerebral blood flow

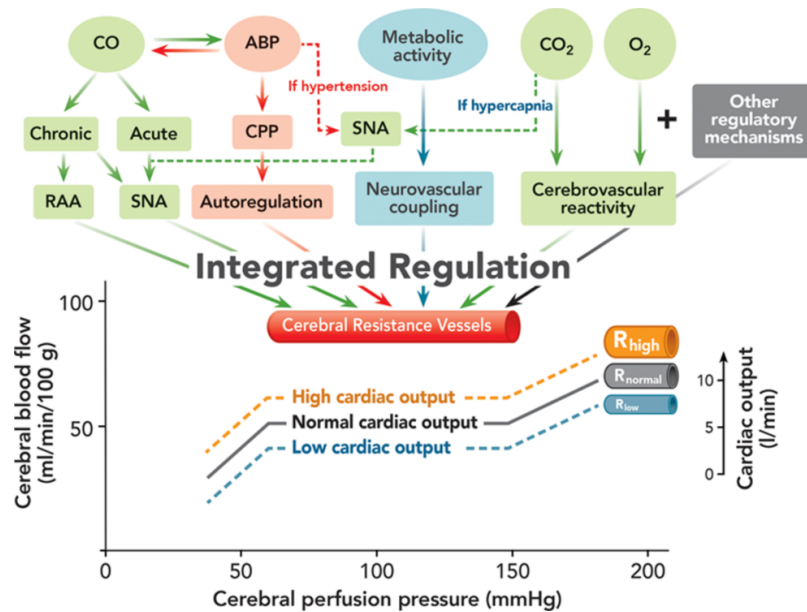
Meng and colleagues recently proposed a revised conceptual framework of the integrated regulation of brain perfusion in order to consider all CBF-regulating mechanisms with the effects of blood pressure and CO on brain perfusion in one concordant context⁷. This was an important consideration because blood pressure and CO are related but different systemic hemodynamic parameters, and they may change simultaneously but exerting distinctive effects on brain perfusion⁴⁷ (**figure 1-6**).

The autoregulatory curve should be regarded as a dynamic process, meaning that its shape, plateau, and the lower and upper limits may change depending on the integrated effect of these CBF-regulating mechanisms including the CO. As CBF regulation is multifactorial, these various processes, no matter how distinctive, must exert their effects simultaneously on the cerebral resistance vessels and jointly generate only one consequence that is the extent of the CVR. Different mechanisms may affect different segments of these cerebral resistance vessels (i.e. sympathetic stimulation constricts large cerebral arteries, whereas an increase in ABP constricts the arterioles).

Therefore, how CBF is affected after a change in any of the regulatory processes depends on how these mechanisms are integrated. Different mechanisms likely have different degrees of regulatory power likely determined by the physiologic priority in the context of the clinical situation. The one with the major regulatory power plays a dominant role, whereas one with minor power plays a smaller role.

The effect of CO on CBF can be appreciated within the framework of cerebral autoregulation. When CO is decreased, the plateau descends slightly reflecting the smaller decrease in CBF, and vice versa. However, how the lower and upper limits of the Lassen's curve are changed and whether the plateau tilts when the CO is altered is still unknown.

Figure 1-6. Integrated regulation of brain perfusion. The calibre of the resistance vessels is determined by the interaction of different physiological mechanisms of CBF regulation: 1) cardiac output (CO) via sympathetic nervous activity (SNA) and renin–angiotensin–aldosterone system (RAA); 2) ABP and CPP via cerebrovascular autoregulation; 3) cerebral metabolic activity (neurovascular coupling); 4) cerebrovascular reactivity to CO₂ and O₂. The plateau of the curve shifts downward when CO is reduced and upward when is augmented. The position of the plateau is determined by the caliber (R, high-normal-low) of the cerebral resistance vessels. Taken from Meng et al. *Anesthesiology* 2015, (123): 1198-208.



1.1.2 Monitoring cerebral blood flow

As previously stated, the best approach to measure CBF is with the aid of direct perfusion methods, such as ¹³³Xe clearance, MRI or PET, which all enable calculation of absolute CBF values.

Nevertheless, for practical reasons including availability and the capacity to measure CBF continuously at the bedside, different methods that measure surrogate measurements of CBF have been adopted along the last 3 decades. Among them the thermal-diffusion rCBF monitors may quantify perfusion in absolute physiological units [$\text{mL (100 g brain tissue)}^{-1} \text{min}^{-1}$], but it's an invasive technology and signals show lot of fluctuations that seem to be artificial⁴⁸. With similar intentions, laser-Doppler flowmetry was largely investigated years ago but now is rarely used in clinical practice as it is invasive, indirect and has a biological zero⁴⁹.

A special mention must be made regarding jugular venous bulb oximetry, frequently used as a bedside measure of global cerebral oxygen delivery and extraction and as a tool to estimate adequacy of the global CBF. As CBF and metabolism ($CMRO_2$) are usually coupled, during a period of stable cerebral metabolism, CBF can be estimated from the arterio-venous (jugular) oxygen content difference across the cerebral circulation ($AVDO_2$).

$$AVDO_2 = \frac{CMRO_2}{CBF}$$

As a consequence, $AVDO_2$ may be considered a measurement of the flow-metabolism coupling⁵⁰.

Near infrared spectroscopy is a noninvasive optical monitoring technique that utilizes infrared light to estimate brain tissue oxygenation and provide indirect information about CBF. Infrared light is emitted from light emitting diodes and detected by phosphodiode optodes placed over the scalp of the frontal lobes. However, NIRS technique and normative saturation values vary among the different manufactured monitors making both comparisons and interpretations difficult. But technology is still evolving, and besides these recognized limitations it may provide a bedside tool for an accurate measure of CBF in the near future³⁰.

Nevertheless, among all the described techniques TCD has established itself as a reference monitor due to its very good dynamical response while being non-invasive. TCD is the only diagnostic tool that can provide continuous reliable information about cerebral haemodynamics in real time and over extended periods.

1.1.3 Transcranial Doppler

TCD is a non-invasive bedside monitor that uses a Doppler transducer to measure red blood cells (RBC) velocity and pulsatility of the CBF in the circle of Willis large basal cerebral arteries. Its first use in neurology was reported in 1982 by Aaslid and colleagues, mainly to detect and monitor vasospasm after subarachnoid hemorrhage⁵¹. Since then, its use has spread in the monitoring of various brain injuries such as acute ischemic stroke or traumatic brain injury (TBI)^{52,53}. TCD has also been extensively studied in the setting of clinical brain death⁵⁴.

The advantages of TCD are low cost, easy availability, virtually no complications, and the possibility of frequent repeated examinations and continuous monitoring. It has limited ability to detect distal branches of intracranial vessels and being a “blind procedure” its accuracy relies on the knowledge and experience of the explorer.

Ultrasound examination of a vessel is referred to as insonation. The TCD probe is placed over different “acoustic windows” that are specific areas of skull where there is no bone or the cranial bone is thin. The *transtemporal* window is the most commonly used to insonate anterior, middle and posterior cerebral arteries. It should be noted that 8-10% of the population does not have an adequate acoustic window⁵⁵. The other ultrasonic windows are *transorbital* for the carotid siphon, *suboccipital* for the basilar and vertebral arteries, and *submandibular* for the more distal portions of the extracranial internal carotid artery.

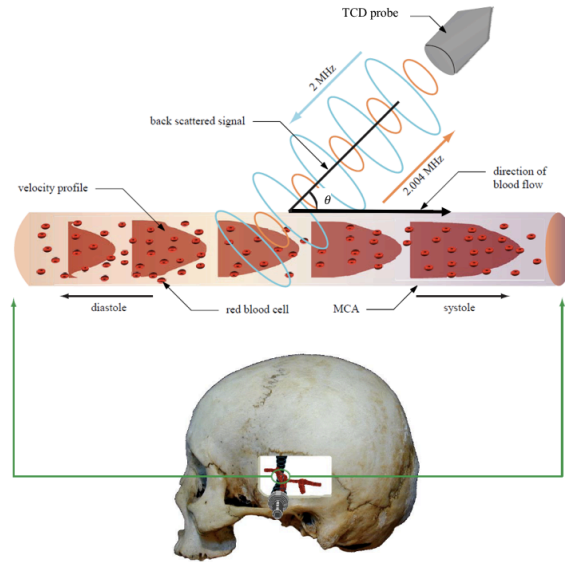
Principle of transcranial Doppler

TCD does not allow direct visualization of insonated vessels (as with “duplex” devices), rather it is an indirect evaluation based on the physical principle described in 1842 by Christian Doppler⁵⁶.

As it can be seen in **figure 1-7**, TCD uses low frequency focused pulsed wave probes to insonate the major cerebral vessels. This TCD probe emits an ultrasonic beam with a known low frequency of 2 MHz, referred to as f_0 and propagation speed c towards the moving target, in this case RBCs. This ultrasonic beam is produced from piezo-electric crystals that have been stimulated electrically and crosses the skull at the “acoustic windows”. This beam bounces off the moving erythrocytes (the echo perceived) within the insonated artery at an altered frequency, f_e , which is dependent on the velocity of the RBCs. The difference between the reflected and the transmitted sound frequencies is called the “Doppler shift” or “Doppler effect” (f_d), and this enables the detection of tissue motion and blood flow velocities.

$$f_d = f_e - f_0$$

Figure 1-7. TCD employs a 2-MHz ultrasound probe because skull bone attenuates about 90% of the waves and attenuation is lower for the low frequencies. This signal is reflected from the moving RBCs of the middle cerebral artery (MCA) with a positive or negative frequency shift (Doppler shift). The faster the erythrocytes are moving, the higher Doppler shift. *Modified and reproduced with permission from the Brain Physics Lab, University Neurosurgery Unit, Addenbrooke's Hospital, Cambridge, UK.*



The complex signals resulting from the reflections of moving RBC are received by the transducer and converted to an electric signal that is processed with the use of spectral analysis into individual velocities by a method called Fast Fourier Transform (FFT) to obtain a waveform that allows accurate determination of blood flow velocities and direction of flow. The flow velocity of the RBC is calculated as

$$FV = \frac{c \times f_d}{2 \times f_0}$$

But as the FV determined by TCD is dependent on the cosine of the angle of insonation, then

$$FV = \frac{c \times f_d}{2 \times f_0 \times \cos \theta}$$

where θ is the angle between the direction of the ultrasonic beam and the direction of the CBF (**figure 1-7**). Hence, at 0° the TCD-calculated and the “real” velocity are equal (as cosine of $0^\circ = 1$). But the anatomic limitations related to the insonation of the transtemporal window (most commonly used to insonate anterior, middle and posterior cerebral arteries) only allow signal captures at narrow angles ($<30^\circ$) minimizing the error to $<15\%$ ⁵⁷.

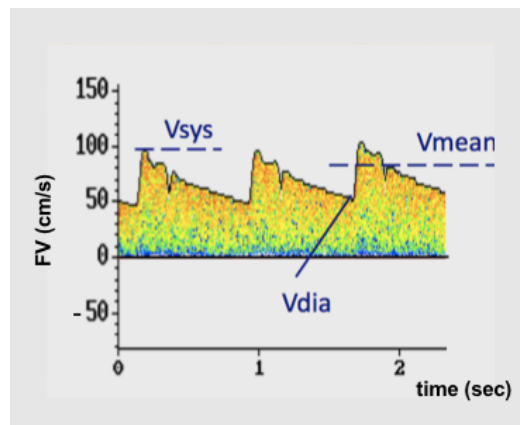
As TCD measures RBC velocity and not flow, changes in flow velocity (FV) only represent true changes in CBF when both the angle of insonation and the diameter of the vessel insonated

remain constant. There is controversial evidence about changes in the diameter of the middle cerebral artery (MCA) with changes in ABP, PaCO₂, or the use of anesthetic or vasoactive agents^{58,59}. Provided these limitations are recognized, this technique can be utilized as a surrogate marker of CBF.

Practical applications of transcranial Doppler

The TCD system displays information as a velocity-time waveform. The peak systolic (FVs) and the end-diastolic (FVd) blood flow velocities are measured from the waveform display (**figure 1-8**). Classically it's been considered that FVd reflects the degree of downstream vascular resistance, whereas FVs depends on upstream determinants such as CO, ABP and carotid blood flow. The flow velocity waveform is determined by the ABP waveform, the viscoelastic properties of the elastic bed, and blood rheology.

Figure 1-8. Pulsed wave TCD spectrum (or sonogram) for three cardiac cycles from the middle cerebral artery (MCA). V_{sys} = systolic blood flow velocity; V_{dia} = diastolic blood flow velocity; V_{mean} = mean blood flow velocity. *Modified and reproduced with permission from the Brain Physics Lab, University Neurosurgery Unit, Addenbrooke's Hospital, Cambridge, UK.*



Main information from the TCD is derived from the following calculated parameters:

- Mean flow velocity (FVm) calculated as follows:

$$FVm = \frac{FVs + (FVd \times 2)}{3}$$

The range of normal values for adults was determined by Aaslid *et al.*⁵¹. The different arteries can be identified according to the insonated acoustic window, the transducer position, depth, direction of blood flow, their Doppler spectra (velocities) and their response to carotid compression⁶⁰.

- Waveform pulsatility

Classically it has been stated that the pulsatility of the FV waveform reflects the distal CVR in the absence of vessel stenosis, vasospasm, arterial hypotension, or profound anemia⁶⁰. Different indices have been defined as descriptors of this physical property.

1.1.3.1 Pulsatility index definition

The Gosling pulsatility index (PI) describes changes in the morphology of the flow velocity (FV) waveform. Defined in 1974, it is a relationship between the difference of systolic flow velocity (FVs) and diastolic flow velocity (FVd) divided by mean flow velocity (FVm)⁶¹. It is the most frequently used TCD parameter to theoretically determine the flow resistance. Normal PI ranges from 0.6 to 1.1 with no significant side-to-side or cerebral interarterial differences in healthy conditions. A PI higher than 1.2 is being classically assumed to represent high resistance to CBF.

$$PI = \frac{FVs - FVd}{FVm}$$

Spectral analysis of the TCD flow velocity signal allows the calculation of the first Fourier pulsatility index (also called 'spectral' PI, sPI) which substitutes the peak-to-peak numerator by the first harmonic from the spectral analysis⁶². According to Aaslid, this resulting index is more reliable than Gosling PI as *f1* is not influenced by artifacts⁶³.

$$sPI = \frac{f1}{FVm}$$

The Pourcelot resistance index (RI) is another TCD parameter and it is assumed to represent flow resistance distal to the site of insonation⁶⁴. Values below 0.75 are considered normal.

$$RI = \frac{FVs - FVd}{FVs}$$

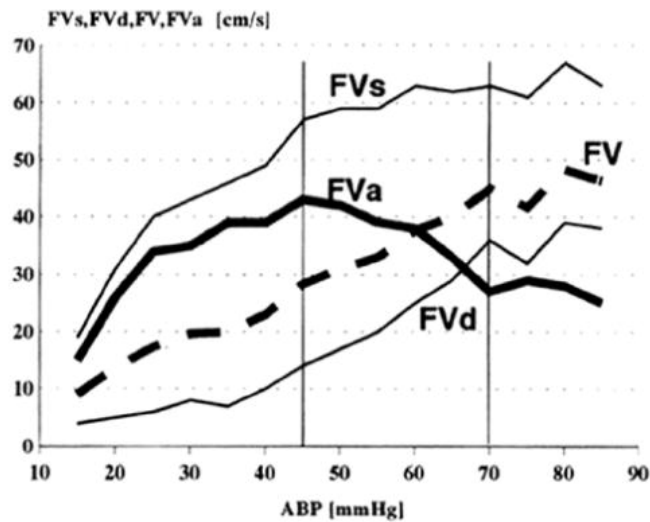
All three indices are theoretically independent of the angle of insonation and have no units. Studies have shown a strong correlation between the Gosling PI and the Pourcelot RI for all arteries⁶² and many authors consider that the three values provide an equal amount of information.

As PI reflects both extrinsic resistance (such as during increased ICP) and intrinsic resistance (such as during hyperventilation), the inherent change in vascular tone with age or diabetes may also influence PI value⁶⁵. Large pulse pressure amplitude is quite common in older patients as their blood vessels become stiff and lose their compliance.

Indeed, the CBF velocity is a dynamic measurement reflecting the instantaneous driving pressure (i.e. systolic and diastolic ABP). With lowering ABP, FVs and FVd react differently, as it has been seen both experimentally⁶⁶ and in the clinical setting (see figure 1-9), so

according to the PI formula, a low diastolic ABP should inevitably result in a high PI value (e.g. a patient with significant aortic insufficiency will have a high PI value).

Figure 1-9. Experimental study in rabbits during haemorrhage-induced hypotension showing how TCD diastolic blood flow velocity (FVd) starts to fall sooner than systolic FV (FVs). The progressive increasing divergence between FVs and FVd increases the amplitude of pulsations (FVa) and, in consequence would increase the PI. *Reproduced with permission from the Brain Physics Lab, University Neurosurgery Unit, Addenbrooke's Hospital, Cambridge, UK.*



1.1.3.2 Clinical applications of pulsatility index

For the last three decades many authors have investigated the usefulness of PI in the *assessment of distal CVR*, and many experimental and clinical studies in different settings have supported this interpretation attributing greater PI to higher CVR⁶⁷. However, PI does not describe CVR under all circumstances⁶⁸ and conclusions regarding its accuracy and reliability remain controversial as far as clinical decisions are concerned^{69,70}. As an example, the role of PI in subarachnoid haemorrhage is discussed by some authors as it seems to correlate better with outcome than with TCD-diagnosed vasospasm⁷¹.

Reports on the usefulness of TCD-PI *to assess ICP and CPP noninvasively* in different groups of patients are mixed^{72,73}, but overall its value is very limited⁷⁴. However, extreme values of PI can be used in support of a decision for invasive ICP monitoring and recent studies consider PI a valuable in-hospital screening tool to identify and follow up patients at risk for second neurologic deterioration⁷⁵.

Related to this, the increase in TCD-PI when CPP falls cannot be interpreted as a phenomenon able to indicate the lower limit of autoregulation because PI always goes up when lowering CPP, no matter the patient autoregulation status⁷⁶. However, it has demonstrated to be a useful indicator of cerebral hemodynamic asymmetry and an indicator of low CPP⁷⁷.

1.2 Intracranial Pressure

The human brain (parenchymal brain tissue) weighs about 1400 grams and occupies the majority of the intracranial compartment (83%). Cerebrospinal fluid (CSF) and cerebral blood volume (mainly its venous content) occupy approximately 11% and 6% of intracranial volume, respectively^{6,78}. Most of the intracranial blood volume (about 200 mL) is contained in the venous sinuses and pial veins, which constitute the capacitance vessels of the cerebral circulation.

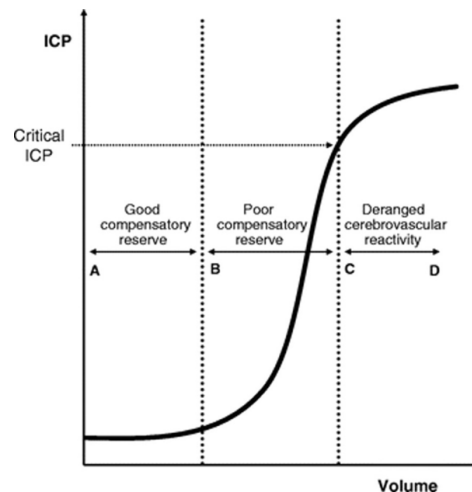
ICP is the force that these three elements exert inside the rigid cranial vault. According to the *Monro-Kellie doctrine* the sum of the volume of blood, CSF and brain parenchyma must remain constant within the fixed dimensions of the rigid non-expandable skull. In other words, the total volume of the intracranial compartment must remain constant if ICP is to remain constant^{79,80}.

ICP is a complex variable, consisting of four components modulated by different physiological mechanisms: (1) inflow and volume of arterial blood, (2) venous blood outflow, (3) CSF circulation, and (4) brain parenchymal (swelling) or mass lesions. The importance of ICP is not always associated with its absolute value, but with monitoring of its dynamics in time and with identifying which of these mentioned components are responsible for the observed pattern of intracranial hypertension. This is essential, as every component that elevates ICP requires different countermeasures (like short-term hyperventilation to control 1; head elevation to control 2; extraventricular drainage (EVD) to control 3; osmotherapy or neurosurgery to control component 4)⁸¹.

CSF plays a major role assuring favourable mechanical conditions for the central nervous system. Although there is not enough volume of CSF to have the brain 'floating' in this fluid, the fact of having a continuous fluid environment equilibrates all gradients of the ICP within the central nervous system (according to Pascal's law) with no risks for volume shifts or herniations under normal conditions⁶. Also, both formation and drainage of CSF are related to CSF pressure according to the Davson equation⁸². Therefore, when circulation of CSF is normal, CSF adopts a very important compensatory role with lumbar subarachnoid space acting as a reservoir⁸³.

The *cerebrospinal pressure-volume curve* is nonlinear and expresses the compensatory reserve^{84,85}. Three parts of the ICP-volume curve can be described (**figure 1-9**). The curve is flat at lower intracranial volumes, meaning ICP remains low and stable despite changes in intracranial volume. This is due to good compensatory mechanisms as the venous blood and CSF pools are considered to have the highest compliances of all compartments and are the first to be affected by raising ICP. However, when these compensatory reserves are reduced or exhausted, the curve rapidly turns exponentially upwards. This part of the curve represents a phase of low compensatory reserve, where ICP increases considerably, even with relatively small increases in intracranial volume. At the end, at high levels of ICP, the curve flattens again, and ICP approximates to the mean arterial blood pressure (ABP). A further increase in ICP leads to a collapse of the cerebral arterial bed⁶.

Figure 1-9. Cerebrospinal pressure-volume curve. Dashed lines marked as B and C determine the three parts of the curve described in the text. *Reproduced with permission from the Brain Physics Lab, University Neurosurgery Unit, Addenbrooke's Hospital, Cambridge, UK.*



Intracranial *compliance* is a concept that is directly related to the pressure-volume interaction, and it is defined as the change in volume (dV) due to a given change in pressure (dP). The inverse of the compliance is called *elastance* (dP/dV), also known as the volume-pressure response, and it can be described quantitatively by the pressure volume index (PVI), which is the volume required to raise ICP tenfold⁸⁶. Compliance decreases with increasing ICP, while elastance increases with rising ICP.

Cerebrospinal compliance is a quite complex parameter because is the sum of the CSF space compliance (associated to CSF buffering capacity), arterial bed compliance and venous compliance. After exhaustion of all CSF buffering capacity (150-170 mL), venous blood volume (around 70 mL) is the next buffer, while arterial compliance is controlled by active modification of arterial wall smooth muscles.

Normal ICP in the horizontal position tends to range between 5 and 15 mmHg, although simple coughing or sneezing can transiently elevate ICP to a pressure of 50 mmHg⁸⁷. The limit of ‘abnormal pressure’ depends on pathology, but in head injury current data support 20-25 mmHg as an upper threshold above which treatment is required for intracranial hypertension⁸⁸.

Different methods of monitoring ICP have been described. The “gold standard” technique to measure ICP is a catheter inserted into the lateral ventricle (usually via a small right frontal burr hole) and connected to a closed external drainage system with an attached pressure transducer. The reference point for the external pressure transducer is the foramen of Monro, which in practice is equated to the external auditory meatus.

The reason for them to be considered the gold standard is related to previously mentioned *Pascal's principle* (or the principle of transmission of fluid-pressure), a principle in fluid

mechanics that states that “a pressure change occurring anywhere in a confined incompressible fluid (as CSF in this case) is transmitted throughout the fluid such that the same change occurs everywhere”⁸⁹. In other words, when CSF circulation is normal (an essential requirement) the values of ICP will be the same in the whole closed system⁹⁰.

The advantages of external ventricular drainages are its low cost, the possibility of repetitive recalibrations, the administration of intrathecal medications (e.g. urokinase-type plasminogen activator tissue to clear intraventricular blood clots) and that it serves as a treatment modality to allow drainage of CSF, which aids in lowering the ICP.

Disadvantages are related to the fact of being the most invasive of all the ICP monitoring options. Difficulties with insertion (e.g. in patients with brain swelling and small ventricles) increase the risk for track hematomas resulting in further brain damage. Also intraventricular catheters have infection rates (2-27%) directly related to the duration of catheterization (more than 5 days) and the frequency of EVD manipulation (EVD sampling)⁹¹.

The most common alternative would be *intraparenchymal probes* consisting of a thin cable with an electronic or fiberoptic transducer at the tip. These monitors are inserted directly in the right or left prefrontal area (via a small hole drilled in the frontal skull) and have very low complication rates (infection rates or risk of major bleeding below 2%) but a small drift of the zero reference may occur due to inability to recalibrate over time. Also measurements are going to be influenced by the presence of intraparenchymal gradients⁹².

As a substitute for the intraparenchymal probes, *subdural and epidural* probes can be used, but the accuracy of these devices is lower limiting its use to coagulopathic patients due to its lower risk for intracranial haemorrhage⁹³.

Despite eventual complications that might raise from invasive monitoring (infections, brain tissue lesions and haemorrhage), direct methods still remain the only option if indicated⁸⁸. When direct ICP measurement is contraindicated or not available, a reliable non-invasive method would have a major impact in clinical practice, at least in the early stages of treatment, when it could act as a screening tool.

Investigations have been made in order to achieve a reliable (both in number and pattern) *non-invasive ICP monitor* (nICP) and many different methods have been described (tympanic membrane displacement, optic nerve sheath diameter, different TCD methods, ABP pulse, ABP-FV transmission, evoked potentials ...). Unfortunately, at this moment, all of them either have a significant lack of accuracy (about +/- 15 mmHg) or have one of these 3 problems: do not measure the absolute value of ICP, have calibration problems or cannot monitor nICP continuously⁹⁴.

ICP monitoring has become a standard of care after severe traumatic brain injury (TBI); however, we do not yet have any class 1 evidence that ICP or more extensive haemodynamic monitoring improves patient outcome⁹⁵. The 2016 4th Edition of the Brain Trauma Foundation clinical practice guidelines for adults recommend, with a level of evidence IIB, that severe TBI patients susceptible for treatment (Glasgow Coma Scale after resuscitation ≤ 8 and abnormal scan) should be managed according to continuous invasively ICP monitoring⁸⁸. It is remarkable that ICP monitoring itself contributes little to outcome without proper interpretation and

secondary analysis of the observed signal. Instead, a positive outcome depends on how the data from the monitor are used and whether an effective treatment exists.

Related to this subject, a controversial study by Chesnut et al demonstrated that there was no difference in primary outcome in TBI patients who received ICP monitoring⁹⁶. However, while this trial has internal validity, it has not been externally validated and did not test whether treatment of ICP per se makes a difference, but rather compared two management protocols (patients with or without ICP monitoring)⁹⁶.

Anyway, many cohorts studies that included a large number of patients have demonstrated that an ICP value above 20 mmHg (or over 22 mmHg according to the last edition of the Brain Trauma Foundation [BTF] guidelines for severe TBI) is independently associated with a higher risk of death and disability⁹⁷.

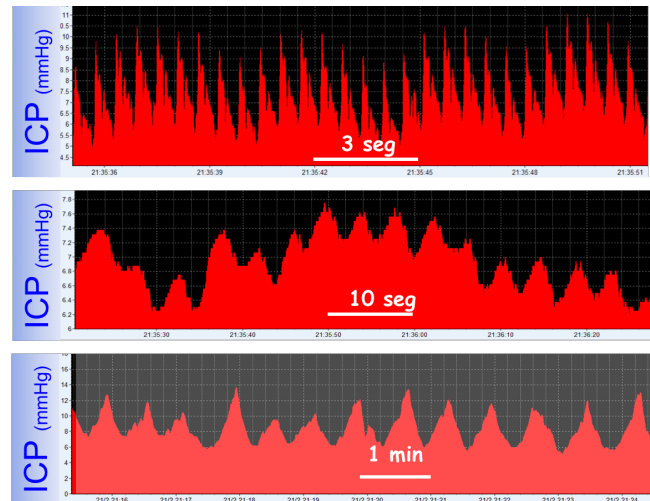
We cannot forget that monitoring must be continuous when possible because punctual measurements (for example manually end-hour values recorded by a nurse) may induce severe errors⁹⁸. Also, evaluating only the trends of the mean value of ICP (mICP) alone leaves a lot of information besides⁹⁹. As an example, reduced ICP variability may be a better outcome predictor than mean ICP¹⁰⁰.

Waveform analysis of intracranial pressure

ICP is not a static value as it exhibits cyclic variation based on the superimposed effects of cardiac contraction, respiration and intracranial compliance. That explains why ICP waveforms include a complex sum of three distinct quasiperiodic components: heart rate pulse, respiratory waves, and slow vasogenic waves. Although these components overlap on a background of randomly changing mean ICP, they can be isolated and quantified using spectral analysis¹⁰¹.

By definition, a frequency spectrum is a graph showing the intensity of individual phasic components plotted against their specific frequency. In the case of ICP waveform, the area under the curve can be used to quantify the magnitude of each specific component at their characteristic range (that is, heart rate 50-180 bpm, respiratory waves 8-20 cycles/min, and slow waves 0.3-3 cycles/min). However, if the recording is long enough they can be identified in a time-trend recording (**Figure 1-10**).

Figure 1-10. Intracranial pressure waveform recording: *Top panel* = pulse pressure waves; *middle panel* = respiratory waves; *Lower panel* = slow vasogenic B waves. *Modified and reproduced with permission from the Brain Physics Lab, University Neurosurgery Unit, Addenbrooke's Hospital, Cambridge, UK.*



- Pulse pressure waveform

When spectral analysis in frequency domain is performed, the pulse waveform has a fundamental frequency (also called first harmonic) equivalent to the heart rate, and several harmonic components. The amplitude of the ICP fundamental component (so called i_1) is useful for the evaluation of various indices describing cerebrospinal dynamics.

However, time-domain analysis is a good alternative as the amplitude of the fundamental component (i_1) and peak-to-peak amplitude of ICP pulsation (AMP) during one heartbeat have an excellent linear relationship, so both methods seem to be equivalent.

When ICP is recorded continuously we can identify the shape of the pressure pulse (**Figure 1-10**). Pulsatile CSF flow can be observed in the aqueduct cerebri and in the cervical region of the subarachnoid space⁸³ and is undoubtedly associated with this pulse wave of CSF pressure, as it is related to the pulsatile arterial blood inflow and venous outflow.

Pulse waveform is almost always present in recordings of ICP and includes information about cerebral blood stroke volume. This ICP beat-to-beat waveform consists of three relatively constant components analogous to the components of the arterial pulse wave that reflect various aspects of the cerebral vascular bed (see **figure 1-11**).

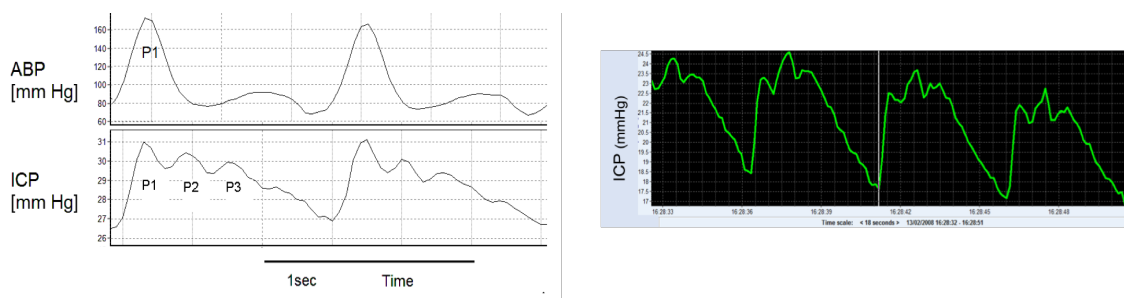
The first peak (P1) is the *percussion wave*, and is derived from arterial pulsations of the large intracranial vessels (due to arterial pressure being transmitted from the choroid plexus to the ventricle). It has a sharp peak and is fairly constant in amplitude.

The second wave (P2), also known as the *tidal wave*, is derived from brain elasticity, is much more variable in shape and amplitude, and ends on the dicrotic notch.

The relation between P1 and P2 provides us information on cerebrospinal compliance and pulse amplitude of ICP is positively related to pulse amplitude of blood flow velocity. The origin of the *dicrotic wave* (P3, not always seen) keeps being a subject of disputes, but it is believed to correlate with the arterial dicrotic notch (closure of the aortic valve), and usually tapers down to ICP diastolic position¹⁰².

Under normal conditions of low ICP, the three peaks relate to each other as $P1 > P2 > P3$. But when brain compliance decreases and ICP starts to rise the ICP pulse waveform modifies with an increase in amplitude followed by an inversion of the P2/P1 ratio that eventually becomes greater than 1.0 (so $P1 < P2 > P3$). Therefore, continuous monitoring of ICP and observation of pulse waveform at bed side helps to understand the individual relationship between volume and pressure for each patient.

Figure 1-11. Component peaks of the ICP waveform. Left: P1 = percussion wave; P2 = tidal wave; P3 = dicrotic wave. Right: inversion of the P2/P1 ratio. *Modified and reproduced with permission from the Brain Physics Lab, University Neurosurgery Unit, Addenbrooke's Hospital, Cambridge, UK.*



- Respiratory waves

These waves are almost always present in ICP recordings and are related to the frequency of the respiratory cycle (usually 8-20 cycles per minute in patients on mechanical ventilation, **figure 1-10**). The pressure signal is complex as both arterial and venous factors contribute to their shape.

- Slow waves

All components that have a spectral representation within the frequency limits of 0.05 to 0.0055 Hz (20 seconds-3 minutes) can be classified as slow waves¹⁰¹. They occur due to fluctuations of CBF that lead to changes in intracranial blood volume and hence in ICP. The origin and reason for the presence of these slow vasogenic repetitive waves is still under debate (a response to ABP variations, a cyclic demand of brain metabolites...). Healthy subjects can have small amplitude (≤ 3 mmHg) slow waves, and complete absence of slow waves is a bad predictor in head-injured patients. On the other hand, reduced intracranial compliance must be suspected if amplitude increases above 8 mmHg.

Although slow waves are not as precisely defined as in the original Swedish neurosurgeon Nils Lundberg's thesis¹⁰³, his descriptions had a significant impact in our understanding about ICP:

- Lundberg A waves, also known as '*plateau waves*', are pathological slow vasogenic waves that lead to increases in ICP up to 50-100 mm Hg, lasting from minutes to hours. Their particular aspects will be extensively discussed in the following section as they are a main subject of this thesis¹⁰⁴.
- B waves have lower amplitudes (< 50 mmHg) and have a repetitive character (frequency of 0.5-2 per minute). They are thought to be related to cerebral vasocycling secondary to multiple mechanisms of CBF control working together.
- C waves occur at a rate of 4-8 min⁻¹ with limited duration and amplitude, and have been documented in healthy individuals. Therefore, they are probably of little pathological significance⁶.

1.3 Critical Closing Pressure

Cerebral perfusion pressure is described as the difference between ABP and ICP if we assume that ICP represents the effective downstream pressure of the cerebral circulation. However, it has been shown that the real downstream pressure of the cerebral circulation is often higher than ICP, and this pressure has been called cerebral critical closing pressure (CCP).

This CCP or zero-flow pressure is the level of ABP at which small cerebral vessels collapse and CBF is interrupted¹⁰⁵. Its value is always greater than ICP, and it was first introduced and described by Burton in 1951 with a theoretical model suggesting that the difference between CCP and ICP is explained by the tone of the small cerebral vessels, so-called wall tension (WT). WT is related to cerebrovascular resistance. Therefore CCP for cerebrovascular circulation would be calculated as follows^{105,106}:

$$CCP = ICP + WT$$

An accurate calculation of CCP is important for different reasons. First, it helps to understand cerebral hemodynamic physiology. Second, it discloses the real value at which brain circulation would stop, helping to take clinical decisions regarding management of ABP, ICP and vascular tone (i.e. a low ICP may be linked to a high WT, and therefore CCP could be a sign of alarm). And third, because CCP value is used in several dynamic cerebral autoregulation models¹⁰⁷.

However, traditional methods for estimating CCP from TCD assume linearity between ABP and CBF and underestimate CCP values. Also, these classic methods occasionally render negative values with no clear physiological interpretation¹⁰⁸ and mean a clear methodological limitation^{107,109}.

Some of these methods included TCD-ABP pulse-waveform-based methods, as the one proposed by Michel¹⁰⁹ that stated that

$$CCP = ABP - A1 \frac{FV}{F1}$$

where A1 and F1 are the pulse amplitudes of the fundamental harmonics of ABP and FV waveforms, obtained from the fast Fourier transform (FFT).

Aiming to overcome these drawbacks, Varsos et al recently described a multiparameter impedance-based mathematical model for an reliable calculation of CCP¹¹⁰.

Resistance is a concept used for direct current, whereas impedance is the alternating current equivalent. In Varsos model, impedance is used instead of resistance, based on the pulsatile characteristics of the cerebral circulation. A simplified electrical model of the cerebrovascular bed was described with arterial compliance (Ca) and resistance (Ra or CVR) set in parallel, such that the impedance to flow is considered as a function of heart rate. The introduction of parameters describing the cerebral circulation aids in the understanding of factors influencing the dynamics of CCP. The CCP values obtained with this method are physiologically understandable and more meaningful¹¹⁰.

$$CCP = ABP - \frac{CPP}{\sqrt{(Ra \times Ca \times HR \times 2\pi)^2 + 1}}$$

where CPP = ABP - ICP, Ca is the pulsatile compliance of the cerebral arterial bed, Ra is cerebrovascular resistance, and HR denotes heart rate (beat/second). Although Ca and Ra cannot be measured directly, they can be estimated using TCD blood FV and ABP and CPP waveforms according to a complex mathematical algorithm^{111,112}.

This new multiparameter model takes into account the cerebrovascular time constant (also called TAU) of the cerebral circulation. This is a concept derived from the electrical circuits, and it is calculated as the product of cerebrovascular compliance (Ca) and resistance (Ra). Theoretically, TAU reflects the time it takes for the arterial blood load during the cardiac cycle to get through the arterial component of the cerebral circulation¹¹³.

Taking into account all these physiological parameters, this modelling approach allows a better understanding of how CCP and WT react to physiological maneuvers and its translation to the clinical setting. As this methodology disallows negative values, it improves the physiological interpretation of CCP.

According to what is being presented previously, vascular wall tension can be calculated as the difference between CCP and ICP:

$$WT = CCP - ICP$$

The concept of CCP stresses the idea of the “closing margin” (CM), calculated as the difference between mean ABP and CCP, which is referred by some authors as the “effective CPP” and the real driving pressure as it includes the contribution of the wall tension¹¹⁴ (which is not considered in calculation of ‘normal’ CPP).

$$CM = ABP - CCP$$

Providing all these facts, having the chance to determine the CCP for a neurocritical patient would provide an important threshold for that patient's ABP below which irreversible brain ischemia could be developed. In fact, it has been demonstrated that diastolic ABP lower than CCP is associated with loss of measurable blood FV during diastole when TCD is used¹¹⁵.

2 TRAUMATIC BRAIN INJURY

2.1 *Definition and epidemiology*

Traumatic brain injury (TBI) keeps being a major universal health problem that affects 10 million people a year worldwide and remains the leading cause of death and disability among children and adults under 45 years of age¹¹⁶. It is defined as an insult or trauma to the brain caused by external mechanical forces, whereas head injury is a more generic term referring to injuries affecting not only the brain but also other structures of the head¹¹⁷.

The number of publications related to this topic has increased exponentially in the last 10 years reflecting the increasing importance of TBI and its profound socioeconomic consequences. Simple estimates of mortality would seriously underestimate its impact therefore any useful risk prediction model needs to provide estimates of poor neurological outcome other than mortality. This has major importance because, despite public prevention policies, global trends for TBI are predicted to increase¹¹⁸.

The epidemiology of TBI in high-income countries has been changing, with the effects of improvements in road safety being offset by increases in fall-related injuries in an ageing population^{116,119}. According to the Center for Disease Control and Prevention (CDC), in the United States the three leading causes of TBI are falls (28%), motor vehicle crashes (20%) and being hit by or colliding with an object (19%)¹²⁰.

Unfortunately, there is no national registry of head injuries in Spain, but a recent epidemiological study has reported a TBI annual incidence rate of 472.6 per million (period analysed: 2000-2009). Over the last decade, the incidence of this type of injury has fallen significantly when related to the injury traffic crashes. However, TBI incidence among people aged 65 and over injured in non-traffic-related circumstances has risen dramatically¹²¹.

Care of patients with TBI has evolved with improvements in pre-hospital medicine, neuroimaging, and access to multidisciplinary expertise through the development of specialist neurotrauma centers or functional units, together with advances in our understanding of the underlying pathophysiology.

In spite of all these improvements in the last 25 years, including the periodic Brain Trauma Foundation (BTF) publication of their consensus evidence-based international guidelines for treatment of TBI, neither mortality nor morbidity have diminished as much as it could be expected¹²². There are still many unanswered questions regarding the physiopathological phenomena underlying each individual patient.

2.2 *Clinical assessment and classification: the Glasgow Coma Scale*

The Glasgow Coma Scale (GCS) score is the best known and widely accepted scale used in the triage of patients early after TBI to indicate its severity and evaluate any subsequent improvement or deterioration. GCS score was introduced in 1974 in order to have a formal

scheme to overcome ambiguities and aid in the clinical assessment of post-traumatic unconsciousness¹²³.

Since then, it has gained worldwide acceptance as an easily performed and reproducible tool and remains a key measure in neurological assessment after head injury. The GCS score has three components: eye (E), verbal (V) and motor (M) responses to external stimuli and the best or highest responses of each component are recorded¹²⁴.

THE GLASGOW COMA SCALE

Eyes	Open	Spontaneously	4
		To verbal command	3
		To pain	2
		No response	1
Best motor response	To verbal command	Obeys	6
		Localizes pain	5
	To painful stimulus	Flexion - withdrawal	4
		Flexion - decorticate	3
		Extension - decerebrate	2
		No response	1
Best verbal response		Oriented, converses	5
		Disoriented, converses	4
		Inappropriate words	3
		Incomprehensible sounds	2
		No response	1
Total			3-15

In most studies, classification of the severity of the trauma is still based on the admission post-resuscitation GCS, as mild (GCS 15), moderate (GCS 9-14) or severe (GCS ≤ 8). As well as providing a quantitative documentation of the level of consciousness, GCS has been demonstrated to have a powerful predictive value for survival and final outcome in both traumatic and non-traumatic coma^{125,126}. The motor score seems to have a higher accuracy compared with the whole GCS score¹²⁷, but other variables such as age, abnormal motor responses, CT findings, pupillary abnormalities, and episodes of hypoxia and hypotension, have been subsequently introduced to build more complex and accurate prognostic models^{128,129}. Poor autoregulation and loss of pressure-reactivity are also independent predictors of fatal outcome following head injury^{97,130}.

However, GCS does have many limitations. The scale excludes assessment of many important neurological functions, requires serial observations to be effective and is limited to the best response in one limb. It cannot therefore identify asymmetry and has poor diagnostic value. In addition, combining the three components (E/V/M) into a single total score can lead to disparities in assessment of true conscious level. Finally, a complete GCS cannot be obtained in TBI patients with eyelid swelling, sedated and intubated or who are aphasic due to a dominant hemisphere lesion.

That explains why numerous scoring scales have been proposed and validated as an alternative to GCS score, but few of them have gained widespread acceptance¹²⁴. The Full Outline of UnResponsiveness (FOUR) score is one of them as it circumvents many of the limitations of the GCS and has shown an excellent inter-rater agreement¹³¹. It replaces the verbal score of the GCS by assessments of pupil reactions and respiratory pattern, making it more appropriate for patients with fluctuating levels of consciousness and/or intubated.

2.3 *Physiological changes after a traumatic brain injury*

TBI is an evolving process that extends beyond the initial insult. The *primary injury* is the mechanical damage that occurs at the time of the injury and results in shearing of neurons, glia and blood vessels. It includes skull fractures, cerebral contusions and the diffuse axonal injury (DAI) due to white matter shearing injury. Primary injuries are untreatable and only preventable with safety precautions.

However, the extent of brain damage is determined also by the subsequent *secondary (or delayed) brain injury*. It is a sequela of the initial trauma that occurs over time (from minutes to even years after the injury) due to the activation of different biochemical and molecular reactions at the tissue and cellular level, and it may be initiated (or enhanced) by episodes of cerebral hypoperfusion, arterial hypotension, hypoxemia, and flow–metabolism uncoupling. Early medical/surgical interventions may ameliorate these deleterious effects to limit the damages.

Disruption of the cerebral vasculature also participates in this pathogenesis in the form of hypoperfusion, ischemia, hypoxia, haemorrhage, chronic inflammation, blood-brain barrier (BBB) disruption and oedema.

Cerebral edema, the excess accumulation of fluid within the brain, accounts for 50% of deaths in severe TBI¹³². After TBI, cerebral edema forms at the lesion and incorporates into the surrounding tissue. Classification of oedema may be quite complex, but it may be simplified to cytotoxic (occurring immediately after injury) and vasogenic.

Cytotoxic oedema results in water accumulation in cells, is caused by dysregulation of the sodium and potassium pumps in the cell membrane and the BBB remains intact¹³³.

Vasogenic edema results in water accumulation in the extracellular space and is caused by a disruption of the BBB¹³³. It associates with elevated ICP, tissue swelling, changes in blood flow and compression of brain structures.

Any increase in ICP may reduce CPP, reduce CBF and cause ischaemia. Ischaemia can cause a further rise in ICP due to increased cerebral edema and further reduce CPP. This mechanism may develop into a vicious positive-feedback loop, causing irreversible brain damage.

Therefore, ICP is both an important surrogate marker of injured brain and a potential cause for secondary insults.

2.3.1 *Intracranial hypertension*

Acutely raised ICP or intracranial hypertension is a final pathophysiological feature common to many neurocritical conditions including 40 to 60% of severe head injuries, and is a major factor in 50% of all fatalities¹³⁴. Besides, it is an important cause of secondary lesion as it impairs CBF, electrical activity and metabolism. Poor outcome after TBI is associated with sustained high ICP¹³⁵ or low oxygenation⁹⁷.

Sudden increases in ICP decrease CPP, but it may be somewhat compensated by an active cerebral vasodilation to maintain CBF due to cerebral autoregulation. However, recent studies indicate that the CBF response to a sustained decrease in CPP caused by a decrease in ABP or an increase in ICP has key physiological differences. A major one is related to the LLA, as it will be lower when the cause is intracranial hypertension instead of a low ABP^{136,137}.

In addition, the haemodynamic response to increased ICP is complicated by the presence of the 'Cushing response' (a triad of arterial hypertension, changes in heart rate, and breathing abnormalities) that suggests involvement of vital centers within the brain stem¹³⁸. Although its physiological relevance to cerebral haemodynamics remains unclear¹³⁹, a recent experimental study with an animal model of acute intracranial hypertension brought interesting conclusions¹⁴⁰.

First, it seems that the brain has two intrinsic mechanisms to protect itself from hypoperfusion during intracranial hypertension: with moderate increases in ICP (from baseline to 40 mmHg), global CBF (assessed with TCD mean FV) may be maintained mainly by a decrease in vascular WT until maximum vasodilation (autoregulatory response) and some increase in ABP; however, with further intracranial hypertension (ICP ~ 70 mmHg) CPP would be protected by a vigorous Cushing vasopressor response reflected by reductions in HR and increases in ABP. Having ABP above the CCP maintains the 'closing margin' and keeps cerebral vessels open.

Second, regional differences in the control of cerebral perfusion seem to exist with cortical blood flow (measured with LDF) decreasing almost linearly with increasing ICP, whereas global CBF (assessed with TCD FVm) seemed to be well maintained until ICP values > 60 mmHg. These findings reflected topographic differences in regional and global CVR consistent with differential autoregulatory control of cortical and global CBF due to a suspected intrinsic differential vascular reactivity between cortical and non-cortical brain. Different clinical monitoring studies support these differential autoregulatory capacity of the cortical compared to non-cortical areas¹⁴¹⁻¹⁴³.

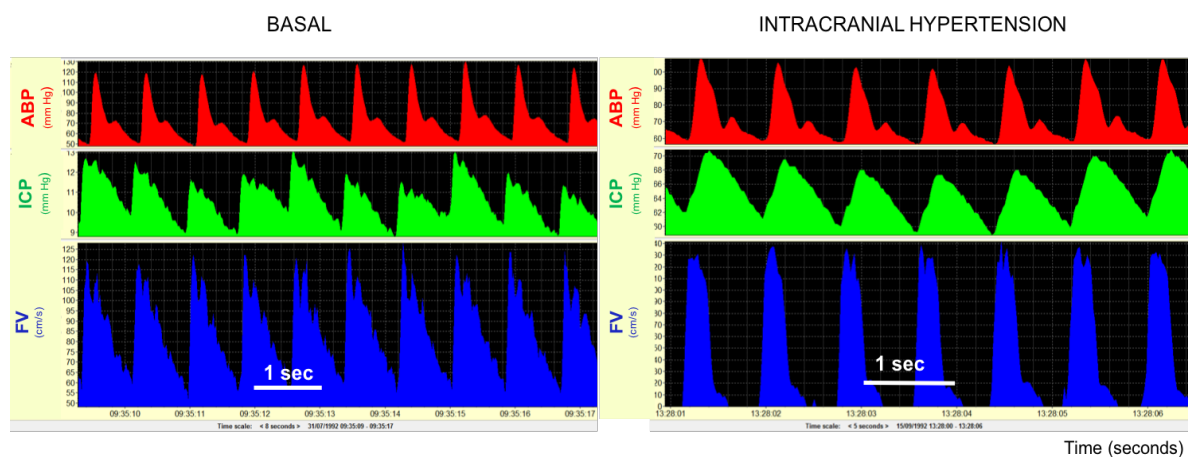
As a last issue, changes in the relationship between ICP pulsatility and mean ICP can be observed. With intracranial hypertension pulse amplitude of ICP (AMP) increased with increasing mean ICP until very high levels of mean ICP were achieved, at which point AMP decreases with increasing mean ICP^{85,144}. This upper breakpoint associates with a low diastolic TCD measured flow velocity and low diastolic closing margin (**figure 2-1**).

TCD derived values have been suggested as a potential non-invasive assessment of ICP and CPP to avoid the inherent risk of invasive ICP monitoring. Different approaches have been employed because, as a general concept, as ICP increases and CPP decreases, TCD flow velocities fall. This fall preferentially affects diastolic values initially, and that explains the decrease of the FVm and progressive increase in PI and RI values.

Although different formulas have been proposed for the prediction of absolute CPP and ICP, results have proved disappointing (with large 95% confidence intervals for predictors), so values are still unacceptable for clinical purposes^{145,146}.

However, different studies have concluded that altered TCD measurements (PI >1.25 and FVd <25 cm/s) upon admission to the emergency departments are associated with early neurological worsening after mild to moderate TBI. According to this TCD may be useful for in-hospital triage to may provide additional information about neurological outcome⁷⁵.

Figure 2-1. ICM+[®] software recordings in the same patient showing the distinctive changes in both the shapes and values (please see the scales) in both ICP and TCD-FV pulsatile components with intracranial hypertension. *Left: basal; Right: intracranial hypertension, where TCD shows a low FVd, a peaked waveform, and higher PI values (if calculated). Modified and reproduced with permission from the Brain Physics Lab, University Neurosurgery Unit, Addenbrooke's Hospital, Cambridge, UK.*



Decompressive craniectomy (DC) is a surgical technique used, among other indications, for patients with TBI with the goal of relieving refractory intracranial hypertension and/or to prevent or reverse cerebral herniation. At the moment significant controversies exist regarding optimal candidate selection, timing of the procedures, technique and neurological outcomes^{147,148}.

The pathophysiology of pressure-flow and cerebral haemodynamic consequences of DC have been reviewed in the last decade, and a study by Timofeev et al justifies the expected sustained reduction of ICP with an improvement in the cerebrospinal compliance due to an enhancement of the pressure-volume relationship. However, intraparenchymal ICP measurements and dynamics are more complicated in the setting of an open cranial vault as similar ICP values may relate to different pressure-volume relationships post-craniectomy.

CBF, brain tissue oxygenation and metabolic effects of DC were recently reported by Lazaridis and Czosnyka¹⁴⁹. Different studies included in their review supported similar TCD findings post-DC with a trend to a bilateral increase in blood FV, being more pronounced ipsilaterally to the site of surgery. Concurrently, PIs on both sides seem to decrease significantly. In addition, studies showing significant augmentation of PbtO₂ and microdialysis-related parameters post-DC are also reported.

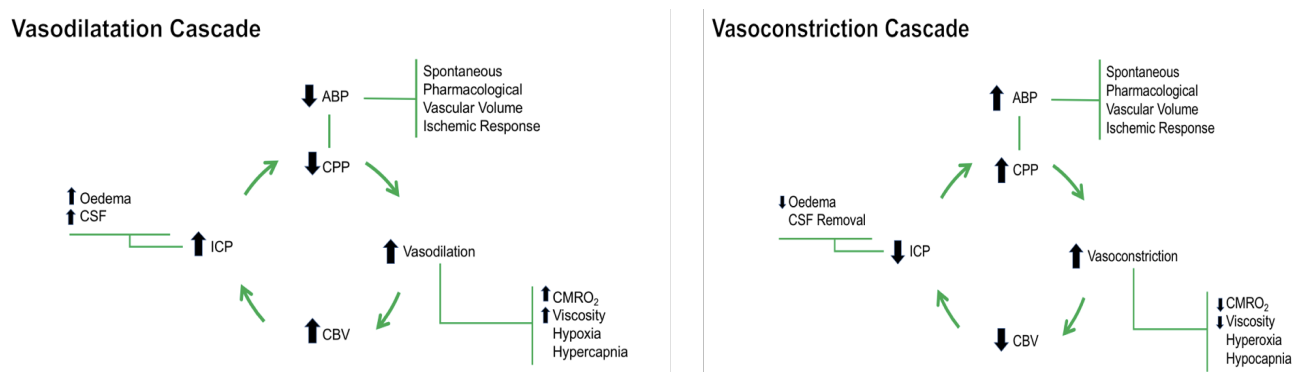
2.3.2 Plateau waves (A waves of Lundberg)

“Sudden rises in intracranial pressure” were first described by Guillaume and Janny in 1951¹⁵⁰, but the term “plateau waves” or “A waves” was introduced by Lundberg in 1960¹⁰³. A plateau wave is classically defined as a sudden substantial elevation of ICP of a magnitude of 20-60 mmHg, above 50 mmHg depending on baseline ICP, that lasts longer than 5 minutes and terminates either spontaneously or in response to treatment (e.g. hyperventilation to induce hypocapnia)^{104,151}. Nowadays, however, duration of plateau waves should not be a strict criterion as elevations of ICP are actively treated in neurocritical patients.

Plateau waves are thought to be caused by a vasodilatory cascade causing a rapidly increasing cerebral blood volume (CBV), which may be triggered by a vasodilatory stimulation, such small oscillations of ABP, brain oxygenation or PaCO₂ levels, in the presence of functioning cerebral autoregulation^{103,152}. The increase in ICP results in a decrease in CPP, leading to further vasodilation (at a second stage after the initial stimulation) in order to compensate for the decreased CPP, resulting in further rise of CBV and further increase in ICP (**figure 2-2, left**). This mechanism would also explain the increment in ICP pulse amplitude¹⁵³.

The reverse of this cycle may arise spontaneously or due to medical management with a vasoconstrictive stimulus that decreases CBV (e.g. hyperventilation aiming hypocapnia for vasoconstriction), and restores normal ICP and CPP¹⁰⁴ (**see figure 2-2, right**).

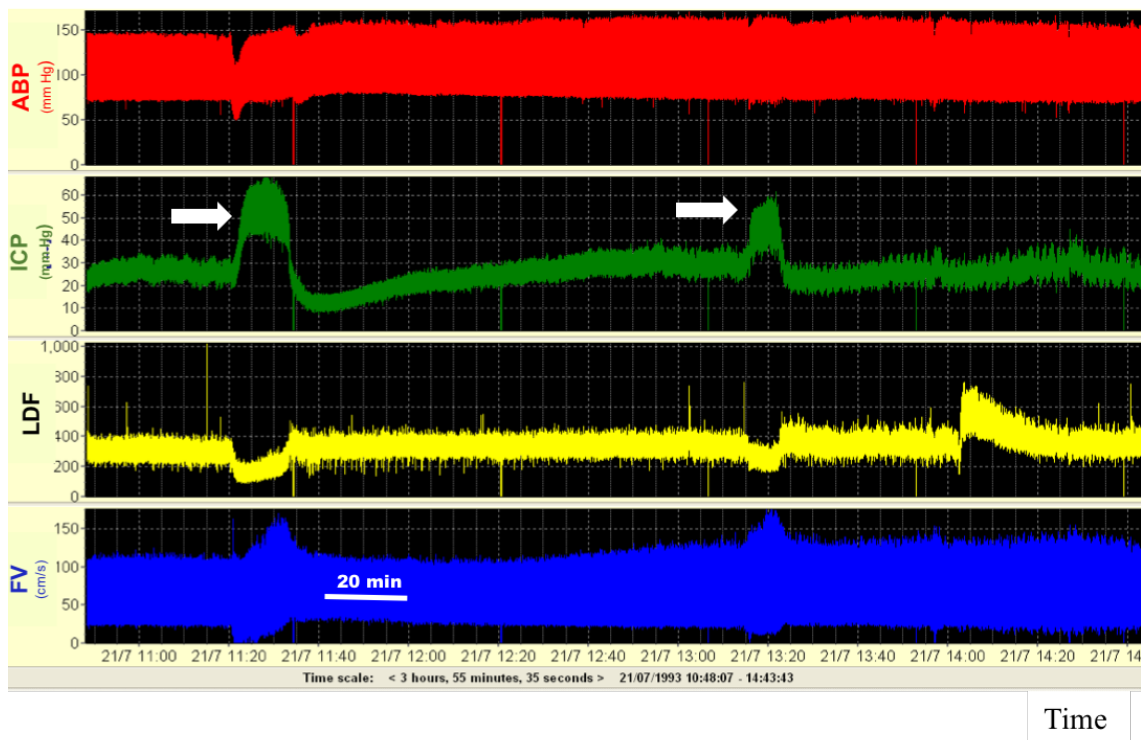
Figure 2-2. Pathophysiology underlying the formation and termination of plateau waves of ICP. Reproduced with permission from the Brain Physics Lab, University Neurosurgery Unit, Addenbrooke’s Hospital, Cambridge, UK.



During plateau waves the profound reduction in CPP is accompanied by a significant decrease in CBF, CVR and brain tissue oxygenation^{28,154}, and the whole cascade lasts until the maximum vasodilation is reached. Recent studies that included autoregulation changes analysis with different secondary indices support this classical model, showing how autoregulation is intact before the onset of the plateau wave but it is disrupted during the crest of the wave^{153,155}.

A transient reactive post-plateau hyperemic response (a significant increase in CBF and brain oxygenation above baseline) may occur as a response to the referred period of brain tissue hypoperfusion and hypoxia¹⁵⁵. The magnitude of this hyperemia seems to be associated with a better autoregulation status and low oxygenation levels at baseline¹⁵³.

Figure 2-3. ICM+[®] software recording of two plateau waves of intracranial pressure (white arrows). ABP arterial blood pressure; ICP intracranial cerebral pressure; LDF laser Doppler flowmetry. FV flow velocity measured with TCD. Note the widening of the FV peak-to-peak amplitude, but mean FV decreases. *Modified and reproduced with permission from the Brain Physics Lab, University Neurosurgery Unit, Addenbrooke's Hospital, Cambridge, UK.*



Plateau waves affect approximately 40% of TBI patients¹⁰⁴, but might also occur in various cerebral pathological conditions with working cerebrovascular reactivity and exhausted cerebrospinal compensatory reserve such as spontaneous subarachnoid haemorrhage^{156,157}, intracerebral haemorrhage¹⁵⁸, brain tumors¹⁵⁹, acute hydrocephalus¹⁵⁸, craniostyostosis¹⁶⁰ and benign intracranial hypertension¹⁵⁸. As soon as these phenomena are identified, the end of the vasodilatory cascade of a plateau wave should be pursued with active treatment because long duration of more than 30 minutes seem to be related to an unfavourable outcome¹⁰⁴. Duration of plateau waves seems to be related to basal autoregulation status, so that the better the autoregulation the longer the duration of plateau waves¹⁵³.

Plateau waves are not a benign phenomena and, at the LLA, there is a risk of zero flow due to the collapse of brain vessels¹¹⁰. This is particularly relevant in the situations of intracranial hypertension with increased LLA.

3 ICM+[®] SOFTWARE FOR MULTIMODAL BRAIN MONITORING

3.1 *Multimodal neuromonitoring*

The last 25 years have meant the entrance in the era of clinical neuromonitoring which is routinely performed in all TBI patients who receive neurocritical care^{161,162}. The combined use of monitors, including the neurological examination, laboratory analysis, imaging studies, and physiological parameters, is common in a platform called multimodality monitoring (MMM). MMM is defined as the simultaneous collection of data from multiple diverse sources associated with a single patient coupled with the ability to view the data in an integrated and time synchronized manner¹⁶².

Twenty to 25 years ago, clinical practice guidelines would only consider invasive ICP monitoring through an EVD (gold standard) or an intraparenchymal probe in a patient with a severe head injury¹⁶³. However, in the last 2 decades we've achieved the possibility to measure parameters related to global or regional cerebral oxygenation both invasively (jugular bulb oxygen saturation) or non-invasively through NIRS techniques¹⁶⁴. Measurement of oxygen saturation in the jugular bulb (SjO₂) provides a means of indirectly assessing the brain ability to extract and metabolize oxygen. Technology allowed us to have dispositives to obtain local oxygenation measurements (brain tissue oxygen pressure – pbtO₂) through the Neurotrend[®] microcatheter or the Licox[®] catheter (polarographic technique with a Clark electrode)¹⁶⁵. Cerebral microdialysis meant a further step as it allowed us to analyze the trends in time of different metabolites in the cerebral cellular interstitium as glucose, glutamate, glycerol or the lactate-to-pyruvate molar ratio and its relation to the brain injury^{166,167}.

All this MMM (ABP, ICP, TCD, NIRS, Licox[®] etc) provide a large volume of data whose analysis can give us a lot of information if well interpreted. But the processing and analysis of these biological signals requires complex informatic systems ("multi-channel digital trend recorders") to present them in a comprehensible way for the treating medical staff so that evolution in time of the different pathophysiological changes can be recognized.

The fast evolution of bioinformatics in critical care has allowed integration of multiple monitors in order to acquire, store, retrieve, and display integrated data in a user-friendly format¹⁶⁸. Besides, including analytic techniques for optimal clinical decision making has also facilitated translational research. As these tools offers the possibility to perform online real-time analysis of the interdependence between the dynamic behaviours of different biological signals, different phenomena of interest may be detected and interpreted (otherwise impossible without computer bedside data analysis)¹⁰¹. Several devices that can integrate these neurocritical care monitoring data are available, with ICM+[®] software being probably the most extended one at this moment.

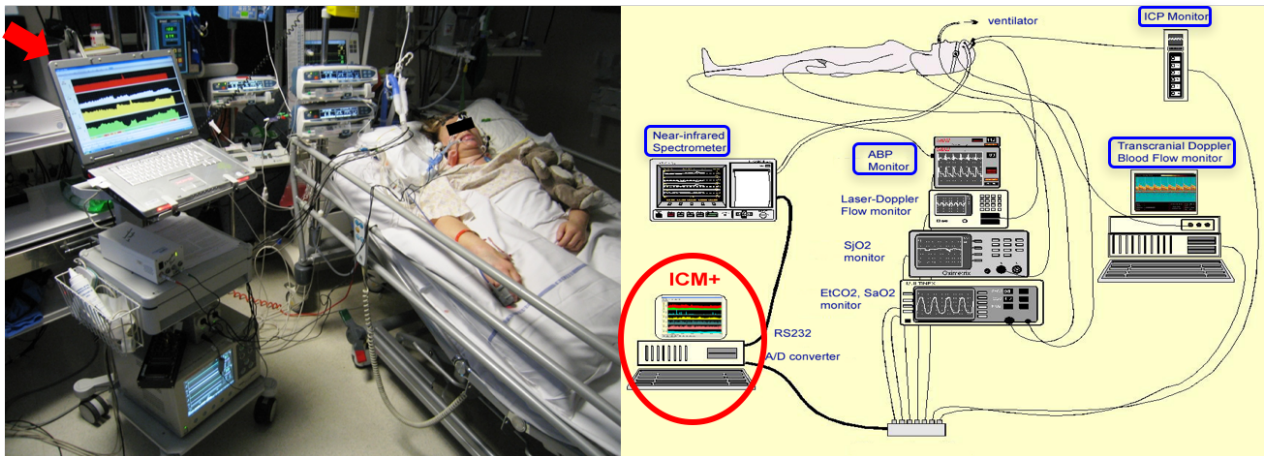
3.2 The ICM+[®] software

The ICM+[®] software (www.neurosurg.cam.ac.uk/icmplus), developed in the Academic Neurosurgery Unit of the Addenbrooke's hospital in Cambridge, United Kingdom, was introduced in clinical practice in the 1990s and is now extended as a clinical and research multimodal neuromonitoring system in neurointensive care in over 120 centres around the world¹⁶⁹.

Its impact has been notorious with an actual integrated database of more than 1000 TBI patients distributed across all ICM+[®] users research centers and over 300 ICM+[®] based publications on PubMed. These facts have led to very important multicenter collaborative data collection projects such as BrainIT¹⁷⁰, CENTER-TBI¹⁷¹ and different optimal CPP projects led by the ICM+[®] core users group^{172,173}.

ICM+[®] is not just a multimodal bedside data collection platform; in fact, data collection is only the prerequisite for its main function which is the real-time analysis and presentation of data. Although major technical improvements have been made in the last 5 years, ICM+[®] is based on software for standard IBM compatible personal computers, equipped with analog-to-digital converter (ADC) and RS232 serial interfaces when needed.

Figure 3-1. Left: example of a patient included in these thesis studies with MMM connected to a laptop running ICM+[®] software (red arrow). Right: schematic description of MMM integrated into ICM+[®]. *Modified and reproduced with permission from the Brain Physics Lab, University Neurosurgery Unit, Addenbrooke's Hospital, Cambridge, UK.*



3.2.1 Principles of ICM+[®] software

- Data collection and storage format

Once all monitors of the patient are connected (through analogue or digital inputs) and communicate with the laptop computer with ICM+[®] software, data from these sources

starts to be collected simultaneously, time synchronized (precisely time stamped), and displayed in an integrated fashion. Data are collected at the highest possible sampling frequency (i.e. higher than the duration of the events to be detected) to avoid missing any clinically significant event (see **figure 3-1**). Collection of continuous or near continuous data has the necessity to review and edit the data so that artifacts can be removed (data cleaning) and missing data dealt (e.g., device disconnection for transfers).

These input variables are also analysed and displayed according to predefined ‘calculation profiles’, and the output data is saved in two separate files:

- First file contains the *time trends* of the analysed signals and all results of calculated indices. These processed data are stored in a unique *.icmp* file (with a proprietary format) along with all the clinical descriptors and annotations introduced during the monitoring of the patient.
- Second file contains digitally *raw data* (input signals defined by the user) that are continuously collected and split into many *.dta* files (also proprietary).

Storing both types of files enables building up a library of signals for off-line post-processing, as software can be reconfigured for previously saved data to be viewed and reanalyzed with a different calculation profile.

- Data analysis and interpretation

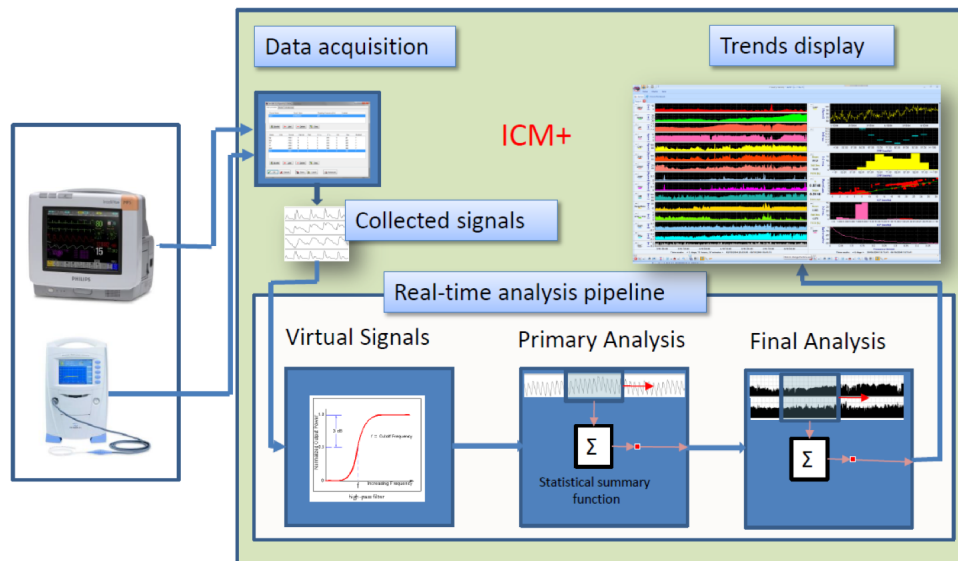
ICM+[®] software uses a wide array of advanced mathematical tools to transform raw data into actionable information by applying different pre-defined calculations profiles (‘data acquisition and analysis configuration profile’). Available functions vary from simple time domain functions such as moving average, to more complex frequency domain computations.

Analyses are broken down into stages, whereby the result (output) of one stage is passed into the next, forming the source data (input) for the next calculation. In the first step ‘Virtual signals’ are selected (the ones providing the raw data) and they form the input to the next stage. Analysis is therefore divided up into a ‘Primary analysis’, one or more ‘Secondary analysis’ (or none), and a ‘Final analysis’. The results and subsequent output are determined by the configuration of the ‘Final Analysis’ only.

So the flow for data occurs as follows (see **figure 3-2**):

Virtual Signals (Input) → Primary Analysis → Secondary Analysis/es → Final Analysis (Output).

Figure 3-2. Analysis pipeline of the ICM+[®] software methodology for data collection and analysis. *Reproduced with permission from the Brain Physics Lab, University Neurosurgery Unit, Addenbrooke's Hospital, Cambridge, UK.*



Besides monitoring of multiple variables describing dynamics of the studied pathology, the software allows both on-line (while monitoring) and offline (retrospective) analysis of the collected data, including calculation of different secondary measures derived from the primary signals (e.g. ABP, ICP or TCD derived FV). The easiest example would be CPP (calculated as ABP minus ICP)⁵, but different indices have been described by using a moving linear correlation coefficient approach applied to the primary analysis results.

On this basis, many secondary indices have been defined along almost 25 years of studies with ICM+[®]. Probably those describing cerebral autoregulation with TCD ('mean velocity index', Mx)²³, cerebrovascular reactivity through correlation of ICP and ABP ('cerebrovascular pressure reactivity index, PRx)¹⁷⁴, and cerebrospinal compensatory reserve (RAP coefficient)¹⁷⁵ have the most relevance and proved to be useful in head injury or subarachnoid haemorrhage (SAH) patients. They can be calculated as a moving correlation coefficient using 10 seconds averages of primary variables over a moving window of 5 minutes in duration. According to the concept of correlation, in a reactive vascular system, these indices are supposed to be close to zero or negative (≤ 0), while positive values close to one signify impaired reactivity.

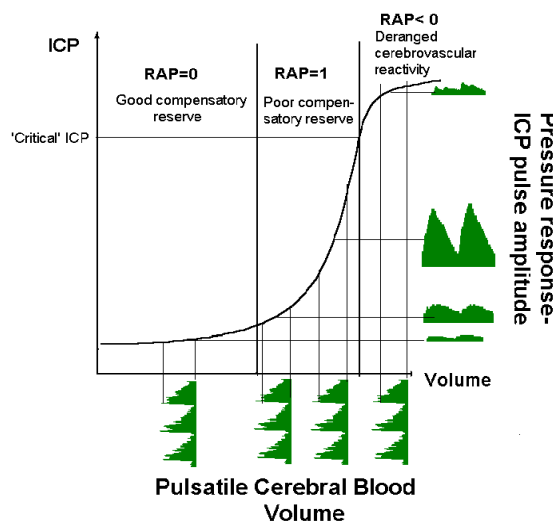
All these secondary indices have been clinically validated and its utility has been demonstrated¹⁶. Recently, a systematic review and meta-analysis has concluded that both PRx and Mx provide a strong prediction of mortality and outcome for patients with TBI¹⁷⁶.

A special mention must be made about the volume-pressure compensatory reserve index (named RAP coefficient), defined as a linear correlation coefficient between the amplitude of ICP wave (AMP) and mean ICP¹⁷⁵. With RAP we can define 3 distinct regions in the pressure-volume curve (**figure 3-3**): first flat indicates a good compensatory reserve with linear

relationship between volume and pressure, so RAP coefficient is close to 0. The second part shows an exponential relationship between volume and ICP, and RAP index is close to 1, indicating a poor compensatory reserve. When the critical level of ICP is achieved and cerebrovascular bed loses its reactivity curve becomes flat again and RAP coefficient becomes negative indicating an exhausted compensatory reserve⁸⁵.

ICM+[®] is extensively used for the analysis of cerebrospinal fluid circulatory and compensatory reserves in hydrocephalic patients. The software includes a pre-defined set up for computerized infusion test with built-in database, and aids decisions about shunting or revisions for shunt failure. Information about the evolution of RAP is very useful for a proper interpretation of these infusion studies for the CSF dynamics analysis¹⁷⁷.

Figure 3-3. Cerebrospinal pressure-volume curve representing the changes in pulse amplitude of ICP and the RAP coefficient (volume-pressure compensatory reserve index). *Reproduced with permission from the Brain Physics Lab, University Neurosurgery Unit, Addenbrooke's Hospital, Cambridge, UK.*

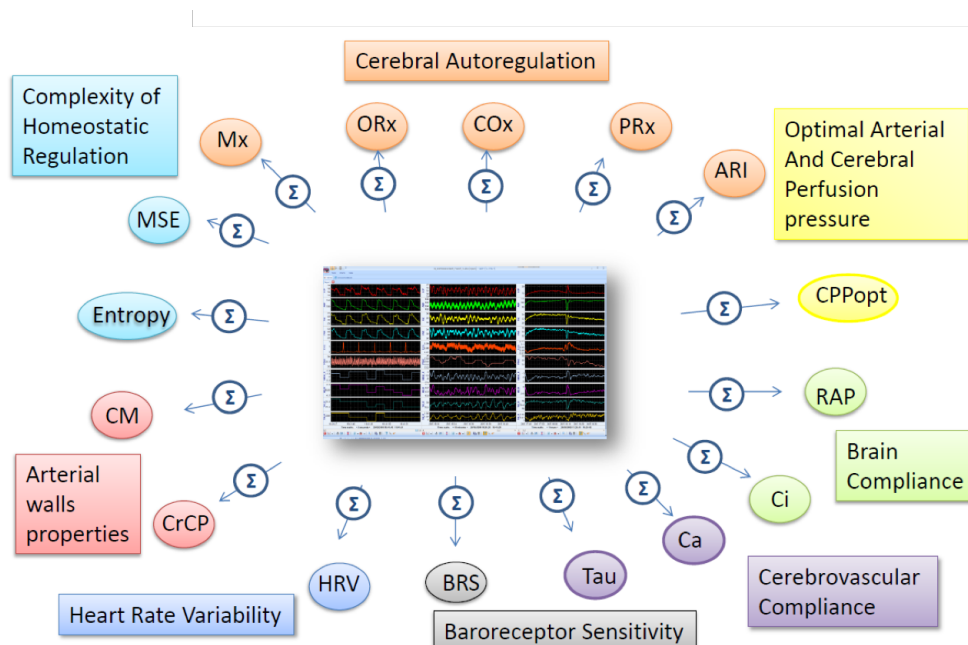


In addition to what has already been explained, the flexibility of ICM+[®] software analysis allows almost unlimited signal analysis and calculation of secondary measures for different fields of research. Some examples include: **(figure 3-4)**.

- Alternative secondary indices related to cerebral autoregulation may be calculated from different CBF surrogate monitors, as NIRS-derived 'cerebral oximetry index' (COx)¹⁷⁸ or pbtO₂ - derived 'oxygen reactivity index' (ORx)¹⁷⁹. Transfer function analysis may be also applied for calculation of the autoregulatory index (ARI)³¹.
- Autoregulation indices are used to identify patient-specific (or optimal) CPP¹⁸⁰ and ICP thresholds that in turn have demonstrated a more robust relationship with outcome than generic population-based thresholds^{173,181,182}.

- Calculating the area under the curve (AUC) above a specific cut point (e.g. ICP > 20 mmHg) provides a measure of pathophysiological “dose” that can be used to track therapy¹⁸¹.
- The ICM+[®] software also includes different analysis tools for various intervention tests like transient hyperaemic response test²², CO₂ reactivity tests¹⁸³, or CSF infusion study¹⁸⁴. Autonomic nervous system can also be monitored through the analysis of the heart rate variability and the baroreflex sensitivity¹⁸⁵.

Figure 3-4. Secondary indices able to be obtained with ICM+[®] software through analysis of the primary multimodal signals. Most of them are described in the previous paragraph. CM closing margin; CPPopt optimal cerebral perfusion pressure; CrCP critical closing pressure; MSE multiscale entropy. *Reproduced with permission from the Brain Physics Lab, University Neurosurgery Unit, Addenbrooke’s Hospital, Cambridge, UK.*



3.2.2 Integrated physiological study of plateau waves

The last 20 years have sent us on a quest to understand more deeply the active processes that may be target for interventions in our patients. The possibility of integrating and analyzing all these signals together means a great improvement to increase our knowledge about the physiopathology underlying the changes that continuously happen in a neurocritical patient. An example would be the study of the plateau waves of intracranial hypertension, also known as A waves, described by the Swedish neurosurgeon Nils Lundberg, back in 1960¹⁰³.

The increase in ICP seen during the plateau wave results in a dramatic decrease in CPP, which is finally below the LLA and therefore causing a decrease in CBF. Prolonged reduced-CBF associated with plateau waves may then provoke a secondary ischemic brain insult, providing they last for a longer period (above 30 minutes); and therefore contribute to a worse outcome after TBI.

Many of these studies were performed by analyzing the changes that on the TCD velocities before, during and after the plateau wave. The characteristics of the cerebral arterial blood flow velocity viewed and analyzed with TCD will bring us additional information about the cerebral haemodynamics.

The most commonly used haemodynamic index is the Gosling pulsatility index (PI), which describes the pulsatility of TCD waveforms⁶¹. For the last three decades many authors have investigated the usefulness of PI in the assessment of distal CVR, non-invasive ICP and CPP in traumatic brain injury (TBI)⁷² and hydrocephalus⁷³. Nevertheless, conclusions regarding its accuracy and reliability remain controversial as far as clinical decisions are concerned^{69,70}. Many experimental and clinical studies have supported the interpretation of PI as a reflection of the distal CVR, attributing greater PI to higher CVR⁶⁷, and this assumption is still accepted nowadays¹⁸⁶.

However, an experimental study in rabbits published by Czosnyka *et al.* had already shown that in physiological conditions hypercapnia decreased both CVR and PI while a reduction in CPP in autoregulating animals caused a decrease in CVR but an increase in PI. These findings suggested a combined change in distal vascular resistance and compliance of the large cerebral arteries⁶⁸.

The proposed vasodilatory mechanism of plateau waves can be examined by estimating critical closing pressure (CCP), which is related to cerebrovascular vasomotor tone represented by wall tension (WT). Past studies under various scenarios¹⁸⁷⁻¹⁸⁹ and physiological stimuli¹⁹⁰ have demonstrated that both changes in ICP and vascular tone cause predictable changes in estimated CCP. Unfortunately, traditional calculation methods for CCP estimation are not very accurate and may produce negative non-physiologic non-interpretable values^{109,191}.

Severe TBI patients MIM with ICM+[®] software permits the early identification of plateau waves, and its off-line analysis allows a better understanding of these intrinsic brain vascular phenomena. This thesis aims to take advantage of this particular pathophysiology to enhance further our knowledge about 1) what factors truly determine TCD pulsatility index; and 2) an accurate and reliable method to calculate critical closing pressure (CCP) and wall tension (WT) changes during plateau waves.

This knowledge may have a positive influence in the management of head injury patients as it would determine a proper interpretation of these often misleading parameters.

Hypothesis and Aims

Based on what has been previously exposed we can present the following working hypothesis:

- In the first study we hypothesized that:
Pulsatility index (PI), calculated from the transcranial Doppler recording of the cerebral blood flow velocity waves and values, is a complex function of various haemodynamic factors and is not solely determined by distal cerebrovascular resistance (CVR). The study compared two groups with opposing changes in CVR (plateau waves vs mild hypocapnic challenge).
- Our second study hypothesis is that:
Calculation of *critical closing pressure (CCP)* and *wall tension (WT)* through a newly defined cerebrovascular impedance model could accurately define the pathophysiological changes during plateau waves of intracranial pressure.

A reliable CCP calculation would allow an accurate estimation of the closing margin (expressed as the difference between arterial blood pressure and CCP) to determine the risk for cerebral circulatory collapse and zero flow.

- In our first study the aims were the following:
 1. To clarify the relationship between TCD pulsatility index (PI), derived from the CBF velocity waveform, and the cerebrovascular resistance (CVR).
 - 1.1 To analyze the behavior of ICP, CPP, PI and CVR during ICP plateau waves.
 - 1.2 To analyze the behavior of ICP, CPP, PI and CVR during transient hyperventilation.
 - 1.3 To compare continuous monitoring recordings of these two opposing physiological conditions where PI increases.
 2. To analyze the relationship between PI and ICP and CPP.
 3. To compare the Gosling PI and the ‘spectral PI’ (calculated in both groups) with a newly described mathematical formula where PI is expressed as a function of cerebrovascular impedance.
 - 3.1 To calculate PI with a newly defined mathematical model
 - 3.2 To correlate TCD-measured PI with PI calculated with the new mathematical model

- In our second study the aims were:
 1. To examine the pathophysiology of the plateau waves applying the concepts of critical closing pressure (CCP) and arterial wall tension (WT).
 2. To calculate critical closing pressure and wall tension with a new multiparametric model based on cerebrovascular impedance.
 3. To compare the modelled CCP (CCPm) and modelled wall tension (WTm) with CCP and WT calculated with a classical method (CCP1 and WT1 respectively).
 4. To evaluate the possible clinical appliance of the calculated CCPm

Subjects and Methods
Results

4.1 Previous preparation of the doctoral candidate

In 2011, I spent a year as an honorary clinical fellow in the Academic Neurosurgery Unit at Addenbrooke's hospital (University of Cambridge, Cambridge, UK).

On his time there he got to develop both clinical work and research:

- *Clinical job*: worked at the Neuroscience Critical Care Unit (NCCU) from January to May 2011. Care of patients included multimodal monitoring and integration with ICM+[®] Software.
- *Research job*: from May 2011 to December 2011 I was involved in the Academic Neurosurgery Unit directed by **Prof. John D. Pickard** and under the supervision of **Prof. Marek Czosnyka**. In that time I developed this project and got involved in another one related to cerebrovascular autoregulation (publication included in the last section, 'Other merits'). Both projects involved clinical monitoring of new admitted patients and analysis of previously recorded data.

This is a reference international group of knowledge related to multimodal monitoring and signal analysis. It is a multidisciplinary team involving neurosurgeons, engineers from different backgrounds and both clinical and research physicians from different specialties (mainly from anaesthetics field, neurointensive care and neurosurgery).

During my time there I got to familiarize with the use of the ICM+[®] software for advanced neurocritical multimodality monitoring and got involved in quite different projects.

Disclosures: ICM+[®] Software is licensed by Cambridge Enterprise, Cambridge, UK. The doctorand declares not to have any conflict of interest. Prof Marek Czosnyka and Dr Piotr Smielewski (both co-authors in the presented publications) have a financial interest in a fraction of the licensing fee.

4.2 Published papers

Description of the design and the results of the studies in each of the two published papers related to the exposed thesis investigation are presented:

PUBLICATION 1

de Riva N, Budohoski KP, Smielewski P, Kasproicz M, Zweifel C, Steiner LA, Reinhard M, Fàbregas N, Pickard JD, Czosnyka M.

Transcranial Doppler Pulsatility Index: What it is and What it Isn't.

Neurocrit Care. 2012 Aug;17(1):58-66.

IF 2016 = 2.752.

-SUMMARY OF THE STUDY-

Background and Purpose: Transcranial Doppler (TCD) pulsatility index (PI) has traditionally been interpreted as a descriptor of distal cerebrovascular resistance (CVR). We sought to evaluate the relationship between PI and CVR in situations where CVR increases (mild hypocapnia) and decreases (plateau waves of intracranial pressure - ICP).

Methods: Recordings from patients with head injury undergoing monitoring of arterial blood pressure (ABP), ICP, cerebral perfusion pressure (CPP) and TCD assessed cerebral blood flow velocities (FV) were analyzed. The Gosling pulsatility index (PI) was compared between baseline and ICP plateau waves (n = 20 patients) or short term (30-60 minutes) hypocapnia (n = 31). In addition, a modeling study was conducted with the 'spectral' PI (calculated using fundamental harmonic of FV) resulting in a theoretical formula expressing the dependence of PI on balance of cerebrovascular impedances.

Results: PI increased significantly ($p < 0.001$) while CVR decreased ($p < 0.001$) during plateau waves. During hypocapnia PI and CVR increased ($p < 0.001$). The modeling formula explained more than 65 % of the variability of Gosling PI and 90% of the variability of the 'spectral' PI ($R=0.81$ and $R=0.95$, respectively).

Conclusion: TCD pulsatility index can be easily and quickly assessed but is usually misinterpreted as a descriptor of CVR. The mathematical model presents a complex relationship between PI and multiple haemodynamic variables.

Transcranial Doppler Pulsatility Index: What it is and What it Isn't

Nicolás de Riva · Karol P. Budohoski · Peter Smielewski ·
 Magdalena Kasprowicz · Christian Zweifel · Luzius A. Steiner ·
 Matthias Reinhard · Neus Fábregas · John D. Pickard ·
 Marek Czosnyka

Published online: 4 February 2012
 © Springer Science+Business Media, LLC 2012

Abstract

Background Transcranial Doppler (TCD) pulsatility index (PI) has traditionally been interpreted as a descriptor of distal cerebrovascular resistance (CVR). We sought to evaluate the relationship between PI and CVR in situations, where CVR increases (mild hypocapnia) and decreases (plateau waves of intracranial pressure—ICP).

Methods Recordings from patients with head-injury undergoing monitoring of arterial blood pressure (ABP), ICP, cerebral perfusion pressure (CPP), and TCD assessed cerebral blood flow velocities (FV) were analyzed. The Gosling pulsatility index (PI) was compared between baseline and ICP plateau waves ($n = 20$ patients) or short term (30–60 min) hypocapnia ($n = 31$). In addition, a modeling study was conducted with the “spectral” PI (calculated using fundamental harmonic of FV) resulting in a theoretical formula expressing the dependence of PI on balance of cerebrovascular impedances.

N. de Riva · K. P. Budohoski · P. Smielewski ·
 M. Kasprowicz · C. Zweifel · L. A. Steiner · M. Reinhard ·
 J. D. Pickard · M. Czosnyka (✉)
 Division of Neurosurgery, Department of Clinical
 Neurosciences, Addenbrooke's Hospital, University
 of Cambridge, Hills Road, Box 167, Cambridge CB2 0QQ, UK
 e-mail: mc141@medschl.cam.ac.uk

Results PI increased significantly ($p < 0.001$) while CVR decreased ($p < 0.001$) during plateau waves. During hypocapnia PI and CVR increased ($p < 0.001$). The modeling formula explained more than 65% of the variability of Gosling PI and 90% of the variability of the “spectral” PI ($R = 0.81$ and $R = 0.95$, respectively).

Conclusion TCD pulsatility index can be easily and quickly assessed but is usually misinterpreted as a descriptor of CVR. The mathematical model presents a complex relationship between PI and multiple haemodynamic variables.

N. de Riva · N. Fábregas
 Department of Anesthesiology, Hospital Clinic,
 Universitat de Barcelona, Barcelona, Spain

M. Kasprowicz
 Institute of Biomedical Engineering and Instrumentation,
 Wrocław University of Technology, Wrocław, Poland

C. Zweifel
 Department of Neurosurgery, University Hospital of Basel,
 Basel, Switzerland

L. A. Steiner
 Department of Anaesthesia, Lausanne University Hospital,
 Lausanne, Switzerland

M. Reinhard
 Department of Neurology, University of Freiburg, Freiburg,
 Germany

M. Czosnyka
 Institute of Electronic Systems, Warsaw University
 of Technology, Warsaw, Poland

Keywords Cerebral hemodynamics · Plateau waves ·
 Transcranial doppler · Traumatic brain injury

Introduction

Transcranial Doppler (TCD) ultrasonography allows repeated, non-invasive investigations of rapid changes in cerebral perfusion. While mean flow velocity (FV) cannot be translated easily into volume blood flow [1] due to the unknown diameter of the insonated vessel, additional information on cerebral haemodynamics may be derived

from the TCD waveform. The most commonly used haemodynamic index is the Gosling pulsatility index [2] (PI), which describes the pulsatility of TCD waveforms. It is calculated as the difference between systolic and diastolic flow velocities divided by the mean velocity $[(FV_{\text{sys}} - FV_{\text{dia}})/FV]$.

For the last three decades many authors have investigated the usefulness of PI in the assessment of distal cerebrovascular resistance (CVR), non-invasive intracranial pressure (ICP) and cerebral perfusion pressure (CPP) in traumatic brain injury (TBI) [3], and hydrocephalus [4]. Conclusions regarding its accuracy and reliability remain controversial as far as clinical decisions are concerned [5, 6]. In subarachnoid hemorrhage (SAH), the role of PI is discussed by some authors as it seems to correlate better with outcome than with TCD-diagnosed cerebral vasospasm [7].

Many experimental and clinical studies have supported the interpretation of PI as a reflection of the distal CVR, attributing greater PI to higher CVR [8], and this assumption is still accepted nowadays [9].

A previous experimental study in rabbits [10] showed that in physiological conditions hypercapnia decreased both CVR and PI while a reduction in CPP in autoregulating animals caused a decrease in CVR but an increase in PI. These findings suggested a combined change in distal vascular resistance and compliance of the large cerebral arteries.

Our hypothesis is that PI is a complex function of various hemodynamic factors and not only of CVR as it is usually interpreted. To clarify the relationship between TCD pulsatility and CVR, we have retrospectively compared clinical data of two different physiological situations where PI increases. The first one is intracranial hypertension, represented by ICP plateau waves, where a major vasodilatory cascade takes place (i.e., CVR decreases) due to a time-dependent positive feedback loop between vasodilation caused by decreasing CPP and increasing ICP [11]. The second group involves patients submitted to a mild hypocapnic challenge, which is known to increase CVR [12] [13]. We also sought to compare measured PI in both groups with a mathematical formula, expressing PI as a function of cerebrovascular impedance.

Subjects and Methods

Patients

From a database of 345 head-injured patients with continuous recordings of ABP, ICP, and TCD (the median age of patients was 29 years [interquartile range (IQR) 20–44], with 75% being male) we have identified all patients where

an ICP plateau wave occurred during the monitored period. This material was partially presented before [14], however not in the context of TCD pulsatility and waveform analysis. Plateau wave data were recorded during daily TCD investigations of cerebral autoregulation [15] performed in head-injured patients, which constituted a part of a standard clinical protocol. Data were retrospectively analyzed as a part of routine clinical audit, with approval of Neurocritical Care Users Committee.

In order to explore the effect of hypocapnia we have used recordings from a previously published study evaluating the effect of moderate hyperventilation on ICP and FV [12]. Data were acquired as part of a research project investigating cerebral physiology and metabolism following TBI, which was approved by the Neurocritical Care Users Committee and the Institutional Research Ethics Committee.

Except for the period of the hypocapnic challenge to assess CO₂ reactivity patients were managed according to an ICP/ CPP oriented protocol which aimed to keep CPP between 60 and 70 mmHg and ICP below 20–25 mmHg [16].

Monitoring and Data Analysis

ABP was monitored invasively from the radial artery using a pressure monitoring kit (Baxter Healthcare CA, USA; Sidcup, UK). ICP was monitored using an intraparenchymal probe (Codman & Shurtleff, MA, USA or Camino Laboratories, CA, USA). FV was monitored from the middle cerebral artery (MCA) with a 2 MHz probe (Multidop T, DWL, Germany) and using the Doppler Box (DWL Compumedics, Germany) or Neuroguard (Medasonic, CA, USA). TCD was performed daily for periods of 10 min to 1 h starting from the day of initiation of invasive monitoring. The decision to discontinue monitoring was made on clinical grounds.

Raw signals were digitized using an analog–digital converter (DT9801, Data Translation, Marlboro, Mass, USA) sampled at a frequency of 50 Hz and recorded using WREC (Warsaw University of Technology) or BioSAn (University of Cambridge, UK) software. ICM+ Software (Cambridge Enterprise, Cambridge, UK, <http://www.neurosurg.cam.ac.uk/icmplus/>) was used for final analysis. All signals were subjected to manual artifact removal. Artifacts consisted of three types: fast bimodal variations more than 20 mmHg from baseline which are related to tracheal suctioning; complete loss of diastolic FV (without signs of increased ICP) or fast, bimodal spikes on TCD due to a poor temporal bone window or incorrect gain settings; absence of the pulse waveform in ABP or ICP which were related to arterial line flushing or transducer malfunction.

The maximal and minimal values of FV from every 2 s period were calculated and treated as the peak-systolic and end-diastolic components, respectively. Second, FV and its peak-systolic and end-diastolic components were averaged over 10 s to give the mean values for FV (FV_m), peak-systolic FV (FV_s), and end-diastolic FV (FV_d). Discrete Fourier transform was used to calculate the fundamental harmonic components for pulse waveforms of ICP, ABP, and FV (denoted as $i1$, $a1$, and $f1$, respectively).

CVR was estimated as 10 s time-averaged CPP divided by the mean FV ($CVR = CPP/FV_m$) [15]. PI was

calculated as the difference between FV peak-to-peak values divided by the mean FV $[(FV_s - FV_d)/FV_m]$. For analyzing TCD pulsatility at a fixed frequency the “spectral” PI was evaluated as $f1/FV_m$.

Finally, a mathematical model of cerebrovascular space, reduced to CVR and cerebral arterial compliance (Ca), was evaluated to express cerebrovascular impedance analytically. From this analysis PI was calculated for a fixed frequency equivalent to heart rate (HR). This relation is defined by the following formula (1) (please see “Appendix” for details of mathematical derivation).

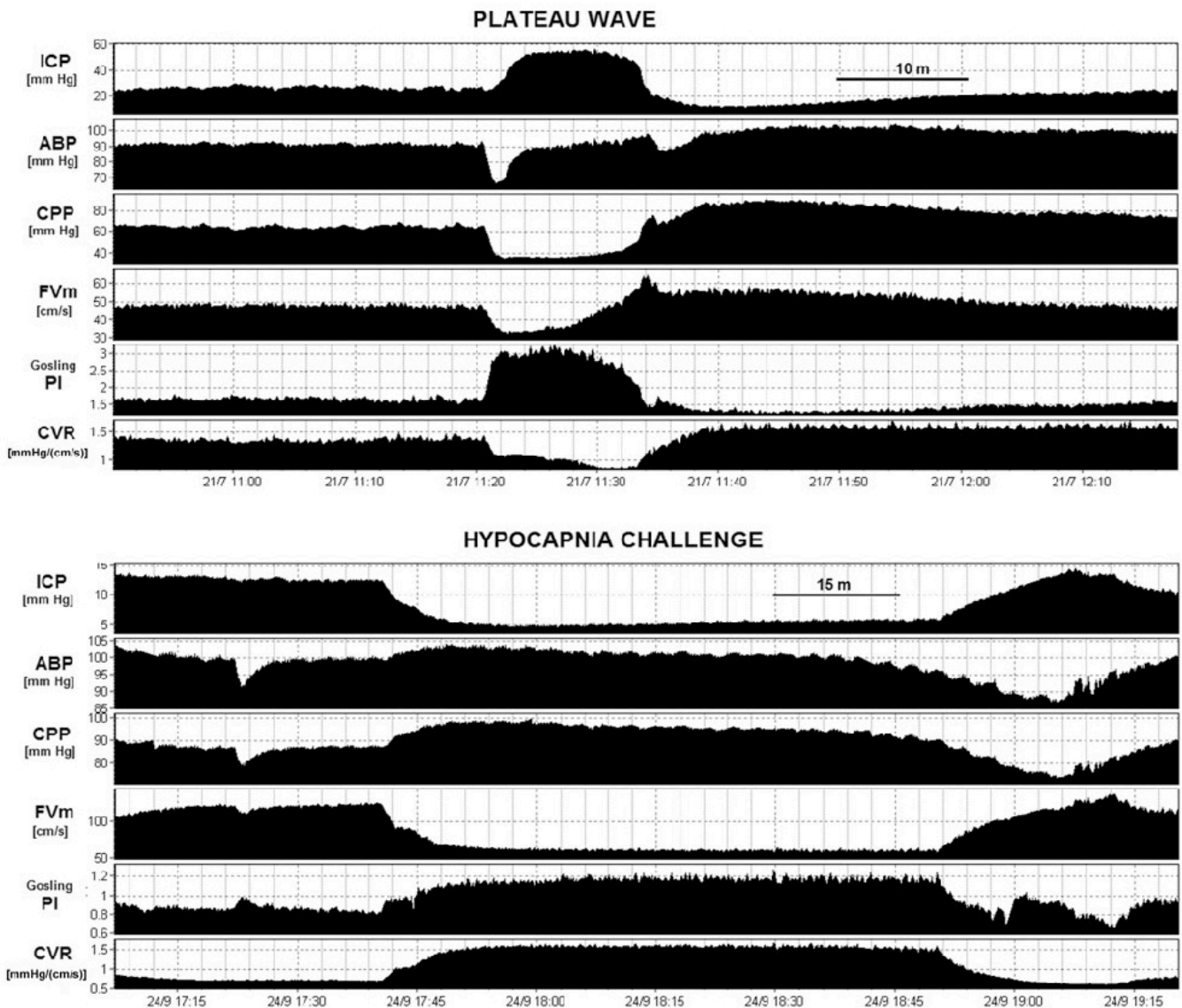


Fig. 1 Timetrends of intracranial pressure (ICP), arterial blood pressure (ABP), cerebral perfusion pressure (CPP), mean cerebral blood flow velocity (FV_m), pulsatility index (PI) and cerebrovascular resistance (CVR) in two different patients with head-injury. *Top panel* plateau wave of ICP. *Bottom* CO_2 vasoreactivity test (hypocapnia).

The figure demonstrates an increase in PI in both situations while CVR decreases during the plateau wave due to the vasodilation but increases during the hypocapnic challenge due to the cerebral vasoconstriction

$$PI = \frac{a1}{CPP} \times \sqrt{(CVR \times Ca \times HR \times 2\pi)^2 + 1} \quad (1)$$

where *a1* is the fundamental harmonic of arterial blood pressure pulse, CPP—mean cerebral perfusion pressure, CVR—cerebrovascular resistance, Ca—cerebral arterial compliance, HR—heart rate.

Statistical Analysis

Changes in ICP, CPP, CVR, and PI between baseline and the observed physiological condition (plateau or hypocapnia) were compared with the paired *t* test. Data are reported as mean ± SD. Calculations were performed using STATISTICA 6.0 (StatSoft, Inc.). *p* < 0.05 was considered significant.

Results

Fifty-one patients were included in the study on plateau waves and hypocapnia. The first cohort included 19 patients (mean age: 24.32 ± 6.02 years, range 17–35 years, five women, 14 men, median admission GCS 5, range 3–12) where 38 events of ICP plateau waves were registered. Studies were carried out 1–10 days after injury (median: day 4). Data obtained from an additional patient who exhibited four plateau waves has been included in the analysis although full demographics were unavailable. Total recording time equaled 30.3 h, with an average of 43.3 min per session (range 16.5–103.5 min).

The second group included 31 patients (mean age: 38 ± 15 years, range 17–70 years, five women, 26 men, median admission GCS: 5, range 3–12). Studies were carried out 1–10 days after injury (median: day 3). Patients were subjected to short term (30–60 min) controlled hyperventilation as part of a standard clinical CO₂ reactivity test.

Examples of time trends of recorded and calculated parameters are presented in Fig. 1.

Changes During Plateau Waves (group 1) and Hypocapnia (group 2)

During the plateau waves the increase in ICP from an average of 24.01 ± 6.91 to 43.53 ± 12.14 mmHg provoked a significant decrease in CPP, FV_m, and FV_d, but an increase in FV_s. The pulse amplitude of ICP and FV (*i1* and *f1*, respectively) increased while the pulse amplitude of ABP (*a1*) did not change (Table 1). During the plateau waves PI increased significantly, whereas CVR decreased (Fig. 2a).

The increase in minute ventilation reduced PaCO₂ from 5.10 ± 0.35 to 4.40 ± 0.34 kPa inducing a small but

Table 1 Mean values of pressure and haemodynamic parameters found in 20 patients before and during plateau waves

Plateau waves (<i>n</i> = 20)			
Parameters	Baseline	Plateau	<i>p</i> value
ICP (mmHg)	24.01 ± 6.91	43.53 ± 12.14 [†]	<0.001
CPP (mmHg)	71.64 ± 10.63	49.37 ± 11.64 [†]	<0.001
FV _m (cm/s)	69.47 ± 29.97	57.94 ± 25.77 [†]	<0.001
<i>i1</i> (mmHg)	2.58 ± 0.85	6.01 ± 2.21 [†]	<0.001
<i>f1</i> (cm/s)	21.90 ± 6.87	25.92 ± 8.55 [†]	<0.001
<i>a1</i> (mmHg)	18.16 ± 3.50	17.31 ± 3.30	NS (0.062)
ABP (mmHg)	95.67 ± 9.15	92.91 ± 9.25*	0.014
HR (cycles/min)	74.26 ± 12.60	73.68 ± 12.26	NS (0.446)
FV _s (cm/s)	127.16 ± 41.05	132.03 ± 43.41	NS (0.055)
FV _d (cm/s)	42.10 ± 21.98	28.92 ± 18.30 [†]	<0.001
PI	1.34 ± 0.38	2.01 ± 0.73 [†]	<0.001
CVR [mmHg/(cm/s)]	1.25 ± 0.61	1.03 ± 0.50 [†]	<0.001

Values are expressed as the mean ± SD. Significant levels of the differences between change in parameters before and during the plateau wave are given (paired *t* test)

a1 pulse amplitude (first harmonic) of ABP, *ABP* arterial blood pressure, *CPP* cerebral perfusion pressure, *CVR* cerebrovascular resistance, *f1* pulse amplitude (first harmonic) of blood FV, *FV_m* mean blood FV in the MCA, *FV_d* diastolic blood FV in the MCA, *FV_s* systolic blood FV in the MCA, *i1* pulse amplitude (first harmonic) of intracranial pressure, *ICP* intracranial pressure, *HR* heart rate, *NS* not significant, *PaCO₂* carbon dioxide arterial partial pressure, *PI* Gosling pulsatility index

* *p* < 0.05; [†]*p* < 0.01

significant decrease in mean ICP (from 16.59 ± 6.68 to 12.73 ± 6.25 mmHg, *p* < 0.001). CPP improved slightly with no significant change in ABP (Table 2). In this group of patients there was a steep decline in all parameters related to FV, however, PI as well as CVR increased significantly (Fig. 2B).

Pulsatility Index and ICP/ CPP

Regression between all points of PI and ICP indicates a correlation coefficient of *R* = 0.7 with linear model 95% prediction margin for ICP of 21 mmHg. Regression between CPP and PI suggests best reciprocal fit, with a correlation coefficient *R* = 0.77 and 95% prediction for CPP around 22 mmHg (Fig. 3).

Pulsatility Index and its Explanation Using the Mathematical Model

Analysis performed combining the results from both groups 1 and 2 showed that the correlation between the calculated

Fig. 2 a The differences in the mean intracranial pressure (ICP), cerebral perfusion pressure (CPP), Gosling pulsatility index (PI), and cerebrovascular resistance (CVR) between baseline and plateau wave of ICP. Data is averaged from recordings of 42 plateau waves encountered in 20 patients. **b** Differences in mean ICP, CPP, Gosling PI, and CVR between baseline and hypocapnic challenge. In all cases, PI significantly increased while CVR decreased in **a** and increased in **b**

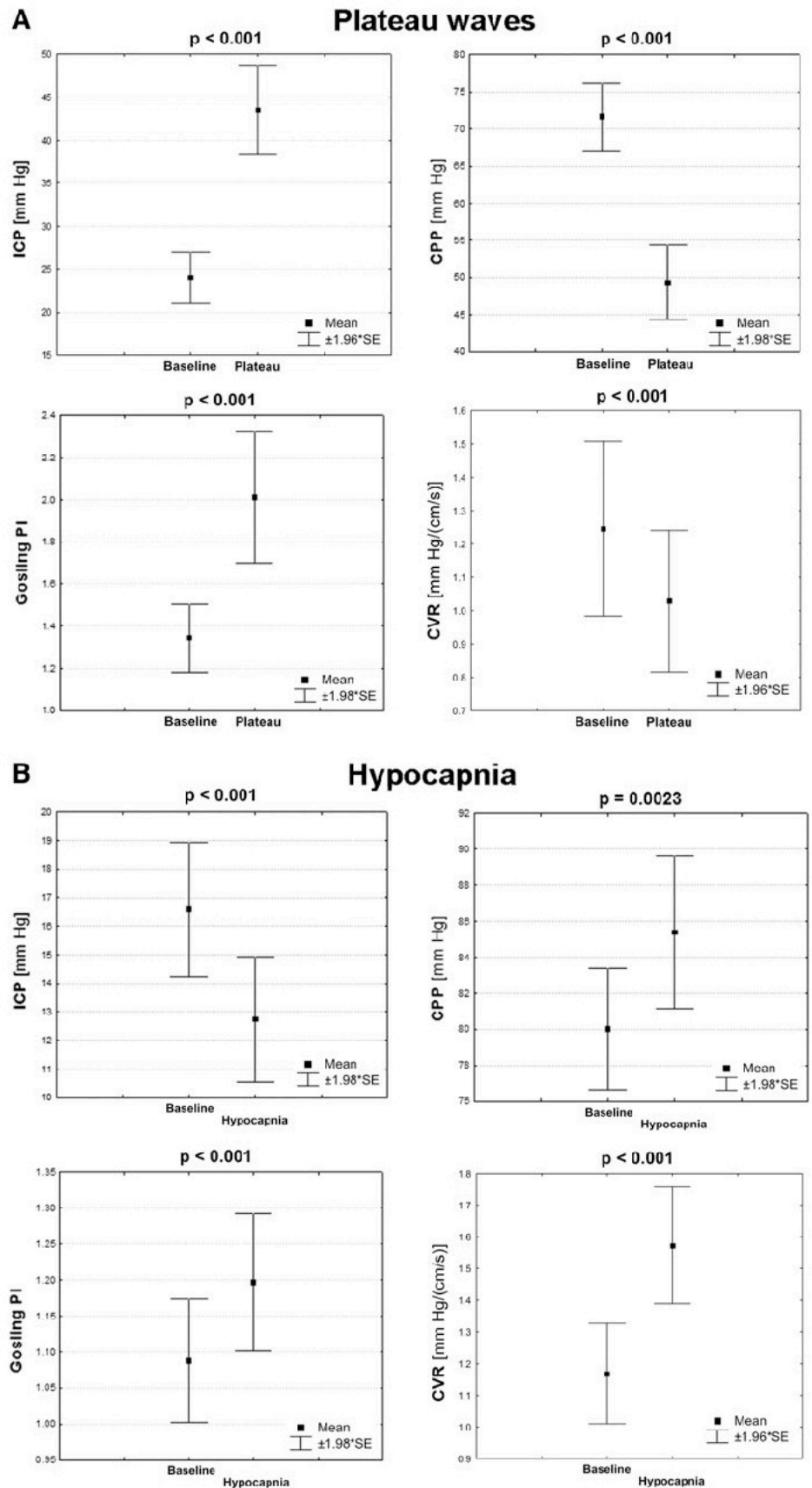


Table 2 Mean values of pressure and haemodynamic parameters found in 31 patients before and during the hypocapnia challenge

Hypocapnia challenge (<i>n</i> = 31)			
Parameters	Baseline	Hypocapnia	<i>p</i> value
PaCO ₂	5.10 ± 0.35	4.40 ± 0.34 [†]	<0.001
ICP (mmHg)	16.59 ± 6.68	12.73 ± 6.25 [†]	<0.001
CPP (mmHg)	80.02 ± 9.57	85.39 ± 12.08*	0.0023
FV _m (cm/s)	77.22 ± 26.33	58.99 ± 17.43 [†]	<0.001
<i>i</i> 1 (mmHg)	1.92 ± 1.63	1.37 ± 1.48 [†]	<0.001
<i>f</i> 1 (cm/s)	23.58 ± 10.45	19.22 ± 8.08 [†]	<0.001
<i>a</i> 1 (mmHg)	20.34 ± 5.09	20.86 ± 5.98	0.432 (NS)
ABP (mmHg)	96.62 ± 9.99	98.13 ± 12.65	0.339 (NS)
HR (cycles/min)	78.58 ± 16.64	78.75 ± 15.74	0.850 (NS)
FV _s (cm/s)	129.26 ± 41.03	103.94 ± 28.68 [†]	<0.001
FV _d (cm/s)	47.86 ± 17.68	35.29 ± 11.03 [†]	<0.001
PI	1.09 ± 0.24	1.20 ± 0.27 [†]	<0.001
CVR	1.17 ± 0.45	1.57 ± 0.52 [†]	<0.001
	[mmHg/(cm/s)]		

Values are expressed as the mean ± SD. Significant levels of the differences between change in parameters before and during the hypocapnia challenge are given (paired *t* test)

*a*1 pulse amplitude (first harmonic) of ABP, *ABP* arterial blood pressure, *CPP* cerebral perfusion pressure, *CVR* cerebrovascular resistance, *f*1 pulse amplitude (first harmonic) of blood FV, *FV_m* mean blood FV in the MCA, *FV_d* diastolic blood FV in the MCA, *FV_s* systolic blood FV in the MCA, *i*1 pulse amplitude (first harmonic) of intracranial pressure, *ICP* intracranial pressure, *HR* heart rate, *NS* not significant, *PaCO₂* carbon dioxide arterial partial pressure, *PI* Gosling pulsatility index

* *p* < 0.05. † *p* < 0.01

Gosling PI and the modeled PI (mPI) using the formula expressed in (1) is high (*R* = 0.81). This correlation improved further (*r* = 0.95) when PI was calculated by using the fundamental harmonic of FV (i.e., “spectral” PI) instead of the FV peak-to-peak pulse amplitude (Fig. 4a, b).

For confirmation of the obtained results the correlations between the mPI with the Gosling PI and the “spectral” PI were analyzed using our whole head-injury database (*n* = 345), achieving comparable average fit (Fig. 4c).

Discussion

The TCD-based pulsatility index is often interpreted as a descriptor of the distal cerebrovascular resistance [9]. However, our study suggests that this concept should be viewed with caution. We have analyzed two clinical situations, plateau waves, and hypocapnia, where opposite changes in CVR are observed. During plateau waves vasodilatation leads to decrease in CVR, increase in cerebral blood volume (CBV) and increase in ICP. During hypocapnia vascular constriction leads to an increase in

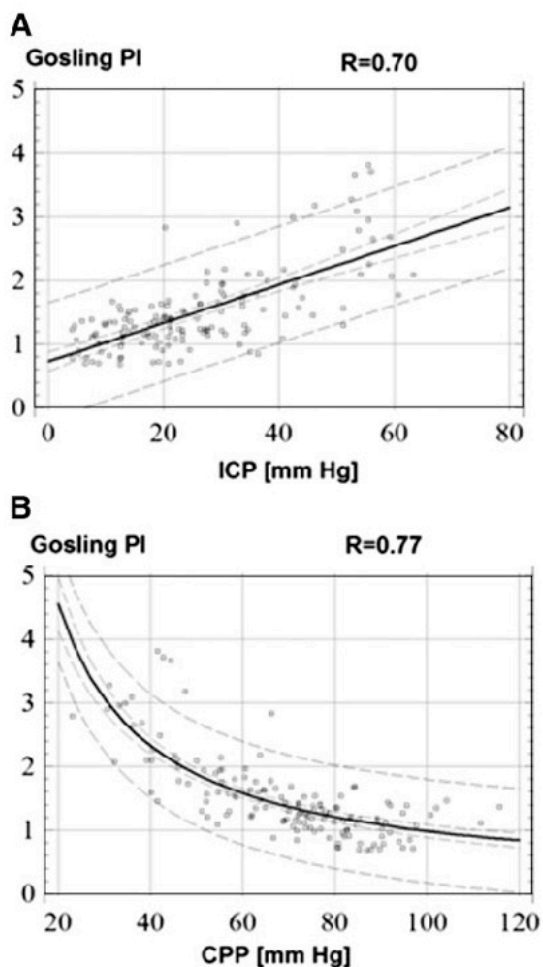


Fig. 3 The relationship between PI and **a** intracranial pressure (ICP) and **b** cerebral perfusion pressure (CPP). Combined data from recordings of plateau waves and hypocapnic challenge are presented. Dashed lines indicate 95% confidence limits for mean (inner) and 95% confidence limits for prediction (outer)

CVR, decrease in CBV, and slight decrease in ICP. Despite opposite changes in CVR we observed that PI in both cases increased, reinforcing the concept that PI cannot be interpreted as an index of CVR alone. Also, in both situations ICP changed inversely (i.e., dramatically increased during plateau waves and slightly decreased during hypocapnia), therefore universal description of rising ICP by rising PI is also questionable.

We have demonstrated by using a mathematical model of cerebrovascular impedance the possible input signals determining the reactions of PI. Analysis of the model suggests that PI is determined by the interplay of the value of CPP, the fundamental harmonic of ABP pulse (*a*1), CVR, compliance of the cerebral arterial bed (*Ca*), and heart rate.

Plateau waves are defined as any sudden elevation of ICP above 50 mmHg that lasts longer than 5 min and

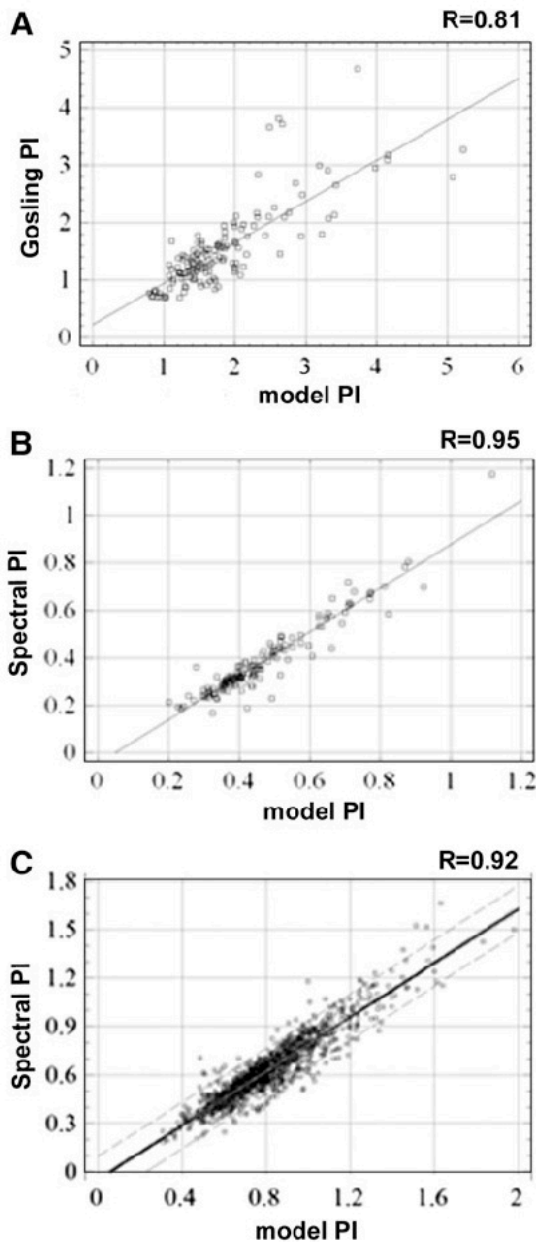


Fig. 4 Scatter plots of the relationship between Gosling PI and the modeled PI calculated using a mathematical model (1). **a** Strong relationship between the predicted Gosling PI and a real Gosling PI and **b** predicted and real “spectral” PI is seen ($R = 0.81$ and $R = 0.95$, respectively). **c** The relationship between “spectral” PI and modeled PI when applied to the whole head-injury database ($N = 345$; $R = 0.92$)

terminates spontaneously or in response to treatment. They are thought to be caused by a vasodilatory cascade, which may be triggered by a sudden decrease in CPP in the presence of functioning cerebral autoregulation [11, 17]. During plateau waves the profound reduction in CPP is accompanied by a decreased cerebral blood flow [15]. On the other hand, the vasodilatation leads to an increase in CBV, which is associated with an increase in cerebral arterial compliance (Ca) [14]. As the pulse amplitude of

ABP ($a1$) remains fairly stable, during plateau waves PI changes inversely to the changes in CPP. Most probably, changes in both Ca and CVR balance each other therefore none of them play a major role in determining PI.

The second group involves patients submitted to short term hypocapnia to assess CO_2 reactivity. Based on the available evidence, the most recent “Guidelines for the management and prognosis of severe traumatic brain injury” still include moderate manipulation of the arterial partial pressure of CO_2 (PaCO_2) as an option to treat raised ICP [18]. The beneficial effect of hyperventilation is due to a reduction in CBV, through vasoconstriction [19]. Therefore, the observed increase in CVR was expected in this group of patients. It has been already shown that changes in CVR are stronger than changes in Ca during controlled changes of PaCO_2 in an experimental setup [20]. Most likely, a similar situation exists during hypocapnia in clinical conditions, therefore the observed increase in PI follows an increase in the product of CVR and Ca combined with a slight decrease in CPP.

According to the described mathematical model (1) (please see “Appendix”) PI is a complex function of many mutually interdependent hemodynamic parameters. PI increases when the amplitude of ABP ($a1$) increases as well as during arterial hypotension and intracranial hypertension through changes in CPP. PI also increases when the product of CVR, Ca, and HR increases [14, 21], which has not been studied thoroughly before. Theoretically, the product of CVR and Ca expresses the time constant of the cerebral arterial bed [21]. The longer this time constant, the longer the time interval which is needed for arterial blood volume to arrive (from the point of TCD insonation) at the cerebral resistive vessels. In the experimental study mentioned above [21], the time constant has been shown to increase with hypocapnia and with reductions in cerebral perfusion pressure (caused by both arterial hypotension and rise in ICP). Similarly the PI in these scenarios will increase.

There are several limitations of this study. First, the sides of TCD insonation and of the ICP probe were not standardized. Although in most of the cases the ICP probe was placed in the right anterior frontal lobe, the side of the analyzed TCD signal depended on the qualities of both the insonated window and the recording. However, we cannot exclude that our data might have been more reliable if it had been based on the average of bilateral TCD readings. Neither can we exclude the influence in cases with unilateral lesions.

Limitations of the method used to calculate CaBV, Ca, and CVR from pulsatile waveforms of FV and ABP for the calculation of the cerebrovascular time constant have been discussed in previous publications [14, 22]. Monitoring the changes in cerebrovascular compliance is difficult to obtain

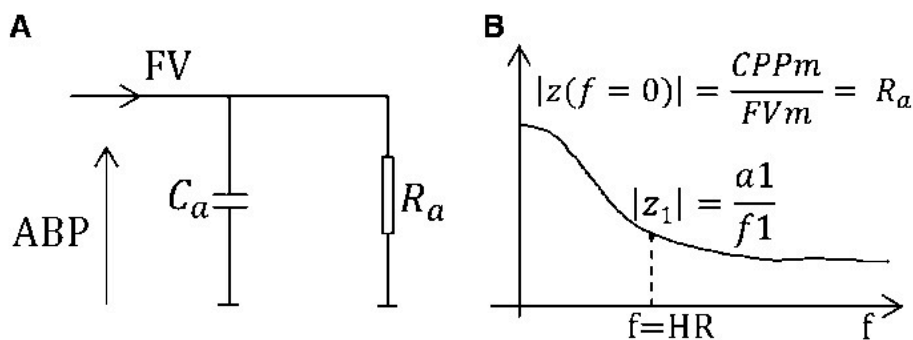


Fig. 5 Simplified input circuit used for the derivation of the formula (4) describing PI (calculated for fixed frequency of heart rate). **a** Input circuit representing a model of cerebral circulation. **b** Diagram of cerebrovascular impedance $|Z(f)|$ as a function of frequency. Two frequencies are considered: $f = 0$ (i.e., DC component) and $f = HR$. Module of impedance for $f = 0$ is equal to R_a , and may be estimated as CPP_m/FV_m . $a1$ pulse amplitude (first harmonic) of ABP, ABP

arterial blood pressure, C_a cerebrovascular compliance, CPP_m mean cerebral perfusion pressure, f frequency, $f1$ pulse amplitude (first harmonic) of blood FV, FV_m mean blood flow velocity in the middle cerebral artery, HR heart rate, PI Gosling pulsatility index, R_a cerebrovascular resistance (in the main part of manuscript expressed as CVR), $|z|$ cerebrovascular impedance, $|z_1|$ cerebrovascular impedance with frequency equal to HR

absolute measures, which requires the application of phase-contrast MRI [23, 24]. Recently Kim et al. developed a computational method allowing a continuous assessment of relative changes in cerebral compartmental compliances based on the relationship between pulsatile components of ABP, ICP, and the cerebral arterial blood volume (CaBV) [14]. This method is estimation only; it does not allow assessing absolute values of Ca but only its relative changes.

In the past another mathematical model was proposed, linking TCD pulsatility index and critical closing pressure [25]. But these formulas differ as the one we present links PI with physiological model parameters.

Conclusion

A mathematical formula describing PI is proposed and it shows a good correlation with the measured values of PI, and hence it is able to explain the major factors influencing PI. The pulsatility index is not dependent solely on CVR but it is a product of the interplay between CPP, pulse amplitude of arterial pressure, cerebrovascular resistance and compliance of the cerebral arterial bed as well as the HR. PI is not an accurate estimator of ICP; it describes CPP in a more accurate manner.

Acknowledgment This study was supported by the National Institute of Health Research, Biomedical Research Centre (Neuroscience Theme), the Medical Research Council (Grants G0600986 and G9439390), and NIHR Senior Investigator Awards (JDP); the Hospital Clinic Grant, Barcelona, Spain (NR) and also by the Swiss National Science Foundation (PBBSP3-125550 to CZ), Bern, Switzerland.

Disclosures ICM+ Software is licensed by Cambridge Enterprise, Cambridge, UK, <http://www.neurosurg.cam.ac.uk/icmplu/>. MC and PS have a financial interest in a fraction of the licensing fee.

Appendix

Mathematical Methods

The input circuit to cerebrovascular space (Fig. 5) can be reduced to cerebrovascular resistance (R_a) and compliance (C_a) of arteries. Under the assumption that input pressure is low, and systolic–diastolic distance is totally contained within the range of autoregulation, the system may be treated as semi-linear.

The pulsatility of the flow (PI), described as the ratio of the fundamental amplitude of the FV waveform divided by mean FV (1)

$$PI = \frac{f1}{FV_m} = \frac{a1}{CPP_m} \times \left| \frac{z(0)}{z(HR)} \right| \quad \left\{ \begin{array}{l} f1 = \frac{a1}{|Z(HR)|} \\ FV_m = \frac{CPP_m}{|Z(0)|} \end{array} \right. \quad (1)$$

where $f1$ is the fundamental harmonic of FV, FV_m is the mean FV, $a1$ is the fundamental harmonic of arterial pulse pressure, CPP_m is the mean cerebral perfusion pressure, $|z(0)|$ is the cerebrovascular impedance at zero frequency, $|z(HR)|$ is the cerebrovascular impedance at frequency equal to heart rate.

Cerebrovascular impedance ($Z(j\omega)$) can be described as a complex function of frequency (2).

$$z(j\omega) = \frac{\frac{R_a}{j\omega Ca}}{R_a + \frac{1}{j\omega Ca}} = \frac{R_a}{j\omega R_a Ca + 1} \quad (2)$$

where ω is the $2\pi f$, j is the imaginary unit, R_a is the cerebrovascular resistance, Ca is the compliance of arteries and arterioles.

$Z(f)$ is described in (3)

$$|z(j\omega)| = \frac{R_a}{\sqrt{R_a^2 Ca^2 \omega^2 + 1}} \quad (3)$$

where R_a is the cerebrovascular resistance, Ca is the compliance of arteries and arterioles.

From here we can derive formula describing the pulsatility index:

$$PI = \frac{a1}{CPP_m} \times \sqrt{(R_a Ca)^2 HR^2 (2\pi)^2 + 1} \quad (4)$$

where PI is the pulsatility index (for fundamental component of HR), $a1$ is the pulse amplitude (first harmonic) of ABP , CPP_m is the mean cerebral perfusion pressure, R_a is the cerebrovascular resistance, Ca is the compliance of arteries and arterioles, HR is the heart rate.

For the Gosling pulsatility index (PI) $a1$ should be substituted by the peak-to-peak amplitude of the ABP pulse. Also, Ca should be derived in a far more complex way, taking into account all harmonics of the ABP pulse and modules of impedances at these frequencies. But the general description of TCD pulsatility as a function of cerebral haemodynamic parameters remains the same.

References

- Kontos HA. Validity of cerebral arterial blood flow calculations from velocity measurements. *Stroke*. 1989;20(1):1–3.
- Gosling RG, King DH. Arterial assessment by Doppler-shift ultrasound. *Proc R Soc Med*. 1974;67(6 Pt 1):447–9.
- Bellner J, Romner B, Reinstrup P, Kristiansson KA, Ryding E, Brandt L. Transcranial Doppler sonography pulsatility index (PI) reflects intracranial pressure (ICP). *Surg Neurol*. 2004;62(1):45–51.
- Behrens A, Lenfeldt N, Ambarki K, Malm J, Eklund A, Koskinen LO. Transcranial Doppler pulsatility index: not an accurate method to assess intracranial pressure. *Neurosurgery*. 2010;66(6):1050–7.
- Figaji AA, Zwane E, Fieggan AG, Siesjo P, Peter JC. Transcranial Doppler pulsatility index is not a reliable indicator of intracranial pressure in children with severe traumatic brain injury. *Surg Neurol*. 2009;72(4):389–94.
- Melo JR, Di Rocco F, Blanot S, et al. Transcranial Doppler can predict intracranial hypertension in children with severe traumatic brain injuries. *Childs Nerv Syst*. 2011;27(6):979–84.
- Soehle M, Chatfield DA, Czosnyka M, Kirkpatrick PJ. Predictive value of initial clinical status, intracranial pressure and transcranial Doppler pulsatility after subarachnoid haemorrhage. *Acta Neurochir (Wien)*. 2007;149(6):575–83.
- Giller CA, Hodges K, Batjer HH. Transcranial Doppler pulsatility in vasodilation and stenosis. *J Neurosurg*. 1990;72(6):901–6.
- Lim MH, Cho YI, Jeong SK. Homocysteine and pulsatility index of cerebral arteries. *Stroke*. 2009;40(10):3216–20.
- Czosnyka M, Richards HK, Whitehouse HE, Pickard JD. Relationship between transcranial Doppler-determined pulsatility index and cerebrovascular resistance: an experimental study. *J Neurosurg*. 1996;84(1):79–84.
- Rosner MJ, Becker DP. Origin and evolution of plateau waves. Experimental observations and a theoretical model. *J Neurosurg*. 1984;60(2):312–24.
- Steiner LA, Balestreri M, Johnston AJ, et al. Sustained moderate reductions in arterial CO2 after brain trauma time-course of cerebral blood flow velocity and intracranial pressure. *Intensive Care Med*. 2004;30(12):2180–7.
- Hsu HY, Chern CM, Kuo JS, Kuo TB, Chen YT, Hu HH. Correlations among critical closing pressure, pulsatility index and cerebrovascular resistance. *Ultrasound Med Biol*. 2004;30(10):1329–35.
- Kim DJ, Kasprovicz M, Carrera E, et al. The monitoring of relative changes in compartmental compliances of brain. *Physiol Meas*. 2009;30(7):647–59.
- Czosnyka M, Smielewski P, Piechnik S, et al. Hemodynamic characterization of intracranial pressure plateau waves in head-injury patients. *J Neurosurg*. 1999;91(1):11–9.
- Helmy A, Vizcaychipi M, Gupta AK. Traumatic brain injury: intensive care management. *Br J Anaesth*. 2007;99(1):32–42.
- Lundberg N. Continuous recording and control of ventricular fluid pressure in neurosurgical practice. *Acta Psychiatr Scand Suppl*. 1960;36(149):1–193.
- Brain Trauma F, American Association of Neurological Surgeon, Congress of Neurological Surgeons, et al. Guidelines for the management of severe traumatic brain injury. XIV. Hyperventilation. *J Neurotrauma* 2007; 24 Suppl 1:S87–S90.
- Raichle ME, Posner JB, Plum F. Cerebral blood flow during and after hyperventilation. *Arch Neurol*. 1970;23(5):394–403.
- Czosnyka M, Richards HK, Reinhard M, et al. Cerebrovascular time constant: dependence on cerebral perfusion pressure and end-tidal carbon dioxide concentration. *Neurol Res*. 2012;34(1):17–24.
- Czosnyka M, Piechnik S, Richards HK, Kirkpatrick P, Smielewski P, Pickard JD. Contribution of mathematical modelling to the interpretation of bedside tests of cerebrovascular autoregulation. *J Neurol Neurosurg Psychiatry*. 1997;63(6):721–31.
- Carrera E, Steiner LA, Castellani G, et al. Changes in cerebral compartmental compliances during mild hypocapnia in patients with traumatic brain injury. *J Neurotrauma*. 2011;28(6):889–96.
- Alperin N, Sivaramakrishnan A, Lichtor T. Magnetic resonance imaging-based measurements of cerebrospinal fluid and blood flow as indicators of intracranial compliance in patients with Chiari malformation. *J Neurosurg*. 2005;103(1):46–52.
- Baledent O, Fin L, Khuoy L, et al. Brain hydrodynamics study by phase-contrast magnetic resonance imaging and transcranial color doppler. *J Magn Reson Imaging*. 2006;24(5):995–1004.
- Michel E, Zemikow B. Goslig's Doppler pulsatility index revisited. *Ultrasound Med Biol*. 1998;24(4):597–9.

PUBLICATION 2

Varsos GA, de Riva N, Smielewski P, Pickard JD, Brady KM, Reinhard M, Avolio A, Czosnyka M.

Critical closing pressure during intracranial pressure plateau waves.

Neurocrit Care 2013 Jun;18(3):341-8.

IF 2016 = 2.752.

-SUMMARY OF THE STUDY-

Critical Closing Pressure (CCP) is the arterial blood pressure (ABP) at which brain vessels collapse and cerebral blood flow (CBF) ceases. Spontaneous increases in intracranial pressure (ICP), termed plateau waves, occur in many neurocritical conditions including head injuries and subarachnoid haemorrhages. The aim of this study was to analyze the behaviour of CCP during plateau waves in order to identify situations at risk for ischaemia.

For calculating CCP, we used a multi-parameter method (CCPm) which is based on the modulus of cerebrovascular impedance. CCPm is expressed with parameters such as cerebral perfusion pressure (CPP), ABP, estimators of cerebrovascular resistance and compliance, and heart rate. Arterial wall tension was estimated as CCPm-ICP.

We analyzed recordings of ABP, ICP and transcranial Doppler based blood flow velocity (FV) from 38 events of ICP plateau waves, recorded in 20 patients after head injury. Overall, CCP increased significantly during plateau waves, by 11.42 ± 8.63 mm Hg ($p < 0.001$). Change in CCPm was correlated to ICP changes ($R = 0.80$ $p < 0.001$). Cerebral arterial wall tension decreased significantly during plateau (28.61 ± 7.05 mm Hg to 18.79 ± 5.60 mm Hg; $p < 0.001$), confirming its vasodilatory origin.

In conclusion, CCP increases during plateau waves of ICP while arterial wall tension decreases. CCPm did not demonstrate the non-physiological negative values that are shown in traditional methods for calculating CCP, allowing the interpretation of CCP in clinical reality where ICP of patients is rising.

Critical Closing Pressure During Intracranial Pressure Plateau Waves

Georgios V. Varsos · Nicolás de Riva · Peter Smielewski ·
John D. Pickard · Ken M. Brady · Matthias Reinhard ·
Alberto Avolio · Marek Czosnyka

Published online: 20 March 2013
© Springer Science+Business Media New York 2013

Abstract

Background Critical closing pressure (CCP) denotes a threshold of arterial blood pressure (ABP) below which brain vessels collapse and cerebral blood flow ceases. Theoretically, CCP is the sum of intracranial pressure (ICP) and arterial wall tension (WT). The aim of this study is to describe the behavior of CCP and WT during spontaneous increases of ICP, termed plateau waves, in order to quantify ischemic risk.

Methods To calculate CCP, we used a recently introduced multi-parameter method (CCPm) which is based on the modulus of cerebrovascular impedance. CCP is derived from cerebral perfusion pressure, ABP, transcranial Doppler estimators of cerebrovascular resistance and compliance, and heart rate. Arterial WT was estimated as CCPm-ICP. The

clinical data included recordings of ABP, ICP, and transcranial Doppler-based blood flow velocity from 38 events of ICP plateau waves, recorded in 20 patients after head injury.

Results Overall, CCPm increased significantly from 51.89 ± 8.76 mmHg at baseline ICP to 63.31 ± 10.83 mmHg at the top of the plateau waves (mean \pm SD; $p < 0.001$). Cerebral arterial WT decreased significantly during plateau waves by 34.3 % ($p < 0.001$), confirming their vasodilatory origin. CCPm did not exhibit the non-physiologic negative values that have been seen with traditional methods for calculation, therefore rendered a more plausible estimation of CCP.

Conclusions Rising CCP during plateau waves increases the probability of cerebral vascular collapse and zero flow when the difference: ABP-CCP (the “collapsing margin”) becomes zero or negative.

G. V. Varsos (✉) · N. de Riva · P. Smielewski ·
J. D. Pickard · M. Czosnyka
Division of Neurosurgery, Department of Clinical
Neurosciences, Addenbrooke’s Hospital,
University of Cambridge, Hills Road,
Cambridge CB2 0QQ, UK
e-mail: gv249@cam.ac.uk

P. Smielewski
e-mail: ps10011@cam.ac.uk

J. D. Pickard
e-mail: jdp1000@medschl.cam.ac.uk

N. de Riva
Department of Anesthesiology, Hospital Clinic,
Universitat de Barcelona, Barcelona, Spain
e-mail: nderiva@clinic.ub.es

K. M. Brady
Baylor College of Medicine,
Texas Children’s Hospital, Houston, TX, USA
e-mail: kmbrady@texaschildrens.org

M. Reinhard
Department of Neurology, University of Freiburg,
Freiburg im Breisgau, Germany
e-mail: matthias.reinhard@uniklinik-freiburg.de

A. Avolio
Australian School of Advanced Medicine,
Macquarie University, Sydney, NSW, Australia
e-mail: alberto.avolio@mq.edu.au

M. Czosnyka
Institute of Electronic Systems, Warsaw
University of Technology, Warsaw, Poland
e-mail: mc141@medschl.cam.ac.uk

Keywords Critical closing pressure · Plateau waves · Intracranial pressure · Mathematical modeling · Wall tension

Introduction

A plateau wave is a sudden substantial elevation of intracranial pressure (ICP) of a magnitude of 20–60 mmHg, depending on baseline ICP, that lasts several minutes and terminates either spontaneously or in response to treatment [1–6]. Plateau waves are caused by rapidly increasing cerebral blood volume (CBV) [7, 8] triggered by a vasodilatory cascade [2], which may be initiated by a vasodilatory stimulation, such as an initial reduction in arterial blood pressure (ABP) (Fig. 1) [5]. The increase in ICP results in a decrease in cerebral perfusion pressure (CPP), which engages pressure autoregulatory mechanisms in a positive feedback-loop with further vasodilation, further rise of CBV and further increase in ICP. The whole cascade loop lasts until maximum vasodilation is reached. Reversing the cascade to a vasoconstrictory cycle may restore ICP to a baseline level [5]. Plateau waves can be observed in various clinical conditions causing exhausted cerebrospinal compensatory reserve, including subarachnoid hemorrhage

[7, 9], head injury [2, 10, 11], brain tumor [12], acute hydrocephalus [3, 13], craniosynostosis [14, 15], and pseudotumor cerebri [3].

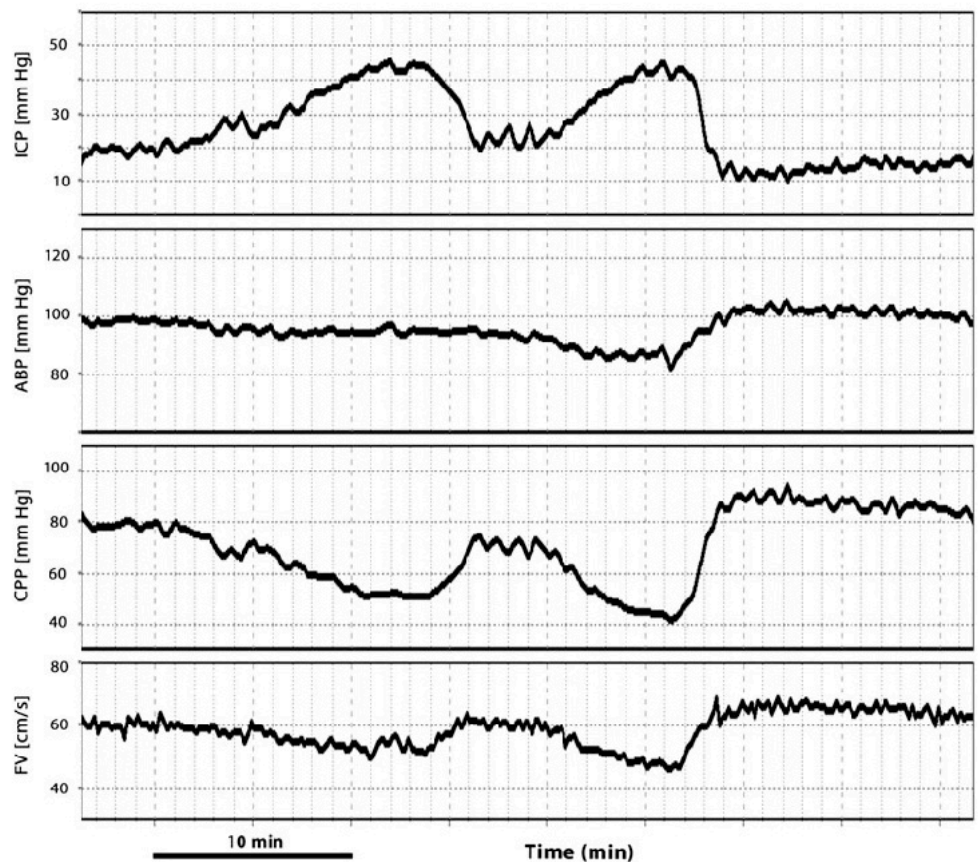
Overall, the increase in ICP seen during the plateau wave results in a dramatic decrease in CPP, usually below the lower limit of autoregulation, therefore causing a decrease in cerebral blood flow (CBF) [5, 6, 16]. Prolonged reduced-CBF associated with plateau waves may then provoke a secondary ischemic brain insult [17], providing they last for a longer period (above 30 min); in that way, plateau waves have been associated with a worse outcome following traumatic brain injury (TBI) [5]. The proposed vasodilatory mechanism of plateau waves can be examined by estimating critical closing pressure (CCP), which is related to cerebrovascular vasomotor tone, represented by wall tension (WT).

CCP or zero-flow pressure was first theoretically described as a concept in 1951 by Burton, who stated that small vessels can collapse when local blood pressure is reduced to a critical value [18]. Since then, CCP has been studied in vascular beds under various conditions [19–21].

Burton's model suggests that CCP is equal to the sum of ICP and vascular WT [18, 22]: $CCP = ICP + WT$.

Past studies performed under various conditions [23–25] and physiological stimuli [26] have demonstrated that both changes in ICP and vascular tone cause predictable changes in

Fig. 1 Example of a sudden increase in intracranial pressure (ICP) that lasts several minutes, termed as plateau wave. A decrease in arterial blood pressure (ABP) triggers a vasodilatory cascade, increasing cerebral blood volume and leading to rising of mean ICP. During this increase, cerebral perfusion pressure (CPP) decreases, as does cerebral blood flow velocity (FV). Gaps left after artefacts removal have been interpolated graphically



estimated CCP. A reliable estimation of CCP from non-invasive traditional transcranial Doppler (TCD) [27, 28] might be clinically useful to estimate changes in ICP non-invasively for patients at risk of elevated ICP, such as in occurrence of plateau waves. Unfortunately, the methods available so far [21, 28] suffer from uncertainty and poor accuracy as they may produce negative non-interpretable values [29].

We recently published a multi-parameter model to calculate CCP (CCPm), which is based on cerebrovascular impedance [30]. In the present study, we retrospectively re-analyzed clinical material [5, 31, 32] with the primary aim to examine the pathophysiology of “plateau waves” using the concept of CCP and arterial WT. The second aim was to verify the performance of CCPm for calculating CCP in clinical practice, by comparing it to traditional methodology.

Subjects and Methods

Patients

From a database of 345 head-injured patients [median age of patients: 29 years (interquartile range 20–44), with 75 % being male] with continuous recordings of ABP, ICP, and short TCD recording periods (up to 1 h sessions daily per patient), we identified a total of 20 patients where at least one ICP plateau wave occurred during the monitored period. A total of 38 plateau waves were recorded and retrospectively analysed for the purpose of our study. The mean length of plateau waves was 13 min with a range of 4–34 min. The median Glasgow Coma Score of the patients at admission was 5 (range from 3 to 12), while the Glasgow Outcome Score varied from good outcome to mortality, with most of the cases (57 %) having an unfavorable outcome (dead, persistently vegetative or severely disabled). Data were recorded during daily routine clinical TCD investigations of cerebral autoregulation [6], performed in head-injury patients, which was included in a standard clinical brain monitoring protocol. This material has been partially presented before [31, 32], however not in the context of CCP analysis. This retrospective analysis was performed as part of an anonymous clinical audit, with approval of Neurocritical Care Users Committee Addenbrooke’s Hospital, Cambridge, UK.

Monitoring and Data Analysis

ABP was invasively monitored from the radial artery with a pressure monitoring kit (Baxter Healthcare CA, USA; Sidcup, UK), zeroed at the level of the heart; ICP was monitored using an intraparenchymal probe (Codman & Shurtleff, MA, USA or Camino Laboratories, CA, USA); Cerebral blood flow velocity (FV) was measured from the middle cerebral

artery with a 2-MHz probe (Multidop T, DWL, Germany) and monitored with the Doppler Box (DWL Compumedics, Germany) or Neuroguard (Medasonic, CA, USA). The TCD recordings were performed daily for periods of 10 min to 1 h starting from the day of initiation of invasive monitoring. The decision to discontinue monitoring was made on clinical grounds.

Raw signals were digitized using an analog–digital converter (DT2814 or DT9801, Data Translation, Marlboro, Mass, USA) sampled at a frequency of 50 Hz and recorded using WREC (Warsaw University of Technology), BioSan (University of Cambridge, UK) or ICM+ (Cambridge Enterprise, Cambridge, UK, <http://www.neurosurg.cam.ac.uk/icmplus/software>). The recorded signals were then subjected to manual artefacts removal and analysed with the ICM+ software.

The amplitudes of the fundamental harmonics of ABP, FV, and ICP (A1, F1, and I1, respectively) were derived using 10-s discrete Fourier transformations. Heart rate (HR) was calculated using spectral position (adjusted using sinc interpolation, as above) of the peak associated with the first harmonic of ABP. All the calculations, including mean values of ABP, ICP, FV, and CPP, were performed over a 10 s long-sliding window [30]. The minimal values of FV from every 2-s period were calculated and treated as end-diastolic components. These components were then averaged over 10 s to give the mean values for end-diastolic FV, termed as FVd.

Calculation of CCP and WT

The multi-parameter estimation of CCP was calculated using the following formula (1):

$$\text{CCPm} = \text{ABP} - \frac{\text{CPP}}{\sqrt{(\text{Ra} \cdot \text{Ca} \cdot \text{HR} \cdot 2\pi)^2 + 1}} \quad (1)$$

where CPP is the mean cerebral perfusion pressure (being calculated as $\text{CPP} = \text{ABP} - \text{ICP}$), Ra denotes cerebrovascular resistance, Ca stands for compliance of cerebral arterial bed, while HR is the heart rate (beats/s).

The above-mentioned formula is based on the analysis of a simple model of cerebrovascular impedance. Details of its derivation have been published previously [5, 30].

On this model, two parameters (Ra and Ca) cannot be measured directly and need to be estimated. Their estimation can be made using TCD blood flow velocity and ABP, CPP waveforms according to the algorithm presented in previous studies [33–35].

Model WT (WTm) was calculated using Dewey’s model [22], which denotes WT to be estimated as the difference between estimation of CCP and ICP

$$\text{WTm} = \text{CCPm} - \text{ICP}$$

The traditional calculation of CCP (termed as CCP1) was performed using the formula proposed by Michel [28]:

$$CCP1 = ABP - A1 \cdot \frac{FV}{F1} \tag{2}$$

where A1 and F1 are amplitudes of the fundamental harmonics of ABP and FV pulse waveforms, respectively.

The traditional calculation of WT was also derived from Dewey’s model, like previously, however with CCP1 instead of CCPm:

$$WT1 = CCP1 - ICP$$

Statistical Analysis

Statistical analysis of the data was conducted with IBM SPSS Statistics 20 package. The analysis included comparison of changes in the group of data of ABP, ICP, FV, CCP1, CCPm, WT1, and WTm from normal baseline ICP to high and stable ICP at the top of the plateau wave. Results are presented in mean value ± standard deviation format. Normal distribution was tested with the Shapiro–Wilk test and paired *t* tests were used to examine the significance of each sample comparison. The level of significance was set at 0.05. Bivariate correlations were used, with *R* being the Pearson correlation coefficient. Bland–Altman method was used to determine the agreement between CCPm and CCP1.

Results

Critical Closing Pressure and Wall Tension During Plateau Waves

Detailed results are given in Table 1. During plateau waves in these subjects, mean ICP increased significantly

(*p* < 0.001) by 21.56 mmHg from baseline to plateau level. CPP decreased significantly by a margin of 31.96 % (*p* < 0.001), while ABP did not endure any significant changes and remained at the same levels. Mean CBF velocity also decreased by 13.8 % (*p* < 0.001), with its diastolic values showing a larger decrement (28.36 %; *p* < 0.001). Plateau waves in these subjects caused a significant increase in CCP by 22.00 % (*p* < 0.001). This result was demonstrated using both the novel and traditional methods of calculating CCP (CCPm and CCP1, respectively, see Table 1). As predicted by the vasodilatory nature of plateau waves, WT decreased significantly by 34.30 % (*p* < 0.001), demonstrated by WTm and confirmed by values of WT1 (*p* < 0.001, see Table 1). As CCP is equal to the sum of ICP and WT, it can be seen in these subjects that the ICP increase during plateau waves which is more pronounced than the decrease in WT, resulting in a net increase in CCP (Fig. 2). In the same figure we can observe that during a plateau wave CCP rises while ABP remains constant. Therefore the “collapsing margin” (ABP–CCP) decreases, presenting an increased risk for brain vessels to collapse (Fig. 3).

Relationship Between the Two Methods of CCP Calculation

When data from both baseline and plateau levels of ICP were considered, there was a strong correlation between CCPm and CCP1 (*R* = 0.87, *p* < 0.001; Fig. 4a) as well as between WTm and WT1 (*R* = 0.69, *p* < 0.001).

Bland–Altman plot (Fig. 4b) was used to demonstrate the overall agreement between CCPm and CCP1 (Bias = 10.06 mmHg, standard deviation of error = 10.60 mmHg). When the average of CCPm and CCP1 was below 40 mmHg, the agreement deteriorated significantly as compared to the values above 40 mmHg (mean difference of 25.02 ± 15.50

Table 1 Mean values and standard deviations (mean ± SD) of measured and calculated variables from baseline to plateau

	Baseline	Plateau	<i>p</i> value (<i>t</i> value, df)
ICP (mmHg)	21.81 ± 6.63	43.37 ± 11.96	<0.001 (12.76, 37)
ABP (mmHg)	94.85 ± 11.25	93.13 ± 10.59	0.141 (1.50, 37)
CPP (mmHg)	73.02 ± 12.92	49.68 ± 14.34	<0.001 (14.22, 37)
FV (cm/s)	62.61 ± 29.91	53.94 ± 28.19	<0.001 (6.39, 37)
FVd (cm/s)	35.12 ± 20.10	25.16 ± 20.72	<0.001 (6.29, 37)
CCPm (mmHg)	51.89 ± 8.76	63.31 ± 10.83	<0.001 (8.15, 37)
CCP1 (mmHg)	40.36 ± 17.44	54.71 ± 17.66	<0.001 (7.86, 37)
WTm (mmHg)	28.61 ± 7.05	18.79 ± 5.60	<0.001 (11.45, 37)
WT1 (mmHg)	18.55 ± 16.64	11.34 ± 14.22	<0.001 (5.77, 37)
Collapsing margin (mmHg)	42.96 ± 12.91	29.82 ± 11.98	<0.001 (9.64, 37)

ABP arterial blood pressure, *CCP1* fundamental harmonic model of critical closing pressure, *CCPm* multi-parameter mathematical model of CCP based on the concept of impedance, *CPP* cerebral perfusion pressure, *FV* mean blood flow velocity in the middle cerebral artery (MCA), *FVd* diastolic blood FV in the MCA, *ICP* intracranial pressure, *WT1* fundamental harmonics model wall tension, *WTm* multi-parameter mathematical model of wall tension based on the concept of impedance, *Collapsing margin* calculated as the difference between ABP and CCPm

Fig. 2 Example of the behavior of critical closing pressure (CCP) during a plateau wave. The multi-parameter mathematical model CCPm was used to demonstrate the increase of CCP during the increase in intracranial pressure (ICP), while the arterial blood pressure (ABP) remained unchanged. The difference between CCP and ICP, demonstrated as the gap between the two corresponding waveforms, indicates the active vasomotor tone, represented as the wall tension (WT). The multi-parameter mathematical model WTm was used to demonstrate the decrease of WT at the top of the plateau in comparison to baseline opening pressure, due to vasodilation compensating for the increase in ICP

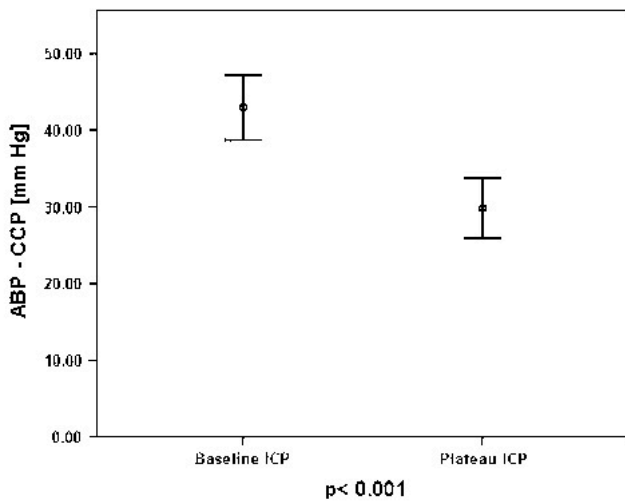
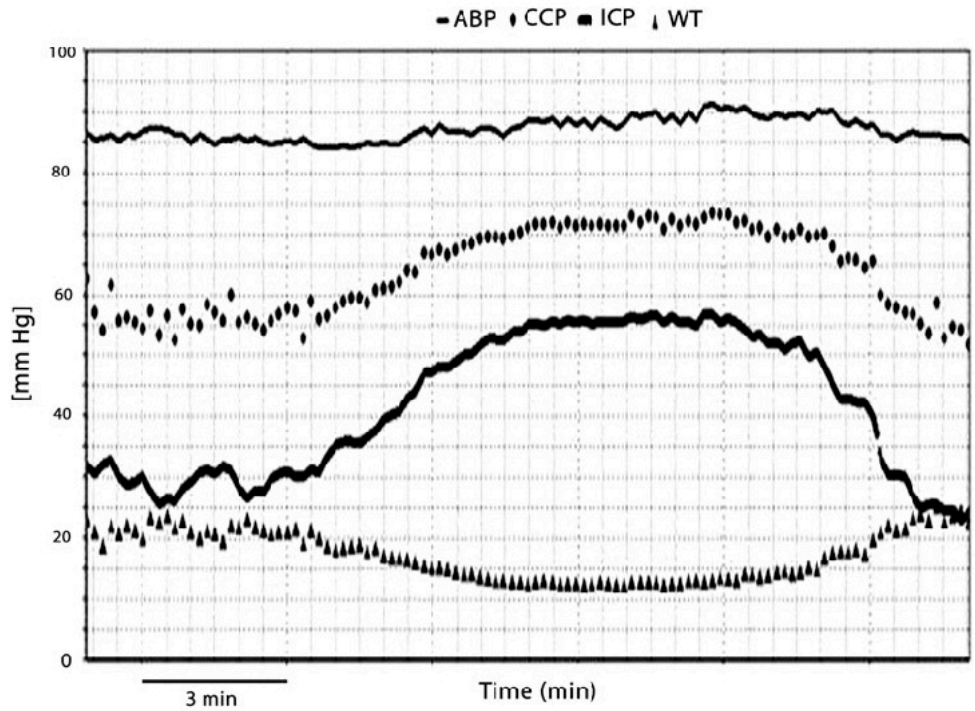


Fig. 3 Difference of mean arterial blood pressure (ABP) to critical closing pressure (CCP) calculated with the module of impedance (CCPm), termed as collapsing margin decreases significantly ($p < 0.001$) from baseline intracranial pressure (ICP) to the plateau level. This denotes the increased risk of brain vessels collapsing during plateau waves in comparison to baseline normal ICP

and 6.68 ± 4.91 mmHg; $p = 0.001$ for values of CCP < 40 mmHg and CCP > 40 mmHg, respectively).

Traditional methods for calculation of zero-flow pressure presents the drawback of the appearance of non-physiologic, negative values of CCP. In our data, CCP1 occasionally rendered negative values during the post-plateau “hyperemia.” This is exemplified in Fig. 5, where the decrease in ICP after the plateau with increasing CPP, ABP, and FV values resulted in CCP1 falling below zero, yielding values

that have no meaning. By contrast, our own estimator CCPm stayed positive during this period.

Discussion

CCP is a metric that has inspired theoretical interest but which has been relatively neglected as a clinical application. In theory, CCP can enhance our understanding in regard of cerebral haemodynamics when CPP is below the lower limit of autoregulation. In that sense, CCP can provide a second, higher-risk threshold of CPP, where CBF ceases completely.

The primary aim of this study was to measure CCP during “plateau waves.” The results show that during the vasodilatory loop of the plateau waves, there is a rise in CCP and a reduction in WT, with both of them being significant. However, the effect of rising ICP is more pronounced than the corresponding vasodilatory response decreasing WT.

The observed increased CCP during plateau waves imposes an elevated risk for brain vessels to collapse, especially if ABP remains constant (example shown in Fig. 2). As can be seen in Fig. 3, the collapsing margin ABP–CCP decreased significantly ($p < 0.001$) in this cohort from baseline ICP to plateau levels, indicating that the probability for brain vessels to collapse is increasing during this phenomenon.

The collapsing margin (ABP–CCP) was once thought to describe cerebral perfusion pressure [22]. However, even

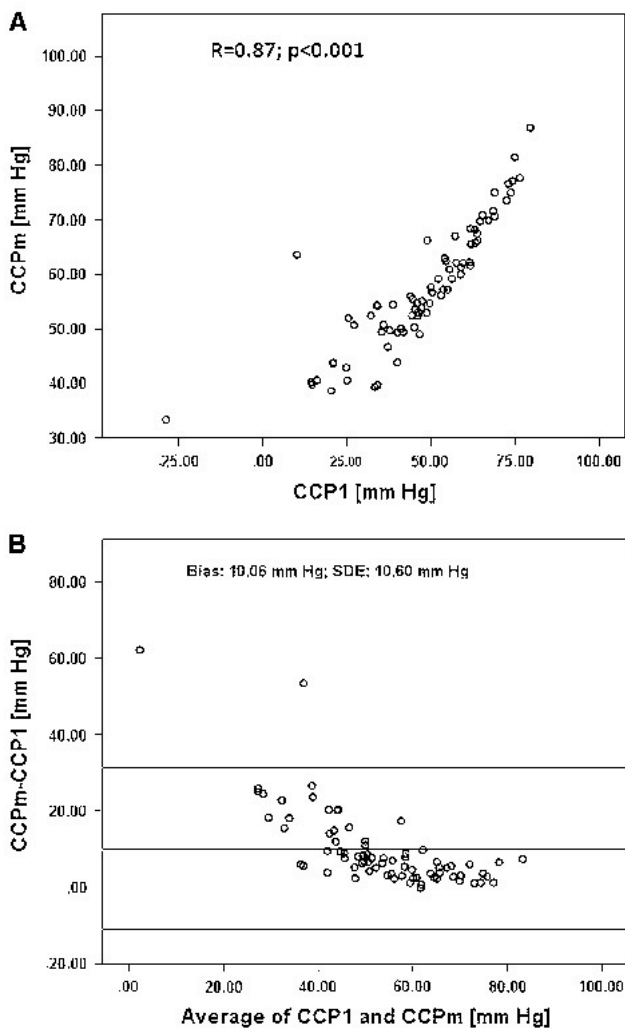


Fig. 4 **a** Correlation between multi-parameter mathematical model CCPm and first harmonic model of critical closing pressure (CCP1) (Pearson correlation coefficient: $R = 0.87$; $p < 0.001$). **b** Bland–Altman test for comparing difference between CCPm and CCP1 to average value of CCP1 and CCPm. Note that after the physiological threshold of 40 mmHg the difference is becoming minimal ($p < 0.001$)

though there is a strong bivariate correlation between CPP and the collapsing margin ($R = 0.844$, $p < 0.001$), the collapsing margin is different from CPP in at least two respects. First, the collapsing margin accounts for changes in WT, which do not influence the CPP equation. Second, the collapsing margin indicates the amount of pressure reserve available to avoid total cease of flow, whereas CPP indicates the perfusion pressure driving CBF and does not have an inherently meaningful threshold.

A reliable calculation for CCP and monitoring of the collapsing margin may have a future role in the care of patients after TBI or stroke. For example, identifying patients with frequent decrements in the collapsing margin may inform selection of patients who would benefit from decompressive craniectomy.

The second aim of this study was to verify the performance of our novel mathematical multi-parameter model for calculating CCP in the clinical cases of plateau waves. It has been proven with experimental animal data that CCPm is well-correlated to the traditional method used to calculate CCP from the fundamental harmonic of pulse-frequency Doppler and pressure changes (CCP1) [30]. The same high correlation is shown in plateau waves of human subjects, further supporting the validity of CCPm. Divergence between CCP1 (traditional) and CCPm (novel) can be seen only when CCP1 has meaninglessly low (or negative) values [29, 30, 36]. The issue of low and negative values of CCP has been a known drawback of traditional calculation methods in cases such as hyperemia, vasospasm, or with artificially elevated diastolic blood flow velocity [29, 36, 37]. In plateau waves, CCP1 rendered negative values in a variety of situations in which changes in amplitude and mean values of FV and/or ABP occurred. The appearance of these values is considered to be a methodological limitation, as there is no physiologic explanation for negative values of WT. By contrast, CCPm, calculated with the concept of impedance was proven to overcome this drawback. CCPm cannot reach non-physiologic negative values, provided physiologic values of ABP, CPP, and FV are used [30, 33], and is, therefore, more clinically relevant.

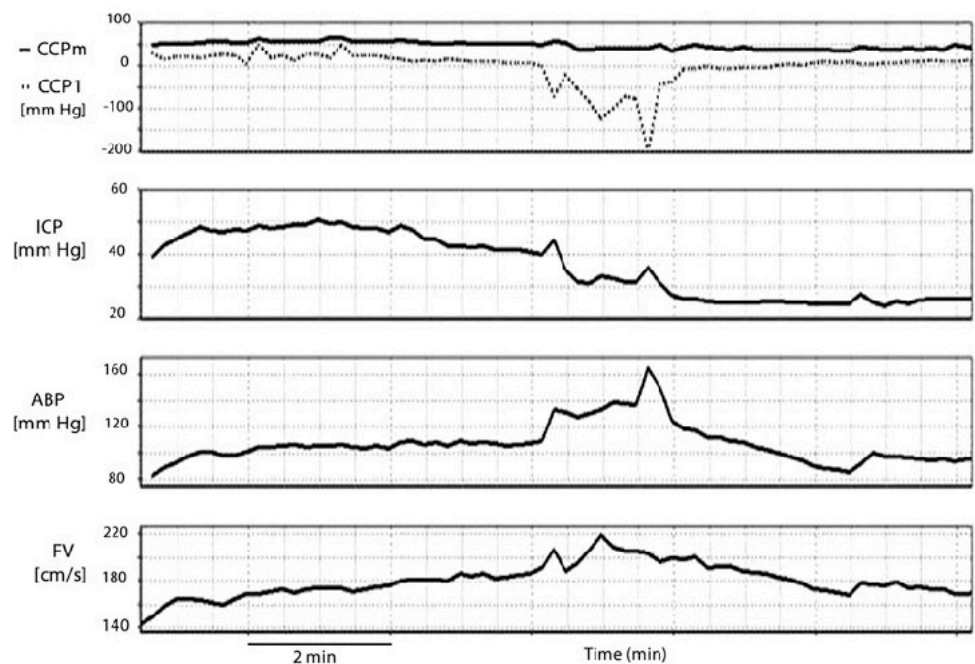
The validity of WT calculation via cerebrovascular impedance was also proven, with WTm being significantly correlated to WT1 ($p < 0.001$) during the plateau waves, as has been also proven in experimental animal data [30]. Like CCPm, the use of WTm has the advantage of consistently positive values, unlike the fundamental harmonic model WT1, which presents senseless negative values. Decrease in WTm is in agreement with modeling data presented previously by Daley [38], although our study takes into account changes in CBF, confirming validity of previous analyses done using ICP and ABP waveforms [38].

Limitations

Due to the small number of patients, we are unable to test an association between the collapsing margin and outcome. Plateau waves, although are observed in 40 % of TBI patients [5], are difficult to be captured with limited time TCD recording in the neurocritical care unit. However, having set the theoretical basis of the collapsing margin, a similar study of a larger cohort of patients is indicated.

The main disadvantage of the multi-parameter mathematical model for calculating CCP (CCPm) is the requirement of invasive ICP monitoring. However, in subjects at risk for plateau waves, measurement, and signal of ICP monitoring are standard care, which increases the clinical relevance of the technique demonstrated in this study.

Fig. 5 Trailing edge of ICP plateau wave. Example of first harmonic model of critical closing pressure (CCP1) demonstrating non-physiologic negative values during the recovery time after the plateau wave. Negative CCP1 were caused by increased values of mean flow velocity (FV). In contrast, the multi-parameter mathematical model CCPm rendered always positive values



Estimation of CCP requires good quality recording of flow velocity through TCD. The TCD monitoring sessions were not continuous like ABP and ICP monitoring but instead were performed for short periods for every patient on a daily basis. The short periods were justified by the difficulty of having continuous TCD measurements, as the head injured patients were treated in a neurointensive care environment, thus subjected to change in position or transfer i.e. for the purpose of an MRI scan, which would result in intervention of TCD recordings. On that basis, it might be possible that not all the occurred plateau waves have been captured. However, as the aim of this study was to estimate CCP during the specific phenomenon of occurring plateau waves and not continuously, this limitation does not affect its purposes.

Conclusion

During plateau waves and increase in ICP, CCP increases significantly while active vasomotor tone, represented by WT, decreases due to vasodilation. Rising CCP in turn can increase the risk for brain vessels to collapse if the difference ABP–CCP termed as “collapsing margin” decreases to zero. In a neuro-intensive environment, monitoring of this collapsing margin can then indicate a “pillow” of safety for the small brain vessels and can be used as a reference point to guidance of treatment in terms of terminal ischemia associated with collapsing vessels. Estimation of CCP based on the impedance methodology does not produce non-physiologic negative values in contrast to the a traditional computations of CCP.

Acknowledgments This study was supported by the National Institute of Health Research, Biomedical Research Centre (Neuroscience Theme), NIHR Senior Investigator Awards (JDP) and the Medical Research Council (Grants G0600986 and G9439390).

Conflict of interest ICM+ Software is licensed by Cambridge Enterprise, Cambridge, UK, <http://www.neurosurg.cam.ac.uk/icmplus/>. MC and PS have a financial interest in a fraction of the licensing fee.

References

- Lundberg N. Continuous recording and control of ventricular fluid pressure in neurosurgical practice. *Acta Psychiatr Scand Suppl.* 1960;36(149):1–193.
- Rosner MJ, Becker DP. Origin and evolution of plateau waves. Experimental observations and a theoretical model. *J Neurosurg.* 1984;60(2):312–24.
- Hayashi M, Handa Y, Kobayashi H, Kawano H, Ishii H, Hirose S. Plateau-wave phenomenon (I). Correlation between the appearance of plateau waves and CSF circulation in patients with intracranial hypertension. *Brain.* 1991;114(Pt 6):2681–91.
- Hayashi M, Kobayashi H, Handa Y, Kawano H, Kabuto M. Brain blood volume and blood flow in patients with plateau waves. *J Neurosurg.* 1985;63(4):556–61.
- Castellani G, Zweifel C, Kim DJ, Carrera E, Radolovich DK, Smielewski P, Hutchinson PJ, Pickard JD, Czosnyka M. Plateau waves in head injured patients requiring neurocritical care. *Neurocrit Care.* 2009;11(2):143–50.
- Czosnyka M, Smielewski P, Piechnik S, Schmidt EA, Al-Rawi PG, Kirkpatrick PJ, Pickard JD. Hemodynamic characterization of intracranial pressure plateau waves in head-injury patients. *J Neurosurg.* 1999;91(1):11–9.
- Hayashi M, Kobayashi H, Kawano H, Yamamoto S, Maeda T. Cerebral blood flow and ICP patterns in patients with communicating hydrocephalus after aneurysm rupture. *J Neurosurg.* 1984; 61(1):30–6.

8. Risberg J, Lundberg N, Ingvar DH. Regional cerebral blood volume during acute transient rises of the intracranial pressure (plateau waves). *J Neurosurg*. 1969;31(3):303–10.
9. Hayashi M, Kobayashi H, Kawano H, Handa Y, Yamamoto S, Kitano T. ICP patterns and isotope cisternography in patients with communicating hydrocephalus following rupture of intracranial aneurysm. *J Neurosurg*. 1985;62(2):220–6.
10. Avezaat CJJ, van Eijndhoven JHM. Cerebrospinal fluid pulse pressure and craniospinal dynamics. A theoretical clinical and experimental study. Thesis. The Hague: A Jongbloed; 1984.
11. Rosner MJ. Pathophysiology and management of increased intracranial pressure. *Care: Neurosurg Int*; 1999. p. 57–112.
12. Matsuda M, Yoneda S, Handa H, Gotoh H. Cerebral hemodynamic changes during plateau waves in brain-tumor patients. *J Neurosurg*. 1979;50(4):483–8.
13. Gjerris F, Borgesen SE, Hoppe E, Boesen F, Nordenbo AM. The conductance to outflow of CSF in adults with high-pressure hydrocephalus. *Acta Neurochir (Wien)*. 1982;64(1–2):59–67.
14. Batorski L, Czosnyka M, Laniewski P, Zaworski W. Application of advanced forms of intracranial pressure analysis in craniostylosis. In: Hoff JT, Betz AL, editors. *Intracranial pressure*, vol. VII. Berlin/Heidelberg/New York: Springer-Verlag; 1989. p. 189–92.
15. Renier D, Sainte-Rose C, Marchac D, Hirsch JF. Intracranial pressure in craniostenosis. *J Neurosurg*. 1982;57(3):370–7.
16. Czosnyka M, Pickard JD. Monitoring and interpretation of intracranial pressure. *J Neurol Neurosurg Psychiatry*. 2004;75:813–21.
17. Schmidt B, Czosnyka M, Schwarze JJ, Sander D, Gerstner W, Lumenta CB, Pickard JD, Klingelhofer J. Cerebral vasodilatation causing acute intracranial hypertension: a method for noninvasive assessment. *J Cereb Blood Flow Metab*. 1999;19(9):990–6.
18. Burton AC. Fundamental instability of the small blood vessels and critical closing pressure in vascular beds. *Am J Physiol*. 1951;164:330–1.
19. Brunner MJ, Greene AS, Sagawa K, Shoukas AA. Determinants of systemic zero-flow arterial pressure. *Am J Physiol* 1983; 245:H453–9.
20. Czosnyka M, Smielewski P, Piechnik S, Al-Rawi PG, Kirkpatrick PJ, Matta BF, Pickard JD. Critical closing pressure in cerebrovascular circulation. *J Neurol Neurosurg Psychiatry*. 1999;66: 606–11.
21. Panerai RB. The critical closing pressure of the cerebral circulation. *Med Eng Phys*. 2003;25:621–32.
22. Dewey RC, Pierer HP, Hunt WE. Experimental cerebral hemodynamics-Vasomotor tone, critical closing pressure, and vascular bed resistance. *J Neurosurg*. 1974;41(5):597–606.
23. López-Magaña JA, Richards HK, Radolovich DK, Kim DJ, Smielewski P, Kirkpatrick PJ, Pickard JD, Czosnyka M. Critical closing pressure: comparison of three methods. *J Cereb Blood Flow Metab*. 2009;29(5):1–7.
24. Panerai RB, Salinet AS, Brodie FG, Robinson TG. Influence of calculation method on estimates of cerebral critical closing pressure. *Physiol Meas*. 2011;32:1–16.
25. Ursino M, Di Giammarco P. A mathematical model of the relationship between cerebral blood volume and intracranial pressure changes: the generation of plateau waves. *Ann Biomed Eng*. 1991;19(1):15–42.
26. Richards HK, Czosnyka M, Pickard JD. Assessment of critical closing pressure in the cerebral circulation as a measure of cerebrovascular tone. *Acta Neurochir (Wien)*. 1999;141(11):1221–7.
27. Aaslid R, Lash SR, Bardy GH, Gild WH, Newell DW. Dynamic pressure–flow velocity relationships in the human cerebral circulation. *Stroke*. 2003;34(7):1645–9.
28. Michel E, Hillebrand S, von Twickel J, Zernikow B, Jorch G. Frequency dependence of cerebrovascular impedance in preterm neonates: a different view on critical closing pressure. *J Cereb Blood Flow Metab*. 1997;17:1127–31.
29. Puppo C, Camacho J, Yelicich B, Moraes L, Biestro A, Gomez H. Bedside study of cerebral critical closing pressure in patients with severe traumatic brain injury: a transcranial Doppler study. *Acta Neurosurg Suppl*. 2012;114:283–8.
30. Varsos GV, Richards H, Kasprovicz M, Budohoski KP, Brady KM, Reinhard M, Avolio M, Smielewski P, Pickard JD, Czosnyka M. Critical closing pressure determined with a model of cerebrovascular impedance. *J Cereb Blood Flow Metab*. 2012;33(2): 235–43.
31. Kim DJ, Kasprovicz M, Carrera E, Castellani G, Zweifel C, Lavinio A, Smielewski P, Sutcliffe MP, Pickard JD, Czosnyka M. The monitoring of relative changes in compartmental compliances of brain. *Physiol Meas*. 2009;30(7):647–59.
32. de Riva N, Budohoski KP, Smielewski P, Kasprovicz M, Zweifel C, Luzius A, Reinhard M, Fabregas N, Pickard JD, Czosnyka M. Transcranial Doppler pulsatility index: what it is and what it isn't. *Neurocrit Care*. 2012;17(1):58–66.
33. Czosnyka M, Richards HK, Reinhard M, Steiner AL, Budohoski K, Smielewski P, Pickard JD, Kasprovicz M. Cerebrovascular time constant: dependence on cerebral perfusion pressure and end-tidal carbon dioxide concentration. *Neurol Res*. 2012;34(1):17–24.
34. Kasprovicz M, Czosnyka M, Soehle M, Smielewski P, Kirkpatrick PJ, Pickard JD, Budohoski KP. Vasospasm shortens cerebral arterial time constant. *Neurocrit Care*. 2011;16(2):213–8; ISSN 1541-6933.
35. Carrera E, Kim DJ, Castellani G, Zweifel C, Smielewski P, Pickard JD, Kirkpatrick PJ, Czosnyka M. Cerebral arterial compliance in patients with internal carotid artery disease. *Eur J Neurol*. 2010;18:711–8.
36. Soehle M, Czosnyka M, Pickard JD, Kirkpatrick PJ. Critical closing pressure in subarachnoid hemorrhage: effect of cerebral vasospasm and limitations of a transcranial Doppler-derived estimation. *Stroke*. 2004;35(6):1393–8.
37. Gazzoli P, Frigerio M, De Peri E, Rasulo F, Gasparotti R, Lavinio A, Latronico N.A case of negative critical closing pressure. Abstracts of the 8th international conference on Xenon CT and related cerebral blood flow techniques: cerebral blood flow and brain metabolic imaging in clinical practice. *Br J Neurosurg*. 2006;20:348.
38. Daley ML, Leffler CW, Czosnyka M, Pickard JD. Plateau waves: changes of cerebrovascular pressure transmission. *Acta Neurochir Suppl*. 2005;95:327–32.

Discussion

The application in neurocritical care of multimodal brain monitoring together with advanced bioinformatics for computerized analysis help clinicians in early detection of secondary insults at the bedside and improve the clinical management of these patients. Besides this obvious contribution, having the chance to do off-line retrospective analysis allows investigators to revisit current concepts in order to improve our knowledge and understanding about their underlying pathophysiology¹⁶⁸. This is an extremely important issue because a significant number of clinical decisions are taken on the basis of data that, if wrongly interpreted, may derive in detrimental clinical decisions¹⁹².

Considering these facts, we decided to revisit the pathophysiology underlying two classical concepts as TCD pulsatility index (PI) and critical closing pressure (CCP) with data obtained from TCD and multimodal monitoring of TBI patients, with the help of advanced bioinformatics (ICM+[®] software) and the support of a multidisciplinary team that included both physicians and engineers (Prof M. Czosnyka, P. Smielewski and GV Varsos) among other contributors. Both parameters had been described for a long time, but conclusions regarding their interpretation and applicability had been controversial for many years and sometimes reporting completely opposing results^{72,73}.

TCD-based pulsatility index (PI) is a haemodynamic index derived from the TCD waveform and is often interpreted as a descriptor of the distal cerebrovascular resistance (CVR)¹⁸⁶.

However, an experimental study in rabbits by Czosnyka *et al.* with a controlled decrease of CVR had already shown that in physiological conditions hypercapnia decreased both CVR and PI while a reduction in CPP in autoregulating animals caused also a decrease in CVR but an increase in PI. So their final conclusion was that PI could not be interpreted simply as an index of CVR in all circumstances⁶⁸.

To our knowledge, no studies had been published since then regarding which factors truly determine and influence the PI value, so we decided to review this concept with analysis of data obtained from the clinical setting. For the development of this first article of this thesis we opted to reanalyse already recorded multimodal monitoring data including TCD from severe TBI patients that had been admitted in a european reference neurocritical care unit (Addenbrooke's hospital, Cambridge, UK) where the doctorand developed this project. We opted for this pathology as it is a prevalent condition that has an extreme health and social impact, and because almost 50% of these patients present intracranial hypertension along their evolution, a deleterious fact that has been proven to be clearly associated with a worse outcome⁹⁷.

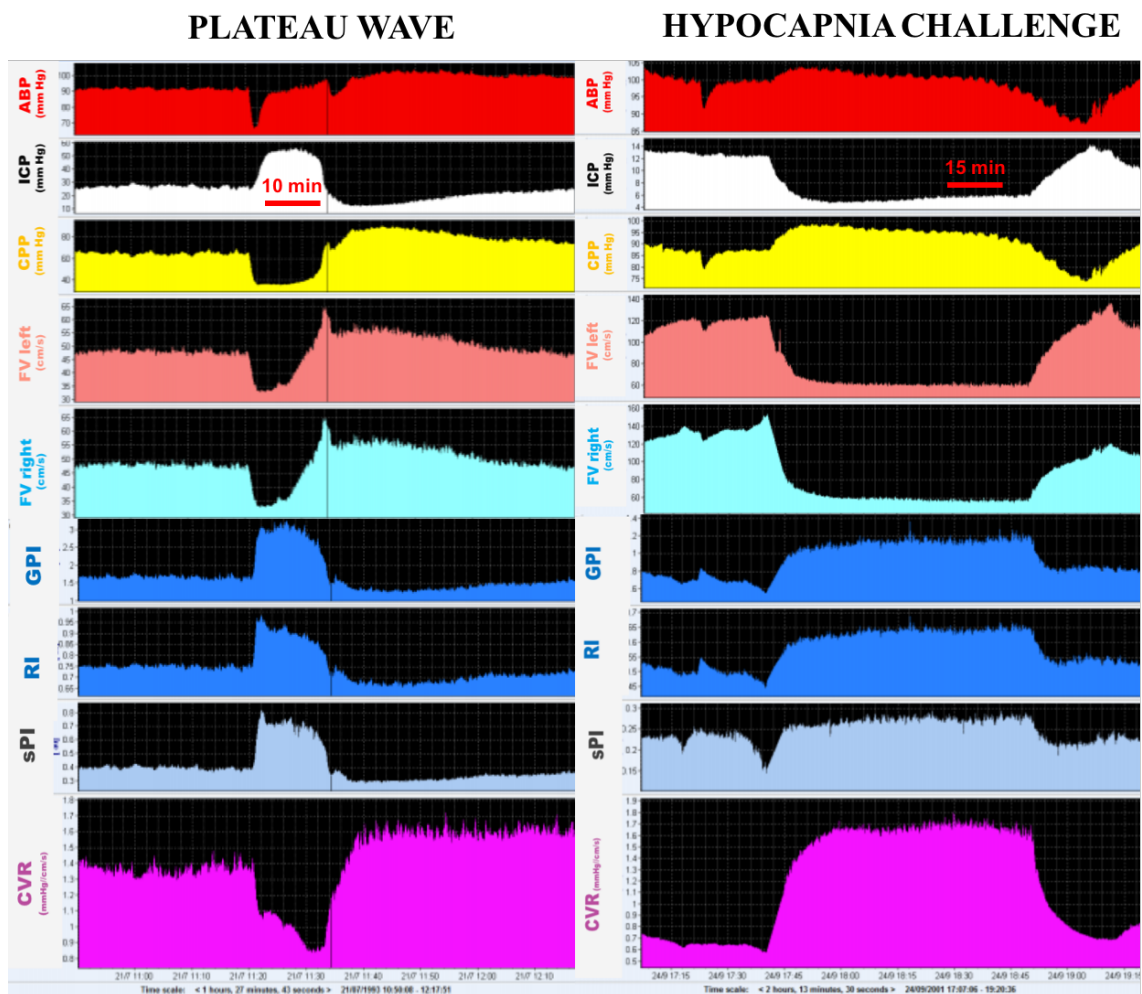
As we wanted to analyse the relation between CVR and PI, we decided to confront two clinical situations, plateau waves and hypocapnia challenges, where opposite changes in CVR are known and observed.

Our first group included 20 severe TBI patients that developed plateau waves of intracranial hypertension. Due to their previously explained pathophysiology, this phenomena represent an excellent model of cerebrovascular vasodilation related to the presence of functioning cerebral autoregulation.

In contrast, we had a second cohort of 31 patients where a short hypocapnia stimulus was applied to assess cerebrovascular vasoreactivity. Hypocapnia increases CVR by cerebral vasoconstriction at the level of the cerebral resistance vessels.

A first analysis of our results prove the concept that TCD-based pulsatility index is wrongly interpreted as merely a descriptor of the distal cerebrovascular resistance¹⁸⁶. During vasodilatation leading to plateau waves, CVR decreases while hypocapnia induces a vascular constriction that leads to an increase in CVR. Despite opposite changes in CVR we observed that PI in both cases increased, reinforcing the concept that PI cannot be interpreted as an index of CVR alone (see figure 1).

Figure 1. Timetrends recordings with ICM+[®] software of arterial blood pressure (ABP), intracranial pressure (ICP), cerebral perfusion pressure (CPP), left and right cerebral blood flow velocities, Gosling pulsatility index (GPI), Pourcelot resistance index (PRI, calculated as [FVs-FVd]/FVm), “spectral” pulsatility index (sPI), and cerebrovascular resistance (CVR) in two different patients of the study. *Top panel* plateau wave of ICP. *Bottom* Hypocapnia in a CO₂ vasoreactivity test. The figure demonstrates an increase in PI in both situations, while CVR decreases during the plateau wave (due to the vasodilation) but increases during the hypocapnic challenge (due to the cerebral vasoconstriction).



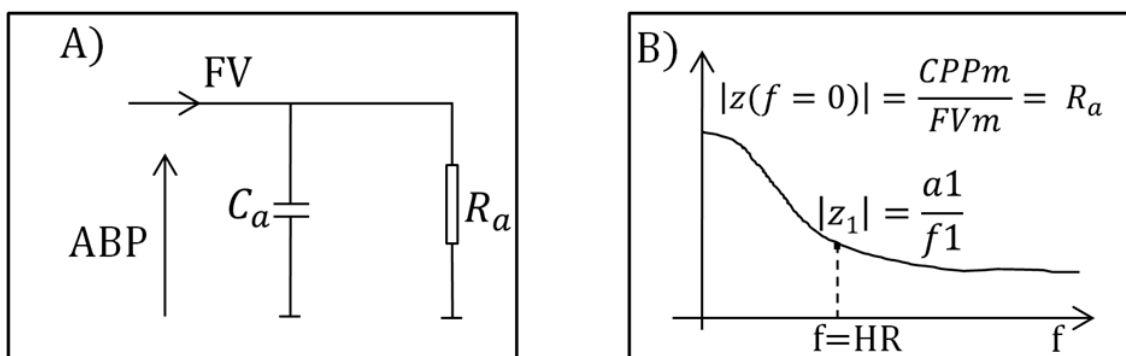
It is also important to consider the fact that in both situations ICP changed inversely (i.e. increased during plateau waves and slightly decreased during hypocapnia), therefore universal description of rising ICP by rising PI is also questionable. In this study combined data from recordings of both cohorts was used to study the regression between all points of PI and ICP and then between CPP and PI, with a best reciprocal fit for CPP. A further-in study by Zweifel et al⁷⁴ concluded that the diagnostic value of PI for direct non-invasive assessment of ICP and CPP is very limited but may have value as a screening tool for identification of patients at risk when highly elevated ICP or dangerously decreased CPP is suspected⁷⁵. But unfortunately PI is not a reliable diagnostic tool for detecting critical clinical thresholds (as ICP > 20 mm Hg or CPP < 60 mm Hg)⁷⁴.

The next step in our investigation was to search for the hemodynamic factors that could determine the reactions of PI. Using the concept of impedance to CBF we described a mathematical model of cerebrovascular impedance where capacitance (i.e. cerebrovascular compliance, C_a) and resistance (cerebrovascular resistance, CVR or R_a) are in parallel such that impedance to flow is considered as a function of heart rate (see figure 2).

It should be noted that resistance is a concept used for direct current (DC), whereas impedance is the AC (alternating current) equivalent. In this model, impedance is used instead of resistance based on the pulsatile characteristics of the cerebral circulation. Details of the mathematical analysis are given in Appendix of the first article, but are beyond the scope of this thesis.

Figure 2. Mathematical model of cerebrovascular impedance. **a)** Simplified electrical model of the cerebrovascular circulation used for the derivation of the formula describing the modelled PI (calculated for fixed frequency of heart rate). [ABP arterial blood pressure, C_a cerebrovascular compliance, FV flow velocity, R_a cerebrovascular resistance].

b) Diagram of cerebrovascular impedance $|Z(f)|$ as a function of frequency (f) in Hz. Two frequencies are considered: $f = 0$ (i.e. direct current component) and $f = HR$. Module of impedance for $f = 0$ is equal to R_a , and may be estimated as CPP_m/FV_m . [a_1 pulse amplitude (first harmonic) of ABP, ABP arterial blood pressure, CPP_m mean cerebral perfusion pressure, f frequency, f_1 pulse amplitude (first harmonic) of blood FV, FV_m mean blood flow velocity in the middle cerebral artery, HR heart rate frequency (beats/min), PI pulsatility index, R_a cerebrovascular resistance (also expressed in the text as CVR), $|z|$ cerebrovascular impedance, $|z_1|$ cerebrovascular impedance with frequency equal to HR].



According to the relations determined in this model of cerebrovascular impedance, PI can be defined by the following formula

$$PI = \frac{a1}{CPP} \times \sqrt[2]{(Ra \times Ca \times HR \times 2\pi)^2 + 1} \quad (\text{formula 1})$$

where $a1$ is the fundamental harmonic of arterial blood pressure, CPP is the mean cerebral perfusion pressure, Ra is the cerebrovascular resistance, Ca is the compliance of the cerebral arterial bed, and HR denotes heart rate (in beats/second). Although Ca and Ra cannot be measured directly, they can be estimated using TCD blood FV and ABP and CPP waveforms according to an algorithm described in previous mathematical studies^{193,194}.

We have demonstrated, by using this mathematical model of cerebrovascular impedance, the possible input signals determining the reactions of PI. Analysis of the model suggests that PI is determined by the interplay of the value of CPP, the fundamental harmonic of ABP pulse ($a1$), cerebrovascular resistance (Ra), compliance of the cerebral arterial bed (Ca), and heart rate.

Plateau waves are defined as any sudden elevation of ICP above 50 mmHg that lasts longer than 5 minutes and terminates spontaneously or in response to treatment. Multimodal brain monitoring helps to distinguish and describe them. They are thought to be caused by a vasodilatory cascade, which may be triggered by vasodilatory events such as small oscillations in ABP, brain oxygenation or arterial CO₂, in the presence of functioning cerebrovascular reactivity and low cerebrospinal compensatory reserve^{103,152}.

These frequent cerebrovascular phenomena in TBI, are not usually associated with worse outcome unless they are longer than 30 minutes¹⁰⁴. Nonetheless, poor outcome after TBI is associated with sustained intracranial hypertension or low oxygenation⁹⁷.

During plateau waves the profound reduction in CPP, usually below the LLA, is accompanied by a decreased CBF¹⁵⁴ and oxygenation¹⁵³. On the other hand, the vasodilatation leads to an increase in cerebral blood volume (CBV), which is associated with an increase in cerebral arterial compliance (Ca)¹⁹⁵. As the pulse amplitude of ABP ($a1$) remains fairly stable, during plateau waves PI changes inversely to the changes in CPP. Most probably, changes in both Ca and Ra balance each other, therefore none of them play a major role in determining PI.

The second group involves patients submitted to short term hypocapnia to assess CO₂ reactivity. Based on the available evidence, the most recent “Guidelines for the Management and Prognosis of Severe Traumatic Brain Injury” still include moderate manipulation of the arterial partial pressure of CO₂ (PaCO₂) as an option to treat raised ICP⁸⁸. The beneficial effect of hyperventilation is due to a reduction in CBV, through vasoconstriction¹⁹⁶. Therefore, the observed increase in cerebrovascular resistance (stated as CVR or Ra) was expected in this group of patients. It has been already shown that changes in Ra are stronger than changes in Ca during controlled changes of PaCO₂ in an experimental setup¹⁹⁴. Most likely, a similar situation

exists during hypocapnia in clinical conditions, therefore the observed increase in PI follows an increase in the product of Ra and Ca combined with a slight decrease in CPP.

According to the described mathematical model (formula 1) PI is a complex function of many mutually interdependent hemodynamic parameters. PI increases when the amplitude of ABP (a_1) increases as well as during arterial hypotension and intracranial hypertension through changes in CPP. PI also increases when the product of Ra , Ca and HR increases^{195,197}, which had not been studied thoroughly before. Theoretically, the product of cerebrovascular compliance (Ca) and resistance (Ra) expresses the time constant of the cerebral arterial bed, also denoted as TAU¹⁹⁷.

As defined in the introduction, TAU is a concept derived from the electrical circuits, and theoretically reflects the time (in seconds) it takes for the arterial blood load during the cardiac cycle to get through the arterial component of the cerebral circulation¹¹³. If the large conductant vessel is poorly compliant, as in cerebral vasospasm, and the resistance is decreased because of vasodilation of arterioles, blood takes less time to get through the arterial circulation (low TAU)¹⁹⁸.

On the other hand, if the conductance vessels compliance is increased and the arterioles are constricted leading to a high cerebrovascular resistance (Ra), blood will stay longer inside the arterial circuit (high TAU). The longer this time constant, the longer the time interval which is needed for arterial blood volume to arrive (from the point of TCD insonation) at the cerebral resistive vessels.

In the experimental study mentioned above¹⁹⁷, the time constant (i.e. TAU) has been shown to increase with hypocapnia and with reductions in CPP (caused by both arterial hypotension and rise in ICP). Similarly the PI in these scenarios will increase.

There are several limitations in this first study of the thesis. First, the sides of TCD insonation and of the ICP probe were not standardized. Although in most of the cases the ICP probe was placed in the right anterior frontal lobe, the side of the analyzed TCD signal depended on the qualities of both the insonated window and the recording. However, we cannot exclude that our data might have been more reliable if it had been based on the average of bilateral TCD readings. Neither can we exclude the influence in cases with unilateral lesions.

Limitations of the method used to calculate cerebral arterial blood volume (CaBV), Ca and Ra from pulsatile waveforms of FV and ABP for the calculation of the cerebrovascular time constant have been discussed in their original publications^{195,199}. Monitoring the changes in cerebrovascular compliance is difficult and in order to obtain absolute measures requires the application of phase-contrast MRI^{83,200}. Years ago Kim et al developed a computational method allowing a continuous assessment of relative changes in cerebral compartmental compliances based on the relationship between pulsatile components of ABP, ICP and the CaBV¹⁹⁵. However, this method is an estimation only, it does not allow to assess absolute values of Ca but only its relative changes.

In the past, another mathematical model had been proposed, linking TCD pulsatility index and critical closing pressure²⁰¹. But these formulas differ as the one we present links PI with physiological model parameters.

The second study (Varsos GV, de Riva N, Smielewski P *et al.*) included in this thesis aims to characterize the proposed vasodilatory pathophysiology of ICP plateau waves by using the concept of critical closing pressure (CCP), which is related to cerebrovascular vasomotor tone, represented by arterial wall tension (WT). The patients included in this second study are the same ones studied in the first article of this thesis (PI investigation) as the “plateau wave group” (n= 20 patients, a total of 38 plateau waves).

CCP is the level of ABP at which small brain vessels collapse and CBF ceases. As such, it is a metric that has inspired theoretical interest but has been relatively neglected as a clinical application. In theory, CCP can enhance our understanding in regard of cerebral haemodynamics when CPP is below the lower limit of autoregulation (LLA). In that sense, CCP may provide a second higher-risk threshold of cerebral perfusion pressure, where CBF ceases completely.

Since Burton’s theoretical model²⁰² ($CCP = ICP + WT$), different *traditional* TCD-derived methods to calculate this zero-flow pressure have been described^{188,203} but present the drawback of frequent negative non-physiologic values of CCP. The first harmonic model of CCP (CCP1) proposed by Michel¹⁰⁹ seems to be the most robust among them¹⁸⁸:

$$CCP1 = ABP - A1 \times \frac{FV}{F1}$$

where $A1$ and $F1$ are amplitudes of the fundamental harmonics of ABP and FV waveforms, obtained from the fast Fourier transfer (FFT) .

The *traditional* calculation of WT was calculated using Dewey’s model as:

$$WT1 = CCP1 - ICP$$

Searching for a more accurate method, and based on the analysis of the same simple model of cerebrovascular impedance previously described to calculate pulsatility index (PI)¹¹¹, Varsos et al reported in 2013 a multi-parameter mathematical model for estimation of CCP (CCPm) according to the following formula (2)¹¹⁰:

$$CCPm = ABP - \frac{CPP}{\sqrt{(Ra \times Ca \times HR \times 2\pi)^2 + 1}} \quad (\text{formula 2})$$

where CPP is the mean cerebral perfusion pressure (calculated as $CPP = ABP - ICP$), Ra denotes cerebrovascular resistance, Ca stands for the pulsatile compliance of the cerebral arterial bed, and HR denotes heart rate (beats/second). As previously explained, Ca and Ra cannot be measured directly and need to be estimated. Their estimation can be made using TCD blood flow velocity and ABP and CPP waveforms according to the previously referred algorithm^{193,194}.

Arterial WT can be associated with these cerebrovascular physiological parameters by creating its multiparameter mathematical descriptor. This model WT (WTm) was calculated also using Dewey's equation, which denotes WT to be estimated as the difference between the mathematical descriptor model of CCP (CCPm) and the measured ICP.

$$WTm = CCPm - ICP$$

Again, it is important to remark the interplay between *Ra* and *Ca* as it was previously exposed. TAU decreases during hypercapnia suggesting a decrease in WT (providing no change in CPP is present) and correspondingly to CCP owing to vasodilation. Similarly, TAU decreases in carotid artery stenosis, where distal vasodilation is present, suggesting again a compensatory decrease in WT and CCP. TAU decreases even further with bilateral carotid stenosis. On the other hand, TAU was shown to increase during a decrease in CPP, both as a result of arterial hypotension or intracranial hypertension, keeping with the expected autoregulatory vasodilation observed with decreased CPP.

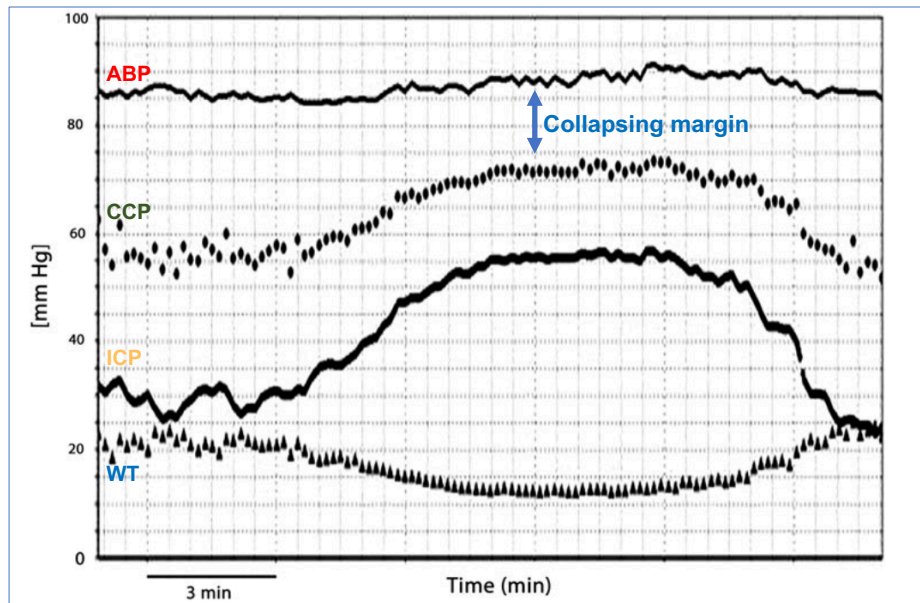
The primary aim of this second study of this thesis was to measure CCP during plateau waves in order to examine their pathophysiology by using the concepts of CCP and arterial WT. Our results show that during the vasodilatory loop of the plateau waves, there is a rise in CCP and a reduction in WT, with both of them being significant ($p < 0.001$). However, the effect of rising ICP is more pronounced than the corresponding vasodilatory response decreasing WT. These results were demonstrated and significant with both the traditional (CCP1 and WT1) and the multi-parameter methods (CCPm and WT) of calculation.

Some investigators have coined the term “effective cerebral perfusion”¹¹⁴ or “closing collapsing margin”²⁰⁴ to refer to the difference between mean ABP and CCP. They argue that this “collapsing margin” would be a better descriptor of the real driving pressure for the arterial cerebral circulation instead of CPP (= ABP-ICP) as CCP is higher than ICP and takes into account the tone of the vessels (i.e. the contribution of wall tension)^{106,107,114}.

However, even though we found a strong bivariate correlation between CPP and the “collapsing margin” ($R = 0.844$, $p < 0.001$), the “collapsing margin” is different from CPP in at least two aspects. First, the “collapsing margin” accounts for changes in WT, which do not influence the CPP equation. Second, the “collapsing margin” indicates the amount of pressure reserve available to avoid total cease of CBF, whereas CPP indicate the perfusion pressure driving CBF and does not have an inherently meaningful threshold.

In our study the observed increased CCP during plateau waves imposes an elevated risk for brain vessels to collapse, especially if ABP remains almost constant. Therefore, the “safety collapsing margin” ($ABP - CCP$) decreased significantly ($p < 0.001$) in this cohort from baseline ICP to plateau levels, indicating that the probability for brain vessels to collapse is increased during this phenomenon (see **figure 3**).

Figure 3. Example of the behaviour of CCP and WT (calculated with the multi-parameter mathematical model) during a plateau wave of intracranial pressure. The “collapsing margin” is referred as the difference between ABP and CCP waveforms. On the other hand, the gap between CCP and ICP waveforms indicates the active vasomotor tone, represented as the wall tension. *ABP* arterial blood pressure, *CCP* critical closing pressure (with the multi-parameter model), *ICP* intracranial pressure, *WT* wall tension (with the multi-parameter model).



Besides the fact that several models of dynamic cerebral autoregulation use CCP in their formulations^{31,205}, a reliable calculation for CCP and monitoring of the “collapsing margin” may have a future role in the care of neurocritical patients.

On one hand, a measurement of CCP for a neurocritical patient would provide a threshold for the patient’s ABP below which irreversible brain ischaemia may be developed. In fact, it has been demonstrated that diastolic ABP lower than CCP is associated with loss of measurable blood FV during diastole when TCD is used¹¹⁵.

Its knowledge would help clinicians to manage ABP, ICP and also vascular tone by itself. Specific patients could have a low ICP but a high WT with a consequent high CCP and a low “closing margin”, while the clinician has a false safety feeling.

Also, identifying patients with frequent decrements in the “collapsing margin” may improve the selection of patients who would benefit from a decompressive craniectomy.

The second aim of this second study was to verify the performance of a novel multiparameter mathematical model for calculating critical closing pressure (CCPm), in clinical cases of sudden increases of ICP like plateau waves. The introduction of parameters describing the cerebral

circulation aids the understanding of factors influencing the dynamics of CCP during plateau waves.

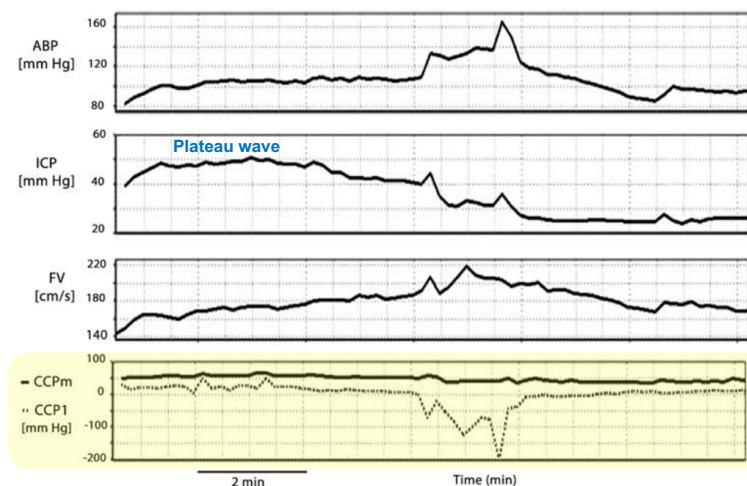
A retrospective analysis of experimental animal data proved that CCPm is well correlated to the traditional method used to calculate CCP from the fundamental harmonic of pulse-frequency TCD and pressure changes (CCP1)¹¹⁰. A more recent clinical study by Puppo *et al.* comparing these same methods also corroborated the experimental findings by Varsos *et al.*¹⁰⁷.

The same high correlation ($R = 0.87$; $p < 0.001$) is seen in this study of plateau waves in clinical patients, further enhancing the conclusion of similarity of the two methods and thus proving the validity of CCPm. Divergence between ‘traditional’ (CCP1) and ‘modeled’ CCP (CCPm) can be seen only when CCP1 achieves non-physiologically low (or negative) values^{108,110,206}, but that makes the agreement too poor to interchange them.

The issue of low and negative non-interpretable values of CCP has been a known drawback of traditional calculation methods in cases like hypercapnia-induced hyperaemia, vasospasm, or with artificially elevated diastolic blood flow velocity^{108,206,207}. In plateau waves, CCP1 rendered negative values in a variety of situations where changes in amplitude and mean values of FV and/or ABP took place. The appearance of these values is considered to be a methodological limitation, as there is no physiological explanation for negative values of WT.

In contrast, CCPm, calculated with the concept of impedance, was proven to overcome this drawback. CCPm cannot render non-physiological negative values when physiological values of ABP, CPP and FV are provided^{110,194}, and is, therefore, more relevant to actual clinical reality complying with CCP definition and concept (see figure 4).

Figure 4. Example of first harmonic model of critical closing pressure (CCP1) demonstrating non-physiologic negative values during the recovery time after a plateau wave. Negative CCP1 were caused by increased values of mean flow velocity (FVm). In contrast, the multi-parameter mathematical model (CCPm) rendered always positive values. *ABP* arterial blood pressure, *CCP1* critical closing pressure (with the first harmonic TCD-derived model), *CCPm* critical closing pressure (with the multi-parameter model), *FVm* mean blood flow velocity in the middle cerebral artery, *ICP* intracranial pressure.



The validity of WT calculation via cerebrovascular impedance was also proven, with WTm being significantly correlated to WT1 ($p < 0.001$) during the plateau waves, as has been also proven in experimental animal data¹¹⁰.

Like CCPm, the use of WTm has the advantage of consistently positive values, unlike the fundamental harmonic model WT1, which presents senseless negative values. Decrease in WTm is in agreement with modelling data presented previously by Daley et al²⁰⁸, although our study takes into account changes in CBF, confirming validity of previous analysis done using ICP and ABP waveforms. Impaired autoregulation has been found to be associated with a lower WT supporting the role of vasoparalysis in the loss of autoregulatory capacity²⁰⁹.

This second study of the thesis has a number of limitations that deserve discussion. First, the small number of patients does not allow to test for an association between the collapsing margin and outcome. Plateau waves, although are observed in 40% of TBI patients¹⁰⁴, are difficult to be captured with limited time (10 minutes to 1 hour) TCD recording in the neurocritical care unit. However, having set the theoretical basis of the collapsing margin, a similar study of a larger cohort of patients is indicated.

The major drawback of the multi-parameter mathematical model for calculating CCP is the requirement of invasive ICP monitoring; and therefore, it cannot be calculated noninvasively. However, in subjects at risk for plateau waves ICP monitoring is a standard care, which increases the clinical relevance of the technique demonstrated in this study. Also, it is recognized that CPP is a more accurate estimate of the transmural pressure gradient and therefore is more relevant to changes in vasomotor tone.

A third remarkable issue is that estimation of CCP requires good quality recording of CBF velocity through TCD in order to obtain an accurate calculation of Ra and Ca . As it's been explained TCD monitoring sessions were not continuous like ABP and ICP monitoring, but instead were performed for short periods for every patient on a daily basis.

The short periods were justified by the difficulty of having continuous TCD measurements, as the head injured patients were treated in a neurointensive care environment, thus subjected to change in position or transfers (e.g. for the purpose of a CT or MRI scan), which would result in intervention of TCD recordings.

On that basis, it might be possible that not all the occurred plateau waves have been captured. However, as the aim of this study was to estimate CCP during the specific phenomenon of occurring plateau waves and not continuously, we think this limitation does not affect its purposes.

It is also important to keep in mind the factors that have been reported to have an influence on CCP values. Hypocapnia (as induced by mild hyperventilation) generally increases CCP due to vasoconstriction, while vasodilatation decreases CCP. Nevertheless, in these patients there was no significant change in PaCO₂ levels as clinical management was performed maintaining normocapnia.

It has been reported that CCP may be disturbed by localised brain lesions with CCP asymmetry corresponding to asymmetrical findings on CT scans in head injury²¹⁰. CCP also reflects asymmetry in common carotid artery stenotic disease and decreases “artificially” during vasospasm²⁰⁶. However, none of these factors were considered in our analysis as the aims of our study were focused on characterizing the vasodilatory pathophysiology of plateau waves with the newly defined method.

As a final remark, the retrospective character of the recordings included in both studies is in fact a limiting factor, but probably not a serious limitation. Multiple use of continuous collection of biological signals for retrospective big data analysis and to conduct mathematical modelling studies is scientifically sound and allows an in-depth study of cerebral haemodynamics.

Conclusions

1. During the plateau waves the increase in intracranial pressure provoked a significant decrease in cerebral perfusion pressure, mean blood flow velocity and diastolic blood flow velocity, but an increase in systolic flow velocity. Pulsatility index increased significantly but cerebrovascular resistance decreased.
2. Hyperventilation challenge induced a small but significant decrease in intracranial pressure. However, pulsatility index as well as cerebrovascular resistance increased significantly.
3. The mathematical formula provided to describe pulsatility index shows a good correlation with the measured values of pulsatility index.
4. The presented mathematical model is able to explain the input signals with influence on pulsatility index.
5. Pulsatility index is not dependent solely on cerebrovascular resistance. It is a product of the interplay between cerebral perfusion pressure, pulse amplitude of arterial pressure, cerebrovascular resistance and compliance of the cerebral arterial bed, as well as the heart rate.
6. Pulsatility index is not an accurate estimator of intracranial pressure; it describes cerebral perfusion pressure in a more accurate manner.
7. During plateau waves of intracranial pressure, critical closing pressure increases significantly while active vasomotor tone, represented by wall tension, decreases due to vasodilation.
8. Estimation of critical closing pressure based on the impedance methodology disallows non-physiologic negative values.
9. Critical closing pressure and wall tension based on the impedance methodology allow an accurate analysis of plateau waves pathophysiology in contrast to the traditional computations.
10. The main disadvantage of the impedance mathematical model is the requirement of invasive intracranial pressure monitoring. But if a good quality recording of transcranial Doppler flow velocity is achieved, the effect of plateau waves may be clinically useful within the other monitoring parameters setting.
11. Multimodality neuromonitoring integrated with bio-informatics analysis (ICM+[®] Software) provide new insights into physiologic variables as pulsatility index and critical closing pressure.

References

1. Williams LR, Leggett RW. Reference values for resting blood flow to organs of man. *Clin Phys Physiol Meas*. 1989;10(3):187-217.
2. Vavilala MS, Lee LA, Lam AM. Cerebral blood flow and vascular physiology. *Anesthesiol Clin North America*. 2002;20(2):247-64, v.
3. Dagal A, Lam AM. Cerebral blood flow and the injured brain : how should we monitor and manipulate it ? 2011. doi:10.1097/ACO.0b013e3283445898.
4. Kandel E. *Principles of Neural Science*. 4th ed. (Kandel, Eric R; Schwartz, James H; Jessell TM., ed.). New York: McGraw Hill; 2000.
5. Gobiet W, Grote W, Bock WJ. The relation between intracranial pressure, mean arterial pressure and cerebral blood flow in patients with severe head injury. *Acta Neurochir (Wien)*. 1975;32(1-2):13-24.
6. Zweifel, Christian; Hutchinson, Peter; Czosnyka M. Intracranial pressure. In: Matta, Basil F; Menon, David K; Smith M, ed. *Core Topics in Neuroanaesthesia and Neurointensive Care*. First Edit. New York: Cambridge University Press; 2011:45-62.
7. Meng L, Hou W, Chui J, Han R, Gelb AW. Cardiac Output and Cerebral Blood Flow. *Anesthesiology*. 2015;123(5):1198-1208. doi:10.1097/ALN.0000000000000872.
8. Fog M. The relationship between the blood pressure and the tonic regulation of the pial arteries. *J Neurol Psychiatry*. 1938;1(3):187-197.
9. Fog M. The reaction of the pial arteries to a fall in blood pressure. *Arch Neurol Psychiatry*. 1937;(37):351-364.
10. Lassen NA. Cerebral blood flow and oxygen consumption in man. *Physiol Rev*. 1959;39(2):183-238.
11. Paulson OB, Strandgaard S, Edvinsson L. Cerebral autoregulation. *Cerebrovasc Brain Metab Rev*. 1990;2(2):161-192.
12. Kontos HA, Wei EP, Navari RM, Levasseur JE, Rosenblum WI, Patterson JL. Responses of cerebral arteries and arterioles to acute hypotension and hypertension. *Am J Physiol*. 1978;234(4):H371-83.
13. Andresen J, Shafi NI, Bryan RM. Endothelial influences on cerebrovascular tone. *J Appl Physiol*. 2006;100(1):318-327. doi:10.1152/jappphysiol.00937.2005.
14. Budohoski KP, Czosnyka M, Kirkpatrick PJ, Smielewski P, Steiner LA, Pickard JD. Clinical relevance of cerebral autoregulation following subarachnoid haemorrhage. *Nat Rev Neurol*. 2013;9(3):152-163. doi:10.1038/nrneurol.2013.11.
15. Tan CO. Defining the characteristic relationship between arterial pressure and cerebral flow. *J Appl Physiol*. 2012;113(8):1194-1200. doi:10.1152/jappphysiol.00783.2012.
16. Czosnyka M, Brady K, Reinhard M, Smielewski P, Steiner LA. Monitoring of cerebrovascular autoregulation: facts, myths, and missing links. *Neurocrit Care*. 2009;10(3):373-386. doi:10.1007/s12028-008-9175-7.
17. McDowall DG. Cerebral blood flow and metabolism in acute controlled hypotension: implications for hypotensive anaesthesia. *Acta Med Scand Suppl*. 1983;678:97-103.
18. Fitch W, Ferguson GG, Sengupta D, Garibi J, Harper AM. Autoregulation of cerebral blood flow during controlled hypotension in baboons. *J Neurol Neurosurg Psychiatry*. 1976;39(10):1014-1022.
19. Strandgaard S. Autoregulation of cerebral blood flow in hypertensive patients. The modifying influence of prolonged antihypertensive treatment on the tolerance to acute, drug-induced hypotension. *Circulation*. 1976;53(4):720-727.
20. Dagal A, Lam AM. Cerebral autoregulation and anesthesia. *Curr Opin Anaesthesiol*. 2009;22(5):547-552. doi:10.1097/ACO.0b013e32833020be.
21. Aaslid R, Lindegaard KF, Sorteberg W, Nornes H. Cerebral autoregulation dynamics in humans. *Stroke*. 1989;20(1):45-52.
22. Giller CA. A bedside test for cerebral autoregulation using transcranial Doppler ultrasound. *Acta Neurochir (Wien)*. 1991;108(1-2):7-14.
23. Czosnyka M, Smielewski P, Kirkpatrick P, Menon DK, Pickard JD. Monitoring of cerebral autoregulation in head-injured patients. *Stroke*. 1996;27(10):1829-1834.
24. Diehl RR, Linden D, Lücke D, Berlitz P. Phase relationship between cerebral blood flow velocity and blood pressure. A clinical test of autoregulation. *Stroke*. 1995;26(10):1801-

- 1804.
25. Zhang R, Zuckerman JH, Giller CA, Levine BD. Transfer function analysis of dynamic cerebral autoregulation in humans. *Am J Physiol.* 1998;274(1 Pt 2):H233-41.
 26. Kontos HA. Validity of Cerebral Arterial Blood Flow Calculations From Velocity Measurements. *Stroke.* <http://stroke.ahajournals.org/content/20/1/1.full.pdf>. Published 1989. Accessed March 9, 2016.
 27. Lang EW, Mehdorn HM, Dorsch NWC, Czosnyka M. Continuous monitoring of cerebrovascular autoregulation: a validation study. *J Neurol Neurosurg Psychiatry.* 2002;72(5):583-586.
 28. Budohoski KP, Zweifel C, Kasprowitz M, et al. What comes first? the dynamics of cerebral oxygenation and blood flow in response to changes in arterial pressure and intracranial pressure after head injury. *Br J Anaesth.* 2012;108(1):89-99. doi:10.1093/bja/aer324.
 29. Lee JK, Brady KM, Mytar JO, et al. Cerebral blood flow and cerebrovascular autoregulation in a swine model of pediatric cardiac arrest and hypothermia. *Crit Care Med.* 2011;39(10):2337-2345. doi:10.1097/CCM.0b013e318223b910.
 30. Badenes R, García-Pérez ML, Bilotta F. Intraoperative monitoring of cerebral oximetry and depth of anaesthesia during neuroanaesthesia procedures. *Curr Opin Anaesthesiol.* 2016;29(5):576-581. doi:10.1097/ACO.0000000000000371.
 31. Tiecks FP, Lam AM, Aaslid R, Newell DW. Comparison of static and dynamic cerebral autoregulation measurements. *Stroke.* 1995;26(6):1014-1019.
 32. Gibbs F A; Gibbs E L; Lennox WG. Changes in human cerebral blood flow consequent on alterations in blood gases. *Am J Physiol.* 1935;(111):557-563.
 33. Meng L, Gelb AW. Regulation of Cerebral Autoregulation by Carbon Dioxide. *Anesthesiology.* 2015;122(1):196-205. doi:10.1097/ALN.0000000000000506.
 34. Grubb RL, Raichle ME, Eichling JO, Ter-Pogossian MM. The effects of changes in PaCO₂ on cerebral blood volume, blood flow, and vascular mean transit time. *Stroke.* 5(5):630-639.
 35. Battisti-Charbonney A, Fisher J, Duffin J. The cerebrovascular response to carbon dioxide in humans. *J Physiol.* 2011;589(12):3039-3048. doi:10.1113/jphysiol.2011.206052.
 36. Artru AA, Colley PS. Cerebral blood flow responses to hypocapnia during hypotension. *Stroke.* 15(5):878-883.
 37. Sobczyk O, Battisti-Charbonney A, Fierstra J, et al. A conceptual model for CO₂-induced redistribution of cerebral blood flow with experimental confirmation using BOLD MRI. *Neuroimage.* 2014;92:56-68. doi:10.1016/j.neuroimage.2014.01.051.
 38. Artru AA, Katz RA, Colley PS. Autoregulation of cerebral blood flow during normocapnia and hypocapnia in dogs. *Anesthesiology.* 1989;70(2):288-292.
 39. Darby JM, Yonas H, Marion DW, Latchaw RE. Local “inverse steal” induced by hyperventilation in head injury. *Neurosurgery.* 1988;23(1):84-88.
 40. Paulson OB, Hasselbalch SG, Rostrup E, Knudsen GM, Pelligrino D. Cerebral blood flow response to functional activation. *J Cereb Blood Flow Metab.* 2010;30(1):2-14. doi:10.1038/jcbfm.2009.188.
 41. Koehler RC, Roman RJ, Harder DR. Astrocytes and the regulation of cerebral blood flow. *Trends Neurosci.* 2009;32(3):160-169. doi:10.1016/j.tins.2008.11.005.
 42. Hägerdal M, Harp J, Nilsson L, Siesjö BK. The effect of induced hypothermia upon oxygen consumption in the rat brain. *J Neurochem.* 1975;24(2):311-316.
 43. Ehrlich MP, McCullough JN, Zhang N, et al. Effect of hypothermia on cerebral blood flow and metabolism in the pig. *Ann Thorac Surg.* 2002;73(1):191-197.
 44. Ogoh S, Brothers RM, Barnes Q, et al. The effect of changes in cardiac output on middle cerebral artery mean blood velocity at rest and during exercise. *J Physiol.* 2005;569(2):697-704. doi:10.1113/jphysiol.2005.095836.
 45. Choi B-R, Kim JS, Yang YJ, et al. Factors Associated With Decreased Cerebral Blood Flow in Congestive Heart Failure Secondary to Idiopathic Dilated Cardiomyopathy. *Am J Cardiol.* 2006;97(9):1365-1369. doi:10.1016/j.amjcard.2005.11.059.

46. Loncar G, Bozic B, Lepic T, et al. Relationship of reduced cerebral blood flow and heart failure severity in elderly males. *Aging Male*. 2011;14(1):59-65. doi:10.3109/13685538.2010.511326.
47. Meng L, Cannesson M, Alexander BS, et al. Effect of phenylephrine and ephedrine bolus treatment on cerebral oxygenation in anaesthetized patients. *Br J Anaesth*. 2011;107(2):209-217. doi:10.1093/bja/aer150.
48. Vajkoczy P, Roth H, Horn P, et al. Continuous monitoring of regional cerebral blood flow: experimental and clinical validation of a novel thermal diffusion microprobe. *J Neurosurg*. 2000;93(2):265-274. doi:10.3171/jns.2000.93.2.0265.
49. Fukuda O, Endo S, Kuwayama N, Harada J, Takaku A. The characteristics of laser-Doppler flowmetry for the measurement of regional cerebral blood flow. *Neurosurgery*. 1995;36(2):358-364.
50. Sutton LN, McLaughlin AC, Dante S, Kotapka M, Sinwell T, Mills E. Cerebral venous oxygen content as a measure of brain energy metabolism with increased intracranial pressure and hyperventilation. *J Neurosurg*. 1990;73(6):927-932. doi:10.3171/jns.1990.73.6.0927.
51. Aaslid R, Markwalder TM, Nornes H. Noninvasive transcranial Doppler ultrasound recording of flow velocity in basal cerebral arteries. *J Neurosurg*. 1982;57(6):769-774. doi:10.3171/jns.1982.57.6.0769.
52. Bouzat P, Oddo M, Payen J-F. Transcranial Doppler after traumatic brain injury. *Curr Opin Crit Care*. 2014;20(2):153-160. doi:10.1097/MCC.0000000000000071.
53. White H, Venkatesh B. Applications of transcranial Doppler in the ICU: a review. *Intensive Care Med*. 2006;32(7):981-994. doi:10.1007/s00134-006-0173-y.
54. de Freitas GR, Andre C. Sensitivity of transcranial Doppler for confirming brain death: a prospective study of 270 cases. *Acta Neurol Scand*. 2006;113(6):426-432. doi:10.1111/j.1600-0404.2006.00645.x.
55. Marinoni M, Ginanneschi A, Forleo P, Amaducci L. Technical limits in transcranial Doppler recording: inadequate acoustic windows. *Ultrasound Med Biol*. 1997;23(8):1275-1277.
56. Doppler C. Über das farbige Licht der Doppelsterne und einiger anderer Gestirne des Himmels (About the coloured light of the binary stars and some other stars of the heavens). *Proc R Bohemian Soc Sci*. 1842;5(2):465-482.
57. Eicke BM, Tegeler CH, Dalley G, Myers LG. Angle correction in transcranial Doppler sonography. *J Neuroimaging*. 1994;4(1):29-33.
58. Strebel SP, Kindler C, Bissonnette B, Tschalèr G, Deanovic D. The impact of systemic vasoconstrictors on the cerebral circulation of anesthetized patients. *Anesthesiology*. 1998;89(1):67-72.
59. Hoiland RL, Ainslie PN. CrossTalk proposal: The middle cerebral artery diameter does change during alterations in arterial blood gases and blood pressure. *J Physiol*. 2016;594(15):4073-4075. doi:10.1113/JP271981.
60. Rasulo FA, De Peri E, Lavinio A. Transcranial Doppler ultrasonography in intensive care. *Eur J Anaesthesiol*. 2008;25(Supplement 42):167-173. doi:10.1017/S0265021507003341.
61. Gosling RG, King DH. Arterial assessment by Doppler-shift ultrasound. *Proc R Soc Med*. 1974;67(6 Pt 1):447-449.
62. Steinmeier R, Laumer R, Bondár I, Priem R, Fahlbusch R. Cerebral hemodynamics in subarachnoid hemorrhage evaluated by transcranial Doppler sonography. Part 2. Pulsatility indices: normal reference values and characteristics in subarachnoid hemorrhage. *Neurosurgery*. 1993;33(1):10-8-9.
63. Aaslid, Rune; Lindegaard KF. Cerebral haemodynamics. In: Aaslid R, ed. *Transcranial Doppler Sonography*. New York: Springer-Verlag; 1986:60-85.
64. Pourcelot L. Diagnostic ultrasound for cerebral vascular disease. In: Donald, Ian; Levi S, ed. *Present and Future of Diagnostic Ultrasound*. Rotterdam: Kooyker Scientific Publications; 1976:141-147.
65. Ahmad M, Legrand M, Lukaszewicz A-C, Charlier P, Mateo J, Payen D. Transcranial

- Doppler monitoring may be misleading in prediction of elevated ICP in brain-injured patients. *Intensive Care Med.* 2013;39(6):1150-1151. doi:10.1007/s00134-013-2885-0.
66. Czosnyka M, Richards H, Kirkpatrick P, Pickard J. Assessment of cerebral autoregulation with ultrasound and laser Doppler wave forms--an experimental study in anesthetized rabbits. *Neurosurgery.* 1994;35(2):287-92-3.
 67. Giller CA, Hodges K, Batjer HH. Transcranial Doppler pulsatility in vasodilation and stenosis. *J Neurosurg.* 1990;72:901-906.
 68. Czosnyka M, Richards HK, Whitehouse HE and JP. Relationship between transcranial Doppler-determined pulsatility index and cerebrovascular resistance: an experimental study. *J Neurosurg.* 1996;84(1):79-84.
 69. Figaji AA, Zwane E, Fieggen AG, Siesjo P, Peter JC. Transcranial Doppler pulsatility index is not a reliable indicator of intracranial pressure in children with severe traumatic brain injury. *Surg Neurol.* 2009. doi:10.1016/j.surneu.2009.02.012.
 70. Roberto Tude Melo J, Di Rocco F, Blanot S, et al. Transcranial Doppler can predict intracranial hypertension in children with severe traumatic brain injuries. doi:10.1007/s00381-010-1367-8.
 71. Soehle M, Chatfield DA, Czosnyka M, Kirkpatrick PJ. Predictive value of initial clinical status, intracranial pressure and transcranial Doppler pulsatility after subarachnoid haemorrhage. *Acta Neurochir (Wien).* 2007. doi:10.1007/s00701-007-1149-6.
 72. Bellner J, Romner B, Reinstrup P, Kristiansson KA, Ryding E, Brandt L. Transcranial Doppler sonography pulsatility index (PI) reflects intracranial pressure (ICP). *Surg Neurol.* 2004. doi:10.1016/j.surneu.2003.12.007.
 73. Behrens A, Lenfeldt N, Ambarki K, Malm J, Eklund A, Koskinen LO. Transcranial doppler pulsatility index: Not an accurate method to assess intracranial pressure. *Neurosurgery.* 2010. doi:10.1227/01.NEU.0000369519.35932.F2.
 74. Zweifel C, Czosnyka M, Carrera E, de Riva N, Pickard JD, Smielewski P. Reliability of the Blood Flow Velocity Pulsatility Index for Assessment of Intracranial and Cerebral Perfusion Pressures in Head-Injured Patients. *Neurosurgery.* 2012;71(4):853-861. doi:10.1227/NEU.0b013e3182675b42.
 75. Bouzat P, Almeras L, Manhes P, et al. Transcranial Doppler to Predict Neurologic Outcome after Mild to Moderate Traumatic Brain Injury. *Anesthesiology.* 2016;125(2):346-354. doi:10.1097/ALN.0000000000001165.
 76. Richards HK, Czosnyka M, Whitehouse H, Pickard JD. Increase in transcranial Doppler pulsatility index does not indicate the lower limit of cerebral autoregulation. *Acta Neurochir Suppl.* 1998;71:229-232.
 77. Schmidt EA, Piechnik SK, Smielewski P, Raabe A, Matta BF, Czosnyka M. Symmetry of cerebral hemodynamic indices derived from bilateral transcranial Doppler. *J Neuroimaging.* 2003;13(3):248-254.
 78. Ropper AH. Brain in a Box. *N Engl J Med.* 2012;367(26):2539-2541. doi:10.1056/NEJMe1212289.
 79. Monro A. *Observations on the Structure and Function of the Nervous System.* Edinburgh: Creech & Johnson; 1783.
 80. Kelly G. Appearances observed in the dissection of two individuals; death from cold and congestion of the brain. *Trans Med Chir Sci Edinb.* 1824;(1):84-169.
 81. Cardim D, Schmidt B, Robba C, et al. Transcranial Doppler Monitoring of Intracranial Pressure Plateau Waves. *Neurocrit Care.* December 2016. doi:10.1007/s12028-016-0356-5.
 82. Davson H. Formation and drainage of the cerebrospinal fluid. *Sci Basis Med Annu Rev.* 1966:238-259.
 83. Balédent O, Fin L, Khuoy L, et al. Brain hydrodynamics study by phase-contrast magnetic resonance imaging and transcranial color doppler. *J Magn Reson Imaging.* 2006;24(5):995-1004. doi:10.1002/jmri.20722.
 84. Löfgren J, von Essen C, Zwetnow NN. The pressure-volume curve of the cerebrospinal fluid space in dogs. *Acta Neurol Scand.* 1973;49(5):557-574.
 85. Avezaat CJ, van Eijndhoven JH, Wyper DJ. Cerebrospinal fluid pulse pressure and

- intracranial volume-pressure relationships. *J Neurol Neurosurg Psychiatry*. 1979;42(8):687-700.
86. Maset AL, Marmarou A, Ward JD, et al. Pressure-volume index in head injury. *J Neurosurg*. 1987;67(6):832-840. doi:10.3171/jns.1987.67.6.0832.
 87. Czosnyka M, Pickard JD. Monitoring and interpretation of intracranial pressure. *J Neurol Neurosurg Psychiatry*. 2004;75:813-821. doi:10.1136/jnnp.2003.033126.
 88. Carney N, Totten AM, O'Reilly C, et al. Guidelines for the Management of Severe Traumatic Brain Injury, Fourth Edition. *Neurosurgery*. September 2016:1. doi:10.1227/NEU.0000000000001432.
 89. Bloomfield L. *How Things Work: The Physics of Everyday Life*. 3rd ed. John Wiley & Sons; 2006.
 90. Ekstedt J. CSF hydrodynamic studies in man. 1. Method of constant pressure CSF infusion. *J Neurol Neurosurg Psychiatry*. 1977;40(2):105-119.
 91. Rebuck JA, Murry KR, Rhoney DH, Michael DB, Coplin WM. Infection related to intracranial pressure monitors in adults: analysis of risk factors and antibiotic prophylaxis. *J Neurol Neurosurg Psychiatry*. 2000;69(3):381-384.
 92. Sahuquillo J, Poca MA, Arribas M, Garnacho A, Rubio E. Interhemispheric supratentorial intracranial pressure gradients in head-injured patients: are they clinically important? *J Neurosurg*. 1999;90(1):16-26. doi:10.3171/jns.1999.90.1.0016.
 93. Poca MA, Sahuquillo J, Topczewski T, Peñarrubia MJ, Muns A. Is intracranial pressure monitoring in the epidural space reliable? Fact and fiction. *J Neurosurg*. 2007;106(4):548-556. doi:10.3171/jns.2007.106.4.548.
 94. Robba C, Bacigaluppi S, Cardim D, Donnelly J, Bertuccio A, Czosnyka M. Non-invasive assessment of intracranial pressure. *Acta Neurol Scand*. 2016;134(1):4-21. doi:10.1111/ane.12527.
 95. Le Roux P, Menon DK, Citerio G, et al. Consensus summary statement of the International Multidisciplinary Consensus Conference on Multimodality Monitoring in Neurocritical Care. *Intensive Care Med*. 2014;40(9):1189-1209. doi:10.1007/s00134-014-3369-6.
 96. Chesnut RM, Temkin N, Carney N, et al. A trial of intracranial-pressure monitoring in traumatic brain injury. *N Engl J Med*. 2012;367(26):2471-2481. doi:10.1056/NEJMoa1207363.
 97. Balestreri M, Czosnyka M, Hutchinson P, et al. Impact of intracranial pressure and cerebral perfusion pressure on severe disability and mortality after head injury. *Neurocrit Care*. 2006;4(1):8-13. doi:10.1385/NCC:4:1:008.
 - 98.owler BK, Fong KC, Czosnyka Z. Importance of ICP monitoring in the investigation of CSF circulation disorders. *Br J Neurosurg*. 2001;15(5):439-440.
 99. Hu X, Glenn T, Scalzo F, et al. Intracranial pressure pulse morphological features improved detection of decreased cerebral blood flow. *Physiol Meas*. 2010;31(5):679-695. doi:10.1088/0967-3334/31/5/006.
 100. Kirkness CJ, Burr RL, Mitchell PH. Intracranial pressure variability and long-term outcome following traumatic brain injury. *Acta Neurochir Suppl*. 2008;102:105-108.
 101. Czosnyka M, Smielewski P, Timofeev I, et al. Intracranial pressure: more than a number. *Neurosurg Focus*. 2007;22(5):E10.
 102. Cardoso ER, Rowan JO, Galbraith S. Analysis of the cerebrospinal fluid pulse wave in intracranial pressure. *J Neurosurg*. 1983;59(5):817-821. doi:10.3171/jns.1983.59.5.0817.
 103. Lundberg N. Continuous recording and control of ventricular fluid pressure in neurosurgical practice. *Acta Psychiatr Scand Suppl*. 1960;36(149):1-193.
 104. Castellani G, Zweifel C, Kim D-J, et al. Plateau Waves in Head Injured Patients Requiring Neurocritical Care. *Neurocrit Care*. 2009;11(2):143-150. doi:10.1007/s12028-009-9235-7.
 105. Nichol J, Girling F, Jerrard W, Claxton E, Burton A. Fundamental instability of the small blood vessels and critical closing pressures in vascular beds. *Am J Physiol*. 1951;164(2):330-344.
 106. Dewey RC, Pieper HP, Hunt WE. Experimental cerebral hemodynamics Vasomotor

- tone, critical closing pressure, and vascular bed resistance. *Neurosurgery*. 1974;41:597-606.
107. Puppo C, Camacho J, Varsos G V., et al. Cerebral Critical Closing Pressure: Is the Multiparameter Model Better Suited to Estimate Physiology of Cerebral Hemodynamics? *Neurocrit Care*. 2016;25(3):446-454. doi:10.1007/s12028-016-0288-0.
 108. Puppo C, Camacho J, Yelicich B, Moraes L, Biestro A, Gomez H. Bedside study of cerebral critical closing pressure in patients with severe traumatic brain injury: a transcranial Doppler study. *Acta Neurochir Suppl*. 2012;114:283-288. doi:10.1007/978-3-7091-0956-4_55.
 109. Michel E, Hillebrand S, Vontwinkel L, Zemikow T, Lorch G. Frequency Dependence of Cerebrovascular Impedance in Preterm Neonates: A Different View on Critical Closing Pressure. *J Cerebral Blood Flow Metab*. 17(1):127-1131.
 110. Varsos G V, Richards H, Kasprowicz M, et al. Critical closing pressure determined with a model of cerebrovascular impedance. *J Cereb Blood Flow Metab*. 2013;33161(10):235-243. doi:10.1038/jcbfm.2012.161.
 111. De Riva N, Budohoski KP, Smielewski P, et al. Transcranial doppler pulsatility index: What it is and what it isn't. *Neurocrit Care*. 2012;17(1):58-66.
 112. Varsos G V., De Riva N, Smielewski P, et al. Critical closing pressure during intracranial pressure plateau waves. *Neurocrit Care*. 2013;18(3):341-348. doi:10.1007/s12028-013-9830-5.
 113. Kasprowicz M, Diedler J, Reinhard M, et al. Time Constant of the Cerebral Arterial Bed in Normal Subjects. *Ultrasound Med Biol*. 2012;38(7):1129-1137. doi:10.1016/j.ultrasmedbio.2012.02.014.
 114. Thees C, Scholz M, Schaller M D C, et al. Relationship between intracranial pressure and critical closing pressure in patients with neurotrauma. *Anesthesiology*. 2002;96(3):595-599.
 115. Varsos G V., Richards HK, Kasprowicz M, et al. Cessation of Diastolic Cerebral Blood Flow Velocity: The Role of Critical Closing Pressure. *Neurocrit Care*. 2014;20(1):40-48. doi:10.1007/s12028-013-9913-3.
 116. Marmarou A, Lu J, Butcher I, et al. IMPACT Database of Traumatic Brain Injury: Design And Description. *J Neurotrauma*. 2007;24(2):239-250. doi:10.1089/neu.2006.0036.
 117. Koliass AG, Guilfoyle MR, Helmy A, Allanson J, Hutchinson PJ. Traumatic brain injury in adults. *Pract Neurol*. 2013;13(4):228-235. doi:10.1136/practneurol-2012-000268.
 118. Menon DK, Zahed C. Prediction of outcome in severe traumatic brain injury. *Curr Opin Crit Care*. 2009;15(5):437-441. doi:10.1097/MCC.0b013e3283307a26.
 119. Langlois JA, Rutland-Brown W, Wald MM. The Epidemiology and Impact of Traumatic Brain Injury A Brief Overview. *J Head Trauma Rehabil*. 2006;21(5):375-378. doi:00001199-200609000-00001 [pii].
 120. Faul, Mark; Xu, Liking; Wald MMCVG. Traumatic Brain Injury in the United States: Emergency Department Visits, Hospitalizations and Deaths 2002–2006. *Atlanta Centers Dis Control Prev Natl Cent Inj Prev Control*. 2010.
 121. Pérez K, Novoa AM, Santamariña-Rubio E, et al. Incidence trends of traumatic spinal cord injury and traumatic brain injury in Spain, 2000–2009. *Accid Anal Prev*. 2012;46:37-44. doi:10.1016/j.aap.2011.12.004.
 122. Brain Trauma Foundation, American Association of Neurological Surgeons, Congress of Neurological Surgeons. Guidelines for the management of severe traumatic brain injury. *J Neurotrauma*. 2007;24 Suppl 1:S1-106. doi:10.1089/neu.2007.9999.
 123. Teasdale G, Jennett B. Assessment of coma and impaired consciousness. A practical scale. *Lancet*. 1974;304(7872):81-84. doi:10.1016/S0140-6736(74)91639-0.
 124. Kornbluth J, Bhardwaj A. Evaluation of Coma: A Critical Appraisal of Popular Scoring Systems. *Neurocrit Care*. 2011;14(1):134-143. doi:10.1007/s12028-010-9409-3.
 125. Balestreri M, Czosnyka M, Chatfield DA, et al. Predictive value of Glasgow Coma Scale after brain trauma: change in trend over the past ten years. *J Neurol Neurosurg Psychiatry*. 2004;75(1):161-162.

126. Sorrentino E, Diedler J, Kasprowicz M, et al. Critical Thresholds for Cerebrovascular Reactivity After Traumatic Brain Injury. *Neurocrit Care*. 2012;16(2):258-266. doi:10.1007/s12028-011-9630-8.
127. Teasdale G, Maas A, Lecky F, Manley G, Stocchetti N, Murray G. The Glasgow Coma Scale at 40 years: standing the test of time. *Lancet Neurol*. 2014;13(8):844-854. doi:10.1016/S1474-4422(14)70120-6.
128. Andrews PJD, Sleeman DH, Statham PFX, et al. Predicting recovery in patients suffering from traumatic brain injury by using admission variables and physiological data: a comparison between decision tree analysis and logistic regression. *J Neurosurg*. 2002;97(2):326-336. doi:10.3171/jns.2002.97.2.0326.
129. Rovlias A, Kotsou S. Classification and Regression Tree for Prediction of Outcome after Severe Head Injury Using Simple Clinical and Laboratory Variables. *J Neurotrauma*. 2004;21(7):886-893. doi:10.1089/0897715041526249.
130. Czosnyka M, Balestreri M, Steiner L, et al. Age, intracranial pressure, autoregulation, and outcome after brain trauma. *J Neurosurg*. 2005;102(3):450-454. doi:10.3171/jns.2005.102.3.0450.
131. Kramer AA, Wijdicks EFM, Snively VL, et al. A multicenter prospective study of interobserver agreement using the Full Outline of Unresponsiveness score coma scale in the intensive care unit. *Crit Care Med*. 2012;40(9):2671-2676. doi:10.1097/CCM.0b013e318258fd88.
132. Marmarou A. Pathophysiology of traumatic brain edema: current concepts. *Acta Neurochir Suppl*. 2003;86:7-10.
133. Badaut J, Ashwal S, Obenaus A. Aquaporins in Cerebrovascular Disease: A Target for Treatment of Brain Edema. *Cerebrovasc Dis*. 2011;31(6):521-531. doi:10.1159/000324328.
134. Saqur, Maher; Zygun, David; Demchuk, Andrew; Manosalva HA. Transcranial Doppler monitoring. In: Miller, Chad M; Torbey MT, ed. *Neurocritical Care Monitoring*. 1st ed. New York: Demos Medical Publishing; 2015:18-34.
135. Vik A, Nag T, Fredrikli OA, et al. Relationship of "dose" of intracranial hypertension to outcome in severe traumatic brain injury. *J Neurosurg*. 2008;109(4):678-684. doi:10.3171/JNS/2008/109/10/0678.
136. Bragin DE, Bush RC, Müller WS, Nemoto EM. High Intracranial Pressure Effects on Cerebral Cortical Microvascular Flow in Rats. *J Neurotrauma*. 2011;28(5):775-785. doi:10.1089/neu.2010.1692.
137. Bragin DE, Statom GL, Yonas H, Dai X, Nemoto EM. Critical Cerebral Perfusion Pressure at High Intracranial Pressure Measured by Induced Cerebrovascular and Intracranial Pressure Reactivity. *Crit Care Med*. 2014;42(12):2582-2590. doi:10.1097/CCM.0000000000000655.
138. Cushing H. Concerning a definite regulatory mechanism of the vaso-motor centre which controls blood pressure during cerebral compression. *Johns Hopkins Hosp Bull*. 1901;(12):290-292.
139. Wan WH, Ang BT, Wang E. The Cushing Response: a case for a review of its role as a physiological reflex. *J Clin Neurosci*. 2008;15(3):223-228. doi:10.1016/j.jocn.2007.05.025.
140. Donnelly J, Czosnyka M, Harland S, et al. Cerebral haemodynamics during experimental intracranial hypertension. *J Cereb Blood Flow Metab*. 2017;37(2):694-705. doi:10.1177/0271678X16639060.
141. Horsfield MA, Jara JL, Saeed NP, Panerai RB, Robinson TG. Regional Differences in Dynamic Cerebral Autoregulation in the Healthy Brain Assessed by Magnetic Resonance Imaging. Meisel A, ed. *PLoS One*. 2013;8(4):e62588. doi:10.1371/journal.pone.0062588.
142. Zweifel C, Czosnyka M, Lavinio A, et al. A comparison study of cerebral autoregulation assessed with transcranial Doppler and cortical laser Doppler flowmetry. *Neurol Res*. 2010;32(4):425-428. doi:10.1179/174313209X459165.
143. Budohoski KP, Czosnyka M, Smielewski P, et al. Cerebral Autoregulation after

- Subarachnoid Hemorrhage: Comparison of Three Methods. *J Cereb Blood Flow Metab.* 2013;33(3):449-456. doi:10.1038/jcbfm.2012.189.
144. Marmarou A. A theoretical model and experimental evaluation of the cerebrospinal fluid system. 1973.
 145. Czosnyka M, Matta BF, Smielewski P, Kirkpatrick PJ, Pickard JD. Cerebral perfusion pressure in head-injured patients: a noninvasive assessment using transcranial Doppler ultrasonography. *J Neurosurg.* 1998;88(5):802-808. doi:10.3171/jns.1998.88.5.0802.
 146. Schmidt EA, Czosnyka M, Gooskens I, et al. Preliminary experience of the estimation of cerebral perfusion pressure using transcranial Doppler ultrasonography. *J Neurol Neurosurg Psychiatry.* 2001;70(2):198-204.
 147. Cooper DJ, Rosenfeld J V., Murray L, et al. Decompressive Craniectomy in Diffuse Traumatic Brain Injury. *N Engl J Med.* 2011;364(16):1493-1502. doi:10.1056/NEJMoa1102077.
 148. Hutchinson PJ, Kolias AG, Timofeev IS, et al. Trial of Decompressive Craniectomy for Traumatic Intracranial Hypertension. *N Engl J Med.* 2016;375(12):1119-1130. doi:10.1056/NEJMoa1605215.
 149. Lazaridis C, Czosnyka M. Cerebral Blood Flow, Brain Tissue Oxygen, and Metabolic Effects of Decompressive Craniectomy. *Neurocrit Care.* 2012;16(3):478-484. doi:10.1007/s12028-012-9685-1.
 150. Guillaume J, Janny P. [Continuous intracranial manometry; physiopathologic and clinical significance of the method]. *Presse Med.* 1951;59(45):953-955.
 151. Czosnyka M, Smielewski P, Piechnik S, et al. Hemodynamic characterization of intracranial pressure plateau waves in head-injured patients. *J Neurosurg.* 1999;91(1):11-19. doi:10.3171/jns.1999.91.1.0011.
 152. Rosner MJ, Necker DP. Origin and evolution of plateau waves. Experimental observations and a theoretical model. *J Neurosurg.* 1984;60:312-324.
 153. Dias C, Maia I, Cerejo A, et al. Pressures, Flow, and Brain Oxygenation During Plateau Waves of Intracranial Pressure. *Neurocrit Care.* 2014;21(1):124-132. doi:10.1007/s12028-013-9918-y.
 154. Czosnyka M, Smielewski P, Piechnik S, Schmidt EA, Al-Rawi PG, Kirkpatrick PJ. Hemodynamic characterization of intracranial pressure plateau waves in head-injured patients. *J Neurosurg.* 1999;91(1):11-19.
 155. Dias C, Maia I, Cerejo A, Smielewski P, Paiva J-A, Czosnyka M. Plateau Waves of Intracranial Pressure and Multimodal Brain Monitoring. In: *Acta Neurochirurgica. Supplement.* Vol 122. ; 2016:143-146. doi:10.1007/978-3-319-22533-3_29.
 156. Hayashi M, Kobayashi H, Kawano H, Yamamoto S, Maeda T. Cerebral blood flow and ICP patterns in patients with communicating hydrocephalus after aneurysm rupture. *J Neurosurg.* 1984;61:30-36.
 157. Hayashi M, Kobayashi H, Kawano H, Handa Y, Yamamoto S, Kitano T. ICP patterns and isotope cisternography in patients with communicating hydrocephalus following rupture of intracranial aneurysm. *J Neurosurg.* 1985;62:220-226.
 158. Hayashi M, Handa Y, Kobayashi H, Kawano H, Ishii H, Hirose S. Plateau-wave phenomenon (I). Correlation between the appearance of plateau waves and CSF circulation in patients with intracranial hypertension. *Brain.* December 1991:2681-2691.
 159. Matsuda M, Yoneda S, Handa H, Gotoh H. Cerebral hemodynamic changes during plateau waves in brain-tumor patients. *J Neurosurg.* 1979;50:483-488.
 160. Renier D, Sainte-Rose C, Marchac D, Hirsch J-F. Intracranial pressure in craniostenosis. *J Neurosurg.* 1982;57:370-377.
 161. Roh D, Park S. Brain Multimodality Monitoring: Updated Perspectives. *Curr Neurol Neurosci Rep.* 2016;16(6):56. doi:10.1007/s11910-016-0659-0.
 162. Le Roux P, Menon DK, Citerio G, et al. Consensus Summary Statement of the International Multidisciplinary Consensus Conference on Multimodality Monitoring in Neurocritical Care: A statement for healthcare professionals from the Neurocritical Care Society and the European Society of Intensive C. *Neurocrit Care.* 2014;21(2):1-26. doi:10.1007/s12028-014-0041-5.

163. Bullock R, Chesnut RM, Clifton G et al. Guidelines for the management of severe head injury. *J Neurotrauma*. 1996;(13):639-734.
164. Highton D, Elwell C, Smith M. Noninvasive cerebral oximetry: is there light at the end of the tunnel? *Curr Opin Anaesthesiol*. 2010;23(5):576-581.
165. Haitzma I, Rosenthal G, Morabito D, Rollins M, Maas AIR, Manley GT. In vitro comparison of two generations of Licox and Neurotrend catheters. *Acta Neurochir Suppl*. 2008;102:197-202.
166. Timofeev I, Carpenter KLH, Nortje J, et al. Cerebral extracellular chemistry and outcome following traumatic brain injury: a microdialysis study of 223 patients. *Brain*. 2011;134(2):484-494. doi:10.1093/brain/awq353.
167. Hutchinson PJ, Jalloh I, Helmy A, et al. Consensus statement from the 2014 International Microdialysis Forum. *Intensive Care Med*. 2015;41(9):1517-1528. doi:10.1007/s00134-015-3930-y.
168. Citerio G, Park S, Schmidt JM, et al. Data collection and interpretation. *Neurocrit Care*. 2015;22(3):360-368. doi:10.1007/s12028-015-0139-4.
169. Smielewski P, Czosnyka M, Steiner L, Belestri M, Piechnik S, Pickard JD. ICM+: software for on-line analysis of bedside monitoring data after severe head trauma. *Acta Neurochir Suppl*. 2005;95:43-49.
170. Piper I, Citerio G, Chambers I, et al. The BrainIT group: concept and core dataset definition. *Acta Neurochir (Wien)*. 2003;145(8):615-28-9. doi:10.1007/s00701-003-0066-6.
171. Maas AIR, Menon DK, Steyerberg EW, et al. Collaborative European NeuroTrauma Effectiveness Research in Traumatic Brain Injury (CENTER-TBI). *Neurosurgery*. 2015;76(1):67-80. doi:10.1227/NEU.0000000000000575.
172. Dias C, Silva MJ, Pereira E, et al. Optimal Cerebral Perfusion Pressure Management at Bedside: A Single-Center Pilot Study. *Neurocrit Care*. 2015;23(1):92-102. doi:10.1007/s12028-014-0103-8.
173. Aries MJH, Czosnyka M, Budohoski KP, et al. Continuous determination of optimal cerebral perfusion pressure in traumatic brain injury. *Crit Care Med*. 2012;40(8):2456-2463. doi:10.1097/CCM.0b013e3182514eb6.
174. Czosnyka M, Smielewski P, Kirkpatrick P, Laing RJ, Menon D, Pickard JD. Continuous assessment of the cerebral vasomotor reactivity in head injury. *Neurosurgery*. 1997;41(1):11-7-9.
175. Czosnyka M, Price DJ, Williamson M. Monitoring of cerebrospinal dynamics using continuous analysis of intracranial pressure and cerebral perfusion pressure in head injury. *Acta Neurochir (Wien)*. 1994;126(2-4):113-119.
176. Rivera-Lara L, Zorrilla-Vaca A, Geocadin R, et al. Predictors of Outcome With Cerebral Autoregulation Monitoring. *Crit Care Med*. 2017;45(4):695-704. doi:10.1097/CCM.0000000000002251.
177. Smielewski P, Czosnyka Z, Kasprowicz M, Pickard JD, Czosnyka M. ICM+: A Versatile Software for Assessment of CSF Dynamics. In: ; 2012:75-79. doi:10.1007/978-3-7091-0956-4_13.
178. Brady KM, Lee JK, Kibler KK, et al. Continuous Time-Domain Analysis of Cerebrovascular Autoregulation Using Near-Infrared Spectroscopy. *Stroke*. 2007;38(10):2818-2825. doi:10.1161/STROKEAHA.107.485706.
179. Jaeger M, Schuhmann MU, Soehle M, Meixensberger J. Continuous assessment of cerebrovascular autoregulation after traumatic brain injury using brain tissue oxygen pressure reactivity. *Crit Care Med*. 2006;34(6):1783-1788. doi:10.1097/01.CCM.0000218413.51546.9E.
180. Steiner LA, Czosnyka M, Piechnik SK, et al. Continuous monitoring of cerebrovascular pressure reactivity allows determination of optimal cerebral perfusion pressure in patients with traumatic brain injury. *Crit Care Med*. 2002;30(4):733-738.
181. Lazaridis C, DeSantis SM, Smielewski P, et al. Patient-specific thresholds of intracranial pressure in severe traumatic brain injury. *J Neurosurg*. 2014;120(4):893-900. doi:10.3171/2014.1.JNS131292.

182. Lazaridis C, Smielewski P, Steiner LA, et al. Optimal cerebral perfusion pressure: are we ready for it? *Neurol Res.* 2013;35(2):138-148. doi:10.1179/1743132812Y.0000000150.
183. Smielewski P, Kirkpatrick P, Minhas P, Pickard JD, Czosnyka M. Can cerebrovascular reactivity be measured with near-infrared spectroscopy? *Stroke.* 1995;26(12):2285-2292.
184. Czosnyka M, Whitehouse H, Smielewski P, Simac S, Pickard JD. Testing of cerebrospinal compensatory reserve in shunted and non-shunted patients: a guide to interpretation based on an observational study. *J Neurol Neurosurg Psychiatry.* 1996;60(5):549-558.
185. Haubrich C. Autonomic system monitoring using ICM+. 2016.
186. Lim MH, Cho YI, Jeong SK. Homocysteine and pulsatility index of cerebral arteries. *Stroke.* 2009. doi:10.1161/STROKEAHA.109.558403.
187. López-Magaña JA, Richards HK, Radolovich DK, et al. Critical closing pressure: comparison of three methods. *J Cereb Blood Flow Metab.* 2009;29:987-993. doi:10.1038/jcbfm.2009.24.
188. Panerai RB, Salinet ASM, Brodie FG, Robinson TG. The influence of calculation method on estimates of cerebral critical closing pressure. *Physiol Meas.* 2011;32(4):467-482. doi:10.1088/0967-3334/32/4/007.
189. Ursino M, Di Giammarco P. A mathematical model of the relationship between cerebral blood volume and intracranial pressure changes: the generation of plateau waves. *Ann Biomed Eng.* 1991;19(1):15-42.
190. Richards HK, Czosnyka M, Pickard JD. Assessment of critical closing pressure in the cerebral circulation as a measure of cerebrovascular tone. *Acta Neurochir (Wien).* 1999;141(11):1221-7-7.
191. Panerai RB. The critical closing pressure of the cerebral circulation. *Med Eng Phys.* 2003;25:621-632. doi:10.1016/S1350-4533(03)00027-4.
192. Chatterjee K. The Swan-Ganz Catheters: Past, Present, and Future: A Viewpoint. *Circulation.* 2009;119(1):147-152. doi:10.1161/CIRCULATIONAHA.108.811141.
193. Carrera E, Kim DJ, Castellani G, et al. Cerebral arterial compliance in patients with internal carotid artery disease. *Eur J Neurol.* 2011. doi:10.1111/j.1468-1331.2010.03247.x.
194. Czosnyka M, Richards HK, Reinhard M, et al. Cerebrovascular time constant: dependence on cerebral perfusion pressure and end-tidal carbon dioxide concentration. *Neurol Res.* 2012;34(1):17-24. doi:10.1179/1743132811Y.0000000040.
195. Kim D-J, Kasprovicz M, Carrera E, et al. The monitoring of relative changes in compartmental compliances of brain. *Physiol Meas.* 2009;30(7):647-659. doi:10.1088/0967-3334/30/7/009.
196. Raichle ME, Posner JB, Plum F. Cerebral Blood Flow During And After Hyperventilation. *Arch Neurol.* 1970;23(5):394-403. doi:10.1001/archneur.1970.00480290014002.
197. Czosnyka M, Piechnik S, Richards HK, Kirkpatrick P, Smielewski P, Pickard JD. Contribution of mathematical modelling to the interpretation of bedside tests of cerebrovascular autoregulation. *J Neurol Neurosurg Psychiatry.* 1997;63:721-731.
198. Kasprovicz M, Czosnyka M, Soehle M, et al. Vasospasm shortens cerebral arterial time constant. *Neurocrit Care.* 2012. doi:10.1007/s12028-011-9653-1.
199. Carrera E, Steiner LA, Castellani G, et al. Changes in Cerebral Compartmental Compliances during Mild Hypocapnia in Patients with Traumatic Brain Injury. doi:10.1089/neu.2010.1377.
200. Alperin N, Sivaramakrishnan A LT. Magnetic resonance imaging-based measurements of cerebrospinal fluid and blood flow as indicators of intracranial compliance in patients with Chiari malformation. *J Neurosurg.* 2005;103(1):46-52.
201. Michel E, Zernikow B. Gosling's Doppler Pulsatility Index Revisited. *Ultrasound Med Biol.* 1998;24(4):597-599. doi:10.1016/S0301-5629(98)00024-6.
202. Burton AC. On the physical equilibrium of small blood vessels. *Am J Physiol.* 1951;164(2):319-329.

203. Aaslid R, Lash SR, Bardy GH, Gild WH, Newell DW. Dynamic pressure-flow velocity relationships in the human cerebral circulation. *Stroke*. 2003;34:1645-1649. doi:10.1161/01.STR.0000077927.63758.B6.
204. Czosnyka M, Smielewski P, Piechnik S, et al. Critical closing pressure in cerebrovascular circulation. *J Neurol Neurosurg Psychiatry*. 1999;66:606-611.
205. Michel E, Zernikow B, von Twickel J, Hillebrand S, Jorch G. Critical closing pressure in preterm neonates: towards a comprehensive model of cerebral autoregulation. *Neurol Res*. 1995;17(2):149-155.
206. Soehle M, Czosnyka M, Pickard JD, Kirkpatrick PJ. Critical closing pressure in subarachnoid hemorrhage: Effect of cerebral vasospasm and limitations of a transcranial Doppler-derived estimation. *Stroke*. 2004;35(6):1393-1398. doi:10.1161/01.STR.0000128411.07036.a9.
207. Gazzoli P, Frigerio M, De Peri E, Rasulo F, Gasparotti R, Lavinio A LN. A case of negative critical closing pressure. *Abstr 8th Int Conf XeCT Relat CBF Tech*. 2006:348.
208. Daley ML, Leffer CW, Czosnyka M, Pickard JD. Plateau waves: changes of cerebrovascular pressure transmission. *Acta Neurochir Suppl*. 2005;95:327-332.
209. Varsos G V., Budohoski KP, Koliass AG, et al. Relationship of Vascular Wall Tension and Autoregulation Following Traumatic Brain Injury. *Neurocrit Care*. 2014;21(2):266-274. doi:10.1007/s12028-014-9971-1.
210. Kumar A, Schmidt EA, Hiler M, Smielewski P, Pickard JD, Czosnyka M. Asymmetry of critical closing pressure following head injury. *J Neurol Neurosurg Psychiatry*. 2005;76(11):1570-1573. doi:10.1136/jnnp.2004.059493.

OTHER SCIENTIFIC MERITS RELATED TO THIS INVESTIGATION

In addition to the presented articles, during the development of this doctoral thesis the doctorand has been co-author of the following scientific publications related to the described multimodality monitoring and signal analysis research line. The related original articles published in international journals are included in this section as annexed documents:

1. Calviello L, **de Riva N**, Donnelly J, Czosnyka M, Smielewski P, Menon DK, Zeiler FA. *Relationship Between Brain Pulsatility and Cerebral perfusion Pressure: Replicated validation Using Different Drivers of CPP Change*. Neurocrit Care. 2017 May 25. doi: 10.1007/s12028-017-0404-9 [Epub ahead of print]. PMID: 28547321. [IF 2016 = 2.752].
2. Zweifel C, Czosnyka M, Carrera E, **de Riva N**, Pickard JD, Smielewski P. *Reliability of the Blood Flow Velocity Pulsatility Index for Assessment of Intracranial and Cerebral Perfusion Pressures in Head Injured Patients*. Neurosurgery. 2012 Oct;71(4):853-61. [IF 2016 = 4.889].
3. Budohoski KP, Lavinio A, **de Riva N**, Smielewski P, Pickard JD, Menon DK, Kirkpatrick PJ, Czosnyka M. *The Relationship Between Cerebral Blood Flow Autoregulation and Cerebrovascular Pressure Reactivity After Traumatic Brain Injury*. Neurosurgery. 2012 Sep;71(3):652-60. [IF 2016 = 4.889].

On the other hand, the doctorand has been an invited speaker for different aspects related to this area of investigation and knowledge:

1. Workshop session in multimodal monitoring “*ICM+ and cerebral autoregulation*”. 9th International Update on Neuroanesthesia and Neurointensive Care, interdisciplinary neuroscience. Barcelona, Spain, April 14-16, 2016.
2. Invited Speaker for the lecture: “*Intracranial Pressure, the Physics Applied to Clinical Practice*”. 5th Congress of the European Academy of Paediatric Societies (EAPS 2014). Barcelona, Spain, October 17-21, 2014.
3. Invited speaker: “*El concepto de PPC óptima y utilidad del concepto de ‘pressure reactivity index’ (PRx) en el manejo individualizado de la autorregulación*”. Curso Pre-Simposium “Monitorización de la autorregulación cerebral en el paciente neurocrítico”. XVII Simposium Internacional de Neuromonitorización y Tratamiento del Paciente Neurocrítico. Barcelona, 15-19 Noviembre 2016.
4. Invited speaker: “*Efectos sobre la autorregulación de los fármacos anestésicos. ¿Está indicada la anestesia inhalatoria en el paciente neurocrítico?*” XVI Simposium Internacional de Neuromonitorización y Tratamiento del Paciente Neurocrítico. Barcelona, 18-22 Noviembre 2014.
5. Invited speaker: “*Monitorización de la autorregulación cerebral*”. VII Reunión de la Sección de Cuidados Intensivos de la Sociedad Española de Anestesiología y Reanimación (SEDAR). VI Curso de Formación en Medicina de Cuidados Intensivos. Hospital Universitario La Fe, Valencia, Spain, May 5-7, 2016.

6. Varsos GV, **de Riva N**, Smielewski P, Pickard JD, Brady KM, Reinhard M, Avolio A, Koliass AG, Hutchinson PJ, Czosnyka M. *Closing margin: a new method for assessing the risk of ischaemia in TBI patients*. 2013 Autumn Meeting of the Society of British Neurological Surgeons. Published in Br J Neurosurg October 2013;27(5):556-576. P-11.

Relationship Between Brain Pulsatility and Cerebral Perfusion Pressure: Replicated Validation Using Different Drivers of CPP Change

Leanne A. Calviello¹ · Nicolás de Riva² · Joseph Donnelly¹ · Marek Czosnyka¹ · Peter Smielewski¹ · David K. Menon^{3,6,7,8} · Frederick A. Zeiler^{3,4,5}

© The Author(s) 2017. This article is an open access publication

Abstract

Background Determination of relationships between transcranial Doppler (TCD)-based spectral pulsatility index (sPI) and pulse amplitude (AMP) of intracranial pressure (ICP) in 2 groups of severe traumatic brain injury (TBI) patients (a) displaying plateau waves and (b) with unstable mean arterial pressure (MAP).

Methods We retrospectively reviewed patients with severe TBI and continuous TCD monitoring displaying either plateau waves or unstable MAP from 1992 to 1998. We utilized linear and nonlinear regression techniques to describe both cohorts: cerebral perfusion pressure (CPP)

versus AMP, CPP versus sPI, mean ICP versus ICP AMP, mean ICP versus sPI, and AMP versus sPI.

Results Nonlinear regression techniques were employed to analyze the relationships with CPP. In plateau wave and unstable MAP patients, CPP versus sPI displayed an inverse nonlinear relationship ($R^2 = 0.820$ vs. $R^2 = 0.610$, respectively), with the CPP versus sPI relationship best modeled by the following function in both cases: $PI = a + (b/CPP)$. Similarly, in both groups, CPP versus AMP displayed an inverse nonlinear relationship ($R^2 = 0.610$ vs. $R^2 = 0.360$, respectively). Positive linear correlations were displayed in both the plateau wave and unstable MAP cohorts between: ICP versus AMP, ICP versus sPI, AMP versus sPI.

Conclusions There is an inverse relationship through nonlinear regression between CPP versus AMP and CPP

Electronic supplementary material The online version of this article (doi:10.1007/s12028-017-0404-9) contains supplementary material, which is available to authorized users.

✉ Leanne A. Calviello
leannecalviello@gmail.com

Nicolás de Riva
nderiva@clinic.cat

Joseph Donnelly
donnellyj87@gmail.com

Marek Czosnyka
mc141@medschl.cam.ac.uk

Peter Smielewski
ps10011@cam.ac.uk

David K. Menon
dkm13@cam.ac.uk

Frederick A. Zeiler
umzeiler@myumanitoba.ca

² Division of Neuroanesthesia, Department of Anesthesiology, Hospital Clinic, Universitat de Barcelona, Barcelona, Spain

³ Division of Anesthetics, Addenbrooke's Hospital, University of Cambridge, Cambridge, UK

⁴ Section of Neurosurgery, Department of Surgery, Rady Faculty of Health Sciences, University of Manitoba, Winnipeg, Canada

⁵ Clinician Investigator Program, University of Manitoba, Winnipeg, Canada

⁶ Neurosciences Critical Care Unit, Addenbrooke's Hospital, Cambridge, UK

⁷ Queens' College, Cambridge, UK

⁸ National Institute for Health Research, Cambridge, UK

¹ Division of Neurosurgery, Department of Clinical Neurosciences, Addenbrooke's Hospital, University of Cambridge, Cambridge, UK

versus sPI display. This provides evidence to support a previously-proposed model of TCD pulsatility index. ICP shows a positive linear correlation with AMP and sPI, which is also established between AMP and sPI.

Keywords Neurocritical care · Traumatic brain injury · Pulsatility index · Intracranial pressure · Cerebral perfusion pressure · Transcranial doppler

Introduction

Multi-modal, high-resolution intracranial monitoring within the critically-ill neurological patient is becoming standard in most high-volume neurocritical care units. Recent endorsement of multi-modal monitoring has come from a multitude of professional societies associated with the critical care management of these patients [1, 2]. To date, traumatic brain injury (TBI) and subarachnoid hemorrhage have dominated the literature on both invasive and noninvasive cranial monitoring, with TBI the focus of most publications [1, 2].

Worldwide interest in noninvasive measurement of various cranial hemodynamic indices has driven the application of transcranial Doppler (TCD) in a variety of scenarios, with the goal of correlating middle cerebral artery (MCA) flow velocity and pulsatility index (PI) to common invasive measures such as intracranial pressure (ICP) and cerebral perfusion pressure (CPP, the calculated difference between arterial blood pressure (ABP) and ICP), as documented within a recent systematic review [3]. The brain is extraordinarily fragile following TBI. Patients are at risk of increasing ICP, and of sudden changes in ABP or CPP that may require immediate clinical intervention. Low CPP is associated with potential instances of delayed cerebral ischemia; conversely, high CPP is associated with edema [4].

PI has been found to be a complex descriptor of several “mutually interdependent” parameters within the brain [4]. Elevated values of PI can signal rising ICP and can additionally inform of both decreasing CPP and of decreasing cerebrovascular resistance. These correlations are particularly relevant to the study of plateau waves, phenomena characterized by unexpected elevations in ICP above 50 mm Hg accompanied by marked depletions of CPP for a duration of at least 5 min that either resolve on their own or through treatment with vasopressors. In addition to plateau waves, alterations of mean arterial pressure (MAP) can upset the balance of CPP in critically-ill neurological patients, due to the fundamental nature of ABP within the CPP derivation. Clinical analysis of unstable, decreasing MAP can assist in the ongoing investigation of the relationships between various cerebral hemodynamic parameters.

To delineate the relationships between CPP, ICP, MAP, and TCD parameters, continuous data series through large ranges of CPP and ICP values would be ideal. Difficulties with long-term, high-quality TCD signal acquisition have led to limited studies in humans correlating TCD measures to CPP, ICP, and MAP [5], with some animal studies documenting the relationship [6] and others utilizing mathematical modeling [7]. Ideally, being able to correlate TCD-based PI with ICP pulse amplitude (AMP), MAP, and CPP could bolster the concept of reliable noninvasive measurement of these hemodynamic parameters. Previous literature has outlined the possibility of an inverse nonlinear correlation between PI and CPP, utilizing “spectral” PI (sPI, defined as the first harmonic of the flow velocity (FV) pulse waveform divided by mean FV) in 51 patients with plateau waves and continuous TCD monitoring [6]. The following relationship between PI and CPP was proposed within the supplementary portion of that same manuscript [4]:

$$PI = \frac{A_1}{CPP_m} \cdot \sqrt{(CVR \cdot Ca)^2 HR^2 \cdot (2\pi)^2 + 1}$$

In this equation, A_1 represents the fundamental harmonic of ABP, CPP_m the calculated mean of recorded CPP values, CVR the cerebrovascular resistance, Ca the cerebral arterial compliance, and HR the heart rate.

Given the complexities in such analyses, we hypothesized that validation of relationships between CPP and indices of cerebrovascular pulsatility (defined using either sPI or AMP) would be strengthened by demonstrating similar relationships in contexts where the drivers of CPP change were different. Consequently, in this study, we used a unified method to compare the same relationship in clinical conditions where CPP is affected either by increasing ICP or by the oscillations of unstable MAP. The aim of our study was to describe and compare the relationships between spectral PI and various invasively-derived cerebral hemodynamic measures across two groups of TBI patients demonstrating either plateau waves or unstable MAP while continuously recording flow velocities with TCD. These patients were of interest given the continuous data recorded through a wide range of CPP values, allowing us to potentially gain a better insight into the relationship between TCD and invasively-monitored parameters. The following relationships are described for each cohort: ICP versus AMP, ICP versus sPI, AMP versus sPI, CPP versus AMP, and CPP versus sPI.

Methods

Patients

From a database of 1023 head-injured patients with continuous ICM+ (Intensive Care Monitoring) monitoring and

TCD recordings of ABP and ICP, we performed a retrospective review of recorded data for patients exhibiting ICP plateau waves during the period from 1992 to 1998. We were primarily observing physiological effects in subsets of TBI patients, with plateau waves of special interest because they are relatively uncommon. Each recording lasted for a maximum of 15–30 min. These patients have previously been described within other published studies [6, 8, 9] and were selected to evaluate the relationship between CPP versus sPI and CPP versus AMP over a large range of CPP that was observed secondary to large fluctuations in ICP, as seen during plateau waves. 5643 minute-by-minute data points for each variable were analyzed across all patients.

Furthermore, we retrospectively analyzed a second cohort of severe TBI patients with unstable MAP to determine the relationship between CPP versus sPI and CPP versus AMP during wide fluctuations in CPP secondary to unstable MAP. The definition of “unstable MAP” describes mean ABP during recording changing by a minimum of 15 mm Hg in either a monotonic or a fluctuating manner. All patients in both cohorts suffered moderate–severe TBI and were admitted to the Neurosciences Critical Care Unit (NCCU) at Addenbrooke’s Hospital, Cambridge. Patients were managed according to an ICP-oriented protocol which aimed to keep ICP below 20 mm Hg. Institutional ICP protocols were employed during the patients’ NCCU stay, to provide homogeneity of care between patients. Of note, these patients were not treated via CPP-directed therapies, as this was not the standard of care within the NCCU at that time. Thus, fluctuations in CPP seen during plateau wave recordings are natural CPP responses, with no influence of vasoactive substances during recording. On the other hand, patients within the unstable MAP cohort may have received vasopressors in an attempt to stabilize blood pressure; however, this was not titrated to CPP goals.

Monitoring

All patients underwent both invasive and noninvasive monitoring throughout their ICU stay. Raw data signals from select monitoring devices were recorded and electronically stored using WREC software (Warsaw University of Technology).

ABP was continuously monitored both invasively (from the radial artery using a pressure monitoring kit [Baxter Healthcare CA, USA; Sidcup, UK]) and noninvasively. ICP was monitored using an intraparenchymal probe with strain gauge sensors (Codman & Shurtleff, MA, USA, or Camino Laboratories, CA, USA). Mean and peak blood flow velocities (FV_m and FV_x, respectively) were monitored from the MCA with a 2 MHz probe.

Raw data recordings within the plateau wave cohort patients included only 20–40 min of continuous data,

focusing on the immediate periods before, during, and after ICP plateau waves. Within the unstable MAP cohort, raw data recording occurred throughout the entire period of unstable blood pressures.

Monitoring of above brain modalities was conducted as a part of standard NCCU patient care using an anonymized database of physiological monitoring variables in neurocritical care. Data on age, injury severity, and clinical status at hospital discharge were recorded at the time of monitoring on this database, and no attempt was made to re-access clinical records for additional information. Since all data were extracted from the hospital records and fully anonymized, no data on long-term outcomes or patient identifiers were available, and formal patient or proxy consent was not sought.

Data Processing

Processing of raw data signals utilized ICM + software (Cambridge Enterprise, Cambridge, UK; <http://www.neurosurg.cam.ac.uk/icmplus>). Signal artifact removal was first conducted with signal cropping tools within ICM+. CPP was determined from the difference between raw ABP and ICP signals.

Primary analysis involved the calculation of time-averaged mean values for ABP (MAP), ICP, cerebral blood FV, and CPP. These means were calculated during 10-s time windows and were updated every 10 s to eliminate overlap. Mean FV was calculated using the data from FV. In addition, we determined the amplitude of the fundamental frequency of FV (F1) and the amplitude of the fundamental frequency of ICP AMP. Both fundamental amplitude calculations were done by applying a 20-sec time window, updated every 10 sec.

Final data processing involved the calculations of sPI over the course of each individual recording utilizing the equation: Mean F1/Mean FV. Mean F1 and FV were calculated utilizing a 10-sec time window, updated every 10 sec.

All data post-processing was exported from each patient to separate comma-separated variable (CSV) files for further statistical analysis.

Statistics

All statistical analyses were conducted utilizing the XLSTAT (Addinsoft, New York, USA; <https://www.xlstat.com/en/>) add-on package to Microsoft Excel (Microsoft Office 15, Version 16.0.7369.1323) and IBM SPSS Statistics 23 software. Post-processing data of individual patients, as CSV documents, were compiled into one CSV document containing all patients and signals described previously. Statistical significance for measured and

derived variables, both within and between the two patient cohorts, was determined utilizing a two-tailed t test, with an alpha set at 0.05.

Various statistical techniques were employed to describe the following relationships in both patient cohorts: ICP versus AMP, ICP versus sPI, AMP versus sPI, CPP versus AMP, and CPP versus sPI.

Relationships between ICP, AMP, and sPI were analyzed utilizing linear regression techniques. Goodness of fit was reported utilizing the Pearson correlation coefficient (r) and the determination coefficient (R^2). All R^2 values were reported. Statistical significance was assigned only if the p value was less than 0.05.

Analysis of the relationship between CPP, AMP, and sPI was conducted utilizing both linear and nonlinear techniques, with goodness of fit reported via R^2 . Nonlinear regression involved the fitting of existing functions within the statistical programs, in addition to manual function fitting utilizing the nonlinear inverse function: $y = a + (b/x)$.

Results

Patient Demographics

A total of 11 patients were eligible for inclusion within the plateau wave cohort of this study, with a total of 18 plateau waves recorded. A total of 9 patients composed the unstable MAP cohort, with 13 separate recordings of unstable blood pressure. Figure 1 displays an example of the ICP, CPP, and MAP recordings from individual patients during plateau waves (Fig. 1a) and unstable blood pressure (Fig. 1b). All available demographic details are listed in Table 1.

Table 2 summarizes the mean ICP, ABP, CPP, HR, FV, and sPI for both the plateau wave and unstable MAP cohorts. Data for the plateau wave cohort were split into measurements before the plateau wave (i.e., “baseline”) and during the plateau wave, with comparison done via two-tailed t test. Data for the unstable MAP cohort were split into the recorded variables during the “Lowest 10%” and “Highest 10%” of recorded arterial blood pressures, with comparison done via two-tailed t test.

Relationships Between CPP, AMP, and sPI During Plateau Waves and Unstable MAP

Linear regression techniques failed to yield satisfactory relationships between CPP and AMP, or CPP and sPI. Their correlation coefficients were poor, and variance measures had large mean squared errors. As the scatterplots for each of these comparisons produced a nonlinear pattern, we utilized nonlinear regression analyses (with functions within

XLSTAT and IBM SPSS Statistics 23 software) to determine the relationships displayed between these variables during ICP plateau waves, using an inverse function that we have previously theorized to characterize this relationship. Nonlinear regression analysis for CPP versus sPI in each individual plateau wave patient is shown in Appendix A of the Supplementary Materials. Nonlinear regression analysis for CPP versus sPI in each unstable MAP patient is shown in Appendix B of the Supplementary Materials.

The results of both the nonlinear regression across the compiled plateau wave patient data for CPP versus sPI are shown in Fig. 2a. Similarly, the nonlinear regression for CPP versus AMP is shown for Fig. 2b. The corresponding results for the compiled unstable MAP patient data are shown in Fig. 3a and Fig. 3b, respectively.

CPP versus AMP

Nonlinear regression analysis of the relationship between CPP and AMP in plateau wave patients produced an inverse relationship between CPP and AMP ($R^2 = 0.610$). Nonlinear regression analysis of the relationship between CPP and AMP in unstable MAP patients produced an inverse relationship between the two parameters ($R^2 = 0.36$).

CPP versus sPI

Similarly, nonlinear regression analysis of the relationship between CPP and sPI in the plateau wave cohort produced an inverse relationship ($R^2 = 0.820$), best described by the following function:

$$sPI = a + (b/ CPP)$$

with CPP measured in mm Hg, and the statistical analysis concluding: $a = -0.03$ and $b = 26.4$. When the individual plateau wave patients were analyzed via nonlinear regression, the mean and standard deviation for the values of “ a ” and “ b ” were: $a = 0.005 \pm 0.061$, $b = 23.61 \pm 6.33$.

Similarly, nonlinear regression analysis of CPP versus sPI in the unstable MAP cohort demonstrated an inverse relationship between CPP and sPI ($R^2 = 0.61$), as shown in Fig. 3a. As seen within the plateau cohort’s nonlinear regression of CPP versus sPI, the model of best fit was the same as in plateau waves, showing the same function (with CPP measured in mm Hg, $a = -0.061$ and $b = 25.3$). When the individual unstable MAP patients were analyzed via nonlinear regression, the mean and standard deviation for the values of “ a ” and “ b ” were: $a = -0.144 \pm 0.391$, $b = 27.43 \pm 21.72$. Interestingly, both relationships closely resemble and support the inverse nonlinear relationship between CPP and PI previously proposed by de Riva et al. [4].

The “ a ” and “ b ” values calculated for each patient cohort were compared in a two-tailed independent-samples

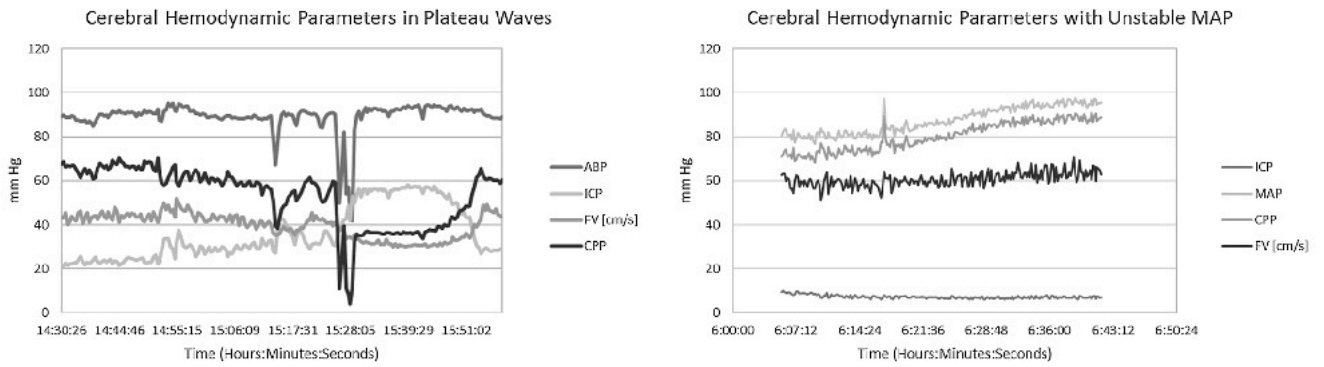


Fig. 1 ICP, CPP, and MAP recordings in both plateau wave and unstable MAP patients. *ABP* arterial blood pressure, *CPP* cerebral perfusion pressure, *FV* flow velocity, *ICP* intracranial pressure, *MAP* mean arterial pressure, *mm Hg* millimeters of mercury

Table 1 Plateau wave and unstable MAP patient demographics

Patient cohort	Number of patients	Mean age (years)	Male: female ratio	Median admission GCS	Glasgow outcome scale at discharge	
Plateau wave	11	27.2 (range: 17–76)	8:3	5 (range: 3–10)	GOS	# of patients
					Dead	2
					PVS	0
					Severe disability	5
					Moderate disability	4
Unstable MAP	9	25.1 (range: 17–60)	5:4	5 (range: 3–7)	GOS	# of patients
					Dead	2
					PVS	1
					Severe disability	5
					Moderate disability	1
Good	0					

GOS utilized within this study is an inverted GOS, with 5 = death and 1 = good outcome

GCS Glasgow Coma Scale, GOS Glasgow Outcome Scale, # number, MAP mean arterial pressure, PVS persistent vegetative state

Table 2 Measured and derived signals in plateau and unstable MAP cohorts

	Plateau wave recordings					Unstable MAP recordings				
	Baseline		Plateau			Lowest 10% of MAP		Highest 10% of MAP		
	Mean	SD	Mean	SD	<i>p</i> value	Mean	SD	Mean	SD	<i>p</i> value
MAP (mm Hg)	96.93	10.12	95.06	8.39	0.52	71.96	15.96	103.65	20.05	0.0002
A1 (mm Hg)	16.41	2.32	15.96	2.25	0.53	15.61	3.76	19.10	5.30	0.07
ICP (mm Hg)	25.60	5.92	50.12	8.66	<0.0001	21.8	10.58	20.65	10.64	0.78
AMP (mm Hg)	2.23	0.73	6.41	1.64	<0.0001	2.51	2.16	1.71	1.15	0.25
CPP (mm Hg)	71.34	12.73	44.94	10.29	<0.0001	50.16	14.91	83.00	19.77	<0.0001
sPI (a.u.)	0.29	0.16	0.48	0.23	0.004	0.51	0.27	0.28	0.12	0.01

MAP mean arterial pressure, CPP cerebral perfusion pressure, ICP intra-cranial pressure, AMP fundamental amplitude of ICP, PI pulsatility index, mm Hg millimeter of Mercury, SD standard deviation, A1 fundamental amplitude of arterial blood pressure

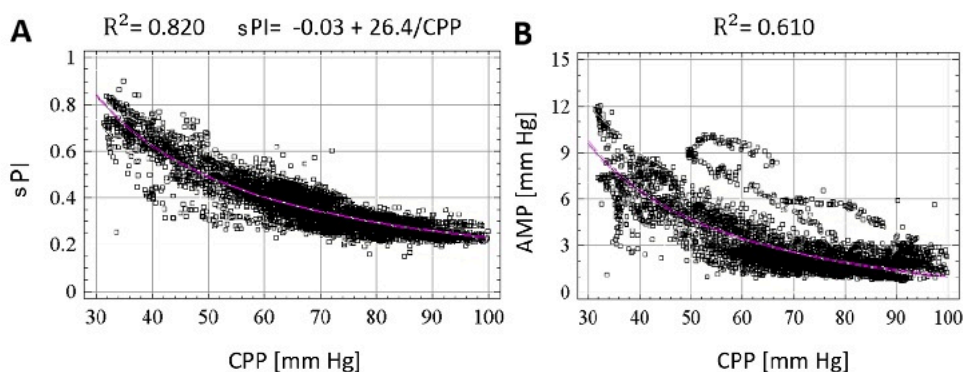


Fig. 2 Nonlinear regression analysis of CPP versus sPI (F1/FV) and CPP versus AMP in plateau cohort. **a** Nonlinear regression of CPP versus sPI. **b** Nonlinear regression of CPP versus AMP. AMP ICP pulse amplitude, CPP cerebral perfusion pressure, F1 amplitude of

fundamental frequency of FV, FV mean blood flow velocity in the mean cerebral artery (MCA), mm Hg millimeter of mercury, sPI spectral pulsatility index

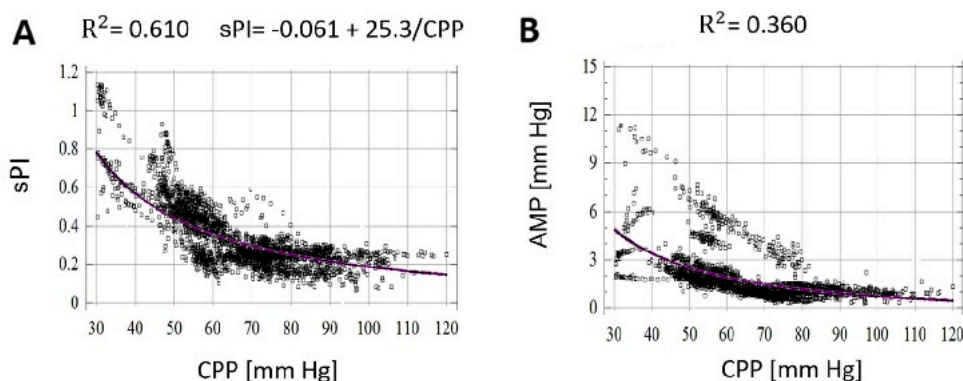


Fig. 3 Nonlinear regression analysis of CPP versus sPI (F1/FV) and CPP versus AMP in unstable MAP cohort. **a** Nonlinear regression of CPP versus sPI. **b** Nonlinear regression of CPP versus AMP. AMP ICP pulse amplitude, CPP cerebral perfusion pressure, F1 amplitude

of fundamental frequency of FV, FV mean blood flow velocity in the mean cerebral artery (MCA), mm Hg millimeter of mercury, sPI spectral pulsatility index

t test to evaluate significant differences between the plateau wave versus unstable MAP cohorts. Levene's test for equality of variances was assumed and dictated a non-significant difference between both the "a" and the "b" values obtained from the two groups ($t[27] = -1.507$, $p = 0.143$ and $t[27] = 0.670$, $p = 0.509$, respectively).

The effects of this hypothesis were further examined to determine whether each group's sets of "a" values were statistically different from the test value of 0 via two-tailed one-sample *t* tests. There was a nonsignificant difference between 0 and the "a" values in unstable MAP patients as well as in plateau wave patients ($t[12] = -1.330$, $p = 0.208$ and $t[15] = 0.300$, $p = 0.768$, respectively).

Relationships Between ICP, AMP, and sPI During Plateau Waves and Unstable MAP

Unlike the case for relationships between CPP versus sPI and AMP (where nonlinear relationships were found),

linear regression techniques yielded robust relationships of ICP with calculated variables in the plateau patient cohort.

The relationship between ICP and AMP across the compiled patient data for the plateau wave cohort is shown in Fig. 4a. A statistically significant linear relationship was described between ICP and AMP ($r = 0.871$, $R^2 = 0.758$). Similarly, a statistically significant linear relationship was described between ICP and sPI ($r = 0.728$, $R^2 = 0.530$), as displayed in Fig. 4b. The relationship between AMP and sPI is displayed in Fig. 4c. Linear regression techniques yielded a significant relationship between AMP and sPI ($r = 0.700$, $R^2 = 0.490$).

While linear regression also demonstrated significant relationships between ICP and AMP across the unstable MAP cohort, these relationships were less robust (Fig. 5). A statistically significant linear relationship was described between ICP and AMP ($R^2 = 0.470$). A very weak linear relationship was described between ICP and sPI ($R^2 = 0.059$), as displayed in Fig. 5b. Finally, the

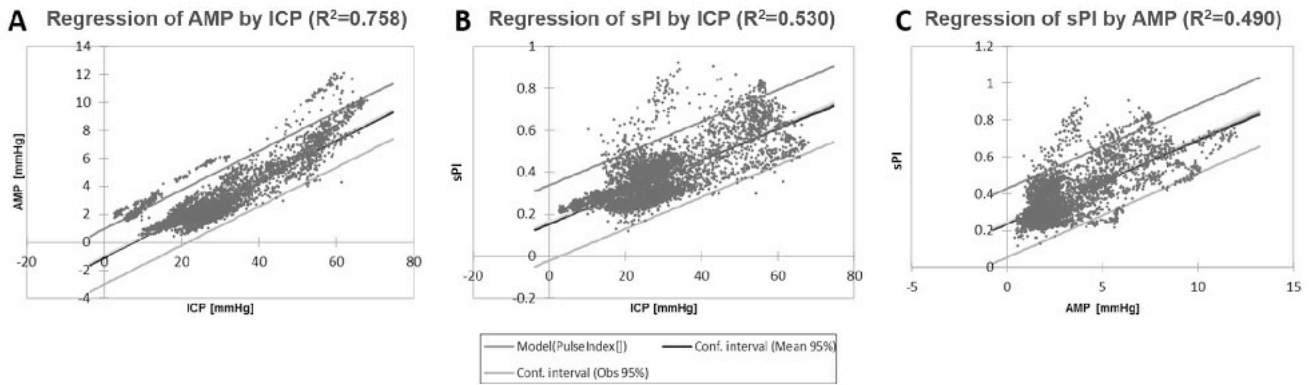


Fig. 4 Linear regression analysis of ICP versus AMP, ICP versus sPI, and AMP versus sPI in plateau cohort. **a** Linear regression of ICP versus AMP. **b** Linear regression of ICP versus sPI. **c** Linear

regression of AMP versus sPI. *AMP* ICP pulse amplitude, *ICP* intracranial pressure, *mm Hg* millimeters of mercury, *sPI* spectral pulsatility index, *R2* coefficient of determination

relationship between AMP and sPI was linear ($R^2 = 0.310$) (Fig. 5c).

Discussion

In the past, observations of brain pulsatility in the scenario of lowering CPP [10] and increasing ICP [11] were reported, although much mixed methodology was used in those works. In this study, we used a unified method to compare the same relationship in clinical conditions where CPP is affected either by increasing ICP or by the oscillations of unstable MAP.

Through the application of linear and nonlinear regression analysis, we have displayed both confirmatory and new results regarding the relationships between TCD-based PI and invasively-measured cerebral hemodynamic indices, ICP and CPP. This is “old” data harvested from the “Cambridge database” of high-resolution recorded signals from the 1990s, as neuro-intensive care TBI patients at that time were not treated according to rigorous CPP-/ICP-

oriented protocol—therefore, incidences of lowering CPP were recorded more easily. This is a relevant major aspect of these data recordings given that it is uncommon to have high-resolution datasets in the absence of CPP-directed therapy post-TBI.

Here, we have demonstrated that large fluctuations in CPP, either via changes in ICP or MAP, hold true the inverse nonlinear relationship between CPP versus sPI, and this relationship can be best described through the function: $PI = a + (b/ CPP)$; with $a \sim 0$ (i.e., plateau patients, $a = -0.03$; unstable MAP, $a = -0.06$) and b almost identical between both cohorts (i.e., plateau patients, $b = 26.4$; unstable MAP, $b = 25.3$). Furthermore, nonlinear regression analysis of each individual patient in both cohorts shows that the value for “ a ” is also close to 0. This was displayed strongly within the plateau wave cohort (mean “ a ” = 0.005; SD = 0.061). The unstable MAP cohort displayed this same relationship, but less substantially (mean “ a ” = -0.144; SD = 0.391). The statement that “ a ” was no different from 0 was further solidified via t test analysis demonstrating no statistically significant

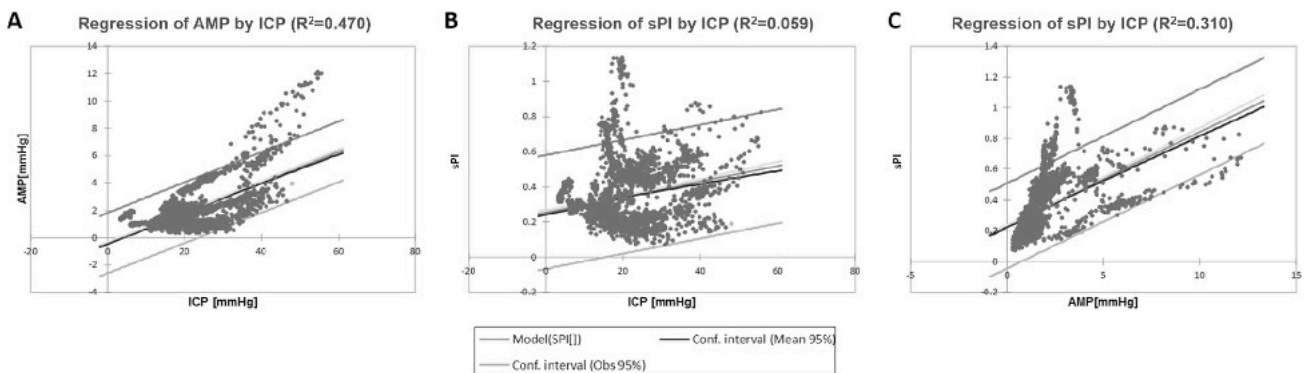


Fig. 5 Linear regression analysis of ICP versus AMP, ICP versus sPI, and AMP versus sPI in unstable MAP cohort. **a** Linear regression of ICP versus AMP. **b** Linear regression of ICP versus sPI. **c** Linear

regression of AMP versus sPI. *AMP* ICP pulse amplitude, *ICP* intracranial pressure, *mm Hg* millimeters of mercury, *sPI* spectral pulsatility index, *R2* coefficient of determination

difference between “ a ” and 0 in both cohorts. Therefore, if “ a ” is essentially equal to 0, then the relationship between CPP versus sPI can be approximated by the relation: $PI = b/ CPP$, with $b \sim 25$. This closely models the relation proposed by de Riva et al. [6] and provides the first evidence in support of this mathematical relation between CPP and PI in human models.

Secondly, we have also demonstrated the positive linear correlations between ICP versus AMP, ICP versus sPI, and AMP versus sPI in both the plateau wave and unstable MAP cohorts. Linear regression analysis of ICP versus AMP displayed the most robust linear relationship. Although the relationship between ICP versus nonspectral methods of PI calculation had been already described [12–15], limited literature exists by utilizing spectral methods for PI determination. Furthermore, the relationship between ICP versus AMP and AMP versus sPI is seldom described, leaving our manuscript as a nice and clear example of their linear relationships.

Third, it is also remarkable that the relationship between CPP and AMP also followed an inverse nonlinear relationship through nonlinear regression techniques. Again, this was also confirmed for both plateau wave and unstable MAP cohorts.

On the other hand, ICP seems to have a stronger link to intra-cranial/extra-vascular parameters (i.e., AMP, with an $R^2 = 0.758$) compared to intra-vascular measurements (i.e., sPI, with an $R^2 = 0.530$). Conversely, we could show that CPP displays a stronger relationship to intra-vascular parameters (i.e., sPI, with an $R^2 = 0.820$) versus extra-vascular intra-cranial measures (i.e., AMP, with an $R^2 = 0.610$).

As a last point, the fact that sPI is a smooth inverse function of CPP makes it very difficult to prove that the CPP level below which sPI starts to increase could denote the lower limit of autoregulation. This would mean that the brain is on the verge of becoming unable to maintain a constant level of blood flow. This thesis was proposed in the past [10], but later experimental challenges have proven it wrong [16].

Clinical Implications

The most recent edition of the Brain Trauma Foundation Guidelines recommends that CPP be directed towards the target range of 60–70 mm Hg. Constraining CPP between these values is thought to prevent either the hyper- or hypoperfusion that could, respectively, increase patient risk of poor outcome. When considering trends across individual patient data, all sPI versus CPP curves suggest that values of sPI around 0.4 correspond to CPP values around 60 mm Hg. In this manner, sPI can easily be interpreted by clinicians as an indicator of the accepted “safe” lower bound of

CPP [17]. Furthermore, through the above analysis we have been able to demonstrate the correlation between TCD-based sPI and CPP. This reinforces previous literature stating that TCD potentially provides the ability for a noninvasive estimation of CPP. Finally, we were able to demonstrate that the relationship between CPP- and TCD-based sPI is maintained during extremes of physiology (i.e., plateau waves and unstable MAP). Thus, if the clinician is to apply this methodology of noninvasive CPP estimation, our data suggest that the relationship between sPI and CPP should hold true, regardless of the individual clinical situation and extremes of physiology seen at the time of measurement.

Limitations

Our study has several limitations that need to be acknowledged. First, our analyses are based on observational data, rather than a prospective recording of response to a change in CPP. Consequently, many confounders may have affected critical variables, and the data access we have (and the relatively small volume of data compatible with ICM+ during this period) does not allow us to fully account for these. Second, our results are derived from only 11 sets of patient data containing 18 distinct plateau waves and nine datasets containing 13 instances of variable MAP. Consequently, extrapolation of this data to all patients with TBI is not possible, and confirmation of the described relationships will need to occur through comparative analysis of larger datasets.

Third, our nonlinear regression techniques for the relationships between CPP versus AMP and CPP versus sPI described the best fit with an inverse nonlinear function. However, with a total of only 20 patients, larger datasets are needed to better delineate and further prove this inverse relationship. Given that our patient population was so small, the next step is to validate our findings within a large TBI cohort to show that the proposed relationship holds. The relation yielded via nonlinear regression cannot be extrapolated and must serve only as a point of interest in the relationship between CPP versus AMP and CPP versus sPI, providing preliminary supporting evidence for the theorized nonlinear relation previously described in the literature [6]. Fourth, within the unstable MAP cohort, it is difficult clinically to isolate pure MAP from pure ICP contributions to changes in CPP. These patients exhibit significant fluctuations in various physiologic measures, as it is shown in Table 2. Finally, patients with severe TBI and plateau waves are an extreme cohort of critically ill patients, with injuries that may yield abnormal physiologic brain properties. Therefore, the relationships described in this small study cannot necessarily be applied to all TBI patients.

Conclusions

In severe TBI patients with plateau waves or unstable MAP, the relationships between CPP and pulsatility of brain signals are inversely proportional, no matter the mechanism that lowers CPP. ICP versus AMP, ICP versus sPI, and AMP versus sPI display positive linear correlations.

Open Access This article is distributed under the terms of the Creative Commons Attribution 4.0 International License (<http://creativecommons.org/licenses/by/4.0/>), which permits unrestricted use, distribution, and reproduction in any medium, provided you give appropriate credit to the original author(s) and the source, provide a link to the Creative Commons license, and indicate if changes were made.

References

1. Le Roux P, Menon DK, Citerio G, et al. The international multidisciplinary consensus conference on multimodality monitoring in neurocritical care: evidentiary tables: a statement for healthcare professionals from the neurocritical care society and the European society of intensive care medicine. *Neurocrit Care*. 2014;21(Suppl 2):S297–361.
2. Le Roux P, Menon DK, Citerio G, et al. Consensus summary statement of the international multidisciplinary consensus conference on multimodality monitoring in neurocritical care: a statement for healthcare professionals from the neurocritical care society and the European society of intensive care medicine. *Intensive Care Med*. 2014;40(9):1189–209.
3. Cardim D, Robba C, Bohdanowicz M, et al. Non-invasive monitoring of intracranial pressure using transcranial doppler ultrasonography: is it possible? *Neurocrit Care*. 3 Mar 2016. [Epub ahead of print].
4. de Riva N, Budohoski KP, Smielewski P, et al. Transcranial Doppler pulsatility index: what it is and what it isn't. *Neurocrit Care*. 2012;17(1):58–66.
5. Czosnyka M, Guazzo E, Iyer V, et al. Testing of cerebral autoregulation in head injury by waveform analysis of blood flow velocity and cerebral perfusion pressure. *Brain Edema*. 1994;IX:468–71.
6. Czosnyka M, Richards H, Kirkpatrick P, Pickard J. Assessment of cerebral autoregulation with ultrasound and laser Doppler wave forms—an experimental study in anesthetized rabbits. *Neurosurgery*. 1994;35(2):287–92.
7. Ursino M, Giullioni M, Lodi CA. Relationships among cerebral perfusion pressure, autoregulation, and transcranial Doppler waveform: a modeling study. *J Neurosurg*. 1998;89(2):255–66.
8. Czosnyka M, Smielewski P, Piechnik S, et al. Hemodynamic characterization of intracranial pressure plateau waves in head-injury patients. *J Neurosurg*. 1999;91(1):11–9.
9. Varsos GV, de Riva N, Smielewski P, et al. Critical closing pressure during intracranial pressure plateau waves. *Neurocrit Care*. 2013;18(3):341–8.
10. Chan KH, Miller JD, Dearden NM, et al. The effect of changes in cerebral perfusion pressure upon middle cerebral artery blood flow velocity and jugular bulb venous oxygen saturation after severe brain injury. *J Neurosurg*. 1992;77(1):55–61.
11. Avezaat CJ, van Eijndhoven JH, Wyper DJ. Cerebrospinal fluid pulse pressure and intracranial volume-pressure relationships. *J Neurol Neurosurg Psychiatry*. 1979;42(8):687–700.
12. Cardim D, Robba C, Donnelly J, et al. Prospective study on noninvasive assessment of intracranial pressure in traumatic brain-injured patients: comparison of four methods. *J Neurotrauma*. 2016;33(8):792–802.
13. Morgalla MH, Magunia H. Noninvasive measurement of intracranial pressure via the pulsatility index on transcranial Doppler sonography: Is improvement possible? *J Clin Ultrasound*. 2016;44(1):40–5.
14. Bellner J, Romner B, Reinstrup P, Kristiansson KA, Ryding E, Brandt L. Transcranial Doppler sonography pulsatility index (PI) reflects intracranial pressure (ICP). *Surg Neurol*. 2004;62(1):45–51.
15. Donnelly J, Czosnyka M, Harland S, Varsos GV, Cardim D, Robba C, et al. Cerebral haemodynamics during experimental intracranial hypertension. *J Cereb Blood Flow Metab*. 18 Mar 2016. pii: 0271678X16639060. [Epub ahead of print].
16. Richards HK, Czosnyka M, Whitehouse H, Pickard JD. Increase in transcranial Doppler pulsatility index does not indicate the lower limit of cerebral autoregulation. *Acta Neurochir Suppl*. 1998;71:229–32.
17. Brain Trauma Foundation guidelines for the management of severe traumatic brain injury: 4th ed. Guidelines for the management of severe traumatic brain injury. Brain Trauma Foundation; 2016 [cited 16 Feb 2017]. https://www.braintrauma.org/uploads/13/06/Guidelines_for_Management_of_Severe_TBI_4th_Edition.pdf.

Reliability of the Blood Flow Velocity Pulsatility Index for Assessment of Intracranial and Cerebral Perfusion Pressures in Head-Injured Patients

Christian Zweifel, MD*‡
 Marek Czosnyka, PhD*
 Emmanuel Carrera, MD*
 Nicolas de Riva, MD*
 John D. Pickard, MD, FMedSci*
 Peter Smielewski, PhD*

*Academic Neurosurgical Unit, University of Cambridge Clinical School, Cambridge, United Kingdom; ‡Department of Neurosurgery, University Hospital of Basel, Basel, Switzerland

Correspondence:

Christian Zweifel, MD,
 Academic Neurosurgical Unit,
 Department of Clinical Neurosciences,
 Level 4, A Block,
 Addenbrooke's Hospital,
 Cambridge CB2 2QQ,
 United Kingdom.
 E-mail: zweifelch@gmx.ch

Received, November 29, 2011.

Accepted, June 20, 2012.

Published Online, July 11, 2012.

Copyright © 2012 by the
 Congress of Neurological Surgeons



WHAT IS THIS BOX?

A QR Code is a matrix barcode readable by QR scanners, mobile phones with cameras, and smartphones. The QR Code above links to Supplemental Digital Content from this article.

BACKGROUND: It has been postulated that the Gosling pulsatility index (PI) assessed with transcranial Doppler (TCD) has a diagnostic value for noninvasive estimation of intracranial pressure (ICP) and cerebral perfusion pressure (CPP).

OBJECTIVE: To revisit this hypothesis with the use of a database of digitally stored signals from a cohort of head-injured patients.

METHODS: We analyzed prospectively collected data of patients admitted to the Cambridge Neuroscience critical care unit who had continuous recordings of arterial blood pressure, ICP, and cerebral blood flow velocities (FVs) using TCD. PI was calculated $(FV_{sys} - FV_{dia})/FV_{mean}$ over each recording session. Statistical analysis was performed using Spearman rank correlation, receiver-operator-characteristics methods, and modeling of a nonlinear PI-ICP/CPP graph.

RESULTS: Seven hundred sixty-two recorded daily sessions from 290 patients were analyzed with a total recording time of 499.9 hours. The correlation between PI and ICP was 0.31 ($P < .001$) and for PI and CPP -0.41 ($P < .001$). The 95% prediction interval of ICP values for a given PI was more than ± 15 mm Hg and for CPP more than ± 25 mm Hg. The diagnostic value of PI to assess ICP area under the curve ranged from 0.62 (ICP >15 mm Hg) to 0.74 (ICP >35 mm Hg). For CPP, the area under the curve ranged from 0.68 (CPP <70 mm Hg) to 0.81 (CPP <50 mm Hg). Probability charts for elevated ICP/lowered CPP depending on PI were created.

CONCLUSION: Overall, the value of TCD-PI to assess ICP and CPP noninvasively is very limited. However, extreme values of PI can still potentially be used in support of a decision for invasive ICP monitoring.

KEY WORDS: Cerebral perfusion pressure, Critical care, Diagnostic value, Head injury, Intracranial pressure, Pulsatility index

Neurosurgery 71:853–861, 2012

DOI: 10.1227/NEU.0b013e3182675b42

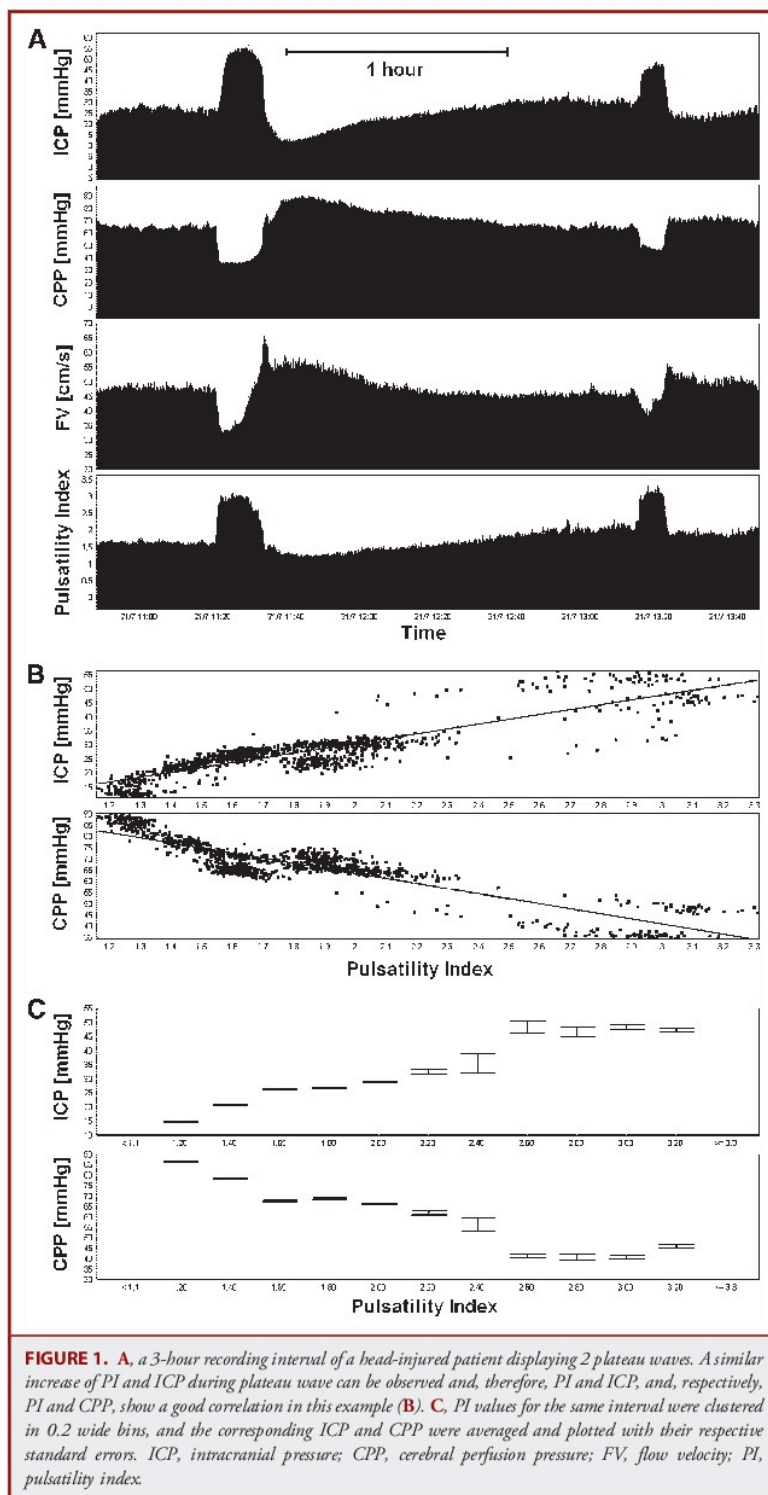
www.neurosurgery-online.com

It is generally accepted that a reliable noninvasive tool for screening for evidence of increased intracranial pressure (ICP) and decreased cerebral perfusion pressure (CPP) would

ABBREVIATIONS: ABP, arterial blood pressure; AUC, area under the curve; CPP, cerebral perfusion pressure; FV, flow velocity; ICP, intracranial pressure; PI, pulsatility index; ROC, receiver-operating-characteristic; TBI, traumatic brain injury; TCD, transcranial Doppler

Supplemental digital content is available for this article. Direct URL citations appear in the printed text and are provided in the HTML and PDF versions of this article on the journal's Web site (www.neurosurgery-online.com).

be highly valued in clinical practice. Past efforts have involved attempts to estimate ICP based on measurements of intraocular pressure,¹ tympanic membrane displacement,² and, more recently, ultrasonography assessment of the optic nerve sheath diameter.³ Transcranial Doppler (TCD) ultrasonography is probably the most widely investigated tool for its potential to assess ICP and CPP noninvasively in many populations of patients: traumatic brain injury (TBI),^{4–8} subarachnoid hemorrhage,^{4,9} hydrocephalus,¹⁰ pediatrics,^{11,12} and others. One of the measures derived from the TCD flow velocity (FV) waveform that has been discovered to reflect changes in ICP and CPP is the pulsatility index (PI), a ratio of pulse amplitude to its mean



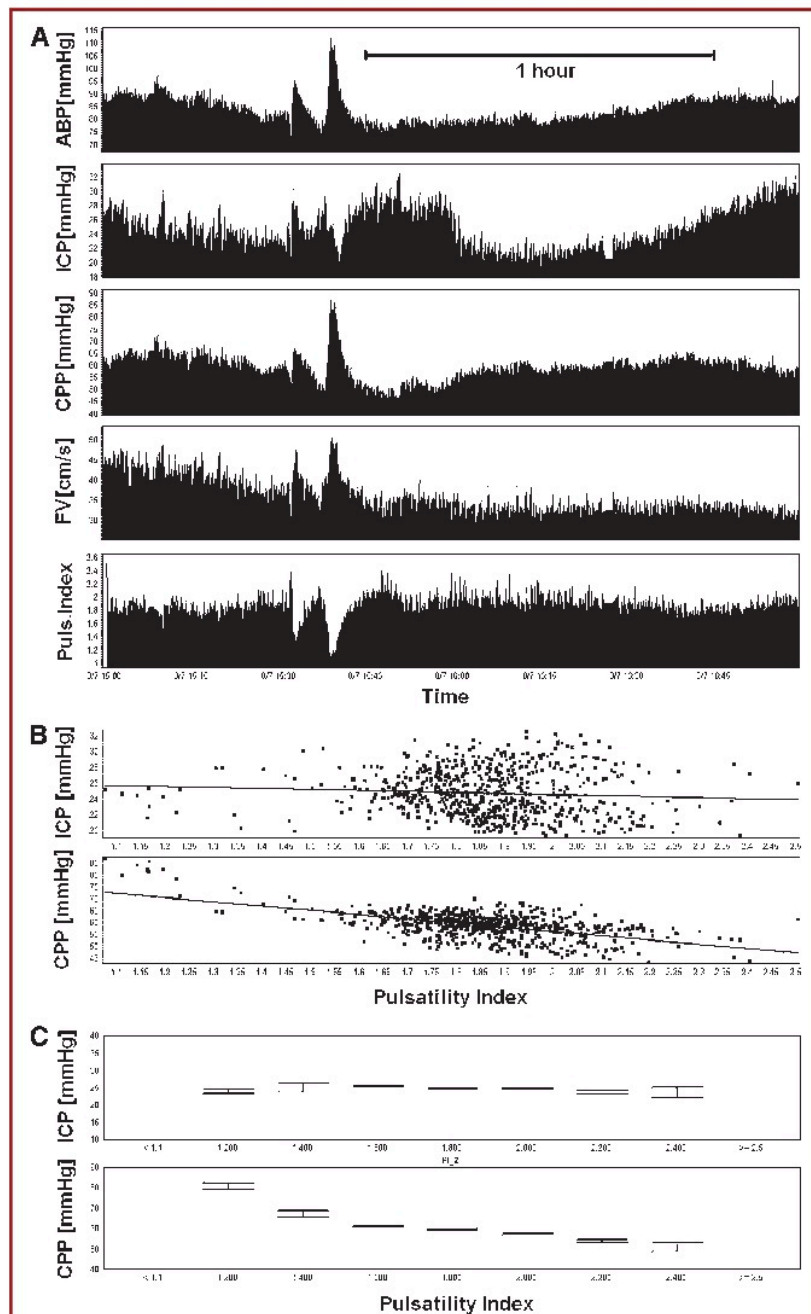


FIGURE 2. Shown is a 2-hour recording interval of a head injured patient. **A**, 2 peaks of ABP elevations led to a consecutive increase of CPP and FV and lowering of PI. ICP showed just a minor change during ABP increase. **B** and **C**, the correlation between PI and ICP was almost not existent during the recording interval. On the other side, there is a stronger correlation between PI and CPP in this example. ABP, arterial blood pressure; ICP, intracranial pressure; CPP, cerebral perfusion pressure; FV, flow velocity; PI, pulsatility index.

value.¹³ The index, being a ratio of velocities, does not rely on the knowledge of the diameter of the insonated vessel and thus can be directly compared between patients. Its version using peak-to-peak amplitude, termed the Gosling PI, is usually displayed in the modern TCD machines and is thus readily available for diagnostic interpretations. However, reports on its usefulness for predicting ICP and CPP are mixed.

A particularly positive report supporting the use of PI assessing ICP was from Bellner et al⁴ in 2004 in a cohort of 81 adult patients with mainly TBI and subarachnoid hemorrhage. They found a strong correlation between PI and ICP ($r = 0.938$, $r < 0.0001$) and a sensitivity and specificity of 0.89 and 0.92 to detect ICP higher than 20 mm Hg. Brandi et al⁵ demonstrated in a cohort of 45 TBI patients that the estimated value of ICP by using PI measure had a median difference from the real ICP of -3.2 mm Hg with a standard deviation of ± 12.6 mm Hg and concluded that PI was useful to screen for patients at risk of increased ICP. Similarly, Melo et al¹² reported a sensitivity of 0.94 and a specificity of 0.41 to diagnose ICP higher than 20 mm Hg in pediatrics with severe TBI when end-diastolic velocity was below 25 cm/s or PI was higher than 1.31. They also concluded that TCD was a valuable screening tool to identify those children who need continuous invasive ICP monitoring.

Other researchers have been far more reserved on this subject. Behrens et al¹⁰ studied ICP-PI relationship in patients with communicating hydrocephalus during a CSF infusion test. They found that in their cohort the 95% prediction interval to assess ICP was as high as ± 25 mm Hg and therefore concluded that PI does not reliably estimate ICP. Figaji et al found only a weak

relationship ($r = 0.36$, $P = .04$) between PI and ICP in children.¹¹ They reported that, with increasing PI, the specificity for detecting ICP >20 mm Hg increases, but sensitivity becomes very low, so that PI cannot be a reliable noninvasive indicator of ICP.

The relationship between the pulsatility index and ICP/ CPP has been recently studied by using a simplified model of cerebrovascular circulation.¹⁴ Analysis presented there clearly shows that PI is indeed related to the inverse of CPP, but that the relationship is complex, and it depends on further factors like arterial blood pressure and its pulse amplitude, cerebrovascular compliance and resistance, as well as the heart rate.^{14,15}

All in all, a complex and unclear picture of the relationship between PI, ICP, and CPP, emerges. This is potentially a serious problem, because investigators who follow the more enthusiastic reports and rely on TCD for an initial assessment of ICP/ CPP may be making clinically harmful decisions. We have therefore decided to revisit this issue in our relatively large database of recordings from patients with severe head trauma.

PATIENTS AND METHODS

Data were collected prospectively from patients admitted to the Neurosciences Critical Care Unit at Addenbrooke’s Hospital (Cambridge University Hospitals NHS Foundation Trust) between 1992 and 2009

TABLE. Baseline Characteristics^a

	Patients (n = 290)
Age, y	32.8 (± 15.9)
GCS on admission	6 (± 3)
MABP (mmHg)	92.7 (± 11.7)
ICP (mmHg) (mean)	20.0 (± 9)
CPP (mmHg) (mean)	72.8 (± 13.3)
HR (min^{-1}) (mean)	80.4 (± 16.8)
RR (min^{-1}) (mean)	13.8 (± 3.1)
Fv max (cm/s)	114.7 (± 40.2)
Fv mean (cm/s)	62.0 (± 25.5)
Fv min (cm/s)	34.1 (± 17.9)
Mean PI	1.2 (± 0.4)
GOS at 6 mo^b	
1 dead	58
2 vegetative state	7
3 severe disability	69
4 moderate disability	48
5 good recovery	63

^aMABP, mean arterial blood pressure; HR, heart rate; RR, respiratory rate; FV, flow velocity; GCS, Glasgow Coma Scale; GOS, Glasgow Outcome Scale; ICP, intracranial pressure; CPP, cerebral perfusion pressure; PI, pulsatility index.

^bGOS available for 245 of 290 patients.

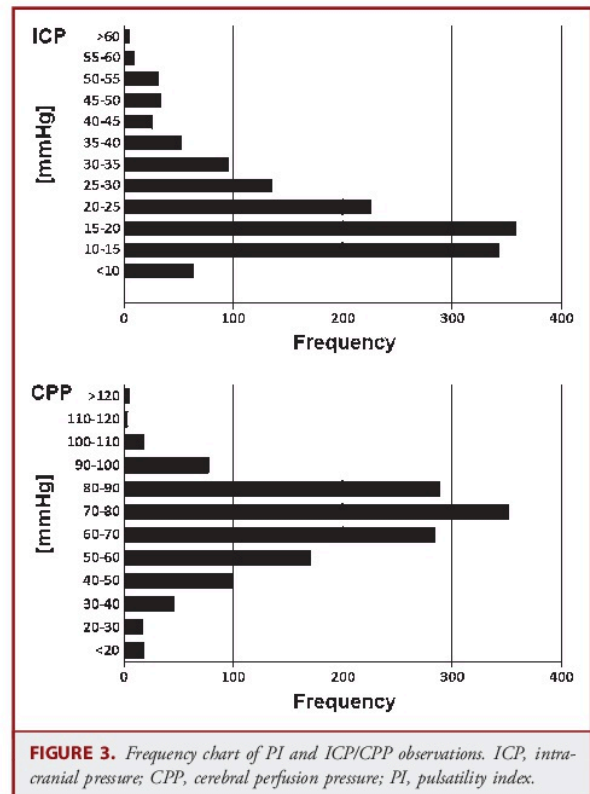


FIGURE 3. Frequency chart of PI and ICP/ CPP observations. ICP, intracranial pressure; CPP, cerebral perfusion pressure; PI, pulsatility index.

with closed head injury who had ICP and concomitant TCD monitoring. The data were acquired as part of daily routine investigation of cerebral autoregulation.¹⁶ The database only included patients with a satisfactory quality of flow velocity recording. No information with regard to number of recordings/patients rejected due to poor ultrasound window was retained. For the early recordings, the Neurocritical Users Committee approved their anonymous use in a form of clinical audit. For the later ones, individual consent was obtained from the family or next of kin. Different treatment protocols were used over the years: before 2003, a pure CPP-oriented therapy was administered¹⁷; since 2003, a mixed ICP/ CPP protocol has been used with a restricted use of vasopressors.¹⁸

Signal Acquisition

ICP was either monitored using an intraparenchymal probe (Codman ICP MicroSensor, Codman & Shurtleff Inc., Raynham, M) or an extra-ventricular drainage system with a pressure transducer (Baxter). During recording, the extraventricular drainage was closed. Arterial blood pressure (ABP) was measured directly from the radial or femoral artery (Baxter Healthcare Corp CardioVascular Group, Irvine, California), which was zeroed at the heart level. FV in the middle cerebral artery was monitored using TCD with a 2-MHz probe (model PCDop 842; Scimed, Bristol, England; since 2008: Multidop T, DWL, Germany). These signals were digitized using A/D converter (DT9801, Data Translation, Marlboro, Massachusetts), sampled at frequency 50 Hz. Before analysis, signal artifacts such as arterial line flushing and repositioning of Doppler probes were removed. The data acquisition and analysis was done using a laptop PC running ICM+ software (<http://www.neurosurg.cam.ac.uk/icmplus>).¹⁹

Statistics

Discrete variables were summarized using counts (percentage) and continuous variables using means (\pm standard deviation). Significance was set at $P \leq .05$. PI was continuously calculated by using the Gosling formula $(FV_{sys} - FV_{dia})/FV_{mean}$ and averaged over consecutive 10-second-long periods in keeping with the process of calculating trends of mean values of ICP, FV, and CPP adopted for this project (Figures 1 and 2). To deal with the problem of autocorrelated data points (correlation between consecutive data points), as well as effects of varying recording durations, ICP and CPP data samples from each patient were divided into bins according to PI. Bin width of 0.2 was chosen as a compromise between PI resolution and amount of averaging needed. Center values of PI for each bin along with the mean values of ICP and CPP within each bin were subsequently taken for further statistical analysis. In addition, 1 average value of PI per patient was calculated to determine its association with outcome (Spearman, Kruskal-Wallis). Receiver-operating-characteristic (ROC) curve analyses were performed to determine performance of PI as a diagnostic index for detection of elevated ICP (or decreased CPP). The ROC curve is created by plotting the true positive rate (sensitivity) against the corresponding false positive rate (1-specificity) for different cutoff points of a parameter²⁰ (in this case PI). The area under the curve (AUC) is a measure of how well PI can detect elevation of ICP above (or decrease of CPP below) given threshold for which the curve was constructed. In our case, the AUCs were calculated for ICP thresholds of 15, 20, 25, 30, and 35 mm Hg and CPP thresholds of 70, 65, 60, 55, and 50 mm Hg. It is generally considered that, in medicine, an AUC <0.7 is not a useful diagnostic tool. An AUC >0.8 is a good diagnostic tool, and an AUC >0.9 an excellent diagnostic tool.

Finally, 2 sets of empirical second-order polynomial models were formulated to chart the probability of ICP, and CPP, respectively, of exceeding different thresholds given measured value of PIs (see Supplemental Digital Content 1, <http://links.lww.com/NEU/A476>).

RESULTS

The cohort consisted of 290 head-injured patients with a mean age of 32.8 (\pm 15.9). The mean Glasgow Coma Scale on admission was 6 (\pm 3). The mean FV of all patients was 62.0 cm/s (\pm 25.5), and only 4 patients had an average FV above 120 cm/s. And although the Lindegaard ratio was not measured, the fact that none of the patients had an average FV higher than 180 cm/s suggests that traumatic vasospasm was unlikely in our cohort.

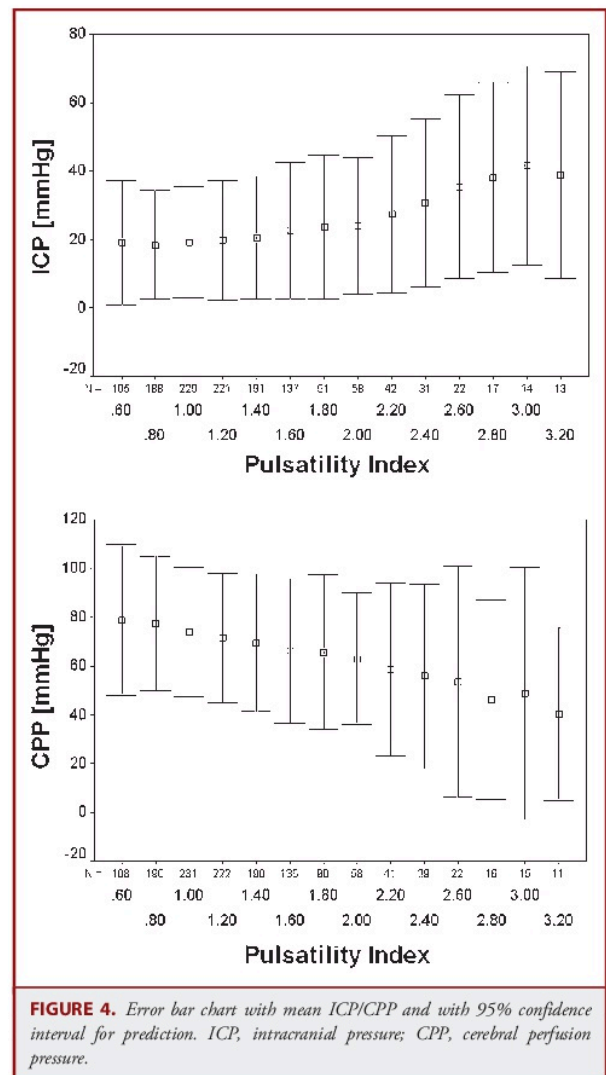


FIGURE 4. Error bar chart with mean ICP/ CPP and with 95% confidence interval for prediction. ICP, intracranial pressure; CPP, cerebral perfusion pressure.

Further baseline characteristics of patients are shown in the Table.

A total of 762 recorded daily sessions were analyzed adding up to the total recording time of 499.9 hours, yielding 1385 PI-ICP and PI-CPP pairs. An example of PI/ICP and PI/CPP scatter plot, as well as the corresponding binning from a single patient, is shown in Figure 1 and Figure 2. Distribution of PI/ICP and PI/CPP pairs across all patients is shown in Figure 3. Of all PI-ICP pairs, 44.7% corresponded to ICP values above 20 mm Hg. Similarly, 25% of all PI-CPP data pairs corresponded to CPP values below 60 mm Hg.

Among the individual recordings, there were those in which PI and ICP (and CPP) showed very high correlation (Figure 1), and those in which a PI and ICP correlation was nonexistent (Figure 2). Correlation analysis (Spearman) performed across all patients revealed highly significant but rather poor association between PI and ICP of 0.31 ($P < .001$) and, somewhat better for PI and CPP of -0.41 ($P < .001$).

The mean and 95% confidence interval for prediction of ICP and CPP for a given PI is charted in Figure 4. The confidence interval for ICP ranged from ± 15 mm Hg to ± 35 mm Hg, and for CPP from about ± 25 mm Hg to ± 50 mm Hg.

Results of ROC analysis are presented in Figure 5, which shows that the diagnostic value improves (ie, higher AUC) with increasing ICP or decreasing CPP thresholds. For ICP, the AUC ranged from 0.62 (ICP >15 mm Hg) to 0.74 (ICP >35 mm Hg), and for CPP, the AUC ranged from 0.68 (CPP <70 mm Hg) to 0.81 (CPP <50 mm Hg). The ROC for a critical ICP threshold of 20 mm Hg was 0.64; for a critical CPP threshold of 60 mm Hg, it was 0.75.

Probability charts for ICP and CPP with respect to PI are shown in Figure 6. Such constructed charts can be used to assess the probability of increased ICP/decreased CPP given measured PI. With a PI of 1.8, for example, the probability of ICP exceeding 25 mm Hg is approximately 40%. Similarly, the probability of decreased CPP to levels below 60 mm Hg is approximately 37%.

The outcome of our cohort was assessed with the Glasgow outcome scale and was available for 245 patients. The correlation between PI and outcome was 0.078 ($P = .22$, Spearman). The Kruskal-Wallis test showed that there was no significant difference between the medians of PI in the 5 outcome groups ($P = .33$).

DISCUSSION

The aim of this study was to evaluate the association between the TCD-derived PI and ICP/CPP in a cohort of 290 head-injured patients. Although one can find examples of a good correlation between PI and ICP/CPP within a single recording (eg, Figure 1), overall there appears to be only a weak association between PI and ICP and between PI and CPP. Also, the rather wide 95% confidence interval for prediction of ICP and CPP reflects the limitation of PI as a diagnostic tool in this respect. ROC analysis showed that the predictive value of PI can indeed be relatively high, with AUC values exceeding 0.75; however, this is the case

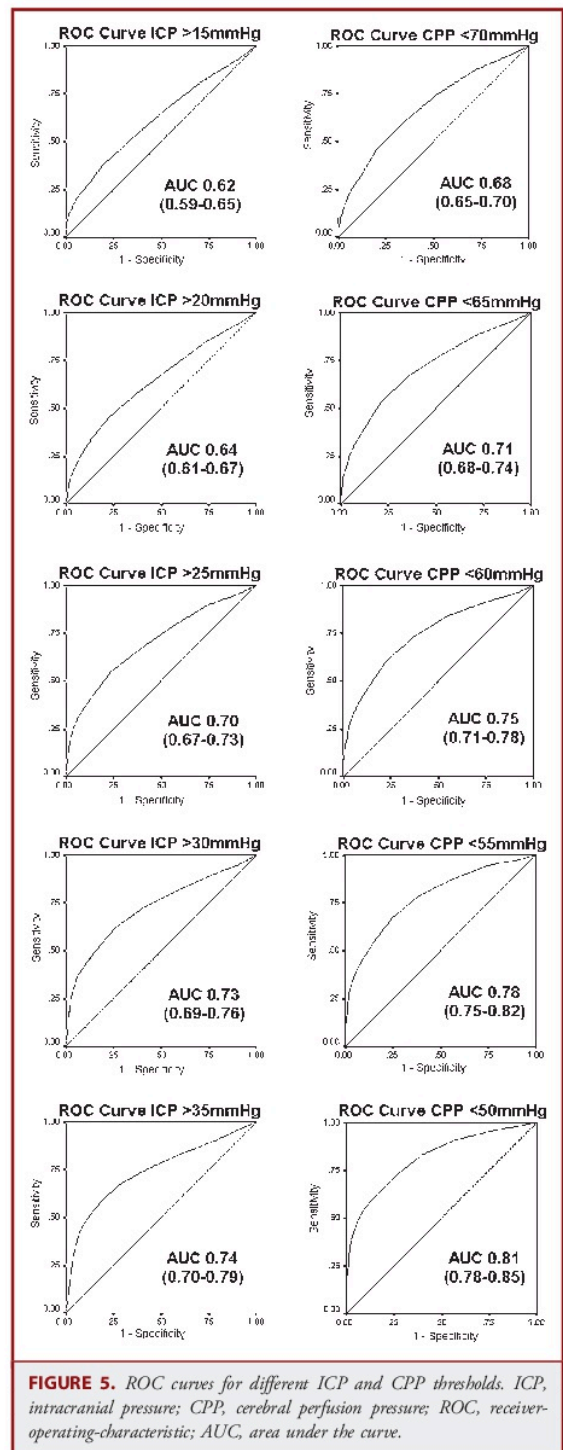


FIGURE 5. ROC curves for different ICP and CPP thresholds. ICP, intracranial pressure; CPP, cerebral perfusion pressure; ROC, receiver-operating-characteristic; AUC, area under the curve.

only for highly elevated ICP (>35 mm Hg) and low CPP values (<55 mm Hg). For detecting critical clinical thresholds (ICP >20 mm Hg, CPP <60 mm Hg), PI is certainly not a reliable diagnostic tool.

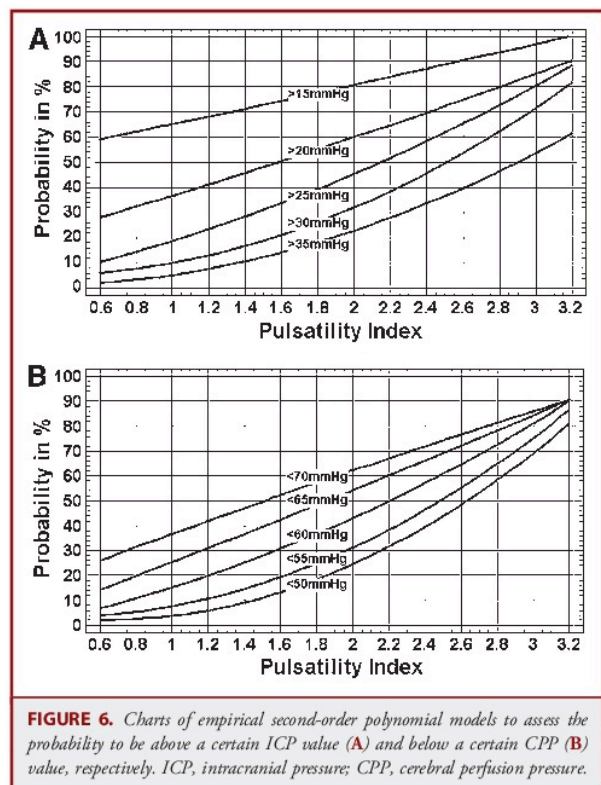
Our results are in accordance with a study published by Behrens et al,¹⁰ mentioned earlier, in which the authors analyzed the PI-ICP relationship during lumbar infusion studies in patients with normal pressure hydrocephalus. With this setting it was possible to investigate the PI-ICP relationship across a wide range of ICP values from baseline up to 50 mm Hg and they found a relationship between PI and ICP of 0.47 ($R^2 = 0.22$). What distinguished that project from other more optimistic ones like Bellner et al⁴ or Brandi et al⁵ was a much larger range of ICP studied, thus allowing for more exhaustive examination of the PI-ICP relationship. In our present study, a large number of recordings including several daily examinations for each patient ensured that our ICP data were similarly widely distributed. In particular, in more than one-fourth of data pairs, ICP exceeded 25 mm Hg. This might explain why our results support findings of Behrens et al¹⁰ and are contrary to the other 2 studies mentioned.

Various TCD-derived formulae have been proposed for ICP and CPP estimation. Whereas some include ABP^{21,22} as a variable, others only include PI.^{4,5} A retrospective study of Brandi et al⁵ compared different formulae and concluded that the one proposed by Bellner⁴ have higher predictive value than those of Schmidt et al²² and Edouard et al.²¹ The conclusion of Brandi et al⁵ was questioned in a review of Lavinio and Menon²³ where the authors reasoned that the Schmidt and Edouard formulae are more suitable for clinical use because they tend to underestimate ICP less than the ones by Bellner et al⁴ and Brandi et al.⁵ Our results show a rather wide 95% confidence interval of prediction, and this indicates that any formula based solely on PI will not provide satisfactory results.

Other approaches to noninvasive assessment of ICP have been reported.²⁴ In particular, ultrasonography based assessment of the optic nerve sheath diameter has gained significant interest. A recently published meta-analysis showed that this technique has a pooled sensitivity of 0.9, a specificity of 0.85, and a summarized AUC of 0.9 to detect elevated intracranial hypertension.³ Another TCD-based method using dual-depth insonation of extraocular and intraocular arteries with simultaneous application of external pressure to the orbit even offers a direct measurement of ICP with relatively high degree of accuracy.²⁵ These techniques, and others, although far from perfect, will perform much better than TCD alone, and, in particular, PI, for estimation of ICP. However, the temptation to use such a readily available index as a diagnostic tool for elevated ICP, a notion supported by some positive experience reported in the literature, often seems too great to resist. So, is there a way that PI can be interpreted safely in terms of its relation to ICP?

Our results clearly show that TCD-PI is a poor and clinically inadequate predictor of ICP that cannot provide a replacement for direct ICP measurement, nor can it compete with other more sophisticated methods of noninvasive assessment of ICP. Particularly

when ICP and CPP are close to the critical thresholds, the diagnostic accuracy is very inadequate. However, with a more empirical approach, PI may still have a clinical value as a screening tool for identification of patients at risk.^{7,12,22} The scientific foundation of the actual guidelines (European Brain Injury Consortium guidelines, European Neurointensive Care and Emergency Medicine, Brain Trauma Foundation)²⁶⁻²⁸ for the indication of invasive ICP monitoring is based on the probability of increased ICP, and, again, this is based on assessment of clinical and imaging data. Probably the most widely used Brain Trauma Foundation guidelines recommend ICP monitoring when the Glasgow Coma Scale after resuscitation is ≤ 8 and an abnormal CT scan is present.²⁷ If the CT scan results are normal, there is a likelihood of about 10% to 15% that a head-injured patient will develop intracranial hypertension. Similarly, we can take this concept and apply it to PI assessment. According to our distribution and the derived probability graph (Figure 6), we can state that, if PI is ≤ 1 , there is a chance of about just 15% that the CPP is below 60 mm Hg. If PI is ≤ 0.8 , there is a likelihood of about 10% that CPP is below 60 mm Hg. On the other hand, if PI is ≥ 2.2 , the probability of low CPP below 60 mm Hg is about 50%; if PI is ≥ 3 , the probability increases to 80%. In this context, a prospective observational study published by Bouzat et al⁷ showed that PI has a prognostic value for secondary deterioration of patients with mild to moderate



brain injury. Instead of associating PI directly with ICP and CPP, they associate PI with a clinical follow-up. They found that, in patients with mild to moderate head injury and no evidence of severe head injury on initial CT, a PI ≥ 1.25 is significantly associated with the occurrence of secondary neurological deterioration. And this really suggests a role for a quick TCD check in accident and emergency medicine. Although we have rather discredited PI as a method for assessment of ICP, taking the full clinical picture in context, and given the probability charts, like the ones in Figure 6, TCD-PI may still offer support for screening for patients at risk of brain hemodynamic deficit who require invasive ICP monitoring.

Limitations

There are several limitations of this study. First, because of logistical reasons, the distribution of duration of individual recordings and their date postadmission as well as their number per patient in our study was very uneven. In order to deal with this problem, PI, ICP, and CPP values were averaged for each patient (within respective 0.2 wide bins of PI) to establish 1 PI-ICP and PI-CPP profile per patient. Hence, we cannot provide reliable information about within-patient variability of our PI-based estimates. However, because our results are similar to previous reported studies in which within-patient variability has been taken into account,^{10,11} we believe that the averaging approach we took was not a major confounding factor in our present study. Second, the side of TCD insonation and the side of ICP probe location was not standardized. It has been described that unilateral brain swelling may influence noninvasive CPP determination by use of TCD.²² Third, the examinations were performed over a period of 17 years. We may not exclude that changes in the treatment regime, interoperator reliability of multiple TCD investigators, and changes in the technical equipment may have influenced the results. Intraventricular drain for ICP monitoring was used from 1992 to 1993, and later only sporadically. On the other hand, our goal was to assess the suitability of PI for assessment of ICP (and CPP) irrespective of these factors. And last, TCD is not suitable for all patients, because the lack of temporal ultrasonic window has been reported in up to 10% of patients.²⁹

CONCLUSION

The diagnostic value of TCD FV pulsatility index for direct noninvasive assessment of ICP and CPP is very limited. However, because its measurement can be readily and repeatedly performed, and given careful probability-led interpretation, PI may still have value as a diagnosis-supporting tool where highly elevated ICP or dangerously decreased CPP is suspected.

Disclosures

The software for brain monitoring ICM+ (www.neurosurg.cam.ac.uk/icmplus) is licensed by the Cambridge Enterprise Limited (University of Cambridge). Drs Smielewski and Czosnyka have a financial interest in a fraction of the licensing fee. This work was supported by National Institute of Health Research, Biomedical Research Centre (Neuroscience Theme), the Medical Research Council (grants

G0600986 and G9439390) and NIHR Senior Investigator Awards (to J.D.P.); and also by the Swiss National Science Foundation (PBBS3-125550 to C.Z. and PASSMP3-124262 to E.C.), Bern, Switzerland. EC was additionally supported by the SICPA Foundation, Lausanne, Switzerland. The authors have no personal financial or institutional interest in any of the drugs, materials, or devices described in this article.

REFERENCES

- Kirk T, Jones K, Miller S, Corbett J. Measurement of intraocular and intracranial pressure: is there a relationship? *Ann Neurol*. 2011;70(2):323-326.
- Shimbles S, Dodd C, Banister K, Mendelow AD, Chambers IR. Clinical comparison of tympanic membrane displacement with invasive ICP measurements. *Acta Neurochir Suppl*. 2005;95:197-199.
- Dubourg J, Javouhey E, Geeraerts T, Messerer M, Kassai B. Ultrasonography of optic nerve sheath diameter for detection of raised intracranial pressure: a systematic review and meta-analysis. *Intensive Care Med*. 2011;37(7):1059-1068.
- Bellner J, Romner B, Reinstrup P, Kristiansson KA, Ryding E, Brandt L. Transcranial Doppler sonography pulsatility index (PI) reflects intracranial pressure (ICP). *Surg Neurol*. 2004;62(1):45-51; discussion 51.
- Brandt G, Béchir M, Sailer S, Haberthür C, Stocker R, Stover JF. Transcranial color-coded duplex sonography allows to assess cerebral perfusion pressure noninvasively following severe traumatic brain injury. *Acta Neurochir (Wien)*. 2010;152(6):965-972.
- Homburg AM, Jakobsen M, Enevoldsen E. Transcranial Doppler recordings in raised intracranial pressure. *Acta Neurol Scand*. 1993;87(6):488-493.
- Bouzat P, Francony G, Decléty P, et al. Transcranial Doppler to screen on admission patients with mild to moderate traumatic brain injury. *Neurosurgery*. 2011;68(6):1603-1609.
- Gura M, Elmaci I, Sari R, Coskun N. Correlation of pulsatility index with intracranial pressure in traumatic brain injury. *Turk Neurosurg*. 2011;21(2):210-215.
- Soehle M, Chatfield DA, Czosnyka M, Kirkpatrick PJ. Predictive value of initial clinical status, intracranial pressure and transcranial Doppler pulsatility after subarachnoid haemorrhage. *Acta Neurochir (Wien)*. 2007;149(6):575-583.
- Behrens A, Lenfeldt N, Ambarki K, Malm J, Eklund A, Koskinen LO. Transcranial Doppler pulsatility index: not an accurate method to assess intracranial pressure. *Neurosurgery*. 2010;66(6):1050-1057.
- Figaji AA, Zwane E, Fieggen AG, Siesjo P, Peter JC. Transcranial Doppler pulsatility index is not a reliable indicator of intracranial pressure in children with severe traumatic brain injury. *Surg Neurol*. 2009;72(4):389-394.
- Melo JR, Di Rocco F, Blanot S, et al. Transcranial Doppler can predict intracranial hypertension in children with severe traumatic brain injuries. *Childs Nerv Syst*. 2011;27(6):979-984.
- Gosling RG, King DH. Arterial assessment by Doppler-shift ultrasound. *Proc R Soc Med*. 1974;67(6 pt 1):447-449.
- de Riva N, Budohoski KP, Smielewski P, et al. Transcranial Doppler pulsatility index: what it is and what it isn't [published online ahead of print February 4, 2012]. *Neurocrit Care*. doi: 10.1007/s12028-012-9672-6.
- Czosnyka M, Richards HK, Whitehouse HE, Pickard JD. Relationship between transcranial Doppler-determined pulsatility index and cerebrovascular resistance: an experimental study. *J Neurosurg*. 1996;84(1):79-84.
- Czosnyka M, Smielewski P, Piechnik S, Steiner LA, Pickard JD. Cerebral autoregulation following head injury. *J Neurosurg*. 2001;95(5):756-763.
- Rosner MJ, Rosner SD, Johnson AH. Cerebral perfusion pressure: management protocol and clinical results. *J Neurosurg*. 1995;83(6):949-962.
- Patel HC, Menon DK, Tebbs S, Hawker R, Hutchinson PJ, Kirkpatrick PJ. Specialist neurocritical care and outcome from head injury. *Intensive Care Med*. 2002;28(5):547-553.
- Smielewski P, Czosnyka M, Steiner L, Belestri M, Piechnik S, Pickard JD. ICM+: software for on-line analysis of bedside monitoring data after severe head trauma. *Acta Neurochir Suppl*. 2005;95:43-49.
- Zou KH, O'Malley AJ, Mauri L. Receiver-operating characteristic analysis for evaluating diagnostic tests and predictive models. *Circulation*. 2007;115(5):654-657.
- Edouard AR, Vanhille E, Le Moigno S, Benhamou D, Mazoit JX. Non-invasive assessment of cerebral perfusion pressure in brain injured patients with moderate intracranial hypertension. *Br J Anaesth*. 2005;94(2):216-221.

22. Schmidt EA, Czosnyka M, Gooskens I, et al. Preliminary experience of the estimation of cerebral perfusion pressure using transcranial Doppler ultrasonography. *J Neurol Neurosurg Psychiatry*. 2001;70(2):198-204.
23. Lavinio A, Menon DK. Intracranial pressure: why we monitor it, how to monitor it, what to do with the number and what's the future? *Curr Opin Anaesthesiol*. 2011;24(2):117-123.
24. Rosenberg JB, Shiloh AL, Savel RH, Eisen LA. Non-invasive methods of estimating intracranial pressure. *Neurocrit Care*. 2011;15(3):599-608.
25. Ragauskas A, Daubaris G, Dziugys A, Azelis V, Gedrimas V. Innovative non-invasive method for absolute intracranial pressure measurement without calibration. *Acta Neurochir Suppl*. 2005;95:357-361.
26. Andrews PJ, Citerio G, Longhi L, Polderman K, Sahuquillo J, Vajkoczy P. NICEM consensus on neurological monitoring in acute neurological disease. *Intensive Care Med*. 2008;34(8):1362-1370.
27. Bratton SL, Chestnut RM, Ghajar J, et al. Guidelines for the management of severe traumatic brain injury. VI. Indications for intracranial pressure monitoring. *J Neurotrauma*. 2007;24(suppl 1):S37-S44.
28. Maas AI, Dearden M, Teasdale GM, et al. EBIC-guidelines for management of severe head injury in adults. European Brain Injury Consortium. *Acta Neurochir (Wien)*. 1997;139(4):286-294.
29. Dagal A, Lam AM. Cerebral blood flow and the injured brain: how should we monitor and manipulate it? *Curr Opin Anaesthesiol*. 2011;24(2):131-137.

Supplemental digital content is available for this article. Direct URL citations appear in the printed text and are provided in the HTML and PDF versions of this article on the journal's Web site (www.neurosurgery-online.com).



AHEAD.

Science moves forward. Fields evolve. And careers are not static. If you're interested in putting your leadership skills to work, the Congress of Neurological Surgeons is interested in you. The CNS offers the insight, innovation and information that pave the way to your future. Hone your leadership skills, advance your education and further your career by joining the one organization focused on fresh ideas and the future of neurosurgery.

Think ahead. We are.

For more information about member benefits or to apply today, visit w3.cns.org/apply.

 **CNS**

Phone: 847-240-2500
toll free: 1-877-5L74CNS
membership@cns.org
www.cns.org

The Relationship Between Cerebral Blood Flow Autoregulation and Cerebrovascular Pressure Reactivity After Traumatic Brain Injury

Karol P. Budohoski, MD*
 Marek Czosnyka, PhD*
 Nicolas de Riva, MD*‡
 Peter Smielewski, PhD*
 John D. Pickard, FMedSci*§
 David K. Menon, PhD¶||
 Peter J. Kirkpatrick, FMedSci*
 Andrea Lavinio, MD||

*Division of Neurosurgery, Department of Clinical Neurosciences, Addenbrooke's Hospital, University of Cambridge, Cambridge, United Kingdom; ‡Department of Anaesthesiology, Hospital Clinic de Barcelona, Universitat de Barcelona, Barcelona, Spain; §Wolfson Brain Imaging Centre, Department of Clinical Neurosciences, Addenbrooke's Hospital, University of Cambridge, Cambridge, United Kingdom; ¶University Department of Anaesthesia, Addenbrooke's Hospital, University of Cambridge, Cambridge, United Kingdom; ||Department of Anaesthesia, Cambridge University Hospitals NHS Foundation Trust, Addenbrooke's Hospital, Cambridge, United Kingdom

Correspondence:

Karol P. Budohoski, MD,
 Department of Neurosurgery,
 Medical Center for Postgraduate
 Training,
 Mazovia Brodnowski Hospital,
 Ul. Kondratowicza 8,
 03-242 Warsaw, Poland

Received, December 15, 2011.
 Accepted, May 9, 2012.
 Published Online, May 30, 2012.

Copyright © 2012 by the
 Congress of Neurological Surgeons

BACKGROUND: Cerebrovascular pressure reactivity is the principal mechanism of cerebral autoregulation. Assessment of cerebral autoregulation can be performed by using the mean flow index (Mx) based on transcranial Doppler ultrasonography. Cerebrovascular pressure reactivity can be monitored by using the pressure reactivity index (PRx), which is based on intracranial pressure monitoring. From a practical point of view, PRx can be monitored continuously, whereas Mx can only be monitored in short periods when transcranial Doppler probes can be applied.

OBJECTIVE: To assess to what degree impairment in pressure reactivity (PRx) is associated with impairment in cerebral autoregulation (Mx).

METHODS: A database of 345 patients with traumatic brain injury was screened for data availability including simultaneous Mx and PRx monitoring. Absolute differences, temporal changes, and association with outcome of the 2 indices were analyzed.

RESULTS: A total of 486 recording sessions obtained from 201 patients were available for analysis. Overall a moderate correlation between Mx and PRx was found ($r = 0.58$; $P < .001$). The area under the receiver operator characteristic curve designed to detect the ability of PRx to predict impaired cerebral autoregulation was 0.700 (95% confidence interval: 0.607-0.880). Discrepancies between Mx and PRx were most pronounced at an intracranial pressure of 30 mm Hg and they were significantly larger for patients who died ($P = .026$). Both Mx and PRx were significantly lower at day 1 postadmission in patients who survived than in those who died ($P < .01$).

CONCLUSION: There is moderate agreement between Mx and PRx. Discrepancies between Mx and PRx are particularly significant in patients with sustained intracranial hypertension. However, for clinical purposes, there is only limited interchangeability between indices.

KEY WORDS: Cerebral autoregulation, Cerebrovascular reactivity, Intracranial pressure, Transcranial Doppler, Traumatic brain injury

Neurosurgery 71:652-661, 2012

DOI: 10.1227/NEU.0b013e318260feb1

www.neurosurgery-online.com

Cerebral blood flow autoregulation describes the intrinsic ability of the brain to maintain a stable cerebral blood flow (CBF) despite fluctuations in cerebral perfusion pressure (CPP).¹⁻⁴ In the acutely injured brain,

cerebral autoregulation may be dysfunctional, leading to episodes of hypoperfusion or hyperemia.^{5,6} It has been shown that poor autoregulation is associated with unfavorable clinical outcome following traumatic brain injury (TBI) and subarachnoid hemorrhage, suggesting that both hypo- and hyperperfusion may play a part in secondary brain insults.⁷⁻¹²

Cerebrovascular pressure reactivity describes the ability of vascular smooth muscle cells to react to changes in transmural pressure,¹³ and is thought to be one of the principal mechanisms governing CBF autoregulation.^{4,5,13,14} Intuitively, it should be possible to distinguish various mechanisms of

ABBREVIATIONS: ABP, arterial blood pressure; BF, cerebral blood flow; CBV, cerebral blood volume; CPP, cerebral perfusion pressure; FV, flow velocity; GCS, Glasgow Coma Scale; GOS, Glasgow Outcome Scale; ICP, intracranial pressure; Mx, mean flow index; PRx, pressure reactivity index; ROC, receiver operator characteristic; TBI, traumatic brain injury; TCD, transcranial Doppler

autoregulatory failure. For instance, impairment of pressure reactivity may lead to a loss of autoregulation and significant fluctuations in CBF. However, in other circumstances CBF may be disrupted despite a functioning myogenic mechanism of vascular dilation/constriction, ie, intact pressure reactivity.

The transcranial Doppler mean flow index (Mx) and the arterial blood pressure (ABP)/intracranial pressure (ICP)-derived pressure reactivity index (PRx) are 2 commonly used methods to assess CBF autoregulation and cerebrovascular pressure reactivity, respectively.^{9,15} These indices rely on spontaneous changes of ABP or CPP and are calculated using the time correlation method.^{9,15} Both Mx and PRx have been shown to be predictors of outcome after TBI. However, there seem to be intrinsic differences in the prognostic information derived from Mx and PRx. PRx demonstrates a better discriminatory power between fatal and nonfatal outcome (mortality),¹⁵⁻¹⁷ and Mx demonstrates a better discriminatory power between favorable and unfavorable outcome (functional outcome).⁹ Both Mx and PRx, when averaged over specific CPP thresholds, demonstrate a U-shaped curve suggesting a specific relationship with the level of CPP, which may be used to individualize CPP management.^{6,18,19} Both methods have been validated,²⁰⁻²³ showing good agreement with other dynamic indices of autoregulation,^{20,24} as well as the static rate of autoregulation.²¹⁻²³ Additionally, PRx has been compared with positron emission tomography and has been shown to be significantly related to global oxygen extraction fraction.²¹ Mx and PRx are modulated by cerebral metabolic rate of oxygen²¹ as well as PaCO₂.²⁵⁻²⁷ Although a relationship between Mx and PRx has been described before,^{17,21,28-30} a detailed description of the factors that influence that relationship has not been performed.

At present, the readily available invasive monitoring has meant that PRx has largely replaced Mx in the assessment of autoregulation following head injury. Transcranial Doppler (TCD) monitoring over a longer period is cumbersome in critically ill patients, whereas continuous intraparenchymal ICP monitoring can be performed without significant risks of complications over days or even weeks. The advantages of long-term monitoring include increased accuracy and predictive value as well as improved ability of optimizing CPP thresholds.^{6,19} However, it is unclear whether the 2 methods can be used interchangeably, or whether both should be used as separate parameters equally contributing to a more complete assessment of the cerebral autoregulatory status.

We attempted to address this issue by assessing the degree of correlation between the 2 indices in datasets that included simultaneous Mx and PRx recordings obtained from patients after head injury. Furthermore, we wanted to determine the factors that are responsible for any potential divergence of the 2 modalities.

PATIENTS AND METHODS

A prospectively collected database of ICP, ABP, TCD recording, and clinical details from 345 TBI patients admitted to the Neurosciences Critical Care Unit between 1992 and 2010 was screened. The inclusion criteria were the availability of data regarding the severity of injury assessed

with Glasgow Coma Scale (GCS), outcome assessed with Glasgow Outcome Scale (GOS) at 6 months postinjury, and availability of monitoring data of ICP, ABP, and TCD. The minimal monitoring duration considered adequate for reliable calculation of autoregulatory indices was 30 minutes. Patients who underwent decompressive craniectomy had continuous TCD monitoring discontinued. Therefore, in those patients, only recordings before decompressive craniectomy were considered. All recordings were performed as an element of routine daily assessment of autoregulation in TBI patients in our center. Data collection and analysis was approved by the Neurocritical Care Users' Committee and the Institutional Research Ethics Committee. The database is continuously extended when new patients are studied and serves as a material source for conceptual, technical, and clinical hypothesis setting studies.

All patients were sedated and mechanically ventilated. From 1996 onward, all TBI patients were managed according to an updated version of the ICP/ CPP-oriented protocol.³¹ ICP was maintained below 20 mm Hg and CPP above 70 mm Hg. Reduction of ICP was achieved with a stepwise escalation approach by means of head positioning, sedation (continuous infusion of propofol or midazolam), cerebrospinal fluid drainage, use of osmotic agents (20% mannitol and/or hypertonic saline depending on electrolyte levels and renal function), induced hypothermia, and moderate hyperventilation. CPP was maintained with fluid expansion, the use of inotropes, and vasopressors. Intracranial hypertension refractory to medical management was treated with either decompressive craniectomy or central nervous system depressants, typically barbiturates. Mechanical ventilation was titrated to maintain a PaCO₂ level of 4.5 to 5.0 kPa (34-38 mm Hg).

Monitoring and Data Analysis

ABP was monitored invasively from the radial artery by use of a pressure-monitoring kit (Baxter Healthcare, Deerfield, Illinois; Sidcup, United Kingdom). ICP was monitored using an intraparenchymal probe (Codman & Shurtleff, Raynham, Massachusetts, or Camino Laboratories, San Diego, California). Flow velocity (FV) was monitored from the middle cerebral artery by using Doppler Box (DWL Compumedics, Germany) or Neuroguard (MedaSonics, Fremont, California). ABP and ICP signals were monitored continuously. TCD was performed daily for periods from 10 minutes to 3 hours starting from the day of initiation of invasive monitoring. The decision to discontinue monitoring was made on clinical grounds.

Raw signals were sampled and recorded by using home-designed software (WREC, Warsaw University of Technology, Poland; BioSan, University of Cambridge, United Kingdom; and ICM+, Cambridge Enterprise, Cambridge, United Kingdom) and retrospectively reanalyzed using professional ICM+ software (Cambridge Enterprise, Cambridge, United Kingdom). All signals were subject to an automated artifact removal process as well as manual correction. The automated artifact removal process applied a "not-a-number" value to all samples that did not fit preset criteria for valid samples. ABP was considered as valid when ABP peak-to-peak amplitude and diastolic ABP were >30 mm Hg and <200 mm Hg, respectively. FV was used when its peak-to-peak amplitude and diastolic FV was >10 cm/s and <180 cm/s. Subsequently, ABP, ICP, and FV signals were detrended by using a low-pass filter. The detrended signals were used for calculating Mx and PRx.

Calculation of Autoregulation and Pressure-Reactivity Indices

Calculation of the autoregulatory indices was based on previously described methodology.^{9,15} Mx was calculated as a moving Pearson

correlation coefficient between FV and CPP from a window of 30 consecutive samples, each averaged over 10 seconds, with an update of 1 sample. Similarly, PRx was calculated as a moving Pearson correlation coefficient between ICP and ABP from a window of 30 consecutive samples, each averaged over 10 seconds, with an update of 1 sample. Positive values of Mx and PRx indicate impaired autoregulation or pressure reactivity (passive transmission), whereas zero and negative values indicate an intact vascular regulatory mechanism. This methodology relies on spontaneous, slow fluctuations of blood pressure and/or cerebral perfusion pressure, and therefore does not require application of any external stimuli. Both indices were calculated from the whole duration of each daily monitoring session and formed minute-by-minute time series. For this analysis, PRx was not calculated continuously, throughout the whole hospitalization, but intermittently, only when simultaneous TCD recordings were available. The absolute difference between Mx and PRx (|Mx-PRx|) was calculated using the averaged value of Mx and PRx from a single monitoring session.

Statistical Analysis

Statistical analysis was performed using SPSS 16.0 (IBM, Armonk, New York). To avoid multiple sampling, all outcome analysis was performed using patient-averaged values from all recording sessions. Binary logistic regression was performed to assess the influence of age, admission GCS, ABP, ICP, CPP, PRx, Mx, and |Mx-PRx| on outcome (favorable vs unfavorable and death vs survival). A receiver operator characteristic (ROC) curve was designed to detect the ability of Mx and PRx to predict favorable and fatal outcome. A second ROC curve was designed to detect the ability of the overall (averaged per patient) PRx to predict impaired cerebral autoregulation (Mx >0.2).³² Empirical regression was used to plot the time trend of Mx and PRx changes over time and to average Mx, PRx, and |Mx-PRx| across ICP and CPP thresholds. For comparison between outcome groups and days postinjury, the 2-tailed *t* test was used. *P* < .05 was considered significant.

Outcome was assessed 6 months postinjury with the GOS. Outcome groups were dichotomized into death vs survival (GOS 1 vs 2, 3, 4, and 5), or favorable vs unfavorable outcome (GOS 1, 2, and 3 vs GOS 4 and 5).

RESULTS

There were a total of 486 recordings containing the required signals with a duration >30 minutes. The recordings were obtained from 201 patients. Seventy-eight percent of the patients were male, and the median age was 23 (range, 11-78). The median GCS was 6 (interquartile range 4-8). There was a 23% mortality rate within the analyzed cohort, and a broadly even distribution of patients between favorable and unfavorable outcome categories (49% vs 51%) (Table 1).

Agreement Between Mx and PRx

We analyzed the overall correlation between Mx and PRx and the ability of PRx to predict impaired cerebral autoregulation defined as Mx >0.2.³² Figure 1 demonstrates 2 different sets of monitoring: one with good agreement between Mx and PRx (*r* = 0.55) and one with large discrepancies. The overall correlation between Mx and PRx (averaged from all recordings) was moderate, but highly significant (*r* = 0.58; *P* < .001) (Figure 2). The area under the ROC curve designed to detect the ability of PRx to predict impaired cerebral autoregulation was 0.700 (95% CI: 0.607-0.880). Furthermore, an average PRx = -0.02 during the first 2 days after hospitalization could predict impaired cerebral autoregulation with a sensitivity of 70% and specificity of 63%.

Relationship of Mx and PRx to Outcome

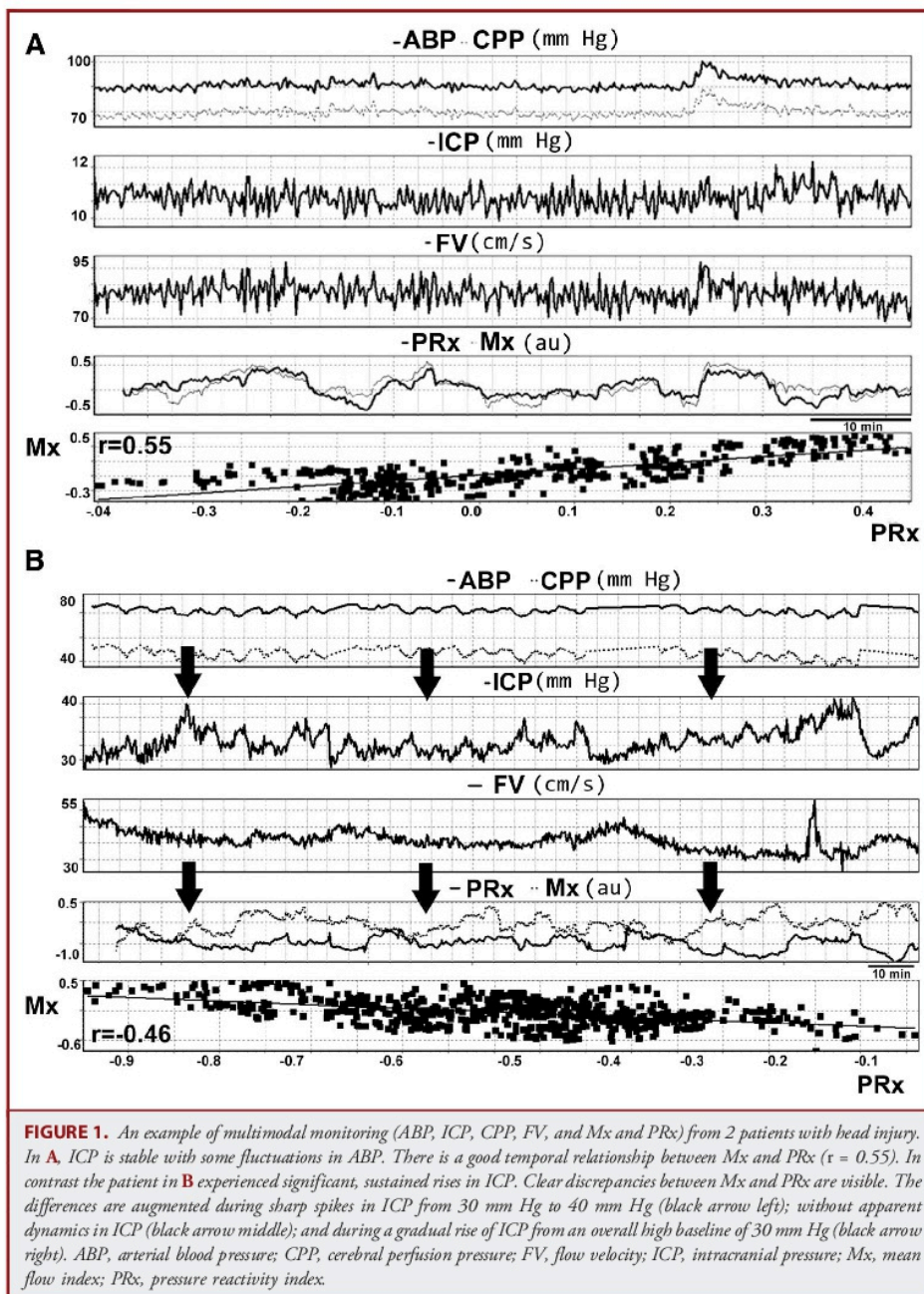
Table 1 demonstrates the differences in the baseline characteristics of the analyzed patients, whereas Table 2 summarizes the relationship

TABLE 1. Baseline Characteristics Split by Outcome Group With Intergroup Comparison and Statistical Significance^a

Parameter	Overall	Value by Outcome Group					
		Dead	Alive	P Value	Unfavorable	Favorable	P Value
n (% of total)	201 (100)	46 (23)	155 (77)	n/a	104 (51)	97 (49)	n/a
Males, n (%)	157 (78)	38 (82)	119 (76)	n/a	84 (80)	71 (73)	n/a
Age, median (range)	23 (11-78)	30 (16-78)	32 (11-76)	.146	34 (11-78)	32 (13-76)	.408
GCS, median (IQR)	6 (4)	5 (3)	7 (5)	.015^b	5 (4)	7 (5)	.010^b
GOS median (IQR)	3 (2)	1 (0)	4 (2)	n/a	2 (2)	4 (1)	n/a
ABP (mean ± SD)	93 ± 11 mm Hg	97 ± 11	92 ± 11	.007^b	95 ± 10	91 ± 12	.014^b
ICP (mean ± SD)	18 ± 9 mm Hg	21 ± 13	17 ± 8	.022^b	19 ± 10	17 ± 8	.991
CPP (mean ± SD)	75 ± 12 mm Hg	76 ± 16	74 ± 12	.479	75 ± 12	74 ± 11	.335
FV (mean ± SD)	60 ± 21 cm/s	66 ± 23	59 ± 20	.077	63 ± 22	59 ± 19	.179
PRx (mean ± SD)	0.00 ± 0.25	0.07 ± 0.32	-0.03 ± 0.23	.020^b	0.04 ± 0.26	-0.05 ± 0.23	.024^b
Mx (mean ± SD)	0.04 ± 0.26	0.12 ± 0.29	0.01 ± 0.25	.018^b	0.09 ± 0.26	-0.03 ± 0.25	.002^b
Mx-PRx (mean ± SD)	0.25 ± 0.19	0.28 ± 0.22	0.23 ± 0.17	.026^b	0.25 ± 0.20	0.24 ± 0.20	.46

^aABP, arterial blood pressure; CPP, cerebral perfusion pressure; FV, transcranial Doppler flow velocity; GCS, Glasgow Coma Scale; GOS, Glasgow Outcome Scale; ICP, intracranial pressure; IQR, interquartile range; Mx, mean flow index; |Mx-PRx|, absolute difference between Mx and PRx; PRx, pressure reactivity index; SD, standard deviation; n/a, not available.

^bSignificant (*P* < .05) in intergroup comparison.

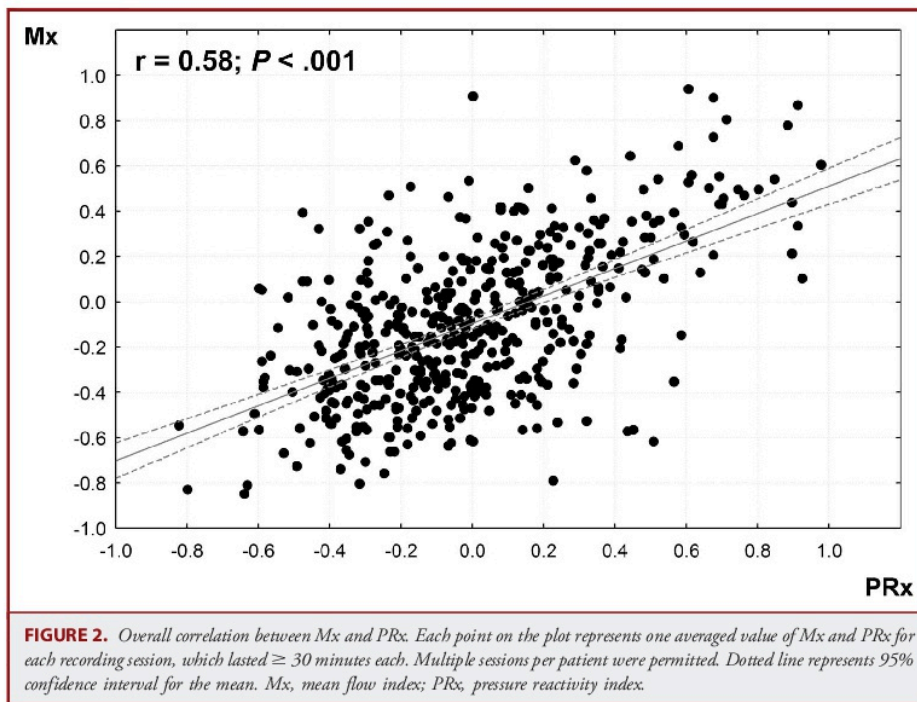


of Mx and PRx with outcome by use of ROC curve analysis and binary logistic regression to determine independent predictors.

The Influence of ICP

Both Mx and PRx showed a relationship with the level of CPP. When averaged PRx values obtained from all recordings were

plotted against CPP, a U-shaped curve was obtained, demonstrating the presence of a CPP level that is associated with the best pressure reactivity (65-75 mm Hg) as previously described by Steiner et al.⁶ However, when Mx values obtained from all patients were plotted against CPP, a descending curve was obtained (Figure 3A). Furthermore, the curve obtained using Mx



was shifted toward higher perfusion pressures (around 90 mm Hg), demonstrating sensitivity toward low-pressure states.

Both indices of autoregulation demonstrate a direct relationship with ICP. Although the changes are similar in direction, Mx increases more gradually, beginning to show changes at an ICP level of 20 mm Hg, whereas PRx demonstrates a sharper change at an ICP above 30 mm Hg (Figure 3B).

Temporal Relationship of Mx and PRx

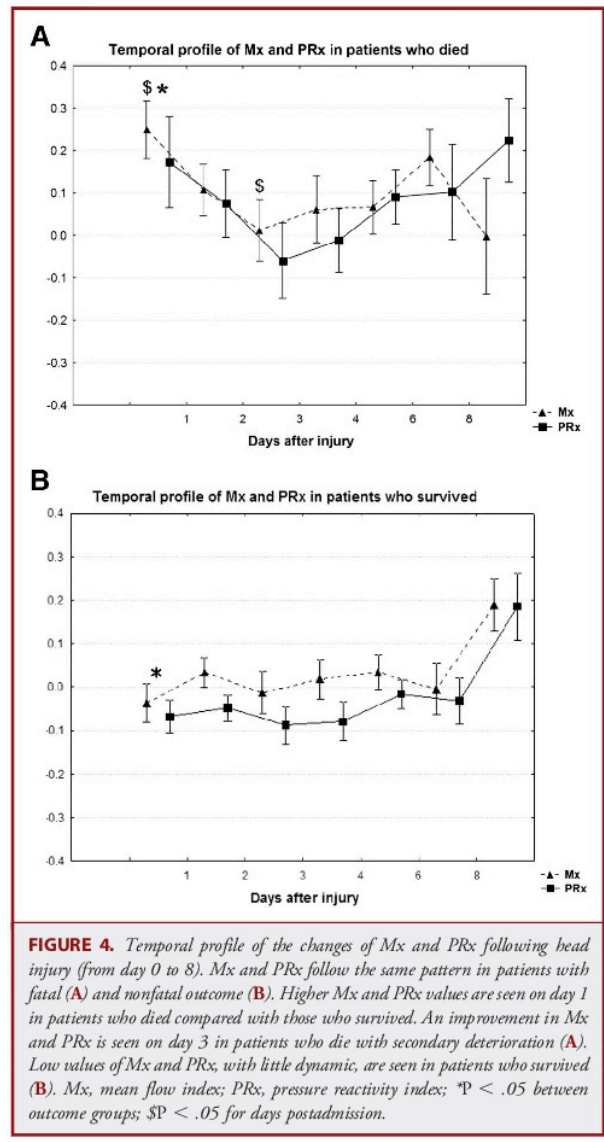
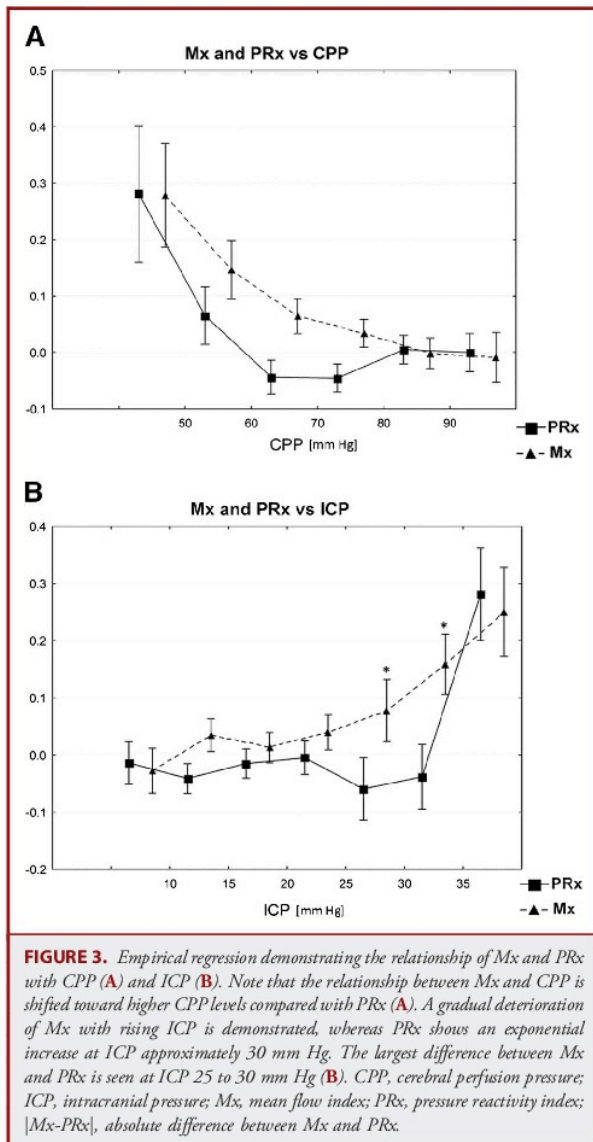
The time trends of Mx and PRx with respect to days postinjury were similar (Figure 4). Patients who died on day 1 postinjury had higher values of both indices ($Mx = 0.25 \pm 0.28$ vs $Mx = -0.02 \pm 0.27$, $P = .002$; and $PRx = 0.17 \pm 0.44$ vs $PRx = 0.07 \pm 0.24$, $P = .003$ for those who died and those who survived, respectively). In the group who died there was a decrease

TABLE 2. ROC Curve Analysis of the Ability of the Analyzed Parameters to Predict Unfavorable and Fatal Outcome and Binary Logistic Regression of the Relationship of the Analyzed Parameters to Outcome^a

	Unfavorable Outcome						Fatal Outcome					
	ROC Curve			Binary Regression			ROC Curve			Binary Regression		
	AUC	95%CI	P Value	B (SE)	Wald χ^2	Sig.	AUC	95%CI	Sig.	B (SE)	Wald χ^2	P Value
GCS	0.625	0.558-0.692	<.001 ^b	0.197 (0.054)	13.2	<.001 ^b	0.638	0.564-0.713	.001 ^b	0.243 (0.077)	9.9	.002 ^b
Age	0.566	0.494-0.639	.073	-0.019 (0.010)	3.5	.060	0.593	0.507-0.679	.023 ^b	-0.013 (0.012)	1.2	.264
ABP	0.582	0.510-0.653	.027 ^b	-8.337 (5.727)	2.1	.145	0.574	0.482-0.666	.126	2.762 (4.750)	0.3	.561
ICP	0.578	0.507-0.650	.034 ^b	8.299 (5.726)	2.1	.147	0.585	0.492-0.678	.077	-2.798 (4.750)	0.3	.556
CPP	0.513	0.440-0.586	.726	87.317 (5.727)	2.1	.146	0.495	0.400-0.591	.928	-2.776 (4.750)	0.3	.559
Mx	0.649	0.584-0.714	<.001	-0.089 (0.652)	5.6	.018 ^b	0.606	0.518-0.695	.003 ^b	-0.172 (0.701)	0.1	.806
PRx	0.579	0.512-0.647	.023 ^b	-1.433 (0.605)	0.6	.893	0.658	0.566-0.750	.001 ^b	-1.806 (0.776)	5.4	.020 ^b
Mx-PRx	0.540	0.467-0.612	.284	-0.640 (0.855)	0.6	.454	0.558	0.473-0.647	.179	-1.070 (1.021)	1.1	.294
Constant	n/a	n/a	n/a	1.886 (1.199)	2.5	.116	n/a	n/a	n/a	2.485 (1.427)	3	.082

^aABP, arterial blood pressure; AUC, area under the curve; CI, confidence interval; CPP, cerebral perfusion pressure; FV, transcranial Doppler flow velocity; GCS, Glasgow Coma Scale; GOS, Glasgow Outcome Scale; ICP, intracranial pressure; IQR, interquartile range; Mx, mean flow index; NS, not significant; PRx, pressure reactivity index; |Mx-PRx|, absolute difference between Mx and PRx; ROC, receiver-operator characteristic; SE, standard error; SD, standard deviation; n/a, not available.

^bIndicates statistical significance ($P < .05$).



(significant only for Mx) in Mx and PRx values on day 3 compared with day 1 postinjury (Mx = 0.25 ± 0.28 vs Mx = 0.01 ± 0.25, P = .01 and PRx = 0.17 ± 0.44 vs PRx = -0.06 ± 0.30, P = .09 on day 1 and day 3, respectively). The trends of Mx and PRx in patients who survived were also comparable with Mx and PRx values lower than in patients who died (Figure 4).

The Absolute Difference Between Mx and PRx

Although a moderate correlation between Mx and PRx was observed, there were situations where Mx and PRx did not demonstrate agreement (Figure 1B). Overall, Mx was slightly

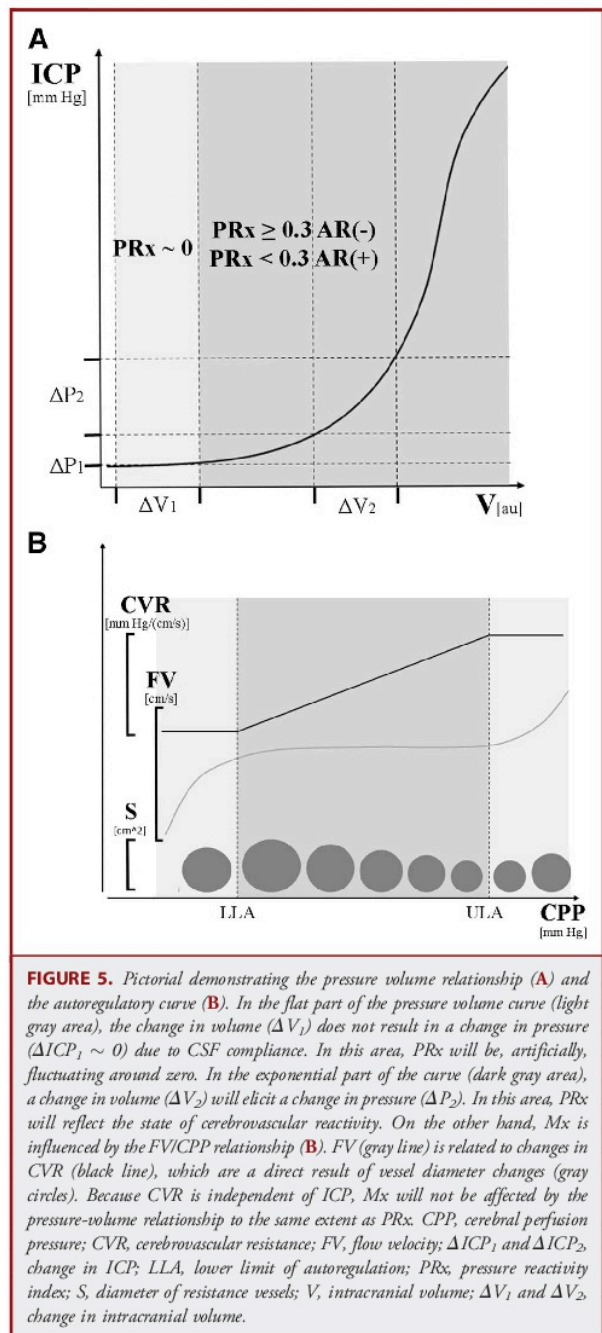
higher than PRx, regardless of the initial GCS and the day postinjury (Mx = 0.04 ± 0.26 and PRx = 0.00 ± 0.25); however, this difference was not statistically significant. We observed that the absolute difference between Mx and PRx was related to the level of ICP. The difference increased with increasing ICP reaching a maximum at ICP of 30 mm Hg and subsequently decreased (Figure 3). There was no obvious relationship between the absolute Mx-PRx difference and the level of CPP. However, it was observed that the absolute difference between Mx and PRx was larger in patients who died as a result of the sustained injury (P = .026) (Table 1).

DISCUSSION

We have shown that PRx distinguishes between fatal and nonfatal outcome, whereas Mx distinguishes between favorable and unfavorable outcome. An abnormal PRx previously has been shown to be predictive of unfavorable outcome.^{16,17} For this study we used only monitoring periods of 30 min or longer in which simultaneous calculation of Mx and PRx was possible. This approach limited the availability of monitoring data to approximately 1 hour/day. Other studies, however, used continuous, long-term monitoring of PRx, potentially making outcome associations more robust. PRx showed an expected relationship with CPP, confirming previous results.⁶ In contrast to earlier work,¹⁸ we have not demonstrated a complete U-shaped curve when Mx has been plotted against CPP. However, the lowest Mx value was found at the same CPP level (90 mm Hg) as in earlier studies.¹⁸ In the analyzed dataset, there were very few recordings with a CPP above 90 mm Hg, which could account for the absence of the ascending arm of the U-shaped curve as a rise in Mx at high CPP levels was previously seen for CPP above 90 mm Hg.¹⁸

Our results demonstrate that the agreement between Mx and PRx is primarily influenced by the level of ICP, with the biggest discrepancy observed for an ICP value of 30 mm Hg. Furthermore, we have shown that the difference between Mx and PRx is greater in patients with fatal outcomes. This finding is concordant with the fact that patients with a fatal outcome have, on average, higher ICP.³³ Additionally, we have observed that, in patients who die, both Mx and PRx demonstrate severely disturbed CBF autoregulation and pressure reactivity during the first 2 days of hospitalization. In contrast, patients who survived had, on average, preserved both CBF autoregulation and pressure reactivity throughout the whole monitoring period. Despite a statistical difference in Mx and PRx values between the analyzed groups, statements about the overall state of autoregulation are prone to misinterpretation. One possible way to overcome this problem in future studies is to calculate the time spent above certain thresholds of Mx and PRx using described methodology.³⁴

In the majority of cases, autoregulatory failure was represented by a simultaneous increase in Mx and PRx (Figure 1A), suggesting that both CBF autoregulation and pressure reactivity are impaired. Furthermore, the time course of the changes in PRx and Mx after TBI were similar. The impairments seen during the first 2 days after hospitalization distinguished patients who died from those who survived (Figure 4). Interestingly, in patients who died, significant improvements in the state of autoregulation were seen during the first 3 days postinjury.³⁵ Furthermore, PRx was found to have good accuracy in predicting impaired cerebral autoregulation, regardless of whether the analysis was based on the whole monitoring period or the first 2 days of hospitalization. These findings support the assumption that pressure reactivity, ie, the ability of vasoconstriction and vasodilation in response to CPP changes, is an important mechanism of CBF autoregulation. Accordingly, Mx and PRx could be viewed as indices monitoring 2 aspects of the same process.



There were, however, recordings with a significant discrepancy between Mx and PRx (Figure 1B). Overall, the absolute difference between Mx and PRx was a function of increasing ICP and was maximal at an ICP of approximately 30 mm Hg. There was a clear

difference in the response of Mx and PRx to increasing level of ICP. Although Mx started to show impairments when ICP reached 15 to 20 mm Hg and increased steadily thereafter, PRx rose dramatically after ICP reached 30 mm Hg (Figure 3). As a result, with ICP between 20 and 30 mm Hg, the discrepancy between Mx and PRx suggested episodes of impaired CBF autoregulation despite functioning pressure reactivity. PRx is calculated from changes in ICP in response to fluctuations of blood pressure. An assumption is made that the observed changes in ICP are coupled with changes in cerebral blood volume (CBV) and therefore represent vasomotor reactions. However, small CBV changes may be successfully buffered by the compliance of the cerebrospinal fluid (CSF).³⁶ Because the intracranial pressure-volume relationship is nonlinear, the degree of buffering may be different at different ICP levels (Figure 5).³⁶ PRx does not include information about CSF compliance, which may significantly confound the obtained measurements. On one hand, a functioning vasoconstriction/vasodilatation mechanism (pressure reactivity) may be insufficient to maintain CBF (CBF autoregulation). Such a situation would result in the observed discrepancy between PRx and Mx. Another possibility is that at low levels of ICP, where the CSF compliance is high and the pressure-volume curve is flat, CBV changes will not be transferred to changes in ICP, artificially forcing PRx to fluctuate around zero (Figure 5). Similarly, high levels of ICP with exhausted CSF compliance may cause accentuation of PRx. It is possible that both mechanisms are responsible for the observed effects simultaneously. The effect of increased CSF compliance on PRx has been reported previously following decompressive craniectomy. The results are equivocal, with 1 study suggesting an improvement in PRx³⁷ and another a further derangement following craniectomy.³⁸ Although definitive conclusions have not been drawn from these studies because of the limited number of patients, the discrepancies support confounding influence of CSF compliance on PRx.

Interestingly, our results demonstrate that patients with a large discrepancy between Mx and PRx were more likely to have a fatal outcome. Previous studies that analyzed the relationship between ICP and outcome after TBI have shown that patients who do not survive a head injury have, on average, a higher ICP level (27 mm Hg) than those who survive (16 mm Hg).³⁵ Although this provides 1 facile explanation for the observed differences, the documented discrepancy between the 2 indices suggests that, at an elevated ICP, functioning pressure reactivity may not be sufficient to sustain a stable CBF, and that this autoregulatory failure is better reflected by Mx. However, the clinical significance of this finding remains to be determined, and studies that address the question of cerebral autoregulation in the context of cerebral compliance are warranted.

Limitations

First, both indices of autoregulation (Mx and PRx) are noisy. Improving signal/noise ratio requires time averaging over long periods. Although continuous recordings over long periods are

feasible by use of PRx, it is challenging to obtain a stable signal using TCD technology for more than 1 hour, making Mx time-limited. For methodological clarity, we have compared Mx and PRx calculated only from periods where both signals were available. This approach disadvantages PRx.

Second, both PRx and Mx are only surrogate measures of autoregulation, because they do not measure CBF directly. Therefore, the observed changes and discrepancies may be a result of factors that do not have a direct translation to CBF, but rather influence only the calculation method.

All patients were treated with CPP/ICP-directed therapy.³¹ The effect of vasopressors on slow wave activity (essential for reliable calculation of PRx and Mx) and the state of cerebral autoregulation is unknown. We are, therefore, unable to make a definite statement regarding the effect of therapy on the measured indices and their interrelationship, particularly at high ICP levels, where vasopressors were likely to be used.

It has previously been shown that autoregulatory indices are influenced by the cerebral metabolic rate of oxygen and arterial levels of carbon dioxide.²¹ In the present study, we were unable to correct for these confounding factors. Furthermore, the influence of various other physiological stimuli on PRx and Mx was not considered here, which needs to be treated as a limitation of the study.

CONCLUSION

Mx and PRx describe different aspects of the homeostatic phenomenon known as cerebral autoregulation. Both indices are independently associated with outcome after head injury. The discrepancies between Mx and PRx are maximal during sustained increases in ICP to 30 mm Hg, suggesting changes in intracranial compliance influences measurement accuracy, particularly of PRx. Although the discrepancies may offer an insight into the nature of cerebral autoregulatory failure, their clinical significance remains unknown.

Disclosure

This work was supported by the National Institute of Health Research, Biomedical Research Centre (Neuroscience Theme), the Medical Research Council (grants G0600986 and G9439390), and National Institute of Health Research Senior Investigator Awards (to J.D.P. and D.K.M.); by the Clifford and Mary Corbridge Trust of Robinson College, Cambridge, UK, and the St. Catharine's College, University of Cambridge Travel and Research Fund (to K.P.B.); by the Hospital Clinic de Barcelona, Barcelona, Spain (NdR). ICM+ software (Cambridge Enterprise, Cambridge, UK <http://www.neurosurg.cam.ac.uk/icmplust/>) is licensed by the University of Cambridge, Cambridge Enterprise Ltd. P.S. and M.C. have a financial interest in a part of licensing fee. J.D.P. and M.C. are directors of Technicam, UK. The other authors have no personal financial or institutional interest in any of the drugs, materials, or devices described in this article.

REFERENCES

1. Lassen NA. Cerebral blood flow and oxygen consumption in man. *Physiol Rev.* 1959;39(2):183-238.
2. Lassen NA. Autoregulation of cerebral blood flow. *Circ Res.* 1964;15(suppl): 201-204.

3. Harper AM. Autoregulation of cerebral blood flow: influence of the arterial blood pressure on the blood flow through the cerebral cortex. *J Neurol Neurosurg Psychiatry*. 1966;29(5):398-403.
4. Kontos HA, Wei EP, Navari RM, Levasseur JE, Rosenblum WI, Patterson JL Jr. Responses of cerebral arteries and arterioles to acute hypotension and hypertension. *Am J Physiol*. 1978;234(4):H371-H383.
5. Bouma GJ, Muizelaar JP, Bando K, Marmarou A. Blood pressure and intracranial pressure-volume dynamics in severe head injury: relationship with cerebral blood flow. *J Neurosurg*. 1992;77(1):15-19.
6. Steiner LA, Czosnyka M, Piechnik SK, et al. Continuous monitoring of cerebrovascular pressure reactivity allows determination of optimal cerebral perfusion pressure in patients with traumatic brain injury. *Crit Care Med*. 2002;30(4):733-738.
7. Bijlenga P, Czosnyka M, Budohoski KP, et al. "Optimal cerebral perfusion pressure" in poor grade patients after subarachnoid hemorrhage. *Neurocrit Care*. 2010;13(1):17-23.
8. Jaeger M, Schuhmann MU, Soehle M, Nagel C, Meixensberger J. Continuous monitoring of cerebrovascular autoregulation after subarachnoid hemorrhage by brain tissue oxygen pressure reactivity and its relation to delayed cerebral infarction. *Stroke*. 2007;38(3):981-986.
9. Czosnyka M, Smielewski P, Kirkpatrick P, Menon DK, Pickard JD. Monitoring of cerebral autoregulation in head-injured patients. *Stroke*. 1996;27(10):1829-1834.
10. Overgaard J, Tweed WA. Cerebral circulation after head injury. 1. Cerebral blood flow and its regulation after closed head injury with emphasis on clinical correlations. *J Neurosurg*. 1974;41(5):531-541.
11. Cold GE, Jensen FT. Cerebral autoregulation in unconscious patients with brain injury. *Acta Anaesthesiol Scand*. 1978;22(3):270-280.
12. Bouma GJ, Muizelaar JP, Choi SC, Newlon PG, Young HF. Cerebral circulation and metabolism after severe traumatic brain injury: the elusive role of ischemia. *J Neurosurg*. 1991;75(5):685-693.
13. Bayliss WM. On the local reactions of the arterial wall to changes of internal pressure. *J Physiol*. 1902;28(3):220-231.
14. Avezaat CJ, van Eijndhoven JH, Wyper DJ. Effects of hypercapnia and arterial hypotension and hypertension on cerebrospinal fluid pulse pressure and intracranial volume-pressure relationships. *J Neurol Neurosurg Psychiatry*. 1980;43(3):222-234.
15. Czosnyka M, Smielewski P, Kirkpatrick P, Laing RJ, Menon D, Pickard JD. Continuous assessment of the cerebral vasomotor reactivity in head injury. *Neurosurgery*. 1997;41(1):11-17; discussion 17-19.
16. Sorrentino E, Diedler J, Kasprowitz M, et al. Critical thresholds for cerebrovascular reactivity after traumatic brain injury. *Neurocrit Care*. 2012;16(2):258-266.
17. Zweifel C, Lavinio A, Steiner LA, et al. Continuous monitoring of cerebrovascular pressure reactivity in patients with head injury. *Neurosurg Focus*. 2008;25(4):E2.
18. Czosnyka M, Smielewski P, Piechnik S, Steiner LA, Pickard JD. Cerebral autoregulation following head injury. *J Neurosurg*. 2001;95(5):756-763.
19. Bratton SL, Chestnut RM, Ghajar J, et al. Guidelines for the management of severe traumatic brain injury. IX. Cerebral perfusion thresholds. *J Neurotrauma*. 2007;24(suppl 1):S59-S64.
20. Czosnyka M, Smielewski P, Lavinio A, Pickard JD, Panerai R. An assessment of dynamic autoregulation from spontaneous fluctuations of cerebral blood flow velocity: a comparison of two models, index of autoregulation and mean flow index. *Anesth Analg*. 2008;106(1):234-239, table of contents.
21. Steiner LA, Coles JP, Johnston AJ, et al. Assessment of cerebrovascular autoregulation in head-injured patients: a validation study. *Stroke*. 2003;34(10):2404-2409.
22. Lang EW, Mehdorn HM, Dorsch NW, Czosnyka M. Continuous monitoring of cerebrovascular autoregulation: a validation study. *J Neurol Neurosurg Psychiatry*. 2002;72(5):583-586.
23. Smielewski P, Czosnyka M, Kirkpatrick P, Pickard JD. Evaluation of the transient hyperemic response test in head-injured patients. *J Neurosurg*. 1997;86(5):773-778.
24. Steinmeier R, Hofmann RP, Bauhof C, Hübner U, Fahlbusch R. Continuous cerebral autoregulation monitoring by cross-correlation analysis. *J Neurotrauma*. 2002;19(10):1127-1138.
25. Steiner LA, Balestrieri M, Johnston AJ, et al. Effects of moderate hyperventilation on cerebrovascular pressure-reactivity after head injury. *Acta Neurochir Suppl*. 2005;95:17-20.
26. Haubrich C, Steiner L, Kasprowitz M, et al. Short-term moderate hypocapnia augments detection of optimal cerebral perfusion pressure. *J Neurotrauma*. 2011;28(7):1133-1137.
27. Ogoh S, Nakahara H, Ainslie PN, Miyamoto T. The effect of oxygen on dynamic cerebral autoregulation: critical role of hypocapnia. *J Appl Physiol*. 2010;108(3):538-543.
28. Czosnyka M, Smielewski P, Kirkpatrick P, Piechnik S, Laing R, Pickard JD. Continuous monitoring of cerebrovascular pressure-reactivity in head injury. *Acta Neurochir Suppl*. 1998;71:74-77.
29. Eide PK, Czosnyka M, Sorteberg W, Pickard JD, Smielewski P. Association between intracranial, arterial pulse pressure amplitudes and cerebral autoregulation in head injury patients. *Neurol Res*. 2007;29(6):578-582.
30. Lang EW, Lagopoulos J, Griffith J, et al. Cerebral vasomotor reactivity testing in head injury: the link between pressure and flow. *J Neurol Neurosurg Psychiatry*. 2003;74(8):1053-1059.
31. Helmy A, Vizcaychipi M, Gupta AK. Traumatic brain injury: intensive care management. *Br J Anaesth*. 2007;99(1):32-42.
32. Sorrentino E, Budohoski KP, Kasprowitz M, et al. Critical thresholds for transcranial Doppler indices of cerebral autoregulation in traumatic brain injury. *Neurocrit Care*. 2011;14(2):188-193.
33. Balestrieri M, Czosnyka M, Hutchinson P, et al. Impact of intracranial pressure and cerebral perfusion pressure on severe disability and mortality after head injury. *Neurocrit Care*. 2006;4(1):8-13.
34. Vik A, Nag T, Fredrikli OA, et al. Relationship of "dose" of intracranial hypertension to outcome in severe traumatic brain injury. *J Neurosurg*. 2008;109(4):678-684.
35. Menon DK. Cerebral protection in severe brain injury: physiological determinants of outcome and their optimisation. *Br Med Bull*. 1999;55(1):226-258.
36. Marmarou A, Shulman K, LaMorgese J. Compartmental analysis of compliance and outflow resistance of the cerebrospinal fluid system. *J Neurosurg*. 1975;43(5):523-534.
37. Wang EC, Ang BT, Wong J, Lim J, Ng I. Characterization of cerebrovascular reactivity after craniectomy for acute brain injury. *Br J Neurosurg*. 2006;20(1):24-30.
38. Timofeev I, Czosnyka M, Nortje J, et al. Effect of decompressive craniectomy on intracranial pressure and cerebrospinal compensation following traumatic brain injury. *J Neurosurg*. 2008;108(1):66-73.

COMMENT

This study compares 2 measures of cerebral blood flow autoregulation, Mrx, which is the transcranial Doppler mean flow index, and Prx, which is the arterial blood pressure/intracranial pressure-derived pressure reactivity index. The authors' group has described both these measures extensively in previous works. The current study addresses the important question of whether these 2 measures are comparable, or whether they serve as independent biomarkers of cerebral blood flow autoregulation status in patients with severe traumatic brain injury. Prospectively collected data from 201 patients was assessed in a retrospective fashion. A statistically significant and moderately robust relationship was found between Mrx and Prx. The indices appeared to diverge from each other at higher intracranial pressure (above 30 mm Hg). Importantly, both Mrx and Prx were lower in patients who survived compared with those who died. In addition, the temporal course of changes in Mrx and Prx were predictive of outcome.

This work is an important comparison of 2 indices of cerebral physiology that can be measured in the Neurointensive Care Unit. However, as the authors point out, the limits of these derivative measures should be kept in mind. Neither Mrx or Prx are direct measures of cerebral autoregulation, because only a direct measure of cerebral blood flow vs cerebral perfusion pressure can yield the autoregulation curve in a particular patient at a given time point. Although this could not be studied in the current work, in certain clinical situations such as after decompressive craniectomy, the usual relationships between cerebral blood flow, cerebral blood volume, and

intracranial pressure may change because the increased buffering capacity of the opened cranium, making P_{rx} values more difficult to interpret. Hopefully, future studies will help shed more light on whether derivative measures such as M_{rx} and P_{rx} can help guide patient-specific treatment strategies in patients with traumatic brain injury. In particular, can these measures help define the optimal cerebral perfusion pressure goal in individual patients? Is

the time spent above certain thresholds of M_{rx} and P_{rx} related to outcome? And, most importantly, can we use these measures to intervene appropriately in order to improve patient outcomes?

Guy Rosenthal
San Francisco, California



AHEAD.

Science moves forward. Fields evolve. And careers are not static. If you're interested in putting your leadership skills to work, the Congress of Neurological Surgeons is interested in you. The CNS offers the insight, innovation and information that pave the way to your future. Hone your leadership skills, advance your education and further your career by joining the one organization focused on fresh ideas and the future of neurosurgery.

Think ahead. We are.

For more information about member benefits or to apply today, visit w3.cns.org/apply.

 **CNS**

Phone: 847-240-2500
Toll Free: 1-877-517-1CNS
membership@1cns.org
www.cns.org